1-1-2018

Robust Distributed Stabilization of Interconnected Multiagent Systems

Vahid Rezaei
University of Denver

Robust Distributed Stabilization of Interconnected Multiagent Systems

Abstract

Many large-scale systems can be modeled as groups of individual dynamics, e.g., multi-vehicle systems, as well as interconnected multiagent systems, power systems and biological networks as a few examples. Due to the high-dimension and complexity in configuration of these infrastructures, only a few internal variables of each agent might be measurable and the exact knowledge of the model might be unavailable for the control design purpose. The collective objectives may range from consensus to decoupling, stabilization, reference tracking, and global performance guarantees. Depending on the objectives, the designer may choose agent-level low-dimension or multiagent system-level high-dimension approaches to develop distributed algorithms. With an inappropriately designed algorithm, the effect of modeling uncertainty may propagate over the communication and coupling topologies and degrade the overall performance of the system. We address this problem by proposing single- and multi-layer structures. The former is used for both individual and interconnected multiagent systems. The latter, inspired by cyber-physical systems, is devoted to the interconnected multiagent systems. We focus on developing a single control-theoretic tool to be used for the relative information-based distributed control design purpose for any combinations of the aforementioned configuration, objective, and approach. This systematic framework guarantees robust stability and performance of the closed-loop multiagent systems. We validate these theoretical results through various simulation studies.

Document Type

Dissertation

Degree Name

Ph.D.

Department

Electrical Engineering

First Advisor

Margareta Stefanovic, Ph.D.

Second Advisor

Kimon Valavanis

Third Advisor

Jun Zhang

Keywords

Cooperative control, Distributed control, Graph-theoretic control, Large-scale systems, Multi-agent systems, Robust control

Subject Categories

Controls and Control Theory | Electrical and Computer Engineering

Robust Distributed Stabilization of Interconnected Multiagent Systems

---

A Dissertation

Presented to

the Faculty of the Daniel Felix Ritchie School of Engineering and Computer Science

University of Denver

In Partial Fulfillment

of the Requirements for the Degree

Doctor of Philosophy

---

by

Vahid Rezaei

June 2018

Advisor: Dr. Margareta Stefanovic

Author: Vahid Rezaei
Title: Robust Distributed Stabilization of Interconnected Multiagent Systems
Advisor: Dr. Margareta Stefanovic
Degree Date: June 2018

Abstract

Many large-scale systems can be modeled as groups of individual dynamics, e.g., multi-vehicle systems, as well as interconnected multiagent systems, power systems and biological networks as a few examples. Due to the high-dimension and complexity in configuration of these infrastructures, only a few internal variables of each agent might be measurable and the exact knowledge of the model might be unavailable for the control design purpose. The collective objectives may range from consensus to decoupling, stabilization, reference tracking, and global performance guarantees. Depending on the objectives, the designer may choose agent-level low-dimension or multiagent system-level high-dimension approaches to develop distributed algorithms. With an inappropriately designed algorithm, the effect of modeling uncertainty may propagate over the communication and coupling topologies and degrade the overall performance of the system. We address this problem by proposing single- and multi-layer structures. The former is used for both individual and interconnected multiagent systems. The latter, inspired by cyber-physical systems, is devoted to the interconnected multiagent systems. We focus on developing a single control-theoretic tool to be used for the relative information-based distributed control design purpose for any combinations of the aforementioned configuration, objective, and approach. This systematic frame-

work guarantees robust stability and performance of the closed-loop multiagent systems. We validate these theoretical results through various simulation studies.

Acknowledgments

Dedicated to

my Family and Kevin L. Moore

with Love, Appreciation, and Respect.

I would like to express my sincere thanks to Dr. Margareta Stefanovic, my advisor, for the chance of studying distributed control as my Ph.D. research topic at the University of Denver (DU). I highly appreciate the time she spent for my research, her helpful suggestions to improve the quality of this research work, continuous support, and friendship during these years.

My deep gratitude goes to Dr. Kimon Valavanis for his personal interest in my research work, and unconditional support during the time I was a Ph.D. student at DU. I also would like to thank Dr. Jun Zhang for serving on my Ph.D. research committee, and our friendly discussions during the past few years. Many thanks to Dr. Alvaro Arias for his interest in this control-theoretic topic, and for serving as the chair of my research committee.

I further would like to thank Dr. Amin Khodaei and Dean JB Holston for their support, and Dr. Goncalo Martins for his friendship. And, of course, special thanks to Ms. Molly Dunn, Ms. Yvonne Petitt, and Mr. Tim Sheu for their help during the time I was with the dept. of Electrical and Computer Engineering at DU.

I should mention that it is really difficult to write about all people in only one page while, unfortunately, DU also does not allow having a separate dedication page at the beginning of my dissertation.

Contents

List of Figures

Chapter 1

Introduction

"When I want to understand what is happening today or try to decide what will happen tomorrow, I look back."

Omar Khayyam — Mathematician, Astronomer, and Poet (1048-1131)

Looking back though history, we notice that the word "feedback", in engineering, has been introduced during the 20^{th} century in order to describe the parasitic effect of an amplifier's output on the input circuit. In fact, it is more than 2000 years that feedback control systems have been known as parts of human daily life. An interesting point is that control systems are multidisciplinary topics, and are heavily affected by theoretical and practical advances in many fields such as electrical and mechanical engineering as well as mathematics. As an example, we know that the modern control era emerged as a result of advances in (the state space domain) mathematical analysis tools and digital computers. (See [1] for further historical comments on control systems.)

Rise in human population has resulted in the increased "size" of systems which, consequently, increased the dimension of their mathematical models. Initial investigation was around direct generalization of existing control systems theories to the high-dimension systems (previously developed for small-scale systems). This was introduced under the name "centralized" control of "large-scale systems." Theoretical small- to large-scale generalizations could be done independently of the size of large-scale system. However, in practice, some limitations were imposed by the existing computational power of a central digital computer, and sensing, measurement, and communication abilities. Motivated by these practical burdens, the (theoretically) conservative "decentralized" control ideas attracted research interest. In the decentralized scenario, central powerful digital computer of the centralized approach could be replaced by some "small" computing systems receiving updates from the sensing tools at their own local subsystems. (See [2]-[3] for further details on large-scale systems.) The success in decentralized control ideas motivated researchers to think about the large-scale system as a "system of (sub-) systems" or, in other words, a group of individuals.

In parallel, researchers were continuously trying to understand the logic behind collective behavior of biological systems (for example, fish schooling and flocks of bird). Specifically, scientists believed that any collective decision among traveling animals highly depend on their inter-group communication ability which was possibly guided by a leading animal that had some global information regarding the target [4] (e.g., the food resource or geographical position of the destination). An inspiring study was reported in [5] where the authors proposed a discrete-time stochastic model to describe the behavior of some moving objects with differ-

ent initial headings, and numerically showed a simple heading-averaging rule in each moving object's neighborhood could lead all group members to move in the same direction.

Researchers within the control system society were also trying to understand these phenomena and use them in their own engineering problems. For example, knowing about two hypotheses that the lateral position tracking of the preceding bird results in aerodynamic advantages for each follower bird and improved navigation capabilities, reference [6] studied the bird V-formation with a (control) systems-theoretic viewpoint and used the result in automatic highway systems and in-flight formation controls ([7] and [8]). Another research trend was created by visualizing the communication topology using graphs, abstracting the information in some graph-related matrices, and understanding the requirements for achieving agreement among individual subsystems. Of those, we mention [9]-[10] and, particularly, reference [11] that proposed a theoretical foundation for a deterministic equivalent formulation of the numerical study in [5] and also connected that result to graph theory[1].

The outcome of these graph-theoretic ideas was astonishing. From a theoretical viewpoint, the distributed design capability allowed researchers to guarantee a global high-dimension design objective through local low-dimension sub-design problems. From a practical viewpoint, a global behavior such as heading agreement in [5] and [11] could be achieved using some cheap computing systems (com-

[1]Researchers are still following systems-theoretic viewpoints in order to explain their observations in some particular applications. For example, [12] discussed the disturbance propagation in a string of vehicles using such a viewpoint. However, this has been less attractive than graph-theoretic distributed control ideas.

pared to the centralized control schemes), and based on local information exchange within each agent's neighborhood. This could eliminate the need for availability of all agents' absolute measurements with respect to the "same" global coordinate (e.g., in decentralized rendezvous, all moving objects should be equipped with a global positioning system (GPS) while this is not required in distributed rendezvous).

These findings were in parallel to industrial improvements in computation, communication, sensing, and monitoring devices. Specifically, it was possible to integrate the sensing devices with computation and communication tools, and have an enabling technology with a reasonable physical size. As a result of these technological advances, a rapid progress was made in communication-based cooperative control of unmanned systems (e.g., see [13] and [14]) which, inherently, could be suitable applications for all distributed control objectives[2].

All of these multidisciplinary advances, in addition to the wide range of potential applications for the distributed control strategies [16] (e.g., ranging from old-style multi-machine power systems [15] to the smart grid), attracted the researchers' attention to this topic. We further mention that the group "consensus", by itself, was a known fact among researchers [17]. Control systems society was familiar with this topic through distributed decision making problems (see [18]). Problems involving agents and multiagent systems in distributed computation were also studied within the computer science society (see the discussion in [19] and [20]). Thus, all together, this newly emerging topic was named "distributed consensus in multiagent systems" (other names in the literature were very close

[2]The objectives will be discussed in Section 1.1.

to this one). Moreover, successful implementation created new avenues for further theoretical improvements and kept this research area alive and very active within the control systems society as will be discussed in the rest of this Chapter. In Section 1.1, we briefly introduce the terminology and team-based objectives that have been commonly addressed in the literature of graph-theoretic distributed multiagent control. In Section 1.2, we survey the literature of multiagent systems control from the agent modeling and applied control theory viewpoints. In Section 1.3, we discuss the contribution and structure of this dissertation. Finally, in Section 1.4, we summarize this chapter.

1.1 Team-based objectives in cooperative control of multiagent systems: an overview

In this section, we overview main control goals that have been proposed as theoretical and practical team-based objectives. Detailed mathematical information, if required, will be provided in other sections of this dissertation.

The word *multiagent system* refers to the fact that there are several (sub-) systems working as a team toward a common goal. Each system is equipped with its own measurement, sensing, computation, and communication tools. We clarify that by "sensing", we distinguish the agent's ability to measure some aspects of another system's behavior. For example, the range sensor is a sensing tool. (This is different from agent's absolute measurement about its own behavior.) Also, *cooperation* points to the fact that a team of agents are willingly sharing their information in order to accomplish a global task (in addition to meeting

their own local objectives). We have already mentioned that a main feature of the distributed control algorithms is about the possibility of cooperation without absolute measurements of agents' variables. In some references, this is specified by saying the design is based on some *relative measurements* in each neighborhood. Here, the *neighboring agents* are those that share some information with a specific agent[3].

In all cases, with simple words, the objective is agreeing on a common value among all agents. For example, in [5], the agreement was on the moving direction (of all particles). This is named *consensus* in distributed control research studies which, in fact, refers to "any" agreements among agents of a multiagent system that have been achieved as the result of sharing information in agents' neighborhoods. In this sense, we focus on appropriately developing graph-theoretic algorithms based on the relative measurements. These are known to be *consensus algorithms or protocols*.

As a matter of fact, these consensus algorithms only ensure the agreement among agents, without specifying the "agreement" value. The *average consensus* algorithms, however, refer to those revised consensus protocols that ensure agreement on the average of all agents' initial status[4]. Although this value is still unknown, these protocols provide a general sense on the agents' agreed status

[3]In a proximity graph scenario, the neighboring agents are sufficiently close to an agent and belong to its neighborhood area (open connected set), e.g., distance-wise in multi-robot systems, all agents that are inside a circle with the host robot as the center and radius $r > 0$.

[4]By the word "status", we simply point to any possible agreement variables which, for example, could be the internal states of agents in the state space domain.

(we are able to generalize this result to a weighted average consensus by pre-determining the importance of agents' information).

The *rendezvous* specifies the application of consensus algorithms for multi-robot (-vehicle) systems with position of robots as the consensus variable [21]. Since (line-to-sight) sensors have a limited range of applicability and agents are moving in space, the proximity graph plays an important role in a rendezvous of mobile agents [22]. Furthermore, *formation control* refers to the case that agents create a pre-defined geometrical shape. For these moving agents, the connectivity maintenance is a topic of interest for researchers. It aims in ensuring the two neighboring agents will remain each others' neighbors during the cooperative task completion. In *distributed flocking or swarming*, having some (man-made) moving objects and some relative measurements, the algorithm tries to automatically reproduce the observed behavior in nature, e.g., fish chooling and flocks of bird (see [23]-[26]). Here, a main point is about the agents' velocity matching. But, since it usually includes a high-number of moving agents and particularly because the inter-agent distance can be less that the length of each agent, the *collision avoidance* capability has also been considered to enhance the overall reliability of flocking algorithms. Furthermore, in the *distributed attitude alignment*, the consensus variable is pre-specified to be the attitude of agents [27].

A *distributed coverage* algorithm tries to optimize the distribution of agents in order to cover the maximum area "by all agents" based on some information exchange within "each agent's neighborhood." Here, a main concern is about the possible holes (areas not covered by agents). The wireless *sensor network* design is about the best distribution of sensing devices to sense a distributed

plant, for example, monitor a specific area [28]. Since these might be used in remote (hazardous) areas and each sensor has a limited energy resource, the energy consumption is a main constraint that has been discussed in the literature. Additionally, a sensor network may only provide a part of the required information about a plant. Thus, the *distributed estimation or (Kalman) filtering* can be used to discover the hidden behavior (or variables) of a distributed system. Those challenges have been addressed using data fusion or decentralized techniques as well as consensus-based ideas [29]. Sometimes, researchers deal with a large-scale optimization problem with a high-number of decision variables. Whenever these decision variables can be grouped into some subsets of variables, where each corresponds to an individual agent, the *distributed optimization* can be employed to find the solution of a global optimization problem using some local information exchange about the decision variables in each neighborhood. Moreover, *synchronization* has also been investigated in the study of harmonic oscillators, where the objective is achieving a synchronized oscillation frequency using some relative measurements in each neighborhood.

In some cases, there exists an agent that is not willing to change its status based on any of other agents in a multiagent system. This agent may further try to dictate its own decision (or sequence of actions) to all other agents. This can happen by sending its status to other agents via "one-way" direct communication or through some intermediate agents. In the literature, this reference agent is called a *leader*, and all other agents are named *followers*. In this scenario, the objective is designing a (leader-follower) consensus algorithm that ensures an agreement on the leader's status. The *distributed containment control* is proposed to address

leader-follower consensus problems with multiple leaders. A multiagent system is *homogeneous* when it is composed by a set of identical agents described by exactly the same dynamics. Otherwise, we call it a *heterogeneous, non-identical, or non-homogeneous* multiagent system.

Graphs are appropriate tools to model the communication or sensing capabilities in multiagent systems where each node of the graph represents an (dynamical) agent, and each edge stands for a relative measurement or information exchange between the corresponding nodes (agents). The word *connected graph* refers to the fact that the information flow can be completed over the communication graph. This is required to achieve consensus, and simply means all agents are aware of the multiagent systems' global status through receiving updates from one or more neighboring agents over an appropriately designed communication topology. Various important properties of multiagent systems can also be understood by studying the properties of matrices associated to the graph. This will be discussed in next chapters.

1.2 Distributed control of multiagent systems: a brief survey

Several tutorial and survey papers have been published to introduce this field and update researchers about specific trends in the graph-theoretic distributed control of multiagent systems (e.g., see [16] and [30]-[34]). In this section, we provide our own story by observing that the dominant research ideas may fall into the following categories:

- Modeling:
  - Agent-level: The complexity of the agent-level dynamical model can increase the difficulties in designing distributed control algorithms. In the literature, agents are described as scalar systems, low- and high-order structured models, linear time-invariant, and nonlinear dynamics. These models are described in both time- and frequency-domain and, further, the time-domain models are reported in both continuous and discrete forms. We mention that the model selection highly depends on the team-level objective and the availability of required information for cooperation.
  - Multiagent system-level: Similar to the previous case, the complexity of multiagent system-level model can also contribute in the design procedure difficulties. In the existing literature, the agents are usually loosely connected through the distributed control algorithm (we use the "loosely-"connected to describe the connectedness in distributed communication topology and, because it is by design, we can remove it at any time). However, they can also be strongly coupled to each other due to the physical interconnections in addition to the previous loose connection. In both cases, any two agents can be connected in a one-way or two-way manner which we call directed or undirected, respectively.

- Control:
  - Multiagent system-level (cooperative) objective: This is often motivated by the practical need, although it can be also inspired by some theoretical findings. We have already talked about this viewpoint in Section 1.1 (e.g., rendezvous, formation control, flocking, and coverage), and do not re-state that discussion here.
  - Applied theory: Depending on the model complexity and cooperative objective, different control algorithms have been used in the literature of distributed control. Essentially, all existing control theories can be generalized to for the distributed control purpose. However, we point out that the usage of relative-measurements imposes some new challenges compared to the centralized and decentralized control theories.

Depending on the cooperative objective in Section 1.1, there are many ways to describe the dynamic behavior of the multiagent system by a set of differential equations. The control approaches are also chosen based on the cooperative objective, complexity of the model, and the assumptions that have been made based on the available information about multiagent systems. In the rest of this section, we walk through the literature of distributed multiagent control and quickly overview it from both modeling and control aspects. Since this is a broad topic, we limit ourselves to the scope of this research.

1.2.1 Multiagent systems: modeling aspect

The research on this topic was started with a multiagent system of single-integrators:

$$\dot{x}_i = u_i \tag{1.1}$$

where $i \in \{1, 2, ..., N\}$ denotes the agent's number, and N is the total number of agents; and $x_i \in \mathbb{R}$ represents the agent's state variable, and $u_i \in \mathbb{R}$ indicates the control input. We point out two reasons that indicate the usefulness of such initial model selection. As the first point, this model describes the behavior of a moving object whenever x_i is chosen to be the i^{th} agent's $1 - dimension$ position along a line (e.g., in a rendezvous problem of Section 1.1). We can generalize this to higher-dimension spaces, e.g., for the formation control purpose. The second point is about the simplicity of the aggregated model which enables us to focus on the effect of communication between agents.

The initial work was mainly focused on analysis strategies in intuitive manners. Reference [35] proposed the concept of Laplacian potential associated to an undirected graph, cost of communication, and agreement and disagreement subspaces. This reference successfully established a connection between algebraic graph theory to the well-known concepts in (linear) control systems theory [5]. Reference [36] established an alternative approach, and proved the results by proposing a novel candidate Lyapunov function and using some special properties for the underlying communication graph. For a set of integrator agents (1.1), [37] distinguished the controllable and uncontrollable sets of communication topologies by investigating

[5] Algebraic graph theory is a study of matrices associated to each graph and their properties.

the required conditions that a graph topology should satisfy in order to have a controllable leader-follower multiagent system.

An extension to (1.1) was made in [38] that, inspired by the complex networks (e.g., Internet and metabolic networks), proposed $\dot{x}_i = f(x_i) + u_i$ where u_i should be designed with a global knowledge about all sub-dynamics (e.g., using any approaches similar to the consensus algorithms). Furthermore, [39] proposed a scalar nonlinear dynamical model $\dot{x}_i = f(u_i)$ with a deadzone nonlinearity f, and addressed its consensus problem based on LaSalle's invariance principle.

A direct generalization to (1.1) was made by proposing a multiagent system of double-integrator agents (see [40]-[42]):

$$\dot{x}_{i1} = x_{i2}, \quad \dot{x}_{i2} = u_i \tag{1.2}$$

where, from a physical viewpoint, $x_{i1} \in \mathbb{R}$ denotes the i^{th} agent's position, and $x_{i2} \in \mathbb{R}$ stands for its velocity. The consensus problem in a multiagent system of (1.2) was also addressed in [43] by a two-component controller using absolute velocity measurements of agents and, also, relative-state information. Depending on the application and the cooperative task, these models may provide suitable linear approximations of the nonlinear systems. For example, [44] showed that a robot's nonlinear dynamics can be appropriately transformed to a double-integrator model for the purpose of formation control.

Reference [45] introduced a multiagent system of second-order nonlinear agents $\dot{x}_{i1} = x_{i2}$ and $\dot{x}_{i2} = f(x_{i1}, x_{i2}, t) + u_i$ and discussed the second-order consensus $\lim_{t\to\infty} \|x_{i1} - x_{j1}\| = 0$ and $\lim_{t\to\infty} \|x_{i2} - x_{j2}\| = 0$ for $i, j \in \{1, 2, ..., N\}$ with

a nonlinear function f satisfying a Lipschitz-type inequality. The results were based on the graph- and matrix-related definitions and some derivations based on the multiagent system's dynamics. For some locally Lipschitz nonlinearity in velocity state equation $\dot{x}_{i2} = f(x_{i1}, x_{i2}, t) + u_i + w_i$, [46] proposed a linear matrix inequality-based robust H_∞ control technique for the containment control in a (multiple leader-based) second-order multiagent system with a scalar unknown nonlinearity and under a bounded disturbance term. This reference guaranteed a level of H_∞ performance in asymptotic convergence of followers' state variables to a convex hull spanned by all leaders.

Also, with a globally Lipschitz nonlinearity and using LaSalle's invariance principle, [47] addressed the leader-follower consensus in a multiagent system with followers $\dot{x}_{i1} = x_{i2}$ and $\dot{x}_{i2} = f(t, x_{i2}) + u_i$, and a reference $\dot{x}_{01} = x_{02}$ and $\dot{x}_{02} = f(t, x_{02})$. For the same model, [48] discussed a semi-global consensus problem where, proposing a special control structure, the semi-global consensus was only guaranteeing $\lim_{t\to\infty} \|x_{i2} - x_{02}\| = 0$ compared to a second-order consensus problem in [45] (there are some additional conditions that we do not go through for brevity). This reference proposed a special symmetric candidate Lyapunov function and established its results.

The presence of (time-dependent) disturbance may prevent achieving consensus in a multiagent system. In reference [49], a leader-follower consensus (cooperative tracking) problem was discussed for a set of heterogeneous second-order nonlinear multiagent system under a bounded disturbance. In this reference the agents' dynamics were modeled by $\dot{x}_{i1} = x_{i2}$ and $\dot{x}_{i2} = f_i(x_{i1}, x_{i2}) + u_i + w_i$ where w_i was an external disturbance, and f_i were continuously differentiable. The

approach was using a variable-structure controller that was a function of both lumped relative-state measurements $\sum_{j\in\mathcal{N}_i}(x_{i1}-x_{j1})$ in each neighborhood $\mathcal{N}_i$ of the i^{th} agent and their sign functions $sgn(\sum_{j\in\mathcal{N}_i}(x_{i1}-x_{j1}))$.

Using partial-state measurements (without any velocity measurements), this reference also discussed a distributed observer design problem. In reference [50], an adaptive leader-follower consensus problem was addressed assuming a leader $\dot{x}_{01}=x_{02}$ and $\dot{x}_{02}=f_0(x_{01},t)$. In this reference, the nonlinearities were unknown but smooth, such that the neural network ideas could be used to approximate $f_i(x_i)=W_i^T\phi_i(x_i)+\epsilon_i$ with ϕ_i denoting basis function vectors, W_i vectors of constant coefficients, and ϵ_i approximation errors.

There are some other types of integrator-based multiagent systems, for example, [51] proposed a heterogeneous multiagent system including both single- and double-integrator agents. However, an immediate extension to (1.2) was made in [52] as a high-order integrator model of agent:

$$\dot{x}_{i1}=x_{i2},\quad \dot{x}_{i2}=x_{i3},\quad ...,\quad \dot{x}_{i(n_x-1)}=x_{in_x},\quad \dot{x}_{in_x}=u_i \tag{1.3}$$

which can be interpreted as a vehicle's model taking all position, speed, acceleration, and higher-order jerks (limited by the model's dimension) into consideration in the state space model. This model can be viewed as a structured linear time-invariant (LTI) model:

$$\dot{x}_i=Ax_i+Bu_i \tag{1.4}$$

where the state matrix $A \in \mathbb{R}^{n_x \times n_x}$ and control input gain matrix $B \in \mathbb{R}^{n_x \times n_u}$ have the following control canonical structures:

$$A = \begin{bmatrix} 0 & 1 & 0 & \dots & 0 \\ 0 & 0 & 1 & \dots & 0 \\ \vdots & \vdots & \vdots & \ddots & \vdots \\ 0 & 0 & 0 & \dots & 1 \\ a_{n_x 1} & a_{n_x 2} & a_{n_x 3} & ... & a_{n_x n_x} \end{bmatrix} \quad and \quad B = \begin{bmatrix} 0 \\ 0 \\ \vdots \\ 0 \\ 1 \end{bmatrix}$$

with all $a_{n_x j} = 0$ for $j \in \{1, 2, ..., n_x\}$. Reference [53] further added a disturbance term to the highest order integrator equation $\dot{x}_{in_x} = u_i + w_i$ and proposed an H_∞ (high-order) consensus algorithm. Moreover, [54] proposed the dynamic nonlinear agents $\dot{x}_{il} = x_{i(l+1)} + f_{il}(y_i, d_i)$, $x_{k(n_i+1)} = u_i$, and $y_i = x_{i1}$ where only x_{i1} was measurable and $l \in \{1, ..., n_i\}$. Additionally, reference [55] discussed a leader-follower output feedback-based consensus problem for a group of *N+1* identical single-input single-output agents:

$$\begin{aligned} \dot{x}_{i,1} &= x_{i,2} + f_1(x_{i,1}), \quad \dot{x}_{i,2} = x_{i,3} + f_2(x_{i,1}, x_{i,2}), \ ..., \dot{x}_{i,n} = u_i + f_n(x_{i,1}, ..., x_{i,n}) \\ y_i &= x_{i,1} \end{aligned}$$

where subscript 0 denotes the leader and $i \in \{1, 2, ..., N\}$ denote followers. In this reference, the functions f_i are sufficiently smooth and satisfy the Lipschitz inequality with a fixed Lipschitz constant. Reference [56] used a similar multiagent system, but f_i were satisfying a time-varying Lipschitz-type inequality.

A more general version of (1.4) with $a_{n_x j} \neq 0$ has also been discussed in the literature [57]. A multiagent system of (unstructured) LTI agents has also been discussed in the literature. Reference [58] showed that consensus problem can be solved through a set of N local stability problem depending on the eigenvalues of underlying communication graph Laplacian and dynamics of agents, and addressed its formation control problem via Nyquist-based criteria. For such a multiagent systems, [59] proposed a dynamic output feedback strategy to achieve synchronization. Moreover, [60] found a necessary and sufficient condition to achieve consensus using output feedback measurements in an LTI multiagent system. Also, [61] used a reduced-order observer-based algorithm in order to achieve consensus in a multiagent system of LTI agents using relative-output measurements (we point out that, for example, references [43] and [58] are proposing some output feedback approaches as well).

Although a closed-form solution for a nonlinear multiagent system (with an arbitrary state space dimension) is still unknown to the researchers in this field, some efforts have been made in the literature to address the consensus problem for some special classes of nonlinear multiagent systems. Particularly, the state equation (1.5) has been proposed in order to model a class of nonlinear multiagent systems compose by Lur'e dynamical agents:

$$\dot{x}_i = Ax_i + Bu_i + Df_i(x_i) \tag{1.5}$$

where $f_i : \mathbb{R}^{n_x} \to \mathbb{R}^{n_x}$ are some nonlinear functions. Reference [62] discusses an average consensus problem for a multiagent system of (1.5) assuming a globally

Lipschitz nonlinear function f. Furthermore, both (unconstrained) LTI and Lur'e models of a multiagent system were discussed in [63] (using adaptive consensus algorithm). Reference [64] investigated its adaptive leader-follower tracking idea using a leader $\dot{x}_0 = Ax_0 + Br$, and N followers $\dot{x}_i = Ax_i + B(f(x_i) + u_i)$ and $y = Cx_i$ where r is an unknown input with a constant bound and f is an unknown nonlinearity that can be parametrized as $f_i(x_i) = W_i^T \phi(x_i) + \epsilon_i$. Here, W_i denotes the weight matrix (unknown and constant), ϕ indicates a known basis vector, and ϵ represents an approximation error. With a known (homogeneous) nonlinear function $f(x_i, t)$, [65] proposed an observer-based consensus protocol using relative-output measurements (f was used in the observer dynamics).

A single-input single output agent model was introduced in [66] in order to consider a nonlinear multiagent system:

$$\begin{aligned} \dot{x}_i &= f_i(x_i) + g_i(x_i)u_i, \quad y_i = h_i(x_i) + d_i u_i \quad Followers \\ \dot{x}_0 &= f_0(x_0), \quad y_0 = h_0(x_0) \quad Leader \end{aligned}$$

in order to design a feedback linearization-based synchronization approach when $u_i \in \mathbb{R}$, $y_i \in \mathbb{R}$. In this reference, the absolute state variables $x_i \in \mathbb{R}^{n_i}$ were measurable for $i \in \{1, 2, ..., N\}$. Reference [19] introduced Kuramoto coupled oscillators as another nonlinear model to the literature of multiagent control:

$$\dot{\theta}_i = \kappa \sum_{\mathcal{N}_i} sin(\theta_i - \theta_j) + w_i$$

where θ_i denotes the phase and w_i indicates the frequency of the i^{th} oscillator. We may use $\kappa = \frac{K}{N}$ for the normalization purpose in a multiagent system of N oscillators (see [67]).

The nonholonomic mobile robots can be described as follows:

$$\dot{x}_{i1} = u_{i1}cos(\theta_i), \quad \dot{x}_{i2} = u_{i1}sin(\theta_i), \quad \dot{\theta}_i = u_{i2}$$

where the pair (x_{i1}, x_{i2}) specifies the location of the robot that, together with the angle θ_i, builds a state variable vector. Also, the pair (u_{i1}, u_{i2}) denotes the control inputs (the translational and rotational velocity of the robot, respectively). Rigid bodies have also been studied in the literature:

$$M_i(q_i)\ddot{q} + C_i(q_i, \dot{q}_i)\dot{q}_i + g_i(q_i) = \tau_i$$

in which $q_i \in \mathbb{R}^n$ represents a vector of generalized coordinates, and M_i, C_i, and g_i are appropriately defined. We do not go through these very special nonlinear model structures. Instead, in the rest of this subsection, we provide a quick overview of the multiagent systems with modeling uncertainties, and provide a short note about a few existing references that have considered consensus problems for physically interconnected multiagent systems.

There are some studies that have addressed the effect of agent-level uncertainties on the graph-theoretic distributed approaches. References [68] and [69] proposed the following state space model:

$$\dot{x}_i(t) = (A + \Delta A_i(t))x_i(t) + Bu_i(t)$$

which could be interpreted as a homogeneous LTI multiagent system in the presence of heterogeneous modeling uncertainties in agents' system state matrices, where $\Delta A_i(t) = DF_i(t)E$ and $F_i^T F_i \leq \delta I$ were satisfied for known matrices D and E, and a positive scalar δ.

Reference [70] addressed a similar issue for multiagent systems with $\Delta A_i(t) = BE_i(t)$ and $E_i^T E_i \leq \delta I$, and [71] discussed the case that $\Delta A_i^T \Delta A_i \leq \delta I$. Also, [72] proposed a consensus algorithm for high-order integrator agents subject to a set of scalar nonlinearities. Reference [63] developed consensus algorithms for linear multiagent systems subject to the Lipschitz nonlinearity, and [73] discussed the consensus of multiagent systems under the state- and control input-dependent norm bounded unknown matched nonlinearities. Nevertheless, in these studies, each agent's modeling uncertainty was a function of its own variables.

Reference [74] proposed the concept of coupled multiagent systems by introducing the state-dependent graphs where the dependency was a result of relative-state information exchange in the distributed consensus algorithm. We mention that this coupling is still by communication, and the same as [75] that will be discussed in the next subsection. The coupled-state, -input, and -output multiagent systems has also been discussed in [76]. In this reference, the coupling could be part of the system's dynamics. Additionally, for a state-coupled multiagent system $\dot{x}_i = Ax_i + Bu_i + F\sum_{\mathcal{N}_i}(x_i - x_j)$, [77] proposed a distributed control protocol in order to minimize the effect of disturbance on the agreement value. Here, the state coupling structure could be different from the communication topology. However, these studies were limited to the completely known and linearly coupled multiagent systems. In a different research, based on a linear

matrix inequality (LMI) formulation, [78] introduced an algorithm to address a leader-follower tracking problem in a multiagent system of linearly coupled linear time-invariant agents. Here, the unmatched coupling strength was uncertain and the communication graph was different from the coupling topology. Also, the size of LMIs could increase depending on the number of agents. This reference modified its protocol and developed a gain-scheduled consensus algorithm depending on a measurable variable θ in order to handle the effect of a parameter-dependent state matrix $A(\theta)$ which was a function of the same θ for all agents (note that the other state space matrices were constant values).

In the next section, we continue the literature survey by reviewing the literature from a control-theoretic viewpoint.

1.2.2 Multiagent systems: control aspect

Many control theories have already been applied in order to guarantee the consensus in multiagent systems. In this subsection, within the scope of this dissertation, we only focus on LQ-based approaches. We also provide a short note on a recent application of adaptive control ideas in this field.

Due to its systematic structure, linear quadratic regulator-based control ideas have received attention in the literature of multiagent systems. For a set of dynamically decoupled systems, [79] proposed a global quadratic cost function for a set of individual agents, found a centralized optimal controller, and showed that a sub-optimal stabilizing system could be found by some local tuning parameters in the agent level sub-design problems. In our opinion, this reference could be viewed as a leading research study on LQ-based distributed control systems (compare the

derivations in [79] to [80], and see the usefulness of Kronecker product). Using the name of multiple systems, reference [81] used LQ-based strategy to guarantee an approximately optimal closed-loop system response. In more detail, with a central control viewpoint, [81] found the optimal closed-loop response under an all-to-all communication topology (which corresponds to a complete undirected graph). Then, for an incomplete communication topology, a set of distributed LQ-based control systems was designed such that the response could converge to that of an all-to-all design. Reference [82] mainly focused on using LQ-based ideas to handle a consensus stability problem in a multiagent system. It showed that the consensus can be achieved using local LQ-based designs. Within this viewpoint, [83] addressed an output feedback leader-follower consensus problem based on an agent-level LQR-based Luenberger observer formulation. In this reference, the focus was on developing a solution for the proposed consensus problem and the global optimality of the multiagent system was not discussed.

Based on a similar problem to [79], references [84] and [85] addressed the global optimality problem via their inverse optimal designs[6]. Reference [86] proposed interaction-free and interaction-based cost functions in its linear quadratic regulator formulations for the consensus purpose, where the interaction-related cost function dependent on the graph Laplacian. This reference was limited to a set of single-integrators. Thus, [87] proposed a mixed local (using absolute

[6]In the literature of optimal control, optimality is defined with respect to the given cost function. Therefore, different solutions can be found for different optimal control problems where each of them is optimal with respect to the corresponding cost function. However, in the literature of multiagent systems, the definition is a little bit different. Here, the global optimality refers to a solution of an optimal control problem with a coupled cost function, and sub-optimality of a solution sometimes refers to the solution of an optimal control problem with respect to a decoupled cost function.

state measurements) and multiagent system-level (using relative state information) control system, and guaranteed that a certain level of optimality could be established using an interaction-related cost function subject to an LTI multiagent system. For single- and double-integrator agents, [88] further borrowed the concept of LQR control to find the optimal communication graph topology and weights. In [89], this has been re-investigated for a multiagent system of single- and double-integrators. Reference [90] used an LQR formulation in its leader-follower consensus problem and showed that the global optimality can be achieved for a special choice of weighting matrices in the cost function, and if the absolute measurements are available.

In the literature, the consensus convergence rate has also received attention as an optimality criterion. For a group of single-integrator agents, this is determined by the algebraic connectivity of communication graph (the smallest non-zero eigenvalue of graph Laplacian). Over a fixed communication graph, this can be changed by adjusting the weight of communication graph. Reference [75] proposed an optimization problem to appropriately weigh the communication topology (graph adjacency or Laplacian matrix) in a multiagent system with state-dependent communication topology (also see [91]). In [92], the weights of a communication graph were designed using a semi-definite convex programming approach in order to maximize the consensus convergence speed by changing the second smallest eigenvalue of the corresponding weighted graph. Moreover, the convergence speed has been investigated in [57] for a group of LTI agents (with a control canonical state space representation).

In [58], an analysis approach was proposed to investigate the stability of a formation system. Based on this result, one needs to separately verify the stability of some dynamical systems (with the same dimension as each agent) for all non-zero eigenvalues of the graph Laplacian. In order to overcome this issue, some researchers proposed a two-step design procedure. In [93], the relative measurement was "corrected" by a *coupling strength* $c > 0$, and passed to the distributed consensus protocol. By design, this coupling gain was greater than a threshold value, but bounded within an area named "consensus region" (if we choose a c within this region, then the consensus is guaranteed). Thus, the authors introduced this region as a measure of robustness for their approach (a larger region indicates a less sensitive consensus algorithm). In reference [83], a consensus protocol was introduced where the consensus gain was modified by such a coupling strength $c > 0$ (using the non-modified relative measurements). This reference showed that an unbounded, yet limited from left, consensus region could be obtained using local LQR designs. Thus, the robustness (as defined in [93]) was significantly high. However, in both cases, the threshold on coupling strength c dependent on the smallest non-zero eigenvalue of graph Laplacian matrix. In other words, this global knowledge about the communication graph was required to ensure agreement using these design approaches. This fact may restrict the applicability of a distributed algorithm for a multiagent system including a high-number of agents. Thus, some references proposed adaptive control ideas in order to design *fully distributed* consensus algorithms[7] (e.g., see [73] and [94]-

[7]We just clarify that the name "distributed control" was proposed based on the simplification in implementation (versus the centralized approach, and since the decentralized was already used by the literature of large-scale systems)(see the discussion at the beginning of this chapter).

[95]). These approaches enable us to design some consensus algorithms purely based on some local agent-level information, at the expense of added complexity in implementation compared to the LQR-based ideas that have been discussed in this subsection.

There are several other approaches that have been studied in the literature of multiagent control. For example, model predictive control [96], back-stepping control [97], and sliding mode control [98]. For brevity, we stop surveying the literature at this point. However, when required, further references are introduced in next chapters.

1.3 Contribution and structure of this dissertation

The quick literature survey of this chapter shows that the distributed control of multiagent system can be viewed as a multidisciplinary topic. In particular, we introduce our research as a synergistic combination of three topics: systems and control, graph theory, and optimization (see Figure 1.1). Based on such a viewpoint, in this dissertation, we design a single control-theoretic tool that can be used to address various problems in the control of multiagent systems. These challenges might be due to the control objectives, e.g., consensus, decoupling, stability, tracking, and performance requirements; due to the type of modeling mismatch such as unknown disturbances, agent-level modeling uncertainties, and

However, the "fully distributed" points to a new level of localization in the design procedure (in addition to the implementation).

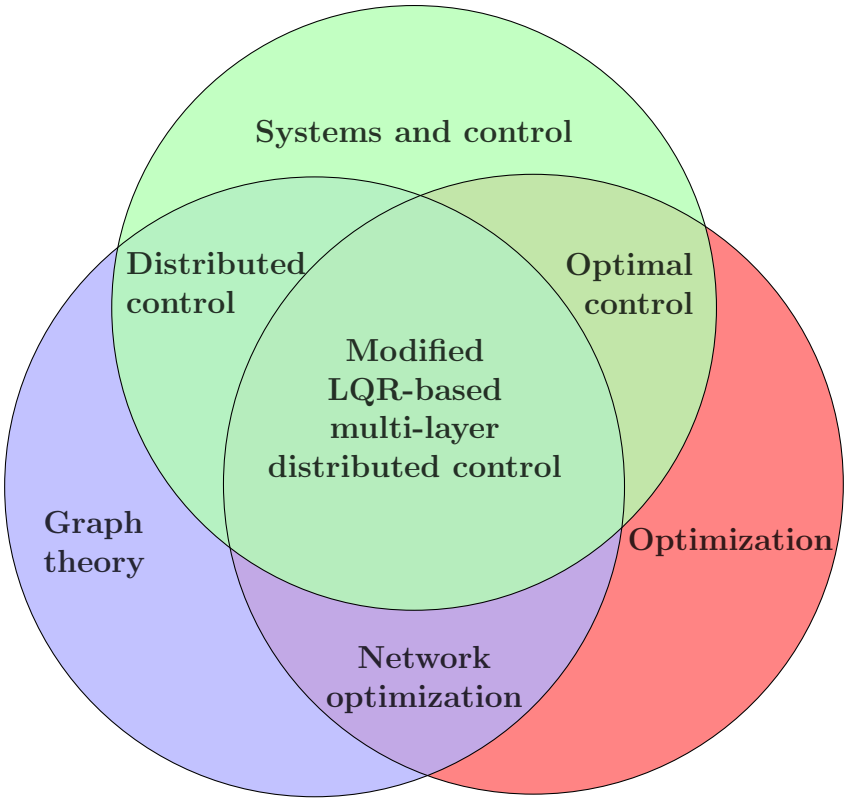

Figure 1.1: Modified LQR-based multi-layer distributed control of physically interconnected multiagent systems as a synergistic combination of three (well-studied) research topics: systems and control, graph theory, and optimization. We skip showing the combination of systems and graph theory ends in interconnected multiagent systems (the distributed control is the result of combining graph theory and control).

linear and nonlinear physical interconnections; or due to the configuration, for example, single- or multi-layer control ideas. These are categorized as follows:

1. Systems and control: The "systems" includes all possible models that have been discussed in Section 1.2. We consider two fairly general classes of multiagent systems' models that have been studied in the literature of multiagent control (see Section 1.2):

(a) Linear models: We model the dynamic behavior of agents by *1)* linear time-invariant state space realization subject to unknown disturbances, and *2)* linear parameter-varying state space realization where the varying parameters denote the operating points of agents, and are unknown. The unknown varying parameters result uncertainty about the system matrices as well as coupling gains.

(b) Nonlinear models: We focus on Lur'e nonlinear multiagent systems which, up to this moment, are among the most complicated state space realizations of multiagent systems. In fact, we introduce the physical couplings through these nonlinear terms, and add the complexity by assuming unknown nonlinearities and unknown interconnected topologies.

In summary, we consider some levels of modeling uncertainties which add the complexity in control of multiagent systems. We discuss our control-theoretic viewpoint under the optimization subject.

2. Graph theory: Similar to the literature, we use graph theory in order to model the communication topology and design a distributed algorithm that is based on some relative measurements. We follow the same idea and model the physical interconnection using the graph notation.

3. Optimization: Based on the relative measurements in agents' local neighborhoods, we use our modified optimization-based formulation in four different ways. The first three items refer to the control objective, and the last one

mainly relies on the first three items to address the network optimization challenge in Figure 1.1:

(a) Robust stability: We propose a modified LQR formulation which, along with some fundamental concepts of the optimal control theory, enables us to systematically design the required distributed control protocols for all of the aforementioned models of multiagent systems in the presence of various sources of modeling mismatches. Unlike the literature, we propose a one-step design approach to find the distributed control gains (see the discussion about coupling strength at page 24). Borrowing some tools from matrix algebra, it further enables us to propose closed-form solutions for the control-layer (including the communication topology) in multiagent systems.

(b) Robust performance (guaranteed convergence rate): In one of our designs, we reformulate the modified LQR formulation and ensure a minimum convergence rate in multiagent systems with unknown physical coupling terms. This is one of the main performance criteria that have been used in the literature of distributed control, yet without any modeling uncertainties. (As will be seen, this formulation enables us to easily guarantee the same behavior in all other designs.)

(c) Robust performance (guaranteed bound on linear quadratic regulatory integral functions): In addition to the robust convergence of all trajectories to the desired point of interest[8] and guaranteed convergence rate

[8]In consensus, this is the agreement value. In stability, this point refers to the origin as equilibrium point. In tracking, the reference signal is the common point for all agents.

for all agents, we prove that the proposed modified LQR formulation results in guaranteed bound on the given linear quadratic cost function.

(d) Multi-layer distributed control framework: Based on a cyber-physical framework, we propose multi-layer configurations to handle the effect of unknown physical coupling terms. We first propose some fixed-gain fully distributed algorithms where the proofs of stability do not require any global knowledge about coupling and communication or physical coupling graphs. This modification enables us to independently change the communication network at each run of the multiagent system without being worried about the re-design or re-implementation of distributed controllers. In addition to robustness with respect to modeling uncertainties in the agent-layer physical couplings' dynamics, we use this "control-layer" communication capability to guarantee an upper-bound on the performance of closed-loop multiagent system and reduce the implementation cost (i.e., the number of communication links can be significantly less than the physical couplings in interconnected multiagent systems). This is done by reformulating cooperative reference tracking problem to a communication graph topology challenge, and systematically addressing it via the proposed modified LQR viewpoint.

The next chapters are organized as follows:

- Chapter 2: We review some topics in matrix analysis, graph theory, control systems, and optimal control theory (proofs can be found in the cited

references). This quick overview is sufficient to support all developments in next chapters.

- Chapter 3: We emphasize that in multiagent systems (with more complicated dynamics than single-integrators), the distributed control designs are affected by both "agent dynamics" and "information exchange topology." We consider two sources of uncertainties in the linear multiagent systems: *1)* unknown persistent disturbance, and *2)* unknown varying operating point. In the former case, the disturbances can have constant (step-like), ramp, and sinusoidal shapes; and we address both leaderless and leader-follower consensus problems. In the latter case, we show that the varying operating point results in uncertainties in all of the state space realization matrices. We find the required consensus protocols, and further prove that some additional requirements should be satisfied to achieve exponential agreement on zero (i.e., after ensuring the consensus in a multiagent system with modeling uncertainty).

- Chapter 4: We consider a multi-agent system of double-integrator agents which is appropriate for motion coordination of multi-vehicle and multi-robot systems that should operate in unknown environments subject to (the road profile or wind). These disturbances persistently excite vehicles' dynamics and prevent agreement among vehicles or robots. For this application, although ensuring agreement, the distributed disturbance rejection leaderless consensus algorithm of Chapter 3 results in an uncontrolled increase in all vehicles' (coordinated) speed. We propose a dynamic output

feedback leaderless stationary algorithm based on the relative information exchanges among vehicles and only a few vehicles' absolute measurements. We systematically design this distributed algorithm by transforming the problem into a static feedback robust control design challenge for low-order modified model of vehicles with fictitious modeling uncertainties. We further propose dynamic leader-follower stationary consensus algorithms for multi-vehicle systems with a static leader, and analytically find the consensus gains based on the design matrices and communication graph topology.

- Chapter 5: Inspired by our observation in ensuring exponential agreement on zero, which is equivalent to the global stabilization at the origin (equilibrium point), we propose the distributed stabilization problem. We discuss that this new distributed stabilization problem can be an interesting topic based on the literature of large-scale systems. We introduce physically coupled modeling uncertainties in parameter-dependent linear and Lur'e nonlinear realizations of heterogeneous multiagent systems. In both cases, we prove that the fixed-gain modified LQR-based distributed control gains can efficiently address the distributed stabilization problem.

- Chapter 6: We propose two classes of multiagent systems: Lur'e nonlinear multiagent systems with heterogeneous nonlinear state coupling terms, and LTI multiagent systems with two different state and control input coupling terms. We assume that the coupling topologies are unknown. Thus, we introduce multi-layer control structures to handle the distributed stabilization problem. In this chapter, we further propose fixed-gain fully distributed

algorithms which are designed and implemented independent of any global knowledge about communication and coupling graph topologies.

- Chapter 7: The result of previous chapters are based on multiagent systems with heterogeneous agents'dynamics. However, we only have considered the stability problem, the order of model is the same for all of agents, the agent-layer dynamics are manipulable (i.e., we can implement local controllers at agent-level subsystems), we left the usage of this additional design degree of freedom (provided by that multi-layer structure) to the future, and the robust performance based on the linear quadratic regulatory cost function criterion is not discussed in those results. In this chapter, we consider the reference tracking problem in mixed-order heterogeneous multiagent systems with partially-known interconnected nonlinear agent-layer dynamics where, unlike the traditional centralized and decentralized control schemes, only a few agents have access to the reference command. We build a multi-layer framework and, by treating each inter-agent communication link as a proportional controller, propose linear distributed protocols and transform the robust cooperative tracking problems to equivalent control-layer communication topology design challenges. Based on this class of multi-layer interconnected multiagent systems, we systematically incorporate control-theoretic concepts and matrix-algebraic tools in order to find analytical solutions for the structurally non-symmetric control-layers that ensure robust stability and performance of the closed-loop systems. We further provide sufficient conditions to establish upper-bounds on the uncertainties in physical agent-layers' dynamics that can be tolerated by the given control-layer commu-

nication topologies. Also, we propose a performance-oriented control-layer design approach based on the given upper-bound on the linear quadratic regulatory integral functions.

- Chapter 8: We briefly overview this dissertation and propose some future work ideas.

1.4 Summary

We start this chapter with a note on the emergence of graph-theoretic distributed control in multiagent systems. Without mathematically formulating the problem, we introduce the multiagent system-level objectives that have been proposed in the literature. We provide a discussion on the evolution of multiagent systems' models and, limiting the literature to the scope of this dissertation, we briefly explain some theoretical trends on LQ-based approaches and fully distributed algorithms in the literature of multiagent control. We finally write about the contribution and structure of this dissertation.

Chapter 2

Preliminaries

"I was lucky. The one thing I did is to pull some things together that were in the air to make dissipativity a concept of its own."

In control, almost from the beginning until the day after tomorrow (2007)

Jan C. Willems — Control systems theoretician (1939-2013)

Along the concepts that have been discussed in Chapter 1, we need some tools in order to attack on the challenges in distributed control of multiagent systems. In particular, the developments of this research are based on matrix analysis, algebraic graph theory, control systems theory, and optimal control theory. These topics are briefly reviewed in this chapter.

This chapter is organized as follows: in Section 2.1, we overview the required concepts in vector and matrix analyses; in Section 2.2, we provide some basic definitions and properties related to the graph theory; in Section 2.3, we present the main concepts in stability analysis of dynamical systems; and, in Section 2.4, we explain some fundamental properties of linear quadratic regulator-based control

systems. Finally, in Section 2.5, we introduce some references that have been used in this chapter.

2.1 Matrix analysis

Analysis of any multivariable (control) systems significantly depends on the properties of matrices and vectors. In this section, we briefly introduce some main tools of linear algebra that are required to analyze control systems.

We first introduce the notation. The symbol $\mathbb{R}$ denotes euclidean space, $\mathbb{C}$ represents the set of complex numbers, and $\mathbb{R}^{n\times m}$ indicates the set of real-valued matrices. The symbol $\mathbf{1}$ stands for a matrix of all ones with appropriate dimension (including non-square matrices), $\mathbf{0}$ stands for a matrix of all zeros, $\mathbf{1}_N$ represents an $N \times 1$ vector of all ones, and I_n denotes an $n \times n$ identity matrix.

The symbol $|a|$ represents the absolute value of a scalar $a \in \mathbb{R}$ or the magnitude of a scalar $a \in \mathbb{C}$. The superscript ^{T} in y^T denotes the transpose of a vector y, and * in y^* represents the conjugate transpose of y. Furthermore, $x = col\{x_i\}\ \forall i \in= \{1, 2, ..., N\}$ denotes $x = [x_1^T, x_2^T, ..., x_N^T]^T$, and $diag\{A_i\}\ \forall i \in \{1, 2, ..., N\}$ represents a diagonal matrix with $A_1, A_2, ...,$ and A_N as its diagonal terms where A_i can be some scalars and matrices.

A square matrix $A \in \mathbb{R}^{n\times n}$ can be characterized by its eigenvalues and eigenvectors. *Eigenvalues* of A, denoted by $\lambda_i \in \mathbb{C}$ for $i \in \{1, 2, ..., n\}$, are the roots of its characteristic polynomial $p(\lambda_i) = det(\lambda_i I_n - A)$, and the non-zero vectors $x_i \in \mathbb{C}^n$ give right eigenvectors of A corresponding to λ_i whenever $Ax_i = \lambda_i x_i$. Also, $y_i \in \mathbb{C}^n$ denote left eigenvectors of A if $y_i^* A = \lambda_i y_i^*$.

For any symmetric matrices $A = [a_{ij}] \in \mathbb{R}^{n\times n}$, where $a_{ij} = a_{ji}$ and $i, j \in \{1, 2, ..., n\}$, $\lambda_i \in \mathbb{R}$ and we sort them as follows:

$$\lambda_{min}(A) = \lambda_1(A) \leq \lambda_2(A) \leq ... \leq \lambda_n(A) = \lambda_{max}(A) \tag{2.1}$$

A symmetric matrix A is positive definite if $x^T Ax > 0$, and positive semi-definite whenever $x^T Ax \geq 0$ for all $x \in \mathbb{R}^n$. These can be examined by $\lambda_{min}(A) > 0$ and $\lambda_{min}(A) \geq 0$, respectively, and are shown by $A \succ \mathbf{0}$ and $A \succcurlyeq \mathbf{0}$. We mention that a positive definite matrix can be written as $A = A^{\frac{1}{2}T} A^{\frac{1}{2}}$ with a square and invertible matrix $A^{\frac{1}{2}}$. Also, $A \succ B$ indicates that $A - B$ is a positive definite matrix. Similarly, $A \succcurlyeq B$ represents a positive semi-definite matrix $A - B$.

For symmetric matrix A, we can use (2.1) to establish some bounds on a quadratic term $x^T Ax$:

Fact 2.1.1. ***(Rayleigh-Ritz inequality)*** *The following inequality is satisfied for all symmetric matrices $A \in \mathbb{R}^{n\times n}$ and vectors $x \in \mathbb{R}^n$:*

$$\lambda_{min}(A)x^T x \leq x^T Ax \leq \lambda_{max}(A)x^T x$$

We use the *vector-norm* operator $\|.\|$ as a real-valued scalar metric for a vector space $\mathbb{V}$ over $\mathbb{R}$. A vector-norm satisfies: *a)* $\|x\| \geq 0$ for any $x \in \mathbb{R}^n$, and $\|x\| = 0$ if and only if $x = \mathbf{0}$, *b)* $\|ax\| = |a|\|x\|$ for all scalar $a \in \mathbb{C}$, and *c)* $\|x+y\| \leq \|x\|+\|y\|$ for any $x, y \in \mathbb{R}^n$. Particularly, the $p-norm$ of a vector $x = col\{x_i\}$ is defined as:

$$\|x\|_p = (\sum_{i=1}^{n} |x_i|^p)^{1/p}, \qquad \forall p \in [1, \infty) \tag{2.2}$$

We can further define the following special norms:

$$\|x\|_1 = \sum_{i=1}^{n} |x_i|, \quad \|x\|_2 = (\sum_{i=1}^{n} |x_i|^2)^{1/2}, \quad \|x\|_\infty = \max_{i \in \{1,\dots,n\}} |x_i|$$

Similarly, for a matrix $A \in \mathbb{R}^{n \times m}$, we define the *matrix-norm*:

$$\|A\|_p = \sup_{x \neq \mathbf{0}} \frac{\|Ax\|_p}{\|x\|_p} \tag{2.3}$$

which is also known as an *induced norm* that is induced by the vector norm (2.2).

The *induced 2-norm* is defined by:

$$\|A\|_2 = \sqrt{|\lambda_{max}(A^T A)|} \tag{2.4}$$

where $\lambda_{max}(A^T A) \in \mathbb{R}$ denotes the maximum eigenvalue of the (symmetric) matrix $A^T A$. The *Kronecker product* $A \otimes B \in \mathbb{R}^{(n_a n_b) \times (m_a m_b)}$ of two matrices $A = [a_{ij}] \in \mathbb{R}^{n_a \times m_a}$ and $B \in \mathbb{R}^{n_b \times m_b}$ is defined as follows:

$$A \otimes B = \begin{bmatrix} a_{11} & a_{12} & \dots & a_{1n_a} \\ a_{21} & a_{22} & \dots & a_{2n_a} \\ \vdots & \vdots & \ddots & \vdots \\ a_{m_a 1} & a_{m_a 2} & \dots & a_{m_a n_a} \end{bmatrix} \otimes B = \begin{bmatrix} a_{11}B & a_{12}B & \dots & a_{1n_a}B \\ a_{21}B & a_{22}B & \dots & a_{2n_a}B \\ \vdots & \vdots & \ddots & \vdots \\ a_{m_a 1}B & a_{m_a 2}B & \dots & a_{m_a n_a}B \end{bmatrix} \tag{2.5}$$

and satisfies the following properties:

- *Basics*:

$$A \otimes (B \otimes C) = (A \otimes B) \otimes C, \qquad (A \otimes B)(C \otimes D) = AC \otimes BD$$
$$(A + B) \otimes (C + D) = A \otimes C + A \otimes D + B \otimes C + B \otimes D$$
$$(A \otimes B)^T = A^T \otimes B^T,\ (A \otimes B)^{-1} = A^{-1} \otimes B^{-1},\ \|A \otimes B\| = \|A\|\|B\|$$

- *Eigenvalues and eigenvectors*: Let (λ_i^A, x_i^A) be the i^{th} eigen-structure (eigen-spectrum or eigenvalue-eigenvector pair) of $A \in \mathbb{R}^{n_a \times n_a}$ for $i \in \{1, 2, ..., n_a\}$, and (λ_j^B, x_j^B) be the j^{th} eigen-structure of $B \in \mathbb{R}^{n_b \times n_b}$ for $j \in \{1, 2, ..., n_b\}$. Then, $(\lambda_i^A \lambda_j^B, x_i^A \otimes x_j^B)$ give all eigenvalue-eigenvector pairs of $A \otimes B$.

- Whenever A and B are symmetric matrices, $A \otimes B$ is a symmetric matrix; A and B are positive (semi-) definite, $A \otimes B$ is positive (semi-) definite; and A and B are nonsingular, $A \otimes B$ is nonsingular.

At the end of this subsection, we provide the statement of Gershgorin disk theorem which can be used to find some bounded regions for the eigenvalues of the given matrix.

Theorem 2.1.1. ***(Gershgorin disk theorem)*** *Let $A = [a_{ij}] \in \mathbb{C}^{n \times n}$ be a matrix where $i, j \in \{1, 2, ..., n\}$. Then, eigenvalues of A are located inside or on n circles $C(a_{ii}, r_i)$ with centers a_{ii} and radius lengths $r_i = \sum_{j \neq i} |a_{ij}|$ which are known as Gershgorin discs.*

For a matrix $A \in \mathbb{R}^{m \times n}$, the *range space* is defined by the set of all linear combinations of the columns in matrix A, which is written as $R(A) = \{Ax | x \in \mathbb{R}^n\}$. The *null space* or *kernel* of A is simply $N(A) = \{x \in \mathbb{R}^n | Ax = \mathbf{0}\}$. It can

be seen that $R(A) = \mathbb{R}^m$ if and only if A has full row rank, and $N(A) = \{0\}$ if and only if A has full column rank.

We mention that a row permutation matrix $\mathcal{P} \in \mathbb{R}^{n\times n}$ is an I_n with switched rows. Multiplying a matrix $A \in \mathbb{R}^{n\times n}$ to $\mathcal{P}$, from left, results in a new matrix A_s with a similar row switching.

Finally, we note that the following fact is always true:

Fact 2.1.2. *For any two vectors $x, y \in \mathbb{R}^n$,and a positive definite matrix $M \in \mathbb{R}^{n\times n}$, we find:*

$$(x+y)^T M(x+y) \leq 2x^T Mx + 2y^T My$$

2.2 Graph theory

Graph-based ideas have been used in different aspects of the control systems (e.g., to find an input-output transfer function using Mason's rule, or in multivariable control systems). Apart from that, graph theory is now playing a significant role in the distributed control of multiagent systems. Particularly, graphs provide a "nice" way to visualize interconnections in multiagent systems, and, furthermore, the graph's associated matrices and their algebraic properties provide a unified framework to analysis or synthesis (closed-loop) controlled multiagent systems. In this subsection, we borrow some basic concepts and definitions from (algebraic) graph theory to build a foundation for our graph-theoretic developments in the next chapters.

A graphs $\mathcal{G}(\mathcal{V}, \mathcal{E})$ is a set of nodes $\mathcal{V} = \{\nu_1, \nu_2, ..., \nu_N\}$ which are connected to each other through a set of edges $\mathcal{E} = \{(\nu_i, \nu_j) | \nu_i, \nu_j \in \mathcal{V}\} \subseteq \mathcal{V} \times \mathcal{V}$. A graph

with no node denotes a null graph, with no edge represents an empty graph, and with only one node gives a trivial graph; and we ignore them in this research. In fact, the edge set $\mathcal{E}$ includes pairwise combinations of all nodes. An edge can be directed (also known as an arc) which results in a set of ordered pairs $(\nu_i, \nu_j) \in \mathcal{E}$, or undirected that ends in a set of unordered pairs where $(\nu_i, \nu_j) \in \mathcal{E}$ implies $(\nu_j, \nu_i) \in \mathcal{E}$. Associated to each node ν_i, depending on the direction of edge, we define the node's *in-degree* and *out-degree* as the number of edges entering and exiting that node, respectively. All information can be lumped in some appropriate matrices, namely, the *adjacency matrix* $\mathcal{A} = [a_{ij}] \in \mathbb{R}^{N\times N}$, *degree matrix* $\mathcal{D} = [deg_i] = diag\{\mathcal{A}\mathbf{1}_N\} \in \mathbb{R}^{N\times N}$ where deg_i denotes the degree of the i^{th} node ν_i (after specifying whether it is in-degree or out-degree of a node), and *Laplacian matrix* $\mathcal{L} = [l_{ij}] \in \mathbb{R}^{N\times N}$ which are defined as follows:

$$\mathcal{A} = \begin{bmatrix} 0 & a_{12} & \dots & a_{1N} \\ a_{21} & 0 & \dots & a_{2N} \\ \vdots & \vdots & \ddots & \vdots \\ a_{N1} & a_{N2} & \dots & 0 \end{bmatrix}, \qquad \mathcal{D} = \begin{bmatrix} \sum_{j=1}^{N} a_{1j} & 0 & \dots & 0 \\ 0 & \sum_{j=1}^{N} a_{2j} & \dots & 0 \\ \vdots & \vdots & \ddots & \vdots \\ 0 & 0 & \dots & \sum_{j=1}^{N} a_{Nj} \end{bmatrix}$$

$$\mathcal{L} = \mathcal{D} - \mathcal{A} = \begin{bmatrix} \sum_{j=1}^{N} a_{1j} & -a_{12} & \dots & -a_{1N} \\ -a_{21} & \sum_{j=1}^{N} a_{2j} & \dots & -a_{2N} \\ \vdots & \vdots & \ddots & \vdots \\ -a_{N1} & -a_{N2} & \dots & \sum_{j=1}^{N} a_{Nj} \end{bmatrix}$$

where $a_{ij} \in \{0, 1\}$ shows the existence of an edge (ν_j, ν_i) with ν_j as the tail and ν_i as the head whenever $a_{ij} = 1$, and no edge from ν_j to ν_i if $a_{ij} = 0$. We

assume that there exists no self-loop, therefore, $a_{ii} = 0$. Based on the in-degree definition, a node ν_j is a neighbor of ν_i whenever there exists a directed edge from ν_j to ν_i. Over an undirected graph, ν_i and ν_j are each other's neighbors whenever they share an edge. We let $\mathcal{N}_i$ be the neighboring set of the i^{th} agent. Then, based on the "in-degree" definition of $\mathcal{A}$, the degree matrix can be rewritten as $\mathcal{D} = diag\{\sum_{j\in\mathcal{N}_i} a_{ij}\}$ where the i^{th} diagonal term represents the number of edges entering to the i^{th} node (a similar change of notation can be readily seen for the diagonal terms in $\mathcal{L}$). The following example shows the relation of these matrices for both directed and undirected graphs.

Example 2.2.1. *Based on the typical graph in Figure 2.1, we find the adjacency $\mathcal{A}_d$, in-degree $\mathcal{D}_d$, and Laplacian $\mathcal{D}_d$ matrices. The edge between ν_1 and ν_2 represents $(\nu_1, \nu_2) \in \mathcal{E}$, and the edge between ν_2 and ν_3 means $(\nu_2, \nu_3), (\nu_3, \nu_2) \in \mathcal{E}$. Removing the directions on edges, we find an undirected graph with the adjacency $\mathcal{A}_u$, degree $\mathcal{D}_u$, and Laplacian $\mathcal{D}_u$ matrices.*

$$\mathcal{A}_d = \begin{bmatrix} 0 & 0 & 0 & 0 & 0 \\ 1 & 0 & 1 & 1 & 0 \\ 0 & 1 & 0 & 0 & 0 \\ 0 & 0 & 1 & 0 & 0 \\ 0 & 0 & 0 & 1 & 0 \end{bmatrix}, \ \mathcal{D}_d = \begin{bmatrix} 0 & 0 & 0 & 0 & 0 \\ 0 & 3 & 0 & 0 & 0 \\ 0 & 0 & 1 & 0 & 0 \\ 0 & 0 & 0 & 1 & 0 \\ 0 & 0 & 0 & 0 & 1 \end{bmatrix}, \ \mathcal{L}_d = \begin{bmatrix} 0 & 0 & 0 & 0 & 0 \\ -1 & 3 & -1 & -1 & 0 \\ 0 & -1 & 1 & 0 & 0 \\ 0 & 0 & -1 & 1 & 0 \\ 0 & 0 & 0 & -1 & 1 \end{bmatrix}$$

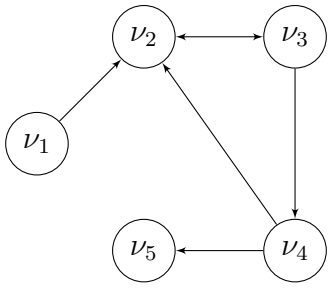

Figure 2.1: A digraph for example 2.2.1 with $(\mathcal{A}_d, \mathcal{D}_d, \mathcal{L}_d)$. Removing all directions on edges, we find an undirected graph with $(\mathcal{A}_u, \mathcal{D}_u, \mathcal{L}_u)$.

$$\mathcal{A}_u = \begin{bmatrix} 0 & 1 & 0 & 0 & 0 \\ 1 & 0 & 1 & 1 & 0 \\ 0 & 1 & 0 & 1 & 0 \\ 0 & 1 & 1 & 0 & 1 \\ 0 & 0 & 0 & 1 & 0 \end{bmatrix}, \ \mathcal{D}_u = \begin{bmatrix} 1 & 0 & 0 & 0 & 0 \\ 0 & 3 & 0 & 0 & 0 \\ 0 & 0 & 2 & 0 & 0 \\ 0 & 0 & 0 & 3 & 0 \\ 0 & 0 & 0 & 0 & 1 \end{bmatrix}, \mathcal{L}_u = \begin{bmatrix} 1 & -1 & 0 & 0 & 0 \\ -1 & 3 & -1 & -1 & 0 \\ 0 & -1 & 2 & -1 & 0 \\ 0 & -1 & -1 & 3 & -1 \\ 0 & 0 & 0 & -1 & 1 \end{bmatrix}$$

We further mention that a graph with no parallel edge and no self-loop is called a *simple graph*. Also, a simple graph with all possible pairs of nodes represents a *complete graph*. A graph $\mathcal{G}_{sub} = (\mathcal{V}_{sub}, \mathcal{E}_{sub})$ is a *subgraph* of $\mathcal{G}$ if $\mathcal{V}_{sub} \subseteq \mathcal{V}$ and $\mathcal{E}_{sub} \subseteq \mathcal{E}$. A *walk with length* m on $\mathcal{G}$ is a finite sequence of nodes $\nu_{i_0}, \nu_{i_1}, ..., \nu_{i_{m-1}}, \nu_{i_m}$ whenever the edges $(\nu_{i_k}, \nu_{i_{k+1}}) \in \mathcal{E}$ for all $k \in \{0, 1, ..., m-1\}$. A walk with no repeated edge is called a *trail*, and a trail with no repeated node is a *path*. Whenever there exists at least one walk between all pairs of nodes, the graph is *connected*. A *tree* is a connected graph with no circuit where, by *circuit*, we mean a path that starts from a node and ends in the same node. A directed graph is *strongly connected* if there exists a directed path from any nodes to all others. A directed graph is *quasi-strongly connected* if one of the following conditions holds for every pair of nodes ν_i and ν_j: *a)* $\nu_i = \nu_j$, *b)* there exists a

directed path $\nu_i - \nu_j$, or *c)* there exist some intermediate nodes ν_l to create a walk from ν_i to ν_j *b* (e.g., with one intermediate node, there exist a path $\nu_i - \nu_l$ and a path $\nu_l - \nu_j$). A node is called a *root* if it receives no information from other nodes (i.e., its in-degree is zero). A directed tree is a walk over $\mathcal{G}$ (thus, a subgraph of $\mathcal{G}$) where each node, except the root, has an in-degree equal to one; and, the *directed spanning tree* of $\mathcal{G}$ is a strongly connected tree that covers all nodes of $\mathcal{G}$ (it is defined over a digraph, and includes the minimum number of directed edges that passes through all nodes). A digraph has a directed spanning tree if and only if it is quasi-strongly connected. Note that a connected graph has at least one spanning tree.

For any (di-) graphs, $\mathbf{1}_N$ is a right eigenvector of $\mathcal{L}$ and zero is its corresponding eigenvalue, i.e., $\mathcal{L}\mathbf{1}_N = \mathbf{0}$ which means $\mathbf{1}_N \in N(\mathcal{L})$. Based on the Gershgorin disk Theorem 2.1.1, we find that all eigenvalues of a graph Laplacian $\mathcal{L}$ lie in some disks $(deg_i, \sum_{j\in\mathcal{N}_i} a_{ij})$ for all $i \in \{1, 2, ..., N\}$. Due to the fact that $deg_i = \sum_{j\in\mathcal{N}_i} a_{ij}$, we conclude that all eigenvalues of $\mathcal{L}$ are inside and on a "big" disk with center $c = \max_i(deg_i)$ and radius $r = \max_i(deg_i)$. For an undirected graph, we further know that $\mathcal{L} = \mathcal{L}^T \succcurlyeq \mathbf{0}$ and $\mathbf{1}_N$ is both right and left eigenvectors corresponding to the eigenvalue zero, and all of its eigenvalues are some real-valued numbers. As a result, these scalars lie on a line connecting the origin to $2\max_i(deg_i)$.

We now summarize some main points about an undirected graph as a fact:

Fact 2.2.1. *a) All eigenvalues of the graph Laplacian $\mathcal{L}$ are nonnegative, b) the graph $\mathcal{G}$ is connected if and only if zero is a simple eigenvalue of $\mathcal{L}$, c) $\mathbf{1}$ is the right and left eigenvector corresponding to the eigenvalue zero of $\mathcal{L}$ ($\lambda_1 = 0$), and d) since $\mathcal{L}$ is a symmetric matrix, there always exists a unitary*

transformation $T \in \mathcal{R}^{N\times N}$ *such that* $T^{-1}\mathcal{L}T = \Lambda$ *where* $\Lambda = Diag_b\{[\lambda_1, \Lambda_d]\}$, $\Lambda_d = diag\{[\lambda_2, \lambda_3, ..., \lambda_N]\}$, *and* $\lambda_i \in \mathbb{R}$ *denotes the* i^{th} *eigenvalue of* $\mathcal{L}$. *For a connected graph, only* $\lambda_1 = 0$, *and* $\Lambda_d \succ \boldsymbol{0}$.

Remark 2.2.1. *It is straightforward to generalize these results to a weighted graph denoted by* $\mathcal{G}(\mathcal{V}, \mathcal{E}, \mathcal{W})$ *where* $\mathcal{W}$ *represents a set of weights associated to the edges in* $\mathcal{E}$. *Then, the graph-related matrices can be modified appropriately with exactly the same properties. For example, the graph Laplacian matrix can be rewritten as* $\mathcal{L}_{ii} = \sum_{j\in\mathcal{N}_i} w_{ij}$ *and* $\mathcal{L}_{ij} = -w_{ij}\ \forall j \neq i$. *In fact, the non-weighted scenario can be viewed as a weighted graph with a threshold operation an the wights (i.e.,* $a_{ij} = 1\ if\ w_{ij} > w_{th}$ *and* $a_{ij} = 0$ *otherwise where* w_{th} *denotes a threshold value). However, except Chapter 7, all results are limited to the non-wighted graph definitions.*

2.3 Control systems theory

In this section, we overview some basic concepts of the control systems theory that have been used for the stability analysis in the next chapters. We start by introducing a state space model of a nonlinear system:

$$\dot{x}(t) = f(x, u, t), \qquad y(t) = h(x, u, t), \qquad x(0) = x_0$$

where $x \in \mathbb{R}^{n_x}$ denotes the state variable, $u \in \mathbb{R}^{n_u}$ represents the control input, and $y \in \mathbb{R}^{n_y}$ indicates the measurement output. For the analysis purpose, we usually substitute $u = k(x)$ and find the following closed-loop system:

$$\dot{x} = f(x, t), \qquad x(0) = x_0 \tag{2.6}$$

In fact, it should be $f'(x,t) = f(x,k(x),t)$. This misuse of notation will not have any adverse effects on the rest of this chapter, but simplifies the notation. This also can be viewed as an unforced state equation whenever $u = 0$ (with full state information). The function $f : \mathbb{D} \to \mathbb{R}^{n_x}$ is piecewise continuous in time[1], and satisfies the *Lipschitz condition* locally around the point x_L over a domain $\mathbb{D} = \mathcal{B}(x_L, r) = \{\|x - x_L\| < r\} \subset \mathbb{R}^{n_x}$. The later condition indicates the existence of a positive Lipschitz constant γ_L such that:

$$\|f(x,t) - f(y,t)\| \leq \gamma_L \|x - y\|, \qquad x, y \in \mathbb{D} \tag{2.7}$$

The global Lipschitz condition refers to the case $\mathbb{D} = \mathbb{R}^{n_x}$. This global property ensures existence and uniqueness of the solution of state equation (2.6) over any time intervals.

As a special case, we know $\dot{x} = f(x,u)$ and $y = h(x,u)$ as an *autonomous* (time invariant) *nonlinear system*. This system may have several equilibrium points which are the solutions of:

$$f(x_{eq}) = \mathbf{0} \tag{2.8}$$

The stability of a nonlinear system should be (separately) analyzed for all equilibrium points. In the following definition, we discuss the stability of an equilibrium point at the origin for a nonlinear system (otherwise, we transfer the origin of dynamical system to the non-zero equilibrium point using appropriate change of variables, and use the same results).

[1]By piecewise continuous, we mean f can be discontinuous at finitely many points, and the left and right limits exist at each discontinuity point.

Definition 2.3.1. *($\delta - \epsilon$ **stability definition**) The $x_{eq} = \mathbf{0}$ is a locally stable equilibrium point of (2.6), with a locally Lipschitz f over a domain $\mathbb{D}$ including the origin and $f(0) = 0$, whenever $\forall \epsilon > 0 \; \exists \; \delta > 0 \;\ni\; \|x\| \leq \delta \Longrightarrow \|f(x)\| \leq \epsilon$; it is a locally asymptotically stable equilibrium point, if it is stable and $\|x - x_{eq}\| \leq \delta \Longrightarrow \lim_{t\to\infty} \|f(x)\| = 0$. These results are globally valid whenever the initial condition can be arbitrarily selected, i.e., $\delta \to \infty$.*

It is a hard task, if not an impossible one, to ensure stability of a complex dynamical system using this $\delta - \epsilon$ definition. Fortunately, the Lyapunov stability results provide some useful tools to verify the stability of a dynamical system without solving the nonlinear differential equation. The following theorem summarizes the Lyapunov's findings.

Theorem 2.3.1. ***(Lyapunov stability)*** *Let conditions of Definition 2.3.1 be satisfied. Let $V(x)$ be a continuously differentiable function over $\mathbb{D}$ and satisfy:*

$$V(x) \geq 0 \quad \forall x \in \mathbb{D} \;\; with \;\; V(x) = 0 \;\; if \; and \; only \; if \;\; x = 0 \tag{2.9}$$

Then, the origin of (2.6) is a stable equilibrium point if:

$$\dot{V}(x) \leq 0 \; \forall \; x \in \mathbb{D} \tag{2.10}$$

Furthermore, the origin is an asymptotically stable equilibrium point if:

$$\dot{V}(x) < 0 \; \forall \; x \in \mathbb{D} \; and \; x \neq 0 \tag{2.11}$$

Rewording these results, a candidate Lyapunov function V satisfying (2.9)-(2.10) is called a positive semi-definite function, and is shown by $V \succcurlyeq 0$; a V satisfying (2.9) and (2.11) is called a positive definite function, and is specified by $V \succ 0$; and a V satisfying $V(x) \to \infty$ whenever $\|x\| \to \infty$ is named a radially

unbounded Lyapunov function. The results of Theorem 2.3.1 are globally valid if the candidate Lyapunov function is radially unbounded. The Lyapunov function-based analysis can also be used to establish the exponential stability of a nonlinear system. We discuss the required conditions in the next theorem.

Theorem 2.3.2. ***(Exponential stability)*** *Assume that conditions of Theorem 2.3.1 are satisfied. The origin is an exponentially stable equilibrium point of the nonlinear system $\dot{x} = f(x)$ whenever there exists a Lyapunov candidate function that satisfies:*

$$a_1\|x\|^b \leq V(x) \leq a_2\|x\|^b, \qquad and \qquad \dot{V}(x) \leq -a_3\|x\|^b \tag{2.12}$$

for some positive constants a_1, a_2, a_3, and b.

As a special case, a strictly proper linear time-invariant dynamical system is given by the following model in the state space domain:

$$\begin{aligned} \dot{x}(t) &= Ax(t) + Bu(t) \\ y(t) &= Cx(t) \end{aligned} \tag{2.13}$$

where $A \in \mathbb{R}^{n_x \times n_x}$ stands for the state matrix, $B \in \mathbb{R}^{n_x \times n_u}$ denotes the input gain matrix, and $C \in \mathbb{R}^{n_y \times n_x}$ specifies the measurement gain matrix. The solution of this first-order differential state equation is given by:

$$x(t) = e^{A(t-t_0)}x(t_0) + \int_{t_0}^{t} e^{A(t-\tau)}Bu(\tau)d\tau \tag{2.14}$$

and, thus, $y(t) = Ce^{A(t-t_0)}x(t_0) + C\int_{t_0}^{t} e^{A(t-\tau)}Bu(\tau)d\tau$.

A linear system has only one equilibrium point located at the origin such that the stability of origin is equivalent to the stability of the system. A complete statement on stability of the linear systems (based on the state space domain notation) depends on the definition of Jordan blocks which we do not need in this

research. In the next theorem, we only characterize the exponential stability of a linear system.

Theorem 2.3.3. *The linear system* (2.13) *is globally exponentially stable if and only if all eigenvalues of A have strictly negative real parts. This result is equivalent to the existence of a solution $P \succ \mathbf{0}$ for the following Lyapunov equation for any $Q \succ \mathbf{0}$:*

$$A^T P + PA = -Q \tag{2.15}$$

Note that, whenever all eigenvalues of A_c in $\dot{x} = A_c x$ have strictly negative real part, $\|x\| \leq \alpha e^{-\sigma t}\|x(0)\|$ is satisfied, and A is called a Hurwitz matrix. In this case, asymptotic stability and exponential stability are equivalent to each other.

Controllability or the weaker condition stabilizability, and observability or the weaker requirement detectability play important roles in designing a controller and stability analysis of a closed-loop system. In the rest, we overview these topics.

For a system at $t_0 = 0$, we first emphasize that the state equation in (2.13) has a response of the form (2.14) where the first term $e^{At}x(0)$ is not affected by the control input u. Thus, the state response for an input u under a zero initial condition is given by $x(t) = \int_{t_0}^{t} e^{A(t-\tau)}Bu(\tau)d\tau$. Then, a reachable set $\mathcal{R} = \mathcal{R}_T$ of the state equation in (2.13) at a time $T > 0$ is defined as the set of all state variables $x(T)$ that can be reached from initial rest condition (at $t = 0$) by a continuous control input u. Now, the controllability is defined as follows:

Definition 2.3.2. *(**Controllability**) The pair (A, B) represents a controllable linear time-invariant system* (2.13) *if $\mathcal{R} = \mathbb{R}^{n_x}$. This controllability property is satisfied if and only if the controllability matrix $\mathcal{C}$ is a full row rank matrix:*

$$Rank(\mathcal{C}) = Rank([B, AB, A^2B, ..., A^{n_x-1}B]) = n_x$$

or, equivalently (if and only if), there exist no nonzero $z \in \mathbb{C}^{n_x}$ *and* $\lambda \in \mathbb{C}$ *to simultaneously satisfy the following conditions:*

$$z^*A = \lambda z^* \qquad and \qquad z^*B = 0$$

In summary, this definition says that there always exists a trajectory to move from an initial state $x(0)$ to a final state $x(t_f)$ at a finite time $t_f > 0$. There always exists a similarity transformation which results in a staircase representation of (2.13):

$$\begin{aligned} \begin{bmatrix} \dot{x}_c \\ \dot{x}_{uc} \end{bmatrix} &= \begin{bmatrix} A_c & A_{12} \\ \mathbf{0} & A_{uc} \end{bmatrix} \begin{bmatrix} x_c \\ x_{uc} \end{bmatrix} + \begin{bmatrix} B_c \\ \mathbf{0} \end{bmatrix} u \\ y &= \begin{bmatrix} C_c & C_{uc} \end{bmatrix} \begin{bmatrix} x_c \\ x_{uc} \end{bmatrix} \end{aligned} \tag{2.16}$$

where (A_c, B_c) represents a controllable pair, and A_{uc} includes all uncontrollable modes of (A, B) in (2.13). This simply says that x_c can be controlled from any initial condition $x_c(0)$ to any final condition $x_c(t_f)$ at a finite time $t_f > 0$ in the presence of an extra term $A_{12}x_{uc}(t)$. Now, we have the following definition:

Definition 2.3.3. *(**Stabilizability**) A linear time-invariant system* (2.13) *is stabilizable if and only if all of its uncontrollable modes are located in the open left-half plane (i.e.,* A_{uc} *is a Hurwitz matrix). Mathematically, this can be verified by ensuring that the matrix* $[A - sI_{n_x},\ B]$ *has full row rank for all eigenvalues of* A *where* $s \in \{\lambda(A) | \Re(\lambda) \geq 0\}$.

The uncontrollability may have different reasons including the insufficient number of inputs. However, close to the topics of this research on multiagent systems, an interestingly uncontrollable system can be obtained after connecting some controllable systems (each serial, parallel, or feedback scenario may result in an uncontrollable coupled dynamical system).

The complete state space model (2.13) includes an output equation $y = Cx$ that models a set of measurements and, under some conditions, can be used to reconstruct all state variables x (we may use them in a feedback framework in order to control a system). The following definition formalize the observability of a linear time-invariant system:

Definition 2.3.4. *(**Observability**) The pair (C, A) represents an observable state space model* (2.13) *whenever it is possible to uniquely reconstruct all state variables $x(t)$ $\forall t \in [0, t_f]$, with $t_f > 0$, using only $u(t)$ and $y(t)$ measurements in that time interval. This property can be verified by a full column rank test of the observability matrix $\mathcal{O}$:*

$$rank(\mathcal{O}) = rank(\begin{bmatrix} C \\ CA \\ \vdots \\ CA^{n_x-1} \end{bmatrix}) = n_x \tag{2.17}$$

or, equivalently (if and only if), there exist no nonzero $x \in \mathbb{C}^{n_x}$ and $\lambda \in \mathbb{C}$ to simultaneously satisfy the following conditions:

$$Ax = \lambda x \qquad and \qquad Cx = 0$$

Similar to the controllability discussion, we always can find a transformed representation which separates observable and unobservable modes of a system (2.13):

$$\begin{aligned} \begin{bmatrix} \dot{x}_o \\ \dot{x}_{uo} \end{bmatrix} &= \begin{bmatrix} A_o & \mathbf{0} \\ A_{21} & A_{uo} \end{bmatrix} \begin{bmatrix} x_o \\ x_{uo} \end{bmatrix} + \begin{bmatrix} B_o \\ B_{uo} \end{bmatrix} u \\ y &= \begin{bmatrix} C_o & \mathbf{0} \end{bmatrix} \begin{bmatrix} x_0 \\ x_{uo} \end{bmatrix} \end{aligned} \tag{2.18}$$

Then, the detectability is defined as follows:

Definition 2.3.5. *(**Detectability**) A linear time-invariant system* (2.13) *is detectable if and only if all of its unobservable modes are located in the open left-half plane (i.e., A_{uo} is a Hurwitz matrix). Mathematically, this can be verified by ensuring that the matrix* $\begin{bmatrix} A - sI_{n_x} \\ B \end{bmatrix}$ *has full column rank for all eigenvalues s of A with $s \in \{\lambda(A) | \Re(\lambda) \geq 0\}$.*

Also, we introduce the duality property in establishing controllability and observability of state space model (2.13):

Lemma 2.3.1. *(**Controller and observer duality**) The controllability of a triple (C, A, B) is equivalent to the observability of a triple (B^T, A^T, C^T), and vice versa.*

Based on these insights, we provide a statement of the Kalman decomposition in the next theorem:

Theorem 2.3.4. ***(Kalman decomposition)*** *Every state space model* (2.13) *can be transformed to an equivalent canonical form:*

$$\begin{aligned}
\begin{bmatrix} \dot{x}_{co} \\ \dot{x}_{cu_o} \\ \dot{x}_{u_c o} \\ \dot{x}_{u_c u_o} \end{bmatrix} &= \begin{bmatrix} A_{co} & \boldsymbol{0} & A_{13} & \boldsymbol{0} \\ A_{21} & A_{cu_o} & A_{23} & A_{24} \\ \boldsymbol{0} & \boldsymbol{0} & A_{u_c o} & \boldsymbol{0} \\ \boldsymbol{0} & \boldsymbol{0} & A_{43} & A_{u_c u_o} \end{bmatrix} \begin{bmatrix} x_{co} \\ x_{cu_o} \\ x_{u_c o} \\ x_{u_c u_o} \end{bmatrix} + \begin{bmatrix} B_{co} \\ B_{cu_o} \\ \boldsymbol{0} \\ \boldsymbol{0} \end{bmatrix} u \\
y &= \begin{bmatrix} C_{co} & \boldsymbol{0} & C_{u_c o} & \boldsymbol{0} \end{bmatrix} \begin{bmatrix} x_{co} \\ x_{cu_o} \\ x_{u_c o} \\ x_{u_c u_o} \end{bmatrix}
\end{aligned} \tag{2.19}$$

which is shown in Figure 2.2. Moreover, the following state space equation gives the completely controllable and observable (sub-) dynamics of (2.13)*:*

$$\begin{aligned}
\dot{x}_{co} &= A_{co} x_{co} + B_{co} u \\
y &= C_{co} x_{co}
\end{aligned} \tag{2.20}$$

In practice, sometimes, we do not have access to all state information x. Therefore, we need to design a state observer to estimate this information. We have shown that the design of an observer can be transformed to a dual stabilization problem based on the Lemma 2.3.1. Now, we provide a statement of the *separation principle* in designing controller and observer gains for an observer-based output feedback control problem.

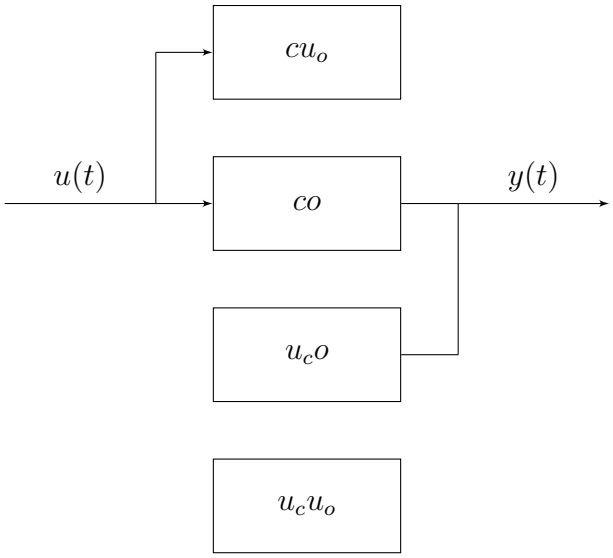

Figure 2.2: A conceptual presentation of the Kalman decomposition. Whenever all modes of cu_o, $u_c o$, and $u_c u_o$ are in the left complex half-plane, we say the system does not have any unstable hidden modes in the sense of Kalman decomposition.

Lemma 2.3.2. ***(Separation principle)*** *The estimated state $\hat{x}$ of* (2.13) *can be found by a Luenberger observer using measurements u and y:*

$$\begin{aligned} \dot{\hat{x}} &= A\hat{x} + Bu + K_o(y - \hat{y}) \\ \hat{y} &= C\hat{x} \end{aligned} \tag{2.21}$$

where $K_o \in \mathbb{R}^{n_x \times n_y}$ denotes an observer gain. Then, $u = K_c\hat{x}$, where $K_c \in \mathbb{R}^{n_u \times n_x}$ represents the feedback control gain, stabilizes (2.13) *whenever K_c results in a Hurwitz matrix $A - BK_c$, and, separately, K_o does the same with $A - K_oC$.*

We now explain a statement of the Bellman-Gronwall lemma that will be used in the next chapters:

Lemma 2.3.3. ***(Bellman-Gronwall lemma)*** *Let $z(t), g(t),$ and $h(t)$ be non-negative piecewise continuous functions of time t. If a function $w(t)$ satisfies the inequality $w(t) \leq z(t) + g(t) \int_{t_0}^{t} h(\tau)w(\tau)d\tau,\ \forall t \geq t_0 \geq 0$; then, we find:*

$$w(t) \leq z(t) + g(t) \int_{t_0}^{t} (z(s)h(s)e^{\int_s^t (h(\tau)g(\tau))d\tau})ds,\ \forall t \geq t_0 \geq 0.$$

2.4 Optimal control theory

The results of Section 2.3 are useful to analyze properties of closed-loop (feedback) system. In parallel, many theoretical research studies have been devoted to the controller synthesis problem. The optimal control is one of the oldest theoretical research topics that, in addition to the stability, guarantees a desired level of performance for the closed-loop system. Particularly, linear quadratic regular-based (LQR-based) ideas have received significant attention in the literature. In this section, we overview the procedure to design an LQR (control) system for a linear time-invariant model (2.13), introduce some basic definitions related to the proposed algorithm, and mention some of the most fundamental properties of the resulting closed-loop system with an LQR optimal controller in the loop.

Specifically, we introduce (2.22) as a performance (integral) cost function to simultaneously quantify the degree of stability and control effort (closeness of x to the origin and size of u, respectively):

$$J(x(0)) = \int_0^{\infty} (x^T Q x + u^T R u)dt \tag{2.22}$$

where $Q \succcurlyeq \mathbf{0}$ and $R \succ \mathbf{0}$ denote the state and input weighting matrices, respectively. We define $\mathcal{U}$ as a set of admissible (linear static state feedback) control signals that stabilize the state equation in (2.13). Then, the optimal linear quadratic regulator problem is defined as the following minimization problem:

$$\begin{aligned} &\underset{u\in\mathcal{U}}{\text{minimize}} && J(x(0)) \\ &\text{subject to} && \dot{x} = Ax + Bu. \end{aligned} \tag{2.23}$$

For any selection of the design matrices Q and R, $J(x(0)) = x^T(0)Px(0)$ gives a lower bound (solution) on the cost function (2.22) for all $u \in \mathcal{U}$, where the matrix $P = P^T$ is the solution of an algebraic Riccati equation:

$$A^TP + PA + Q - PBR^{-1}B^TP = \mathbf{0} \tag{2.24}$$

We assume that the pair (A, B) is stabilizable, and $(Q^{\frac{1}{2}}, A)$ is observable. Then, $u^\star = K_c x = -R^{-1}B^TPx$ gives the minimizer of (2.23) with a unique stabilizing solution $P \succcurlyeq \mathbf{0}$ for the ARE (2.24), i.e., the matrix $A - BR^{-1}B^TP$ is Hurwitz (note that if $Q \succ \mathbf{0}$, then $P \succ \mathbf{0}$). A closed-loop system with this LQ-based control signal has many "nice" properties. We mention the gain margin (robustness) which is, with K_c as the optimal LQ-gain αK_c is still a stabilizing controller for any $\alpha \in (0.5, \infty)$, and phase margin (robustness) that means $e^{j\beta}K_c$ is still a stabilizing controller for any $\beta \in (-60, 60)$ degrees. Particularly, we define the *Hamiltonian*:

$$\mathbf{H} = x^TQx + u^TRu + J_x^T(Ax + Bu) \tag{2.25}$$

where $J_x = \frac{\partial J}{\partial x}$ is calculated along the state trajectory of the system. Moreover, we know that the optimal control signal $u^\star$ satisfies the *Hamilton-Jacobi-Bellman (HJB)* equation $0 = J_t^\star + \min_u\{x^T Q x + u^{\star T} R u^\star + J_x^{\star T}(Ax + Bu)\} = 0$ which, for an infinite horizon LQR problem subject to a linear time-invariant system can be reduced to $\mathbf{H} = 0$ as follows:

$$x^T Q x + u^T R u + J_x^T (Ax + Bu) = 0 \tag{2.26}$$

where we have used $J = J^\star$ and $u = u^\star$ for simplicity. This can be related to the algebraic Riccati equation (2.24) as $0 = x^T Q x + x^T K^T R K x + x^T P(A + BK)x + x^T(A^T + K^T B^T)Px = x^T(Q + K^T R K + PA + PBK + A^T P + K^T B^T P)x = x^T(A^T P + PA + Q - PBR^{-1}B^T P)x$. Based on the necessary condition of optimality $\partial \mathbf{H}/\partial u = \mathbf{0}$, we further find that the following condition is satisfied implementing an optimal control signal:

$$2u^T R + \frac{\partial J}{\partial x}^T B = \mathbf{0} \tag{2.27}$$

When we apply an optimal control signal, the optimal sequence of actions (decisions or policies) will still be the same if we skip part of the sequence and start at any later time on the trajectory. This is known as the *principle of optimality*. These fundamental results play important roles in the developments of this research. We now introduce finite-horizon LQR problem as a more general case than (2.23):

$$\begin{aligned} \min_{u \in \mathcal{U}} \quad & J = x^T(t_f) H x(t_f) + \textstyle\int_0^{t_f} (x(t)^T Q x(t) + u(t)^T R u(t)) dt \\ \text{subject to} \quad & \dot{x}(t) = Ax(t) + Bu(t) \end{aligned} \tag{2.28}$$

where $H = H^T \succcurlyeq \mathbf{0}$ is a terminal cost matrix. In this case, the necessary conditions of optimality are satisfied by $u(t) = -R^{-1}B^T L(t)$ where $x(t)$ and $L(t)$ are solutions of the following matrix differential equation:

$$\begin{bmatrix} \dot{x}(t) \\ \dot{L}(t) \end{bmatrix} = \begin{bmatrix} A & -BR^{-1}B^T \\ -Q & -A^T \end{bmatrix} \begin{bmatrix} x(t) \\ L(t) \end{bmatrix} =: H_M \begin{bmatrix} x(t) \\ L(t) \end{bmatrix} \tag{2.29}$$

in which H_M denotes Hamiltonian matrix. The optimal control signal is then rewritten as follows:

$$u(t) = -R^{-1}B^T P(t)x(t) \tag{2.30}$$

based on the fact that $L(t) = P(t)x(t)$ and $P(t)$ is the solution of Riccati equation $\dot{P}(t) = -A^T P(t) - P(t)A - Q + P(t)BR^{-1}B^T P(t)$ with boundary condition $P(t_f) = H$. In the next chapters, since $P = lim_{t\to\infty} P(t)$, we use (2.28)-(2.30) and establish a relationship between the pattern of zeros in steady solution P of ARE (2.24) and design matrices Q and R in (2.23).

2.5 Bibliography

In this chapter, we have touched the surface of different theoretical concepts ranging from the mathematics to control systems. This brief can be used as a quick reference for the developments in the next chapters. Further details on matrix analysis are available in [99]. Particularly, some main properties of the Kronecker product can be found in [100], and a systems-theoretic viewpoint on norms (of signals and systems) is explained in [101]. References [102]-[103] are

good references to find the usefulness of graphs in the old theoretical developments within the control systems society. But, in our research, a graph visualizes the communication in a multiagent system, and the properties of its associated matrices are used for the distributed control design purpose. In this sense, [104] provides a sufficiently detailed discussion on graph theory that can be used for the analysis of multiagent systems. We just mention that this research is limited to the graphs with non-negative weights (versus the signed graph in [105]). The basic definitions and results about nonlinear systems are explained in [106], and similar findings about linear systems are reported in [107]. Some basic concepts and handy tools in the control systems, including the well-known Bellman-Gronwall lemma, are reviewed in [108]. Reference [109] is a rich source of fundamental concepts in the optimal control theory. Moreover, [110] nicely summarizes some existing research topics and trends about the linear quadratic-based control systems.

Chapter 3

Distributed Consensus in Physically Decoupled Multiagent Systems[1]

"Essentially all models are wrong, but some are useful. ... The practical question is how wrong do they have to be to not be useful."

Empirical model-building and response surfaces (1987)

George E. P. Box — Statistician (1919-2013)

Consensus algorithms have been widely designed to manage the collective behavior among a set of individual agents. Shortly, we recall that the initial research studies focused on proposing some graph-theoretic ideas in order to: *1)* localize the information exchange in multiagent systems and use the relative-measurements,

[1]This chapter is based on the results of [111] and [112]. Each section has its own parameters and variables which are (re-) defined appropriately.

2) analyze the effect of communication topology on the stability and performance of the closed-loop multiagent systems, and *3)* understand the effect of agent's (high-order) dynamics on completing the cooperative task. However, in practice, these models are insufficient to precisely describe the behavior of each individual agent and, also, the collective behavior of a multiagent system.

In this chapter, our primary objective is to study the challenges that have been imposed by relative measurements in the the consensus problem (compared to centralized and decentralized control techniques which are based on the absolute measurements of each subsystem). An overview of the literature in Chapter 1 indicated a trend on more realistic scenarios by adding agent-level modeling uncertainties. Thus, to increase the challenge, we consider two sources of uncertainties in the state-space realization of agents' dynamics: *1)* agent-level unknown external disturbances, and *2)* multiagent system-level unknown varying operating condition. We use our (incomplete) knowledge about these sources of uncertainties, and find some appropriate models which are useful to design the consensus algorithms ensuring agreement among agents of a physically decoupled multiagent system. We assume that only relative-information is available for each distributed algorithm which results in some coupled-by-communication consensus algorithms[2]. We further mention that our modified LQR formulation results in guaranteed consensus without being worried about the selection of coupling strength (see Subsection 1.2.2, page 24).

[2]The word "coupled-by-communication" refers to the fact that this coupling is added by design and can be manipulated accordingly. Such a coupling does not exist in decentralized control.

This chapter is organized as follows: in Section 3.1, we address the leaderless and leader-follower consensus problems in the presence of unknown persistent disturbances. In Section 3.2, we handle the leaderless consensus problem for a multiagent system with multiagent system-level varying operation condition. We summarize our findings and provide some references in Section 3.3. Finally, we collect all proofs in Section 3.4.

3.1 Distributed consensus of linear multiagent systems under persistent disturbances

In this section, we address the consensus problem in the presence of persistent disturbances with unknown magnitudes, and using only relative-output measurements in each agent's neighborhood. The proposed model can handle all constant (step-like), ramp, or sinusoidal disturbances (also, a combination of them). We discuss both leaderless and leader-follower communication topologies, and we further calculate the agreement value of the multiagent system in the leaderless consensus scenario.

3.1.1 Leaderless consensus

3.1.1.1 Problem statement

We consider a multiagent system with the following dynamical agents:

$$\begin{aligned} \dot{x}_i &= Ax_i + Bu_i + \Gamma w_i \\ y_i^r &= \textstyle\sum_{j\in\mathcal{N}_i} C(x_i - x_j) \end{aligned} \tag{3.1}$$

where $i \in \{1, 2, ..., N\}$ indicates the agent's number over an undirected communication topology (graph) $\mathcal{G}$; $x_i \in \mathbb{R}^{n_x}$ denotes the system state variable, $u_i \in \mathbb{R}^{n_u}$ represents the control input vector, $w_i \in \mathbb{R}^{n_w}$ stands for the persistent disturbance vector, and $y_i^r \in \mathbb{R}^{n_y}$ indicates the lumped relative-output measurement of the i^{th} agent with respect to its neighbors; $A \in \mathbb{R}^{n_x \times n_x}$ represents the system state matrix, $B \in \mathbb{R}^{n_x \times n_u}$ indicates the control input matrix, $\Gamma \in \mathbb{R}^{n_x \times n_w}$ stands for the unmatched disturbance input matrix, and $C \in \mathbb{R}^{n_y \times n_x}$ denotes the output matrix. (In general, Γ is not in the range of B, so we call it an unmatched disturbance input matrix. However, the results are valid for the matched case as well.) Each unknown persistent disturbance w_i is modeled by the following disturbance generator:

$$\begin{aligned} \dot{z}_{wi} &= F z_{wi} \qquad with\ z_{wi}(0) = z_{wi}^0 \\ w_i &= \theta z_{wi} \end{aligned} \tag{3.2}$$

where $z_{wi} \in \mathbb{R}^{n_{z_w}}$ stands for the disturbance state, z_{wi}^0 represents the *unknown* initial value of z_{wi}, and $F \in \mathbb{R}^{n_{z_w} \times n_{z_w}}$ and $\theta \in \mathbb{R}^{n_w \times n_{z_w}}$ are two *known* constant matrices that determine the disturbance shape. Some appropriate pairs of (F, θ) are given in Table 3.1 in order to generate a constant (step-like), ramp, or sinusoidal disturbance (we can also consider $F(1,2) = 1$ and $F(2,1) = -\Omega^2$ to generate a sinusoidal disturbance with a frequency equal to $\Omega\ rad/s$). A combination of these disturbances can also be created by augmenting these models.

Now, the *leaderless consensus* is achieved whenever (3.3) is satisfied in the presence of unknown heterogeneous disturbances w_i, for all initial conditions of agents, and over the given undirected graph topology $\mathcal{G}$:

Table 3.1: Examples of persistent disturbances modeled by (3.2).

Type of disturbance	F	θ
Constant	0	1
Ramp	$\begin{bmatrix} 0 & 1 \\ 0 & 0 \end{bmatrix}$	$\begin{bmatrix} 1 & 0 \end{bmatrix}$
Sinusoidal (Ω rad/s)	$\begin{bmatrix} 0 & \Omega \\ -\Omega & 0 \end{bmatrix}$	$\begin{bmatrix} 1 & 0 \end{bmatrix}$

$$\lim_{t\to\infty} (x_i(t) - x_j(t)) = 0 \qquad \forall i, j \in \{1, 2, ..., N\} \tag{3.3}$$

The following assumption holds in the rest of this subsection:

Assumption 3.1.1. *(a) the pair (A, B) represents a stabilizable state space realization, (b) the pair $(\begin{bmatrix} C & \boldsymbol{0} \end{bmatrix}, \begin{bmatrix} A & \Gamma\theta \\ \boldsymbol{0} & F \end{bmatrix})$ characterizes an observable augmented system and disturbance state space realization, and (c) the Moore-Penrose pseudo-inverse $B^\dagger$ exists, (d) the graph $\mathcal{G}$ is connected.*

Let $\lambda_i \in \mathbb{R}$ be the i^{th} eigenvalue of the graph Laplacian matrix $\mathcal{L}$ corresponding to $\mathcal{G}$ for all $i \in \{1, ..., N\}$. Then, we emphasize that an (distributed) observability condition is required for $(\begin{bmatrix} \lambda_i C & \mathbf{0} \end{bmatrix}, \begin{bmatrix} A & \Gamma\theta \\ \mathbf{0} & F \end{bmatrix})$. We decompose this to an unobservable mode with $\lambda_1 = 0$, and observable modes corresponding to the rest of eigenvalues $\lambda_i \neq 0$ and $i \neq 1$. Then, focusing on observable modes, the condition is simplified to Assumption 3.1.1.b.

3.1.1.2 Main results

In order to guarantee the leaderless consensus (3.3) for a multiagent system of agents (3.1)-(3.2), we propose the following consensus algorithm:

$$u_i = K_c^x \sum_{j \in \mathcal{N}_i} (\hat{x}_i - \hat{x}_j) + K_c^w \hat{z}_{wi} \tag{3.4}$$

where $K_c^x \in \mathbb{R}^{n_u \times n_x}$ denotes the system state feedback gain, and $K_c^w \in \mathbb{R}^{n_u \times n_{z_w}}$ stands for the disturbance control gain. The estimated system state $\hat{x}_i \in \mathbb{R}^{n_x}$ and the estimated disturbance state $\hat{z}_{wi} \in \mathbb{R}^{n_{z_w}}$ are obtained using the observer (3.5):

$$\begin{aligned} \dot{\hat{x}}_i &= A\hat{x}_i + Bu_i + \Gamma\hat{w}_i + K_o^x(y_i^r - \hat{y}_i^r) \\ \dot{\hat{z}}_{wi} &= F\hat{z}_{wi} + K_o^w(y_i^r - \hat{y}_i^r) \\ \hat{y}_i^r &= C\textstyle\sum_{j \in \mathcal{N}_i}(\hat{x}_i - \hat{x}_j) \\ \hat{w}_i &= \theta\hat{z}_{wi} \end{aligned} \tag{3.5}$$

where $K_o^x \in \mathbb{R}^{n_x \times n_y}$ represents the system state observer gain, and $K_o^w \in \mathbb{R}^{n_{z_w} \times n_y}$ indicates the disturbance state observer gain.

Remark 3.1.1. *We re-emphasize that the pair (F, θ) is known and the disturbances' initial values are unknown (possibly, there are N different initial values, one for each individual agent's disturbance generator model). Thus, in multiagent system* (3.1)-(3.2)*, agents are subject to persistent disturbances with a similar waveform but different magnitudes. Therefore, although the disturbances are heterogeneous, we can (and do) propose a homogeneous observer* (3.5) *using the same F and θ matrices.*

We define the system state estimation errors $\tilde{x}_i = \hat{x}_i - x_i$ and the disturbance state estimation errors $\tilde{z}_{wi} = \hat{z}_{wi} - z_{wi}$. Also, in order to analyze this multiagent

system over $\mathcal{G}$, let $x = col\{x_i\}$ and $z_{wi} = col\{z_{wi}\}$ be the aggregated system state and disturbance state vectors, respectively; and $\tilde{x} = col\{\tilde{x}_i\}$ and $\tilde{z}_w = col\{\tilde{z}_{wi}\}$ be the aggregated system state and disturbance state estimation error vectors for $i \in \{1, 2, .., N\}$, respectively. Furthermore, let $e_o \triangleq [\tilde{x}^T, \tilde{z}_w^T]^T$ be the aggregated estimation error over $\mathcal{G}$. Now, we find the matrix representation (3.6) for a closed-loop multiagent system of (3.1)-(3.2) and (3.4)-(3.5):

$$\begin{bmatrix} \dot{x} \\ \dot{e}_o \end{bmatrix} = \begin{bmatrix} M_{11} & M_{12} \\ \mathbf{0} & M_{22} \end{bmatrix} \begin{bmatrix} x \\ e_o \end{bmatrix} + \begin{bmatrix} N_1 \\ \mathbf{0} \end{bmatrix} z_w \tag{3.6}$$

where the submatrices are defined as follows:

$$\begin{aligned} M_{11} &= (I_N \otimes A) + (\mathcal{L} \otimes BK_c^x), \quad M_{12} = [(\mathcal{L} \otimes BK_c^x),\ (I_N \otimes BK_c^w)] \\ M_{22} &= \begin{bmatrix} (I_N \otimes A) - (\mathcal{L} \otimes K_o^x C) & (I_N \otimes \Gamma\theta) \\ -(\mathcal{L} \otimes K_o^w C) & (I_N \otimes F) \end{bmatrix}, \quad N_1 = I_N \otimes (\Gamma\theta + BK_c^w) \end{aligned}$$

Because $\mathcal{L}$ is a symmetric matrix, there always exists a unitary transformation T that converts $\mathcal{L}$ to a completely diagonal matrix Λ (see Fact 2.2.1, page 43). We define $\tilde{x}_T = (T^{-1} \otimes I_{n_x})x$, $e_{oT} = diag\{[T^{-1} \otimes I_{n_x},\ T^{-1} \otimes I_{n_{z_w}}]\}e_o$, and $z_{wT} = (T^{-1} \otimes I_{n_{z_w}})z_w$, and find:

$$\begin{bmatrix} \dot{x}_T \\ \dot{e}_{oT} \end{bmatrix} = \begin{bmatrix} \tilde{M}_{11} & \tilde{M}_{12} \\ \mathbf{0} & \tilde{M}_{22} \end{bmatrix} \begin{bmatrix} x_T \\ e_{oT} \end{bmatrix} + \begin{bmatrix} \tilde{N}_1 \\ \mathbf{0} \end{bmatrix} z_{wT} \tag{3.7}$$

with the following submatrices:

$$\tilde{M}_{11} = \begin{bmatrix} A & \mathbf{0} \\ \mathbf{0} & (I_{N-1} \otimes A) + (\Lambda_d \otimes BK_c^x) \end{bmatrix}$$

$$\tilde{M}_{12} = \begin{bmatrix} \mathbf{0} & \mathbf{0} & BK_c^w & \mathbf{0} \\ \mathbf{0} & \Lambda_d \otimes BK_c^x & \mathbf{0} & I_{N-1} \otimes BK_c^w \end{bmatrix} \quad \tilde{M}_{22} = \begin{bmatrix} \tilde{M}_{22}^{11} & \tilde{M}_{22}^{12} \\ \tilde{M}_{22}^{21} & \tilde{M}_{22}^{22} \end{bmatrix}$$

$$\tilde{M}_{22}^{11} = \begin{bmatrix} A & \mathbf{0} \\ \mathbf{0} & (I_{N-1} \otimes A) - (\Lambda_d \otimes K_o^x C) \end{bmatrix}, \quad \tilde{M}_{22}^{21} = \begin{bmatrix} \mathbf{0} & \mathbf{0} \\ \mathbf{0} & -\Lambda_d \otimes K_o^w C \end{bmatrix}$$

$$\tilde{M}_{22}^{12} = I_N \otimes \Gamma\theta, \quad \tilde{M}_{22}^{22} = I_N \otimes F \quad \tilde{N}_1 = I_N \otimes (\Gamma\theta + BK_c^w)$$

We introduce a row permutation matrix $\mathcal{P}$ such that $\eta = [\eta_1^T, \eta_2^T]^T$ can be written as $\eta = \mathcal{P}[x_T^T, \tilde{x}_T^T, \tilde{z}_{wT}^T]^T$. Applying this $\mathcal{P}$ to (3.7), as a transformation matrix, separates the unobservable and uncontrollable mode (corresponding to $\lambda_1 = 0$) from observable and controllable modes (corresponding to $\Lambda_d \neq 0$). In this transformed case, $\eta_1 = [x_{T,1}^T, \tilde{x}_{T,1}^T, \tilde{z}_{wT,1}^T]^T$ and $\eta_2 = [x_d^T, \tilde{x}_d^T, \tilde{z}_{wd}^T]$ where x_d, $\tilde{x}_d$, and $\tilde{z}_{wd}$ are some variables that can be found after removing the first agent's variables respectively from x_T, $\tilde{x}_T$, and $\tilde{z}_{wT}$. The result of this transformation is written as follows:

$$\begin{bmatrix} \dot{\eta}_1 \\ \dot{\eta}_2 \end{bmatrix} = \left[\begin{array}{c|c} P_{11} & \mathbf{0} \\ \hline \mathbf{0} & P_{22} \end{array}\right] \begin{bmatrix} \eta_1 \\ \eta_2 \end{bmatrix} + \begin{bmatrix} Q_1 \\ Q_2 \end{bmatrix} z_{wT} \tag{3.8}$$

where the first row represents the *unobservable and uncontrollable agreement dynamics* and the second row gives the *observable and controllable disagreement dynamics*[3], and the submatrices are partitioned as follows:

$$P_{11} = \left[\begin{array}{c|cc} A & \mathbf{0} & BK_c^w \\ \hline \mathbf{0} & A & \Gamma\theta \\ \mathbf{0} & \mathbf{0} & F \end{array}\right] \quad P_{22} = \left[\begin{array}{c|cc} P_{22}^{11} & P_{22}^{12} & P_{22}^{13} \\ \hline \mathbf{0} & P_{22}^{22} & P_{22}^{23} \\ \mathbf{0} & P_{22}^{32} & P_{22}^{33} \end{array}\right]$$

$$Q_1 = \left[\begin{array}{c} \Gamma\theta + BK_c^w \\ \hline \mathbf{0} \\ \mathbf{0} \end{array}\right] \quad Q_2 = \left[\begin{array}{c} I_{N-1} \otimes (\Gamma\theta + BK_c^w) \\ \hline \mathbf{0} \\ \mathbf{0} \end{array}\right]$$

$$\begin{aligned} P_{22}^{11} &= (I_{N-1} \otimes A) + (\Lambda_d \otimes BK_c^x), \quad P_{22}^{12} = \Lambda_d \otimes BK_c^x \\ P_{22}^{13} &= (I_{N-1} \otimes BK_c^w), \quad P_{22}^{22} = (I_{N-1} \otimes A) - (\Lambda_d \otimes K_o^x C) \\ P_{22}^{23} &= I_{N-1} \otimes \Gamma\theta, \quad P_{22}^{32} = -(\Lambda_d \otimes K_o^w C), \quad P_{22}^{33} = I_{N-1} \otimes F \end{aligned}$$

Since the observer-based consensus algorithm does not receive information about the unobservable mode, we limit the consensus algorithm design to the observable dynamics:

[3]The agreement and disagreement dynamics (and subspaces) are two terms that have been taken from the literature of multiagent systems [104]. Briefly, in this dissertation, they specify the effect of λ_1 (determines the null space of $\mathcal{L}$ in a connected graph) and $\Lambda_d \succ \mathbf{0}$ that includes nonzero eigenvalues of $\mathcal{L}$. Based on the discussion after Assumption 3.1.1, part of the dynamics of the transformed system which is affected by $\lambda_1 = 0$ is not observable (and not controllable). However, the other part can be observed, manipulated, stabilized, and have a convergent behavior $\eta_2 \to \mathbf{0}$ in the transformed multiagent system (3.8). Thus, when the consensus (3.3) is achieved for the non transformed multiagent system (3.6), x_i are affected by the unobservable (uncontrollable) dynamics corresponding to η_1 (note that $x = col\{x_i\}$ can be found by transforming back from (3.8) to (3.6) using two transformation matrices $\mathcal{P}$ and T). Since the limit behavior $x_i = x_j$ shows an agreement, the unobservable (uncontrollable) dynamics of the transformed multiagent system are called "agreement dynamics," and the rest of them are named "disagreement dynamics."

$$\begin{bmatrix} \dot{x}_d \\ \dot{\tilde{x}}_d \\ \dot{\tilde{z}}_{wd} \end{bmatrix} = \underbrace{\left[\begin{array}{c|cc} P_{22}^{11} & P_{22}^{12} & P_{22}^{13} \\ \hline \mathbf{0} & P_{22}^{22} & P_{22}^{23} \\ \mathbf{0} & P_{22}^{32} & P_{22}^{33} \end{array}\right]}_{P_{22}} \begin{bmatrix} x_d \\ \tilde{x}_d \\ \tilde{z}_{wd} \end{bmatrix} + \underbrace{\left[\begin{array}{c} I_{N-1} \otimes (\Gamma\theta + BK_c^w) \\ \hline \mathbf{0} \\ \mathbf{0} \end{array}\right]}_{Q_2} z_{wd} \tag{3.9}$$

which include *N-1* dynamical systems of the form (3.10) $\forall i \in \{2, 3, ..., N\}$:

$$\dot{x}_{di} = Ax_{di} + \lambda_i BK_c^x \hat{x}_{di} + BK_c^w \hat{z}_{wdi} + \Gamma\theta z_{wdi}, \tag{3.10}$$

and another *N-1* dynamical systems given by:

$$\begin{aligned} \dot{\tilde{x}}_{di} &= (A - \lambda_i K_o^x C)\tilde{x}_{di} + \Gamma\theta\tilde{z}_{wdi} \\ \dot{\tilde{z}}_{wdi} &= -\lambda_i K_o^w C\tilde{x}_{di} + F\tilde{z}_{wdi} \end{aligned} \tag{3.11}$$

The effect of unobservable and uncontrollable mode (corresponding to $\lambda_1 = 0$) on the agreement value will be discussed in Lemma 3.1.1. In the next theorem, we convert the "global" (collective) consensus problem (3.3) over graph $\mathcal{G}$ to a set of equivalent "local" stability analysis problems that are affected by non-zero eigenvalues of $\mathcal{L}$.

Theorem 3.1.1. *Let Assumption 3.1.1 be satisfied by multiagent system* (3.1)-(3.2) *over* $\mathcal{G}$. *An observer-based consensus algorithm* (3.4)-(3.5) *solves the consensus problem* (3.3) *if for all* $i \in \{2, ..., N\}$*:*

1. *The Luenberger observer gain* $K_o = \begin{bmatrix} K_o^x \\ K_o^w \end{bmatrix}$ *results in the Hurwitz (closed-loop) matrix* $\begin{bmatrix} A - \lambda_i K_o^x C & \Gamma\theta \\ -\lambda_i K_o^w C & F \end{bmatrix}$ *with appropriate eigenvalues, sufficiently far from the imaginary axis. This matrix corresponds to the observer error dynamics* (3.11).

2. *The control-gain* $K_c = \begin{bmatrix} K_c^x & K_c^w \end{bmatrix}$ *stabilizes* (3.12) *for all nonzero* λ_i*, and rejects the unknown disturbances* $w_{di} = \theta z_{wdi}$.

$$\begin{aligned} \dot{x}_{di} &= Ax_{di} + Bu_{di} + \Gamma\theta z_{wdi} \\ y_{di} &= \lambda_i x_{di} \\ u_{di} &= K_c^x y_{di} + K_c^w z_{wdi} \end{aligned} \tag{3.12}$$

Proof. This proof is given at Subsection 3.4.1. □

Theorem 3.1.1 characterizes some conditions for the stability analysis of agreement (consensus) dynamics. But, this theorem is not useful for the synthesis purpose, because it should be "verified" for "all *N-1* nonzero eigenvalues" of $\mathcal{L}$. Hence, we rewrite (3.12) as follows:

$$\dot{x}_{di} = Ax_{di} + \lambda_i BK_c^x x_{di} + (BK_c^w + \Gamma\theta) z_{wdi} \tag{3.13}$$

and propose the following design procedure:

Design procedure 3.1.1. *The control gains in* (3.13) *can be designed in two steps:*

1. *Disturbance gain* K_c^w*: this gain is designed to minimize* $\|BK_c^w + \Gamma\theta\|$*. Based on the Assumption 3.1.1.c, we find* $K_c^w = -B^\dagger \Gamma\theta$.

2. *State feedback gain K_c^x: using K_c^w of Step 1, we design a feedback gain K_c^x that solves the robust control problem* (3.14) *with a fictitious uncertainty in $B_\lambda \triangleq BD(\lambda_i)$ where $D(\lambda_i) \triangleq \lambda_i I_{n_u}$:*

$$\begin{aligned} \dot{x}_{di} &= Ax_{di} + B_\lambda u_{di} \\ u_{di} &= K_c^x x_{di} \end{aligned} \tag{3.14}$$

We rewrite the state equation in (3.14) as follows:

$$\underbrace{\dot{x}_{di} = Ax_{di} + BD_{\lambda_2} u_{di}}_{\text{Nominal model}} + \underbrace{BD_{\lambda_2} E(\lambda_i) u_{di}}_{\text{Network-induced uncertainty}} \tag{3.15}$$

where we have defined $D_{\lambda_2} \triangleq \lambda_2 I_{n_u}$, such that $0 \prec D_{\lambda_2} \preccurlyeq D(\lambda_i)$, $D(\lambda_i) = \lambda_i I_{n_u}$, and $E(\lambda_i) \triangleq D_{\lambda_2}^{-1} D(\lambda_i) - I_{n_u} \succcurlyeq \mathbf{0}$ are satisfied. In the next remark, we clarify the reason to introduce a robust control problem with a (fictitious) network-induced uncertainty in the state space realization of agents. Also, in the next theorem, we address the design problem in Design procedure 3.1.1.2.

Remark 3.1.2. *In state equation* (3.15)*, we know all B, D_{λ_2}, $E(\lambda_i)$, and u_{di}. However, we consider it as a network-induced uncertainty. As a result, we can find a single consensus protocol that works for all agents. Otherwise, there are $N-1$ nonzero eigenvalues of $\mathcal{L}$ which can be different scalar values. Thus, we may need up to $N-1$ different consensus protocols. As another result, based on this formulation, we propose a one-step design without calculating the coupling strength (see Subsection 1.2.2 at page 24 to find about the two-step design procedure in the literature).*

Theorem 3.1.2. *The solution* $u_{di} = K_c^x x_{di} = -R^{-1} D_{\lambda_2}^T B^T P x_{di}$ *of the modified LQR optimal control problem* (3.16) *subject to the nominal model in* (3.15) *solves the robust control problem of Design procedure 3.1.1.2. The matrix* P *represents the solution of algebraic Riccati equation (ARE)* (3.17)*, and* $Q = Q^T \succ \boldsymbol{0}$ *and* $R = R^T \succ \boldsymbol{0}$ *are the state and control input weighting matrices, respectively. This* K_c^x *provides the required gain in the consensus protocol* (3.4)*.*

$$\min_{u_{di} \in \mathbb{R}^{n_u}} \int_0^\infty (x_{di}^T Q x_{di} + u_{di} R u_{di}) dt \tag{3.16}$$

$$A^T P + PA + Q - PBD_{\lambda_2} R^{-1} D_{\lambda_2}^T B^T P = \boldsymbol{0} \tag{3.17}$$

Proof. This proof is provided at Subsection 3.4.2. □

Theorem 3.1.2 gives the required control gains in Design procedure 3.1.1.2, and so we have found the required result for Theorem 3.1.1.2. The reason to name (3.16) a "modified" LQR problem is that the minimization should be solved subject to a modified model of agents (affected by the communication topology through λ_2). In the next theorem, we address the first part of Theorem 3.1.1 by finding the required observer gains in (3.5) using a modified LQR formulation.

Theorem 3.1.3. *Let* $u_a = K_o^T x_a = -R_a^{-1} D_{a,\lambda_2} C_a^c P_a x_a$ *be the signal that solves the optimal control problem* (3.18) *subject to* (3.19)*. Then, this* $K_o = [K_o^{xT}, K_o^{wT}]^T$ *denotes the observer gain in Theorem 3.1.1.1. The matrix* P_a *indicates the solution of ARE* (3.20)*,* $Q_a = Q_a^T \succ \boldsymbol{0}$ *and* $R_a = R_a^T \succ \boldsymbol{0}$ *are two constant matrices,* $C_a^c = [C,\ \boldsymbol{0}]$*,* $D_{a,\lambda_2} = \lambda_2 I_{n_y}$*,* $E_a(\lambda_i) = D_{a,\lambda_2}^{-1} D_a(\lambda_i) - I_{n_y} \succeq \boldsymbol{0}$*, and* $D_a(\lambda_i) = \lambda_i I_{n_y}$*.*

$$\min_{u_a \in \mathbb{R}^{n_u}} \int_0^\infty (x_a^T Q_a x_a + u_a R_a u_a) dt \tag{3.18}$$

$$\dot{x}_a = A_a^T x_a + C_a^{cT} D_{a,\lambda_2}^T u_a \tag{3.19}$$

$$A_a P_a + P_a A_a^T + Q_a - P_a C_a^{cT} D_{a,\lambda_2}^T R_a^{-1} D_{a,\lambda_2} C_a^c P_a = 0 \tag{3.20}$$

Proof. This proof is given at Subsection 3.4.3. □

Based on the above results, the consensus protocol 3.4 results in a closed-loop multiagent system with stable disagreement dynamics (3.9) while rejecting persistent disturbances in the disagreement subspace. The remaining question is about the final agreement value in the presence of persistent disturbances, and under the effect of unobservable and uncontrollable agreement dynamics. Once the multiagent system's trajectory enters to its agreement subspace, the following lemma is valid (note that the disagreement dynamics are already stabilized).

Lemma 3.1.1. *For a multiagent system of* (3.1)-(3.2)*, if Assumption 3.1.1 is satisfied, the proposed consensus algorithm* (3.4)-(3.5) *results in the following agreement values:*

$$\begin{aligned} x_i^a(t) &= \tfrac{1}{N}\phi_{00}^A \textstyle\sum_{i=1}^N x_i(0) + \tfrac{1}{N}\phi_{11}^{13} \sum_{i=1}^N \tilde{z}_{wi}(0) \\ \tilde{x}_i^a(t) &= \tfrac{1}{N}\phi_{00}^A \textstyle\sum_{i=1}^N \tilde{x}_i(0) + \tfrac{1}{N}\phi_{11}^{23} \sum_{i=1}^N \tilde{z}_{wi}(0) \\ \tilde{z}_{wi}^a(t) &= \tfrac{1}{N}\phi_{11}^{33} \textstyle\sum_{i=1}^N \tilde{z}_{wi}(0) \end{aligned}$$

where the superscript ^{a} stands for the agreement value of each variable, and other parameters are defined as follows:

$$\phi_{00}^{A} = e^{At}, \quad \phi_{11}^{13} = -\int_0^t (e^{A(t-\tau)}\Gamma\theta e^{F\tau})d\tau, \quad \phi_{11}^{23} = \int_0^t (e^{A(t-\tau)}\Gamma\theta e^{F\tau})d\tau, \quad \phi_{11}^{33} = e^{Ft}$$

Proof. This proof is given in Subsection 3.4.4. □

Now, we summarize some observations about the result of previous lemma.

Remark 3.1.3. *Few points about the agreement values in Lemma 3.1.1 are:*

- *We need to note that Lemma 3.1.1 provides the agreement values of "estimation errors"* $\tilde{x}_i^a = \hat{x}_i^a - x_i^a$ *and* $\tilde{z}_{wi}^a = \hat{z}_{wi}^a - z_{wi}^a$. *This fact reflects the definition of closed-loop multiagent system* (3.6). *Then, we find that the final "estimated" values are* $\hat{x}_i^a = x_i^a + \frac{1}{N}\phi_{00}^A \sum_{i=1}^N \tilde{x}_i(0) + \frac{1}{N}\phi_{11}^{23} \sum_{i=1}^N (\hat{z}_{wi}^a(0) - z_{wi}(0)) = \frac{1}{N}\phi_{00}^A \sum_{i=1}^N x_i(0) + \frac{1}{N}\phi_{00}^A \sum_{i=1}^N \tilde{x}_i(0) = \frac{1}{N}\phi_{00}^A \sum_{i=1}^N \hat{x}_i(0)$. *In fact,* $\hat{x}_i^a = \boldsymbol{0}$ *whenever* $\hat{x}(0) = \boldsymbol{0}$. *Also,* $\hat{z}_{wi}^a = z_{wi}^a + \frac{1}{N}\phi_{11}^{33} \sum_{i=1}^N (\hat{z}_{wi}^a(0) - z_{wi}(0))$.

- *For a Hurwitz A,* $\phi_{00}^A \to \boldsymbol{0}$ *as* $t \to \infty$. *Thus, the results of Lemma 3.1.1 can be simplified to the following values:*

$$\begin{aligned} x_i^a &= \lim_{t\to\infty} \tfrac{1}{N}\phi_{11}^{13} \textstyle\sum_{i=1}^N \tilde{z}_{wi}(0) \\ \tilde{x}_i^a &= \lim_{t\to\infty} \tfrac{1}{N}\phi_{11}^{23} \textstyle\sum_{i=1}^N \tilde{z}_{wi}(0) \\ \tilde{z}_{wi}^a &= \lim_{t\to\infty} \tfrac{1}{N}\phi_{11}^{33} \textstyle\sum_{i=1}^N \tilde{z}_{wi}(0) \end{aligned}$$

  which end in the final estimated values $\hat{x}_i^a = x_i^a + \lim_{t\to\infty} \frac{1}{N}\phi_{11}^{23} \sum_{i=1}^N (\hat{z}_{wi}^a(0) - z_{wi}(0)) = \boldsymbol{0}$ *independent of* $\hat{x}(0)$, *and* $\hat{z}_{wi}^a = z_{wi}^a + \lim_{t\to\infty} \frac{1}{N}\phi_{11}^{33} \sum_{i=1}^N (\hat{z}_{wi}^a(0) - z_{wi}(0))$.

3.1.1.3 Simulation verification

Now, we implement our leaderless consensus algorithm over an undirected graph in Figure 3.1 with the following graph Laplacian:

$$\mathcal{L} = \begin{bmatrix} 3 & -1 & 0 & -1 & -1 \\ -1 & 3 & -1 & 0 & -1 \\ 0 & -1 & 2 & -1 & 0 \\ -1 & 0 & -1 & 3 & -1 \\ -1 & -1 & 0 & -1 & 3 \end{bmatrix}$$

In the next examples, we limit ourselves to the constant persistent disturbances (i.e., $F = 0$ and $\theta = 1$ in the disturbance generator model (3.5)). Then, starting from time $t = 0s$, the consensus signal (3.4) can be written as follows:

$$u_i(t) = K_c^x \hat{x}_i^r(t) + K_c^w K_o^w C \int_0^t x_i^r(\tau) - \hat{x}_i^r(\tau) d\tau$$

that is essentially a state-feedback control signal with integral actions on the differences of lumped relative-state measurements $x_i^r = \sum_{j \in \mathcal{N}_i} (x_i - x_j)$ and their

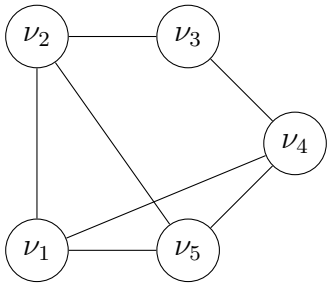

Figure 3.1: An undirected leaderless communication topology $\mathcal{G}$

estimated values $\hat{x}_i^r = \sum_{j\in\mathcal{N}_i}(\hat{x}_i - \hat{x}_j)$. In other words, for a constant disturbance, based on our knowledge about integral control or observer, the tracking error between the estimated lumped relative estimations and the actual lumped relative state variables will converge to zero.

In all cases, we initialize the system and disturbance (generator) state space models by $x_1(0) = [-10, 20]^T, x_2(0) = [15, -15]^T, x_3(0) = [10, 15]^T, x_4(0) = [-30, 20]^T, x_5(0) = [20, -30]^T$, $z_1(0) = 2, z_2(0) = 5, z_3(0) = 3, z_4(0) = 9, z_5(0) = 4$. Also, the disturbance state estimator is initialized by $\hat{z}_i = 0$ for all $i \in \{1, 2, 3, 4, 5\}$. We design the control gains using Design procedure 3.1.1.1 and Theorem 3.1.2, and the observer gains based on Theorem 3.1.3. Then, we calculate our expectations based on the Lemma 3.1.1 and Remark 3.1.3.

In the next example, we consider an unstable multiagent system with a nonzero initial state estimator value.

Example 3.1.1. *(Unstable agent dynamics) Consider the multiagent system* (3.1) *that realizes double-integrator agents by the following state space matrices:*

$$A = \begin{bmatrix} 0 & 1 \\ 0 & 0 \end{bmatrix}, \quad B = \begin{bmatrix} 0 \\ 1 \end{bmatrix}, \Gamma = \begin{bmatrix} 0 \\ 0.4 \end{bmatrix}, \quad C = \begin{bmatrix} 1 & 0 \end{bmatrix}$$

Furthermore, assume that all estate estimators are initialized at zero except $\hat{x}_3 = [10, -15]^T$. *Using the results of Lemma 3.1.1 and Remark 3.1.3, we find:*

$$
\begin{aligned}
x_i^a(t) &= \tfrac{1}{5} e^{At} \textstyle\sum_{i=1}^{5} x_i(0) - \tfrac{1}{5} \int_0^t e^{A(t-\tau)} \Gamma d\tau \sum_{i=1}^{5} \tilde{z}_{wi}(0) \\
&= \tfrac{1}{5} \begin{bmatrix} 1 & t \\ 0 & 1 \end{bmatrix} \textstyle\sum_{i=1}^{5} x_i(0) - \tfrac{8}{100} \int_0^t \begin{bmatrix} t-\tau \\ 1 \end{bmatrix} d\tau \sum_{i=1}^{5} \tilde{z}_{wi}(0) \\
&= \begin{bmatrix} 0.92t^2 + 2t + 1 \\ 1.84t + 2 \end{bmatrix} \\
\hat{x}_i^a(t) &= \tfrac{1}{5} e^{At} \textstyle\sum_{i=1}^{5} \hat{x}_i(0) = \begin{bmatrix} 1 & t \\ 0 & 1 \end{bmatrix} \begin{bmatrix} 2 \\ -3 \end{bmatrix} = \begin{bmatrix} 2 - 3t \\ -3 \end{bmatrix} \\
\hat{z}_{wi}^a &= z_{wi}^a - \tfrac{1}{5} \textstyle\sum_{i=1}^{5} \hat{z}_{wi}(0)
\end{aligned}
$$

where the last term results in $\hat{z}_{w1}^a = -2.6$, $\hat{z}_{w1}^a = 0.4$, $\hat{z}_{w1}^a = -1.6$, $\hat{z}_{w1}^a = 4.4$, $\hat{z}_{w1}^a = -0.6$. *Figures 3.2 and 3.3 depict the simulation verification results.*

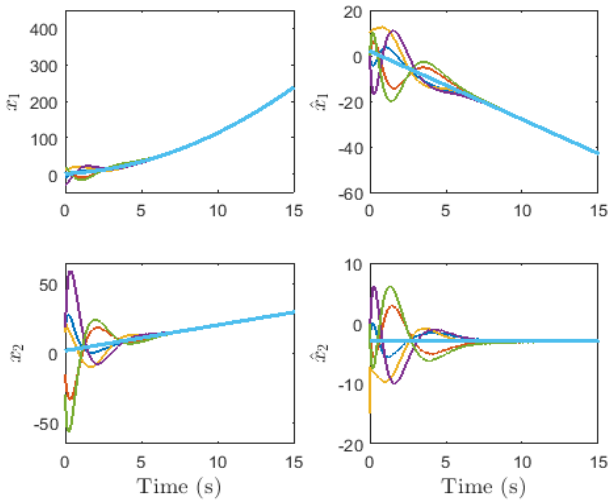

Figure 3.2: The time-varying leaderless agreement in a multiagent system of double-integrators in Example 3.1.1. From Top to bottom, Left: x_{i1} and x_{i2}, and Right: $\hat{x}_{i1}$ and $\hat{x}_{i2}$ for $i \in \{1, 2, ..., 5\}$. The thick light-blue curves show the expected trajectories which are calculated in Example 3.1.1.

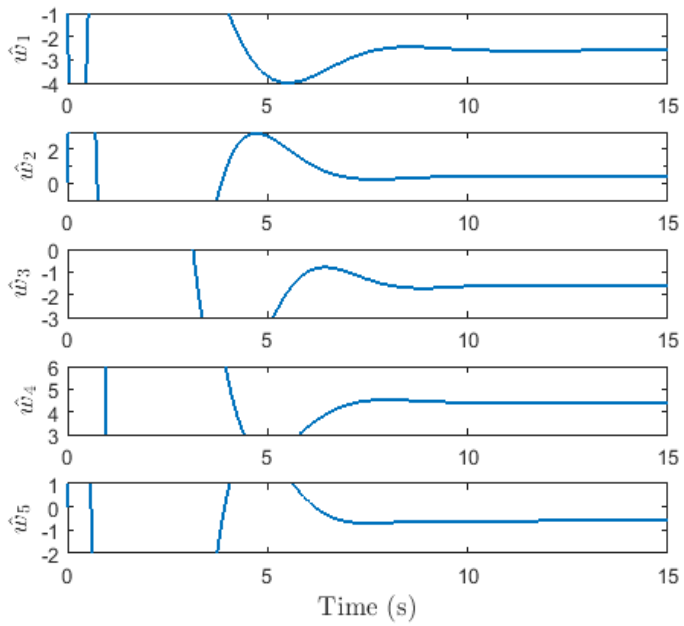

Figure 3.3: Final values of the estimated disturbances in leaderless Example 3.1.1. Top to bottom are $\hat{w}_1$ to $\hat{w}_5$. Along with the Remark 3.1.3, this confirms achieving agreement for some constant disturbances. (Note that the result of this section is focused on the steady-state agreement values, not the transient repose. In solving the proposed LQR problems, our emphasizes was on fast consensus. Thus, we omit the transient response and show the accuracy in calculating the final agreement values. Of course, different responses can be achieved by different trade-offs in selection of state and input weighting matrices.)

Now, we let all state estimators' initial values be zero, and investigate our claim about the state estimators' agreement value in Remark 3.1.3.

Example 3.1.2. *(Unstable agent dynamics) In Example 3.1.1, let* $\hat{x}_3(0) = \boldsymbol{0}$*. Now, the simulation result in Figure 3.4 verifies* $\hat{x}_i^a = \boldsymbol{0}$ *which could be expected based on the discussion in Remark 3.1.3.*

In the next example, we consider a stable multiagent system and observe the discussion in Remark 3.1.3.

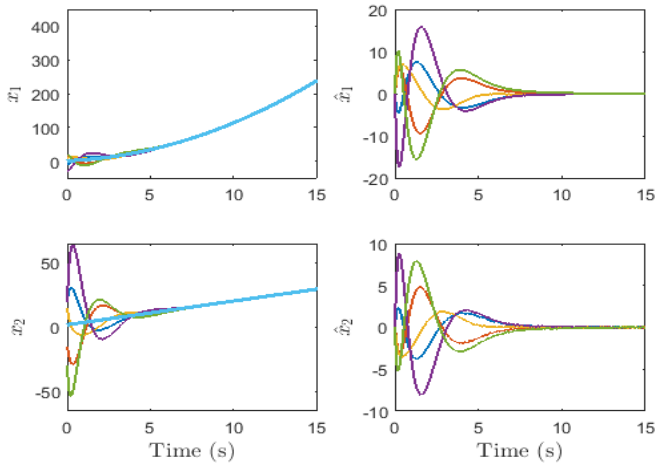

Figure 3.4: The time-varying leaderless agreement in a multiagent system of double-integrators under the same scenario as Example 3.1.1; however, with $\hat{x}_3(0) = \mathbf{0}$. From Top to bottom, Left: x_{i1} and x_{i2}, and Right: $\hat{x}_{i1}$ and $\hat{x}_{i2}$ for $i \in \{1, 2, ..., 5\}$.

Example 3.1.3. *(Stable agent dynamics) Assume a stable multiagent system of agents* (3.1) *specified by the following state space realization:*

$$A = \begin{bmatrix} 0 & 1 \\ -5 & -3 \end{bmatrix}, \quad B = \begin{bmatrix} 0 \\ 1 \end{bmatrix}, \Gamma = \begin{bmatrix} 0 \\ 0.4 \end{bmatrix}, \quad C = \begin{bmatrix} 1 & 0 \end{bmatrix}$$

We expect

$$x_i^a = \frac{1}{5} A^{-1} \Gamma \theta \sum_{i=1}^{5} z_{wi}(0) = \begin{bmatrix} 0.368 \\ 0 \end{bmatrix}, \quad \hat{x}_i^a = 0, \quad \hat{z}_{wi}^a = z_{wi} - \frac{1}{5} \sum_{i=1}^{5} z_{wi}(0)$$

which are confirmed by the simulation result in Figure 3.5 (the $\hat{z}_{wi}^a$ are the same as the previous examples and are not re-presented here).

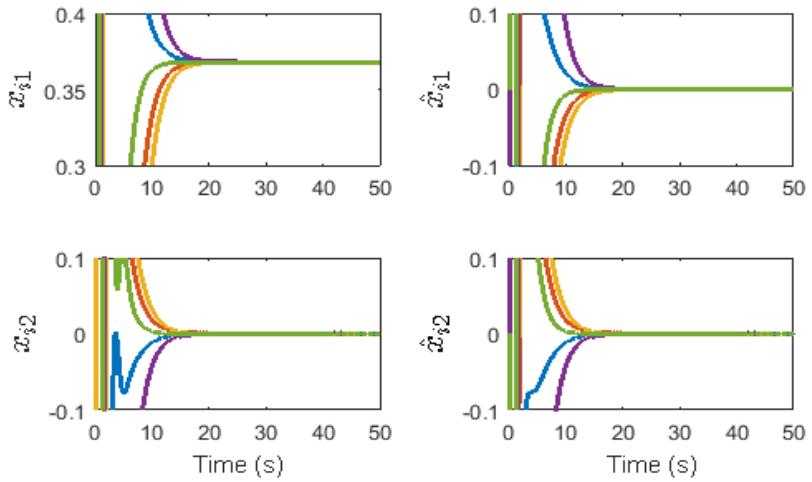

Figure 3.5: Final values of leaderless agents' states and their estimations. From Top to bottom, Left: x_{i1} and x_{i2}, and Right: $\hat{x}_{i1}$ and $\hat{x}_{i2}$ for $i \in \{1, 2, ..., 5\}$.

3.1.2 Leader-follower consensus

3.1.2.1 Problem statement

In the leaderless consensus problem of Subsection 3.1.1, we could ensure agreement on a common value that was a function of initial state and disturbance values. We showed that all state trajectories could converge to the agreement subspace which was built by the unobservable and uncontrollable disagreement dynamics. In this section, we propose a special communication topology and discuss the leader-follower consensus (tracking) problem. An example of this topology is shown in Figure 3.6 where, without loss of generality, we have added a new agent ν_0 to the simulation scenario of Figure 3.1. In this case, a leader agent with the following dynamics is added to the multiagent system:

$$\begin{aligned} \dot{x}_0 &= Ax_0 \\ y_0 &= Cx_0 \end{aligned} \tag{3.21}$$

where the $x_0 \in \mathbb{R}^{n_x}$ denotes the state vector and the $y_0 \in \mathbb{R}^{n_y}$ indicates the output of the leader agent. Assume that follower agents are similar to (3.1) in Subsection 3.1.1. We let these followers communicate to each other over an undirected graph $\mathcal{G}$ (similar to the leaderless scenario in Section 3.1). However, the leader is connected to a set of few followers over some directed edges where this leader and follower communication information (also known as pinning information) is lumped in $\mathcal{B} = diag\{[b_1, b_2, ..., b_N]\}$ where $b_i = 1$ when the i^{th} follower receives information from the leader and $b_i = 0$ otherwise, and $i \in \{1, 2, ..., N\}$.. Having this special leader-follower communication topology $\mathcal{G}_{lf}$, we let $\mathcal{H} = \mathcal{L} + \mathcal{B}$ be its reduced-order Laplacian matrix. Now, the leader-follower problem is solved when (3.22) is achieved by all follower agents $i \in \{1, 2, ..., N\}$ under the unknown disturbances w_i, and any initial conditions over the given graph topology $\mathcal{G}_{lf}$:

$$\lim_{t \to \infty} (x_i(t) - x_0(t)) = 0 \tag{3.22}$$

The following fact is known about any reduced-order Laplacian matrix $\mathcal{H}$:

Fact 3.1.1. *The reduced-order graph Laplacian $\mathcal{H}$ is positive definite if $\mathcal{G}_{lf}$ has a spanning tree with leader agent as the root.*

Furthermore, the following assumption is satisfied in this subsection:

Assumption 3.1.2. *There exists a directed path from the leader to each follower, and x_0 is known for those followers connected to the leader.*

Remark 3.1.4. *Let $\mathcal{L}_{lf} \in \mathbb{R}^{(N+1)\times(N+1)}$ be the graph Laplacian matrix for a leader-follower communication topology $\mathcal{G}_{lf}$ with one leader and N followers. With the leader agent as the root of a spanning tree, this $\mathcal{L}_{lf}$ has a simple zero eigenvalue, and $\mathcal{L}_{lf}$ can be partitioned as follows:*

$$\mathcal{L}_{lf} = \begin{bmatrix} 0 & \boldsymbol{0} \\ -b & \mathcal{H} \end{bmatrix}$$

where $\mathcal{H} = \mathcal{L} + \mathcal{B} \in \mathbb{R}^{N\times N}$, with $\mathcal{L} \in \mathbb{R}^{N\times N}$ as the graph Laplacian matrix of N followers' undirected graph $\mathcal{G}$, and $B \in \mathbb{R}^{N\times N}$ as defined previously. Therefore, we call $\mathcal{H}$ a reduced-order Laplacian matrix because the communication topology can be re-constructed knowing this matrix. Note that, by definition, $\mathcal{L}_{lf}$ has only one zero eigenvalue, and that corresponds to the first row. Also, we already see that $\mathcal{H}$ is a symmetric matrix with real-valued eigenvalues. Thus, we sort all eigenvalues

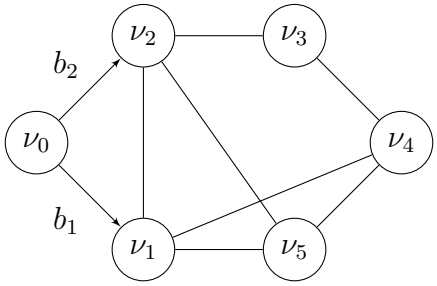

Figure 3.6: A special type of directed leader-follower communication topology $\mathcal{G}_{lf}$ where all followers ν_1-ν_5 communicate over an undirected graph $\mathcal{G}$ with a graph Laplacian matrix $\mathcal{L}$, and few followers (here, ν_1 and ν_2) receive information from the leader ν_0 over some directed edges with non-zero b_i (here, b_1 and b_2). This leader and follower connections can be lumped in a vector $b = [b_1, ..., b_5]^T$. Then, $\mathcal{H} = \mathcal{L} + \mathcal{B}$ represents a reduced-order graph Laplacian matrix for $\mathcal{G}_{lf}$ where $\mathcal{B} = diag\{b\}$.

of $\mathcal{H}$ *as* $0 < \mu_1 \leq \mu_2 \leq ... \leq \mu_N$. *Moreover, we can find a unitary transformation matrix that can convert* $\mathcal{H}$ *to a completely diagonal matrix* $\Lambda = diag\{\mu_i\}$.

3.1.2.2 Main results

Here, we consider a leader-follower multiagent system with a leader (3.21) and N followers (3.1)-(3.2) where the followers' output measurements are changed sa follows:

$$y_i^r = C(\sum_{j\in\mathcal{N}_i}(x_i - x_j) + b_i(x_i - x_0))$$

which include the leader's output whenever $b_i \neq 0$. We propose a dynamic consensus algorithm:

$$u_i = G_c^x\{\sum_{j\in\mathcal{N}_i}(\hat{x}_i - \hat{x}_j) + b_i(\hat{x}_i - x_0)\} + G_c^w\hat{z}_{wi} \tag{3.23}$$

using the following observers:

$$\begin{aligned}
\dot{\hat{x}}_i &= A\hat{x}_i + Bu_i + \Gamma\hat{w}_i + G_o^x(y_i^r - \hat{y}_i^r) \\
\dot{\hat{z}}_{wi} &= F\hat{z}_{wi} + G_o^w(y_i^r - \hat{y}_i^r) \\
\hat{y}_i^r &= \textstyle\sum_{j\in\mathcal{N}_i}(\hat{y}_i - \hat{y}_j) + b_i(\hat{y}_i - y_0) \\
\hat{w}_i &= \theta\hat{z}_{wi}
\end{aligned} \tag{3.24}$$

where $\hat{y}_i = C\hat{x}_i$, $G_c^x \in \mathbb{R}^{n_u\times n_x}$ and $G_c^w \in \mathbb{R}^{n_u\times n_{z_w}}$ denote the state-feedback and disturbance control gain, respectively; and $G_o^x \in \mathbb{R}^{n_x\times n_y}$ and $G_o^w \in \mathbb{R}^{n_{z_w}\times n_y}$ represent the state- and disturbance-observer gains, respectively.

Let $\epsilon_i = x_i - x_0$ be the leader-follower tracking error. Then, $\epsilon = col\{\epsilon_i\}$ denotes the aggregated leader-follower tracking error vector over $\mathcal{G}_{lf}$. Now, we find the augmented leader-follower tracking error, system state estimation error, and disturbance state estimation error dynamics:

$$\dot{\epsilon} = [(I_N \otimes A) + (\mathcal{H} \otimes BG_c^x)]\epsilon + [\mathcal{H} \otimes BG_c^x]\tilde{x} + [I_N \otimes BG_c^w]\tilde{z}_w + [I_N \otimes (BG_c^w + \Gamma\theta)]z_w$$

and

$$\begin{aligned} \dot{\tilde{x}} &= [(I_N \otimes A) - (\mathcal{H} \otimes G_o^x C)]\tilde{x} + [I_N \otimes \Gamma\theta]\tilde{z}_w \\ \dot{\tilde{z}}_w &= -[\mathcal{H} \otimes G_o^w C]\tilde{x} + [I_N \otimes F]\tilde{z}_w \end{aligned} \tag{3.25}$$

We follow an idea similar to Subsection 3.1.1.2, and find the following transformed diagonalized representation:

$$\begin{bmatrix} \dot{\epsilon}_T \\ \dot{e}_{oT} \end{bmatrix} = \begin{bmatrix} \bar{M}_{11} & \bar{M}_{12} \\ \mathbf{0} & \bar{M}_{22} \end{bmatrix} \begin{bmatrix} \epsilon_T \\ e_{oT} \end{bmatrix} + \begin{bmatrix} \bar{N}_1 \\ \mathbf{0} \end{bmatrix} z_{wT} \tag{3.26}$$

where $\epsilon_T \triangleq (T^{-1} \otimes I_{n_x})\epsilon$, and:

$$\begin{aligned} \bar{M}_{11} &= (I_N \otimes A) + \Lambda \otimes BG_c^x, & \bar{M}_{12} &= [(\Lambda \otimes BG_c^x),\ (I_N \otimes BG_c^w)] \\ \bar{M}_{22} &= \begin{bmatrix} \bar{M}_{22}^{11} & \bar{M}_{22}^{12} \\ \bar{M}_{22}^{21} & \bar{M}_{22}^{22} \end{bmatrix}, & \bar{N}_1 &= I_N \otimes (BG_c^w + \Gamma\theta) \\ \bar{M}_{22}^{11} &= (I_N \otimes A) - (\Lambda \otimes G_o^x C), & \bar{M}_{22}^{12} &= I_N \otimes \Gamma\theta \\ \bar{M}_{22}^{21} &= -\Lambda \otimes G_o^w C, & \bar{M}_{22}^{22} &= I_N \otimes F \end{aligned}$$

Based on the Remark 3.1.4, all eigenvalues of $\mathcal{H}$ are positive real numbers (compared to the leaderless consensus where $\lambda_1 = 0$). Thus, we take all (diagonal) subsystems of (3.26) to get (3.27) and (3.28):

$$\begin{aligned} \dot{\epsilon}_{Ti} &= A\epsilon_{Ti} + Bu_{Ti} + \Gamma\theta z_{wTi} \\ y_{\epsilon i} &= \mu_i \epsilon_{Ti} \\ u_{Ti} &= G_c^x y_{\epsilon i} + G_c^w \hat{z}_{wTi} \end{aligned} \tag{3.27}$$

$$\begin{bmatrix} \dot{\tilde{x}}_{Ti} \\ \dot{\tilde{z}}_{wTi} \end{bmatrix} = \left(\begin{bmatrix} A & \Gamma\theta \\ \mathbf{0} & F \end{bmatrix} - \begin{bmatrix} G_o^x \\ G_o^w \end{bmatrix} \begin{bmatrix} \mu_i C & \mathbf{0} \end{bmatrix} \right) \begin{bmatrix} \tilde{x}_{Ti} \\ \tilde{z}_{wTi} \end{bmatrix} \tag{3.28}$$

Now, in the next theorem, we convert the leader-follower consensus task to a stability problem.

Theorem 3.1.4. *Suppose that Assumption 3.1.1.a to c, and Assumption 3.1.2 are satisfied for a leader-follower multiagent system of this subsection. The closed-loop multiagent system with an observer-based consensus algorithm* (3.23)-(3.24) *solves the leader-follower consensus problem* (3.22) *if:*

1. *The observer gain* $G_o = \begin{bmatrix} G_o^x \\ G_o^w \end{bmatrix}$ *results in a Hurwitz matrix* $\begin{bmatrix} A - \lambda_i G_o^x C & \Gamma\theta \\ -\lambda_i G_o^w C & F \end{bmatrix}$ *with eigenvalues in left half plane, sufficiently far away the imaginary axis.*
2. *The control-gain* $G_c = \begin{bmatrix} G_c^x & G_c^w \end{bmatrix}$ *stabilizes* (3.27) *for all eigenvalues of* $\mathcal{H}$*, and rejects the unknown persistent disturbance* $w_{Ti} = \theta z_{wTi}$*.*

Proof. Since $\mu_i > 0$ for all $i \in \{1, 2, ..., N\}$, this proof is similar to that of Theorem 3.1.1 (corresponding to $\lambda_i \neq 0$ for $i \in \{2, ..., N\}$), and we skip it for brevity. □

Also, the design procedure to find appropriate control gains can be summarized as follows:

Design procedure 3.1.2. *The control gains in* (3.23) *can be designed in two steps:*

1. *Disturbance gain* G_c^w*: this gain is designed to minimize the* $\|BG_c^w + \Gamma\theta\|$*. Based on the Assumption 3.1.1.c, the* $G_c^w = -B^\dagger\Gamma\theta$ *rejects the unknown disturbance.*

2. *State feedback gain G_c^x: using a G_c^w of the previous step, we design a feedback gain G_c^x that solves the robust control problem* (3.29) *for a fictitious modeling uncertainty due to $B_\mu \triangleq BD(\mu_i)$ where $D(\mu_i) \triangleq \mu_i I_{n_u}$.*

$$\begin{aligned} \dot{\epsilon}_{Ti} &= A\epsilon_{Ti} + B_\lambda u_{Ti} \\ u_{Ti} &= G_c^x \epsilon_{Ti} \end{aligned} \quad . \tag{3.29}$$

Now, we propose two theorems in order to find these "appropriate" state-feedback and -observer gains. These theorems complete the design of our relative output-based leader-follower consensus protocol.

Theorem 3.1.5. *Assume that $u_{Ti} = G_c^x x_{Ti}$ with $G_c^x = -R_\epsilon^{-1} D_\mu^T B^T P_\epsilon$ solves the modified LQR problem* (3.30) *subject to a dynamical system* (3.31) *where P_ϵ denotes solution of ARE* (3.32)*, $Q_\epsilon = Q_\epsilon^T \succ \boldsymbol{0}$ and $R_\epsilon = R_\epsilon^T \succ \boldsymbol{0}$ are two constant matrices, $D_\mu = \mu_1 I_{n_u}$, and $E(\mu_i) \triangleq D_\mu^{-1} D(\mu_i) - I_{n_u} \succeq \boldsymbol{0}$. Then, this u_{Ti} also stabilizes the uncertain system* (3.33) *which indicates solving the leader-follower consensus problem* (3.22) *using full state feedback measurement.*

$$\min_{u_{Ti} \in \mathbb{R}^{n_u}} \int_0^\infty (\epsilon_{Ti}^T Q_\epsilon \epsilon_{Ti} + u_{Ti} R_\epsilon u_{Ti}) dt \tag{3.30}$$

$$\dot{\epsilon}_{Ti} = A\epsilon_{Ti} + BD_\mu u_{Ti} \tag{3.31}$$

$$A^T P_\epsilon + P_\epsilon A + Q_\epsilon - P_\epsilon B D_\mu R^{-1} D_\mu^T B^T P_\epsilon = \boldsymbol{0} \tag{3.32}$$

$$\dot{\epsilon}_{Ti} = A\epsilon_{Ti} + BD_\mu u_{Ti} + BD_\mu E(\mu_i) u_{Ti} \tag{3.33}$$

Proof. This proof is similar to the proof of Theorem 3.1.2. Also, see the discussion in proof of Theorem 3.1.4. □

Theorem 3.1.6. *Let $u_{\epsilon a} = G_{\epsilon a}^T x_{\epsilon a} = -R_{\epsilon a}^{-1} D_{\epsilon a,\mu} C_{\epsilon a} P_{\epsilon a} x_{\epsilon a}$ be the signal that solves the minimize problem* (3.34) *subject to* (3.35) *where $P_{\epsilon a}$ denotes the solution of*

ARE (3.36), $Q_{\epsilon a} = Q_{\epsilon a}^T \succ \boldsymbol{0}$ *and* $R_{\epsilon a} = R_{\epsilon a}^T \succ \boldsymbol{0}$ *are two constant matrices,* $C_{\epsilon a} = [C,\ \boldsymbol{0}]$, $D_{\epsilon a,\mu} = \mu_1 I_{n_y}$, $E_{\epsilon a}(\mu_i) = D_{\epsilon a,\mu_1}^{-1} D_{\epsilon a}(\mu_i) - I_{n_y} \succeq \boldsymbol{0}$, *and* $D_{\epsilon a}(\mu) = \mu_i I_{n_y}$. *This* $u_{\epsilon a}$ *stabilizes the uncertain models* (3.37), *and, thus,* $G_{\epsilon a}$ *gives the observer gain in Theorem 3.1.4.1.*

$$\min_{u_{\epsilon a} \in \mathbb{R}^{n_u}} \int_0^\infty (x_{\epsilon a}^T Q_{\epsilon a} x_{\epsilon a} + u_{\epsilon a} R_{\epsilon a} u_{\epsilon a}) dt \tag{3.34}$$

$$\dot{x}_{\epsilon a} = A_a^T x_{\epsilon a} + C_{\epsilon a}^T D_{\epsilon a,\mu}^T u_{\epsilon a} \tag{3.35}$$

$$A_a P_{\epsilon a} + P_{\epsilon a} A_a^T + Q_{\epsilon a} - P_{\epsilon a} C_{\epsilon a}^T D_{\epsilon a,\mu}^T R_{\epsilon a}^{-1} D_{\epsilon a,\mu} C_{\epsilon a} P_{\epsilon a} = \boldsymbol{0} \tag{3.36}$$

$$\dot{x}_{\epsilon a} = A_a^T x_{\epsilon a} + C_{\epsilon a}^T D_{\epsilon a,\mu}^T u_{\epsilon a} + C_{\epsilon a}^T D_{\epsilon a,\mu_1} E_{\epsilon a}(\mu_i) u_{\epsilon a} \tag{3.37}$$

Proof. This proof is similar to the proof of Theorem 3.1.3. Also, see the discussion in proof of Theorem 3.1.4. □

3.1.2.3 Simulation verification

Here, we consider the leader-follower communication topology of Figure 3.6 with the following reduced-order Laplacian matrix:

$$\mathcal{H} = \begin{bmatrix} 4 & -1 & 0 & -1 & -1 \\ -1 & 4 & -1 & 0 & -1 \\ 0 & -1 & 2 & -1 & 0 \\ -1 & 0 & -1 & 3 & -1 \\ -1 & -1 & 0 & -1 & 3 \end{bmatrix}$$

Example 3.1.4. *(Stable agent dynamics) Consider the state space model of Example 3.1.3. Assume there exists a leader with an initial condition* $x_0(0) = [15, 15]^T$.

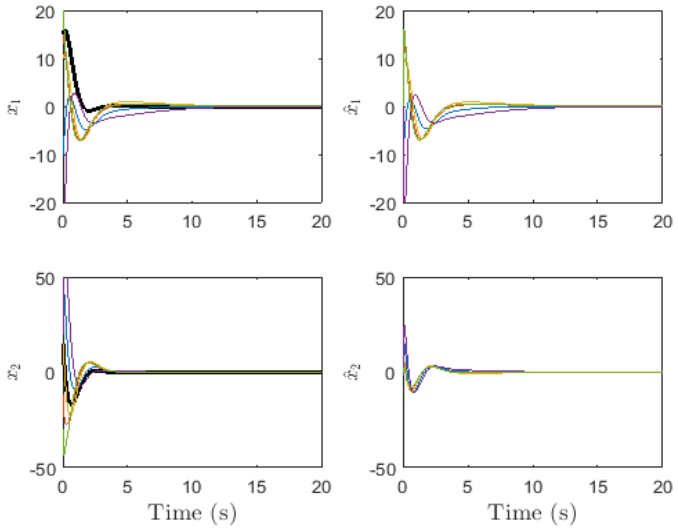

Figure 3.7: Leader-follower tracking problem in Example 3.1.4. From Top to Bottom, Left: x_{i1} and x_{i2}, and Right) $\hat{x}_{i1}$ and $\hat{x}_{i2}$ for $i \in \{0, 1, 2, ..., 5\}$. The thick black curves correspond to the leader agent.

However, now, we assume that followers are subjected to $w_1 = sin(0.5t)$, $w_2 = 1.5sin(0.5t)$, $w_3 = 2sin(0.5t)$, $w_4 = 0.5sin(0.5t)$, *and* $w_5 = sin(0.5t)$. *We use Design procedure 3.1.2.1, Theorem 3.1.5, and Theorem 3.1.6 to find the control and observer gains. The simulation results are depicted in Figures 3.7 and 3.8 that indicate the leader-follower consensus problem* (3.22) *is solved, and the disturbances are estimated precisely. In this example, we note that there exists no* $\mathcal{L}$*-induced null space (unobservable agreement dynamics) to degrade the disturbance estimation performance.*

Example 3.1.5. *(Unstable agent dynamics) Consider an unstable multiagent system with the following state matrix and leave other matrices the same as previous examples in this chapter:*

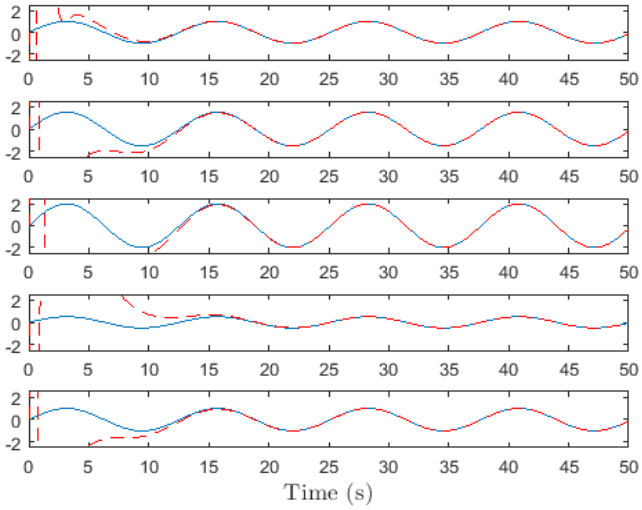

Figure 3.8: Disturbances (solid blue) and their estimated values (dashed red) in leader-follower tracking problem Example 3.1.4. From top to bottom correspond to the disturbances w_1, w_2, w_3, w_4, and w_5.

$$A = \begin{bmatrix} 0 & 1 \\ -1 & 0 \end{bmatrix}$$

which results in an oscillatory time-response by the leader. The leader-follower tracking capability of our algorithm, and disturbance estimation results are depicted in Figure 3.9 and Figure 3.10, respectively.

Example 3.1.6. *(Unstable agent dynamics) Now, consider the example 3.1.1 under a leader-follower tracking scenario. Here, the leader's initial condition is* $x_0 = [0, 5]^T$. *As is depicted in Figure 3.11, followers agree on the leader's position* $x_{01}(t) = 5t$ *and follow it with the leader's velocity* $x_{02} = 5$. *Moreover, the state estimators are able to precisely estimate the agents' state variables using only lumped relative-measurements in their neighborhood. Additionally, Figure 3.12*

shows that the disturbances can also be estimated precisely. We mention that in Example 3.1.1, the constant disturbance was persistently exciting the unobservable (uncontrollable) agreement dynamics and, therefore, we observed an increased velocity in all agents (with constant acceleration which was not shown, but could easily be guessed based on the calculated velocity).

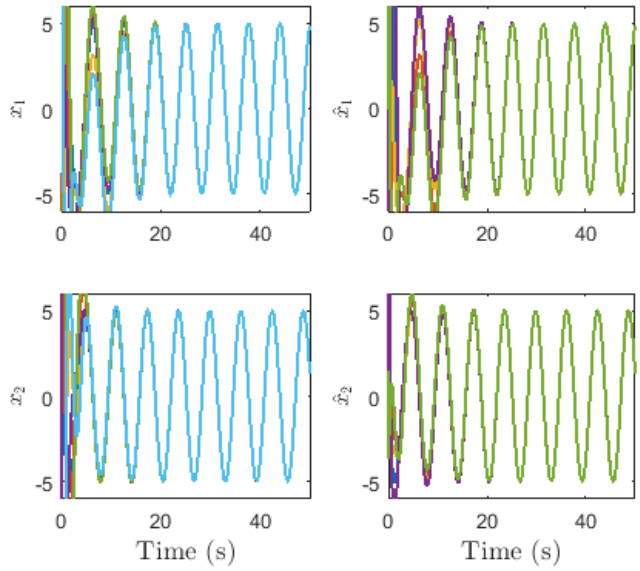

Figure 3.9: Leader-follower tracking problem with an unstable leader in Example 3.1.5. From Top to Bottom, Left: x_{i1} and $\hat{x}_{i1}$, and Right: $\hat{x}_{i1}$ and $\hat{x}_{i2}$ for $i \in \{0, 1, 2, ..., 5\}$.

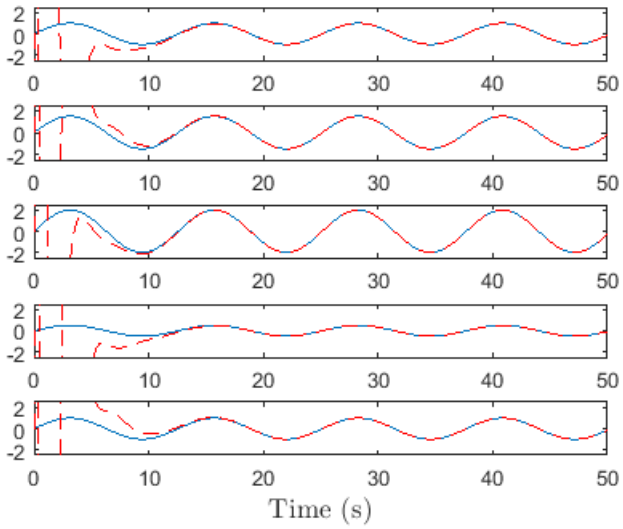

Figure 3.10: Disturbances (solid blue) and their estimated values (dashed red) in leader-follower tracking problem with an unstable leader in Example 3.1.5. From top to bottom correspond to the disturbances w_1, w_2, w_3, w_4, and w_5.

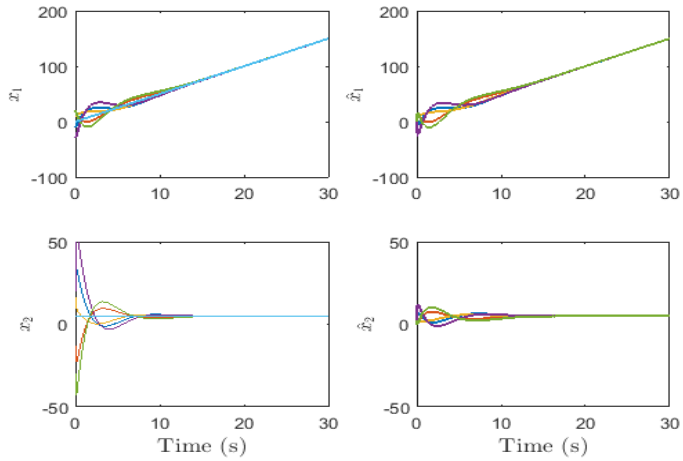

Figure 3.11: Leader-follower tracking problem with an unstable leader in Example 3.1.6. From Top to Bottom, Left: x_{i1} and x_{i2}, and Right: $\hat{x}_{i1}$ and $\hat{x}_{i2}$ for $i \in \{0, 1, 2, ..., 5\}$.

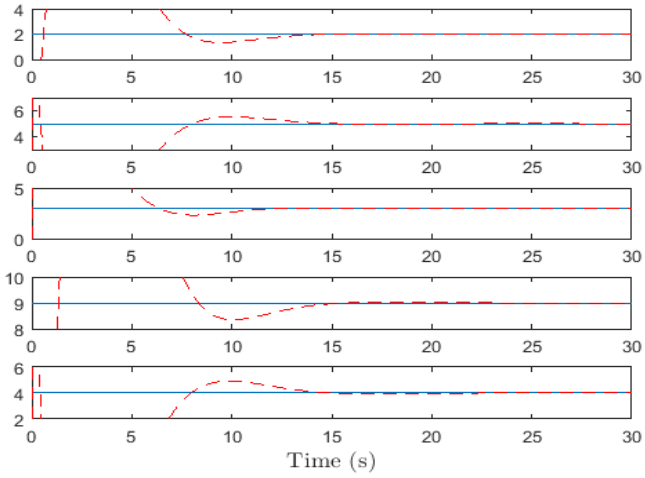

Figure 3.12: Disturbances (solid blue) and their estimated values (dashed red) in leader-follower tracking problem with an unstable leader in Example 3.1.6. From top to bottom correspond to the disturbances w_1, w_2, w_3, w_4, and w_5.

3.2 Distributed leaderless consensus of operating point-dependent linear multiagent systems

The existing consensus algorithms are mainly about completely known linear time-invariant agent models. However, the linear time-invariant model of a dynamical system usually is an approximations of a nonlinear dynamic behavior at some fixed operating conditions. Under a more realistic scenario, the state space realization (2.13) can be generalized to a model with a time-varying triple $(A(t), B(t), C(t))$. In some circumstances, we are able to approximate a nonlinear model with a set of linear models that are characterized by some independent variables that determine, or depend on, the operating condition of a system. Then,

the state space realization (2.13) is rewritten as a parameter-dependent model with the triple $(A(\theta(t)), B(\theta(t)), C(\theta(t)))$.

In this section, we consider a multiagent system where all agents can be characterized by the same unknown independent parameter $\theta(t)$, and propose two linear quadratic regulator formulations which address the leaderless consensus problem based on some fundamental concepts from the optimal control theory in Section 2.4.

3.2.1 Problem statement

Consider a group of agents communicating over an undirected graph $\mathcal{G}$:

$$\dot{x}_i = A(\theta(t))x_i + B(\theta(t))u_i \tag{3.38}$$

where $i \in \{1, 2, ..., N\}$ indicates the agent number, $x_i \in \mathbb{R}^{n_x}$ denotes the state vector, $u_i \in \mathbb{R}^{n_u}$ represents the control input vector, $A(\theta) \triangleq \sum_{m=0}^{n_\theta}(A_m\theta^m) \in \mathbb{R}^{n_x \times n_x}$ stands for the parameter-dependent state matrix, $B(\theta) \triangleq \sum_{m=0}^{n_\theta}(B_m\theta^m) \in \mathbb{R}^{n_x \times n_u}$ refers to the parameter-dependent control input matrix, $A_m \in \mathbb{R}^{n_x \times n_x}$ and $B_m \in \mathbb{R}^{n_x \times n_u}$ denote some known coefficient matrices, and the real-valued scalar parameter $\theta(t) \in [\theta_{min}, \theta_{max}]$ indicates an independent-parameter that determines the operating condition of the multiagent system. The parameter θ is *unknown* but the lower bound $\theta_{min} \in \mathbb{R}$ and the upper bound $\theta_{max} \in \mathbb{R}$ are two known constants. Thus, the state space model (3.38) represents a partially-unknown multiagent system where the unknown independent parameter $\theta(t)$ specifies the multiagent system-level operating point. Proposing a high-order polynomial of

$\theta(t)$ in modeling of state-space realization matrices, enables us to handle the nonlinear dependency of the linearized model to the operating point[4].

In the rest of this section, the objective is achieving the leaderless consensus among a set of N agents (3.38), which is repeated here:

$$\lim_{t\to\infty}(x_i(t) - x_j(t)) = \mathbf{0} \tag{3.39}$$

We consider two different scenarios:

1. For $m \in \{1, 2, ..., n_\theta\}$, assume that neither A_m nor B_m is in the range space of B_0. As a result, we find the following state space model:

$$\begin{aligned} \dot{x}_i &= A_0 x_i + B_0 u_i + w_i(x_i, u_i) \\ w_i(x_i, u_i) &= C_{Ui} x_i + D_{Ui} u_i \end{aligned} \tag{3.40}$$

   where $w_i \in \mathbb{R}^{n_x}$ captures the effect of unknown operating condition in (3.38) and acts as a state- and control input-dependent perturbation. Also, $C_{Ui} = \sum_{m=1}^{n_\theta}(A_m\theta^m)$ and $D_{Ui} = \sum_{m=1}^{n_\theta}(B_m\theta^m)$.

2. For $m \in \{1, 2, ..., n_\theta\}$, assume $B_m = \mathbf{0}$, and A_m be in the range space of B_0:

$$\begin{aligned} \dot{x}_i &= A_0 x_i + B_0(u_i + z_i(x_i)) \\ z_i(x_i) &= C_{Mi} x_i \end{aligned} \tag{3.41}$$

   where $z_i \in \mathbb{R}^{n_u}$ denote the matched uncertain term, due to an unknown operating-point, and $C_{Mi} = B_0^\dagger \sum_{m=1}^{n_\theta}(A_m\theta^m)$.

[4]To provide a physical sense, we may imagine a group of aircraft flying at the same altitude $\theta(t)$ that may change during the time. Specifically, this scenario can be the case for the flight formation control problem. Also, in a wind farm of similar wind turbines, assuming all wind turbines are subjected to the same wind speed, we can show that a first-order polynomial of θ is sufficient to model the wind-dependent behavior of wind turbine in region 3, for the purpose of generator speed or electrical power regulation. However, the high-order polynomial matrices might be required to capture wind turbine's wind-dependent behavior in entire regions 2, 2.5, and 3.

Remark 3.2.1. *Equivalently, instead of assuming the existence of $B_0^\dagger$, we could impose the structural assumption $A(\theta_i) = \sum_{m=0}^{n_\theta}(A'_m\theta_i^m)$ where $A'_0 = A_0$ and $A'_m = B_0A_m$ for $m \in \{1, 2, ..., n_\theta\}$ in order to find a similar multiagent system with a matched uncertainty.*

We design a distributed consensus signal u_i such that the leaderless consensus problem (3.39) is achieved by agents (3.38) (rewritten as (3.40) or (3.41)). The following assumption holds true in this section:

Assumption 3.2.1. *(a) The pair (A_0, B_0) characterizes a stabilizable state space realization, and (b) the graph $\mathcal{G}$ is connected.*

3.2.2 Main results

3.2.2.1 Equivalent multiagent system with unmatched modeling uncertainty

We first rewrite the i^{th} agent's model (3.40) as follows:

$$\begin{gathered} \dot{x}_i = A_0x_i + B_0u_i + w_i(x_i, u_i) \\ w_i(x_i, u_i) = \sum_{m=1}^{n_\theta} w_{mi}(x_i, u_i) \qquad w_{mi}(x_i, u_i) = A_m\theta^m x_i + B_m\theta^m u_i \end{gathered} \tag{3.42}$$

We propose the following distributed consensus protocol:

$$u_i = K_U \sum_{j\in\mathcal{N}_i}(x_i - x_j) \tag{3.43}$$

where $K_U \in \mathbb{R}^{n_u\times n_x}$ denotes the consensus gain for a multiagent system with unmatched uncertainties. Let $x = col\{x_i\}$ be the aggregated state vector and $u = diag\{u_i\}$ be the aggregated control input. We further define $w_m(x, u) =$

$col\{w_m(x_i,u_i)\}$ and introduce $w(x,u) = col\{w_i(x_i,u_i)\} := \sum_{m=1}^{n_\theta} w_m(x,u)$ as the aggregated unmatched uncertainty. Then, we find:

$$\begin{aligned} \dot{x} &= (I_N \otimes A_0)x + (I_N \otimes B_0)u + w(x,u) \\ w_m(x,u) &= (I_N \otimes A_m)\theta^m x + (I_N \otimes B_m)\theta^m u \end{aligned} \tag{3.44}$$

where we have a coupled-by-communication consensus algorithm over $\mathcal{G}$:

$$u = (\mathcal{L} \otimes K_U)x \tag{3.45}$$

which means, we need to design a distributed consensus signal u that is coupled through $\mathcal{L}$. We decompose this coupled consensus signal as follows:

$$u = (\mathcal{L} \otimes I_{n_u})\nu \quad \textit{and} \quad \nu = (I_N \otimes K_U)x \tag{3.46}$$

and, by passing the coupled term into the system's dynamics, find a new representation for the aggregated multiagent system:

$$\begin{aligned} \dot{x} &= (I_N \otimes A_0)x + (\mathcal{L} \otimes B_0)\nu + w(x,\nu) \\ w_m(x,\nu) &= (I_N \otimes A_m)\theta^m x + (\mathcal{L} \otimes B_m)\theta^m \nu \end{aligned} \tag{3.47}$$

which is coupled by two terms $\mathcal{L} \otimes B_0$ (known) and $\sum_{m=1}^{n_\theta}(\mathcal{L} \otimes B_m)\theta^m$ (unknown). Compared to (3.46), we now focus on designing a "decoupled" control signal:

$$\nu = (I_N \otimes K_U)x \tag{3.48}$$

Let $x_T \triangleq (T^{-1} \otimes I_{n_x})x$, $\nu_T \triangleq (T^{-1} \otimes I_{n_u})\nu$, and $w_{mT} \triangleq (T^{-1} \otimes I_{n_x})w_m$ such that $w_T \triangleq (T^{-1} \otimes I_{n_x})w = \sum_{m=1}^{n_\theta} w_{mT}(x_T,\nu_T)$. Based on the Fact 2.2.1, we find a partitioned multiagent system model as follows:

$$\begin{bmatrix} \dot{x}_{T1} \\ \dot{x}_{Td} \end{bmatrix} = \begin{bmatrix} A_0 & \mathbf{0} \\ \mathbf{0} & I_{N-1} \otimes A_0 \end{bmatrix} \begin{bmatrix} x_{T1} \\ x_{Td} \end{bmatrix} + \begin{bmatrix} \mathbf{0} & \mathbf{0} \\ \mathbf{0} & \Lambda_d \otimes B_0 \end{bmatrix} \begin{bmatrix} \nu_{T1} \\ \nu_{Td} \end{bmatrix} + \begin{bmatrix} w_{T1}(x_{T1}) \\ w_{Td}(x_{Td}, \nu_{Td}) \end{bmatrix} \tag{3.49}$$

Now, we need to design a decoupled consensus signal $\nu_T = (I_N \otimes K_U)x_T$ for the decoupled multiagent system model (3.49). Here, $x_T = [x_{T1}^T, x_{Td}^T]^T$, $\nu_T = [\nu_{T1}^T, \nu_{Td}^T]^T$, and $w_T(x_T, \nu_T) = [w_{T1}^T(x_{T1}), w_{Td}^T(x_{Td}, \nu_{Td})]^T$. The (disagreement) aggregated variable x_{Td} is defined by $x_{Td} = [x_{T2}^T, ..., x_{TN}^T]^T$; similarly, we find $\nu_{Td} = [\nu_{T2}^T, ..., \nu_{TN}^T]^T$ and $w_{Td} = [w_{T2}^T, ..., w_{TN}^T]^T$. Furthermore, note that we have used a partitioned diagonal matrix $\Lambda = diag\{[0, \Lambda_d]\}$ where $\Lambda_d = diag\{\lambda_i\}$, and λ_i denote nonzero eigenvalues of $\mathcal{G}$ for $i \in \{2, 3, .., N\}$.

There is no control on the first row of (3.49) that corresponds to the agreement space. (The effect of agreement dynamics will be discussed in Lemma 3.2.1 and Lemma 3.2.2.) The second row of (3.49) corresponds to the controllable disagreement dynamics, and is rewritten as follows:

$$\underbrace{\dot{x}_{Td} = \bar{A}_0 x_{Td} + \bar{B}_0 \nu_{Td}}_{\text{Network-level nominal multiagent system}} \quad + \underbrace{\bar{B}_0 \bar{E} \nu_{Td} + w_{Td}(x_{Td}, \nu_{Td})}_{\text{Network-level uncertainty}} \tag{3.50}$$

where $\bar{A}_0 = I_{N-1} \otimes A_0$, $\bar{B}_0 = I_{N-1} \otimes \lambda_2 B_0$, and $\bar{E} = (\frac{\Lambda_d}{\lambda_2} - I_{N-1}) \otimes I_{n_u}$ (A discussion similar to Remark 3.1.2 at page 70 can be made for introducing the network-level uncertainty in state equation (3.50)). We limit the synthesis of consensus gain K_U to the disagreement dynamics by introducing the reduced-order consensus signal $\nu_{Td} \in \mathbb{R}^{(N-1)n_u}$ with $\bar{K}_U = (I_{N-1} \otimes K_U)$:

$$\nu_{Td} = \bar{K}_U x_{Td} \tag{3.51}$$

We now propose an *auxiliary multiagent system*:

$$\dot{x}_{Td} = \bar{A}_0 x_{Td} + \bar{B}_0 \nu_{Td} + \tau \tag{3.52}$$

where $\tau = [\tau_2^T, ..., \tau_N^T]^T \in \mathbb{R}^{(N-1)n_x}$ denotes a *fictitious control input*[5] that has been added to handle the effect of $w_{Td}(x_{Td}, \nu_{Td}) \in \mathbb{R}^{(N-1)n_x}$.

We briefly re-state that the *distributed consensus algorithm design objective* was to steer disagreement dynamics' trajectory toward the agreement subspace using the consensus protocol (3.51). To design an appropriate consensus gain K_U, we have proposed a disagreement dynamics stabilization problem, and we further have proposed an auxiliary multiagent system model in order to handle the effect of unmatched modeling uncertainties.

Let $\bar{R}_\tau = I_{N-1} \otimes R_\tau$ and $R_\tau = r_\tau I_{n_x}$ where $r_\tau > 0$ is a design parameter. We always can find a quadratic upper bound on w_{Td}:

$$w_{Td}^T \bar{R}_\tau w_{Td} \leq x_{Td}^T \bar{R}_\tau^x x_{Td} + \nu_{Td}^T \bar{R}_\tau^\nu \nu_{Td} =: w_{TdM}^T \bar{R}_\tau w_{TdM} \tag{3.53}$$

using Fact 2.1.2, and Rayleigh-Ritz inequality in Fact 2.1.1. Here, $\bar{R}_\tau^x = I_{N-1} \otimes R_\tau^x$, $\bar{R}_\tau^\nu = I_{N-1} \otimes R_\tau^\nu$, $R_\tau^\nu = r_\tau^\nu I_{n_u}$, and $r_\tau^x, r_\tau^\nu > 0$. An example is provided to clarify successive use of Fact 2.1.2 at page 39.

Example 3.2.1. *Let $n_\theta = 2$. We write $w_{Td} = w_{Td1} + w_{Td2}$ where $w_{Td1} = (I_{N-1} \otimes A_1)\theta x_{Td} + (I_{N-1} \otimes A_)\theta^2 x_{Td}$ and $w_{Td2} = (I_{N-1} \otimes B_1)\theta \nu_{Td} + (I_{N-1} \otimes B_2)\theta^2 \nu_{Td}$. Then, a way to calculate the upper bound* (3.53) *is as follows:*

[5]The numbering matches that of ν_{Td} and, in fact, τ_1 does not exist.

$$
\begin{aligned}
w_{Td}^T \bar{R}_\tau w_{Td} &= (w_{Td1} + w_{Td2})^T \bar{R}_\tau (w_{Td1} + w_{Td2}) \\
&\leq 2 w_{Td1}^T \bar{R}_\tau w_{Td1} + 2 w_{Td2}^T \bar{R}_\tau w_{Td2} \\
&\leq x_{Td}^T (I_{N-1} \otimes A_1^T)(4\theta^2 \bar{R}_\tau)(I_{N-1} \otimes A_1) x_{Td} \\
&\quad + x_{Td}^T (I_{N-1} \otimes A_2^T)(4\theta^4 \bar{R}_\tau)(I_{N-1} \otimes A_2) x_{Td} \\
&\quad + \nu_{Td}^T (I_{N-1} \otimes A_1^T)(4\theta^2 \bar{R}_\tau)(I_{N-1} \otimes A_1) \nu_{Td} \\
&\quad + \nu_{Td}^T (I_{N-1} \otimes A_2^T)(4\theta^4 \bar{R}_\tau)(I_{N-1} \otimes A_2) \nu_{Td} \\
&\leq x_{Td}^T (I_{N-1} \otimes 4(\theta^2 A_1^T R_\tau A_1 + \theta^4 A_2^T R_\tau A_2)) x_{Td} \\
&\quad + \nu_{Td}^T (I_{N-1} \otimes 4(\theta^2 B_1^T R_\tau B_1 + \theta^4 B_2^T R_\tau B_2)) \nu_{Td} \\
&\leq x_{Td}^T \bar{R}_\tau^x x_{Td} + \nu_{Td}^T \bar{R}_\tau^\nu \nu_{Td}
\end{aligned}
$$

where the last term can be easily found by Fact 2.1.1

In Theorem 3.2.1, we provide sufficient conditions to systematically find an appropriate K_U.

Theorem 3.2.1. *Let the signals* $\nu_{Ti} = K_U x_{Ti} = -\lambda_2 R_{\nu f}^{-1} B_0^T P x_{Ti}$ *and* $\tau_i = G x_{Ti} = -R_\tau^{-1} P x_{Ti}$ *solve the minimization problem* (3.54) *subject to the auxiliary system* (3.55) *such that the condition* (3.56) *or* (3.57) *is satisfied. Then, the control signal* (3.51) *exponentially stabilizes the uncertain disagreement dynamics* (3.50). *The matrix* P *denotes the solution of ARE* (3.58), $B_f = \begin{bmatrix} \lambda_2 B_0 & I_{n_x} \end{bmatrix}$, $R_f = Diag_b\{[R_{\nu f}, R_\tau]\}$, $Q_f = Q + R_\tau^x$, *and* $R_{\nu f} = R_\nu + R_\tau^\nu$. *Moreover,* $Q = Q^T \succ \boldsymbol{0}$, $R_\nu = R_\nu^T = r_\nu I_{n_u} \succ \boldsymbol{0}$, $R_\tau = R_\tau^T = r_\tau I_{n_x} \succ \boldsymbol{0}$, *and* $r_\nu, r_\tau > 0$ *are design parameters.*

$$
J_i(x_{Ti}(0)) = \min_{\nu_{Ti}, \tau_i} \int_0^\infty (x_{Ti}^T Q_f x_{Ti} + \nu_{Ti}^T R_{\nu f} \nu_{Ti} + \tau_i^T R_\tau \tau_i) dt \tag{3.54}
$$

$$\dot{x}_{Ti} = A_0 x_{Ti} + \lambda_2 B_0 \nu_{Ti} + \tau_i \tag{3.55}$$

$$Q - 2G^T R_\tau G + K_U^T R_\nu K_U \succ \boldsymbol{0} \tag{3.56}$$

$$Q - 2G^T R_\tau G \succ \boldsymbol{0} \tag{3.57}$$

$$A_0^T P + P A_0 + Q_f - P B_f R_f^{-1} B_f^T P = \boldsymbol{0} \tag{3.58}$$

Proof. This proof is discussed at Subsection 3.4.5. □

We point out that, in LQR formulation (3.54), the effect of modeling uncertainty w_{Td} appears in both Q_f and $R_{\nu f}$. Also, note that post-processing is required to find a suitable control gain K_U, because the conditions (3.56) and (3.57) depend on the control gains K_U and G that should be designed (and are not available at the beginning). Moreover, although we have proved that the disagreement dynamics are exponentially stable, we still are interested in knowing about the agreement value. To do this, we propose a new lemma and specialize it in Remark 3.2.2.

Lemma 3.2.1. *Assume that conditions of Theorem 3.2.2 are satisfied. Then, agents of* (3.44) *reach the following state agreement value for* $i \in \{1, 2, ..., N\}$*:*

$$x_i^f(t) = \frac{1}{N}(e^{At} \sum_{i=1}^{N} x_i(0) + \int_0^t e^{A_0(t-\sigma)} \sum_{i=1}^{N} w_i(x_i(\sigma), u_i(\sigma)) d\sigma) \tag{3.59}$$

where the superscript ^{f} *denotes the final (time-varying) value.*

Proof. This proof is available at Subsection 3.4.6. □

Remark 3.2.2. *For a Hurwitz A, the agreement value is given by:*

$$x_i^f = \lim_{t\to\infty} \frac{1}{N} \int_0^t (e^{A_0(t-\sigma)} \sum_{i=1}^{N} w_i(x_i(\sigma), u_i(\sigma)))d\sigma \tag{3.60}$$

because $e^{At} \to \boldsymbol{0}$ *as* $t \to \infty$.

In Theorem 3.2.1, we established a sufficient condition to ensure an (unknown) agreement among agents (3.44). In Lemma 3.2.1, we found the agreement value and, assuming a Hurwitz A, we derived a simplified agreement value in Remark 3.2.2. Now, in Lemma 3.2.2, we further establish a sufficient condition that guarantees a state agreement on zero for multiagent system (3.44).

Lemma 3.2.2. *State variables of* (3.44) *agrees on zero if* $q < \frac{\beta}{\alpha}$ *where* $q \triangleq \sum_{m=1}^{n_\theta} \kappa_m$, $\kappa_m \triangleq \sqrt{|\mu_{m,M}|}|\theta_{max}^m|$, $\mu_{m,M}$ *denotes the maximum eigenvalue of* $A_m^T A_m$, *and* $\alpha, \beta > 0$ *satisfy* $||e^{A_0 t}|| \leq \alpha e^{-\beta t}$.

Proof. This proof is given at Subsection 3.4.7. □

3.2.2.2 Equivalent multiagent system with matched uncertainty

Now, we solve the consensus problem (3.39) for multiagent systems of (3.41). We show that this simplified structure, compared to (3.40) that has been discussed in previous section, relaxes the post-processing requirement (3.56) or (3.57) in finding an appropriate consensus gain.

For brevity, we only introduce new variables and parameters, and others can be found in previous subsection. We first rewrite (3.41) as follows:

$$\begin{aligned} \dot{x}_i &= A_0 x_i + B_0(u_i + z_i(x_i)) \\ z_i(x_i) &= \textstyle\sum_{m=1}^{n_\theta} z_{mi}(x_i) \\ z_{mi}(x_i) &= B_0^\dagger A_m \theta^m x_i \end{aligned} \tag{3.61}$$

and propose a distributed consensus protocol:

$$u_i = K_M \sum_{j \in \mathcal{N}_i} (x_i - x_j) \tag{3.62}$$

where $K_M \in \mathbb{R}^{n_u \times n_x}$ denotes consensus gain in the presence of matched modeling uncertainty $B_0 z_i(x_i)$. Let $z = col\{z_i\}$ be the aggregated matched uncertainty vector. Now, over $\mathcal{G}$, we model the multiagent system as follows:

$$\begin{aligned} \dot{x} &= (I_N \otimes A)x + (I_N \otimes B_0)(u + z(x)) \\ z_m(x) &= (I_N \otimes B_0^\dagger A_m)\theta^m x \end{aligned} \tag{3.63}$$

where $z(x,u) := \sum_{m=1}^{n_\theta} z_m(x,u)$. In this case, the aggregated consensus protocol appears as a coupled signal:

$$u = (\mathcal{L} \otimes K_M)x \tag{3.64}$$

We decompose this coupled consensus signal as $u = (\mathcal{L} \otimes I_{n_u})\nu$ and $\nu = (I_N \otimes K_M)x$, and pass the coupled term to the multiagent system's dynamics:

$$\begin{aligned} \dot{x} &= (I_N \otimes A_0)x + (\mathcal{L} \otimes B_0)\nu + (I_N \otimes B_0)z(x) \\ z_m(x) &= (I_N \otimes B_0^\dagger A_m)\theta^m x \\ \nu &= (I_N \otimes K_M)x \end{aligned}$$

which results in a coupled dynamics due to $\mathcal{L} \otimes B_0$, and a decoupled (consensus) signal ν. Applying the diagonalization transformation of Proposition 2.2.1 results in a partitioned transformed multiagent system:

$$\begin{bmatrix} \dot{x}_{T1} \\ \dot{x}_{Td} \end{bmatrix} = \begin{bmatrix} A_0 & \mathbf{0} \\ \mathbf{0} & I_{N-1} \otimes A_0 \end{bmatrix} \begin{bmatrix} x_{T1} \\ x_{Td} \end{bmatrix} + \begin{bmatrix} \mathbf{0} & \mathbf{0} \\ \mathbf{0} & \Lambda_d \otimes B_0 \end{bmatrix} \begin{bmatrix} \nu_{T1} \\ \nu_{Td} \end{bmatrix} + \begin{bmatrix} B_0 & \mathbf{0} \\ \mathbf{0} & I_{N-1} \otimes B_0 \end{bmatrix} \begin{bmatrix} z_{T1}(x_{T1}) \\ z_{Td}(x_{Td}) \end{bmatrix} \tag{3.65}$$

where $z_T \triangleq (T^{-1} \otimes I_{n_u})z$. Letting $z_{mT} \triangleq (T^{-1} \otimes I_{n_u})z_m$, the uncertain term is defined by:

$$z_T(x_T) := \sum_{m=1}^{n_\theta} z_{mT}(x_T), \qquad where \quad z_{mT}(x_T) = (I_N \otimes B_0^\dagger A_m)\theta^m x_T$$

The first row of (3.65) represents the uncontrollable agreement dynamics, and the second row models the controllable disagreement dynamics. The design of consensus algorithm is limited to the second row of (3.65) that is rewritten as (3.66)-(3.67) (the potential effects of agreement dynamics, with modeling uncertainty, will be discussed in Lemma 3.2.3 and Lemma 3.2.4):

$$\underbrace{\dot{x}_{Td} = \bar{A}_0 x_{Td} + \bar{B}_0 \nu_{Td}}_{\text{Network-level nominal multiagent system}} + \underbrace{\bar{B}_0 \bar{E} \nu_{Td} + \bar{B}_0 z_{Td\lambda}(x_T)}_{\text{Network-level uncertainty}} \tag{3.66}$$

$$\nu_{Td} = \bar{K}_M x_{Td} \tag{3.67}$$

where $\bar{K}_M = I_{N-1} \otimes K_M$ and $z_{Td\lambda}(x_T) = \frac{1}{\lambda_2} z_{Td}(x_T)$.

Also, defining $\bar{R} = I_{N-1} \otimes R$, $R = rI_{N-1}$, and $r > 0$, we always can find a quadratic upper bound on $z_{Td\lambda}$ as is given below (see Example 3.2.1 at page 97):

$$z_{Td\lambda}^T \bar{R} z_{Td\lambda} \leq x_{Td}^T \bar{R}^x x_{Td} =: z_{Td\lambda M}^T \bar{R} z_{Td\lambda M} \tag{3.68}$$

Theorem 3.2.2 provides sufficient conditions to stabilize the uncertain disagreement dynamics (3.66) and, equivalently, to derive the transformed multiagent system (3.65) to its agreement subspace.

Theorem 3.2.2. *Let $\nu_{Ti} = K_M x_{Ti} = -\lambda_2 R^{-1} B_0^T P_m x_{Ti}$ be the control signal that solves the LQR minimization problem* (3.69) *subject to the i^{th} agent's networked nominal dynamics* (3.70)*. Then, $\nu_{Td} = col\{\nu_{Ti}\}$ exponentially stabilizes the uncertain disagreement dynamics* (3.66)*. Here, P_m denotes the solution of ARE* (3.71)*, and $Q_m = Q + R^x$. Furthermore, $Q = Q^T \succ \boldsymbol{0}$, $R = R^T = rI_{n_u} \succ \boldsymbol{0}$, and $r > 0$ are design parameters.*

$$J_i(x_{Ti}(0)) = \min_{\nu_{Ti}} \int_0^\infty (x_{Ti}^T Q_m x_{Ti} + \nu_{Ti}^T R \nu_{Ti}) dt \tag{3.69}$$

$$\dot{x}_{Ti} = A_0 x_{Ti} + \lambda_2 B_0 \nu_{Ti} \tag{3.70}$$

$$A_0^T P_m + P_m A_0 + Q_m - \lambda^2 P_m B_0 R^{-1} B_0^T P_m = \boldsymbol{0} \tag{3.71}$$

Proof. This proof is provided at Subsection 3.4.8. □

In the next lemma, we find the agreement value of a multiagent system (3.63):

Lemma 3.2.3. *Assume that conditions of Theorem 3.2.2 are satisfied. Then, multiagent system* (3.63) *reaches a state agreement on the following value:*

$$x_i^f(t) = \frac{1}{N}(e^{At}\sum_{i=1}^{N} x_i(0) + \int_0^{\infty} e^{A_0(t-\sigma)}B_0\sum_{i=1}^{N} z_i(x_i(\sigma))d\sigma) \tag{3.72}$$

where $i \in \{1, 2, ..., N\}$ *and the superscript* f *denotes the final (time-varying) value.*

Proof. The proof follows that of Lemma 3.2.1. □

Remark 3.2.3. *For a Hurwitz* A_0*, we know that* $e^{At} \to \boldsymbol{0}$ *as* $t \to \infty$*, and a state-agreement is achieved on the following value:*

$$x_i^f = lim_{t\to\infty}\frac{1}{N}\int_0^{\infty} e^{A_0(t-\sigma)}B_0\sum_{i=1}^{N} z_i(x_i(\sigma))d\sigma \tag{3.73}$$

The next lemma provides a sufficient condition which ensures a state agreement on zero among all agents (3.41).

Lemma 3.2.4. *The agreement value of a multiagent system* (3.63) *is zero if* $s < \frac{\beta}{\alpha||B_0||}$ *where* $s \triangleq \sum_{m=1}^{n_\theta}\rho_m$*,* $\rho_m \triangleq \sqrt{|\varsigma_{m,M}|}|\theta_{max}^m|$*,* $\varsigma_{m,M}$ *denotes the maximum eigenvalue of* $A_m^T B_0^{\dagger T} B_0^{\dagger} A_m$*, and* $\alpha, \beta > 0$ *are such that the Hurwitz matrix* A_0 *satisfies the exponential bound* $||e^{A_0 t}|| \leq \alpha e^{-\beta t}$*.*

Proof. This proof can be derived based on the proof of Lemma 3.2.2. □

3.3 Summary and bibliography

In this chapter, we consider linear multiagent systems subject to different sources of uncertainties. The first case is discussed for both leaderless and leader-follower (communication) topologies using some relative-output measurements. These designs guarantee consensus under different types of unknown disturbances:

constant (step-like), ramp, or sinusoidal (and a combination of them). In the second case, we assume that the operating condition of the multiagent system varies in time, and results in a parameter-varying model of the multiagent system. We propose a leaderless consensus problem, and establish a state agreement that depends on all agents' initial state values, and further found the required condition to achieve a state agreement on zero (which is equivalent to the exponential stability of an uncertain multiagent system model using "relative-state" measurements). We show that all of these results can be systematically guaranteed borrowing some fundamental concepts from the optimal control theory.

Localizing the dynamics of closed-loop multiagent systems, with distributed consensus algorithms in the loop, results in heterogeneous sub-models that depend on non-zero eigenvalues of communication graph Laplacian matrix. In the literature, various viewpoints have been proposed to overcome such a problem and design the same (non-heterogeneous) control gain for all agents. The dominant approaches are based on a two-step procedure where the control gain is designed based local dynamics to be multiplied by a scalar correction factor which depends on the communication network topology. References [82] and [83] introduced a correction factor to modify the algebraic Riccati equation-based control gain and guarantee leaderless consensus in a multiagent system (e.g., based on the formulation of this chapter, we need to implement $ck_{cx},\ ck_{cv}$ in consensus signal (4.4) where c is a correction gain that should be designed independent of the actual gains k_{cx} and k_{cv}), and [93] used the correction gain to modify its relative measurements (e.g., in this viewpoint we need to use modified relative measurements cy_i^r in (4.4)-(4.5) with a modification factor c). In this chapter, we reformulate

the problem as a state-feedback robust control challenge for the nominal networked vehicles' model (identical for al agents) subject to fictitious uncertainties (in general, non-identical for agents). We then provide a systematic one-step approach to find appropriate control and observer gains that guarantee consensus in multiagent systems.

The disturbance rejection (or cancellation), by itself, has received significant attention in the literature of control systems. Particularly, with a known and fixed waveform but unknown magnitude, the persistent disturbance rejection has also been reported in the literature under different names, for example, disturbance accommodation control in [115] which can be combined with state feedback algorithms (as we have done in conjunction with the optimal control ideas of Section 2.4). Recently, this issue has also been discussed in the literature of multiagent systems considering a constant disturbance or integrator agent models (e.g., see [116] and [117]). In a different research work, a leader-follower consensus for a linear time-invariant multiagent system subject to constant disturbances has also been investigated in [118]. Moreover, [119] proposed a consensus algorithm to deal with the disturbances acting on a multiagent system of nonholonomic moving agents.

The parameter-dependent model of Section 3.2 has been seen in many practical cases, including the wind turbine application (e.g., see the references in Sec. III.F [120]). Moreover, the discussion on parameter-dependent aircraft multiagent system at page 93 is inspired by [121]. The proposed methods in this chapter are applicable to the unknown and possibly time-varying operating point scenarios. Alternatively, linear parameter varying and gain scheduling controls

can be applied whenever the independent (scheduling) parameter is measurable. Also, the frequency domain approaches are usually limited to the constant or (practically) very slow-varying parameters. While our ideas are inspired by [122], similar approaches can be found in the literature of control systems theory under the name of *guaranteed-cost control* (e.g., see [110], [123], and [124] with a different set of structural assumptions).

Finally, although it is straightforward to establish the positive definiteness of a reduced-order graph Laplacian matrix $\mathcal{H}$ for a connected leader-follower communication graph (see the partitioning of graph Laplacian matrix in Remark 3.1.4, page 81), a (different) proof is given in [114].

3.4 Appendix: proofs

We have proposed the main results of this chapter through several theorems, lemmas, and propositions. For the sake of readability, we have not discussed their proofs within the main body of this chapter, and, instead, have gathered all of them in this Appendix section. Subsections 3.4.1, 3.4.2, 3.4.3, and 3.4.4 are related to Section 3.1, and Subsections 3.4.5, 3.4.6, 3.4.7, and 3.4.8 focus on the results of Section 3.2.

3.4.1 Proof of Theorem 3.1.1 (page 68)

We first mention that the multiagent system's dynamics (3.6) can be transformed to (3.8) using a similarity transformation that has been discussed in Fact 2.2.1. Therefore, consensus of a closed-loop multiagent system of (2.13)-

(3.2) and (3.4)-(3.5) (or equivalently, the matrix form (3.6)) is the same as deriving all states of (3.8) to the agreement space (described by the first row in (3.8)). In other words, we need to asymptotically stabilize the disagreement dynamics (3.9). Hence, we consider *N-1* sub-systems in (3.10) to design control gains K_c^x and K_c^w, and *N-1* sub-systems in (3.11) to design the observer gains K_o^x and K_o^w. These issues are further detailed in the rest of this proof:

Part 1) Based on the observer error dynamics (3.11), we find that, in fact, we need to design an observer gain $K_o = \begin{bmatrix} K_o^x \\ K_o^w \end{bmatrix}$ for the following augmented system:

$$\begin{bmatrix} \dot{x}_{di} \\ \dot{z}_{wdi} \end{bmatrix} = \underbrace{\begin{bmatrix} A & \Gamma\theta \\ \mathbf{0} & F \end{bmatrix}}_{A_a} \begin{bmatrix} x_{di} \\ z_{wdi} \end{bmatrix}, \qquad y_{di} = \underbrace{\begin{bmatrix} \lambda_i C & \mathbf{0} \end{bmatrix}}_{C_a} \begin{bmatrix} x_{di} \\ z_{wdi} \end{bmatrix} \tag{3.74}$$

We propose a Luenberger observer as follows:

$$\begin{bmatrix} \dot{\hat{x}}_{di} \\ \dot{\hat{z}}_{wdi} \end{bmatrix} = A_a \begin{bmatrix} \hat{x}_{di} \\ \hat{z}_{wdi} \end{bmatrix} + K_a(y_{di} - \hat{y}_{di}), \qquad y_{di} = C_a \begin{bmatrix} x_{di} \\ z_{wdi} \end{bmatrix}$$

in which, whenever Assumption 3.1.1.b is satisfied, an observer gain K_o can always be found to arbitrarily assign eigenvalues of the closed-loop matrix in Theorem 3.1.1.1. Consequently, we can stabilize the observer dynamics (arbitrarily fast).

Part 2) Because of Assumption 3.1.1.b, as is discussed in Part 1 of this proof, the estimation error response in (3.11) converges to zero arbitrarily fast. We

replace the estimated values in (3.10) with the actual variables to get (3.12). Therefore, stabilizing this system for all $i \in \{2, ..., N\}$ confirms our claim in Theorem 3.1.1.2.

3.4.2 Proof of Theorem 3.1.2 (page 70)

All we need is proving that $u_{di} = K_c^x x_{di}$, designed for the nominal model in (3.15), stabilizes the closed-loop system with entire uncertain model (3.15) where the uncertainty is induced by the communication topology (we have $N-1$ possibly different eigenvalues, and introducing this fictitious modeling uncertainty helps finding a homogeneous consensus protocol). We define the following candidate Lyapunov function:

$$V(x_{di}(t)) = x_{di}^T(t) P x_{di}(t)$$

where $P \succ \mathbf{0}$ is the solution of ARE (3.17). At time $t = 0$, $V(x_{di}(0))$ is equal to the LQR cost functional $J(x_{di}(0))$ in (3.16):

$$V(x_{di}(0)) = J(x_{di}(0)) = \min_{u_{di} \in \mathbb{R}^{n_u}} \int_0^\infty (x_{di}^T Q x_{di} + u_{di}^T R u_{di}) dt' \succ 0$$

Therefore, P in the candidate Lyapunov function V is such that the following Hamilton-Jacobi-Bellman equation is satisfied for the nominal dynamics in (3.15):

$$\min_{u_{di} \in \mathbb{R}^{n_u}} (x_{di}^T Q x_{di} + u_{di}^T R u_{di} + V_{x_{di}}^T (A x_{di} + B D_{\lambda_2} u_{di})) = 0$$

where $V_{x_{di}}^T = \frac{\partial V}{\partial x_{di}}$. In particular, implementing $u_{di} = K_c^x x_{di}$ with an optimal gain $K_c^x = -R^{-1} D_{\lambda_2}^T B^T P$, the pairs (x_{di}, u_{di}) satisfy the following equalities:

$$\begin{aligned} x_{di}^T Q x_{di} + u_{di}^T R u_{di} + V_{x_{di}}^T (A x_{di} + B D_{\lambda_2} u_{di}) &= 0 \\ 2 u_{di}^T R + V_{x_{di}}^T B D_{\lambda_2} &= \mathbf{0} \end{aligned}$$

because the algebraic Riccati equation (3.17) is satisfied and $K_c^{xT} = -PBD_{\lambda_2} R^{-1}$ is implemented (the relation between the first equality and algebraic Riccati equation is discussed in Section 2.4). Now, we calculate the time deviation of this candidate Lyapunov function along the uncertain trajectory (3.15) and find:

$$\begin{aligned} \dot{V}(x_{di}) &= V_{x_{di}}^T \dot{x}_{di} \\ &= -x_{di}^T Q x_{di} - x_{di}^T K_c^{xT} R K_c^x x_{di} - 2 x_{di}^T K_c^{xT} R E(\lambda) K_c^x x_{di} \\ &\preccurlyeq -x_{di}^T Q x_{di} \prec 0 \end{aligned}$$

where we have used the fact that $RE(\lambda_i) = (\frac{\lambda_i}{\lambda_2} - 1) R \succcurlyeq \mathbf{0}$ for all $i \in \{2, 3, ..., N\}$. Now, based on the Lyapunov Theorem 2.3.1, the closed-loop system (3.14) is asymptotically stable for all initial values of agents (and for all non-zero λ_i). Based on Theorem 2.3.2, we can further conclude an exponential stability by letting $a_1 = \lambda_{min}(P)$, $a_2 = \lambda_{max}(P)$, $a_3 = \lambda_{min}(Q)$, and $b = 2$.

3.4.3 Proof of Theorem 3.1.3 (page 71)

Based on the Theorem 2.3.1, as the dual to the observer design problem for (3.74), we can find a control signal u_a that stabilizes the following model:

$$\dot{x}_a = A_a^T x_a + C_a^T u_a \tag{3.75}$$

where $C_a^T = C_a^{cT} D_a(\lambda_i)$ create fictitious modeling uncertainties $\forall i \in \{2, 3, ..., N\}$. This is straightforward to rewrite (3.75) and find:

$$\underbrace{\dot{x}_a = A_a^T x_a + C_a^{cT} D_{a,\lambda_2}^T u_a}_{\text{Nominal model}} + \underbrace{C_a^{cT} D_{a,\lambda_2} E_a(\lambda_i) u_a}_{\text{Network-induced uncertainty}}$$

using the Luenberger observer equation (3.75). Now, the problem is reduced to Theorem 3.1.2 with a similar proof. Based on the duality Lemma 2.3.1, this $K_o = [K_o^{xT}, K_o^{wT}]^T$ gives the required observer gain in Theorem 3.1.1.1.

3.4.4 Proof of Lemma 3.1.1 (page 72)

Based on (3.8), dynamics of η_1 and η_2 are decoupled. Also, as a result of Theorem 3.1.1, we know that P_{22} is Hurwitz. Thus, $\eta_2^a = lim_{t\to\infty}\eta_2(t) = 0$. Furthermore, the following time response can be found based on the first-order state equation (3.8):

$$\begin{aligned} x_{T,1}^a &= e^{At} x_{T,1}(0) + \textstyle\int_0^t (e^{A(t-\tau)} B K_c^w e^{F\tau} \tilde{z}_{wT,1}(0)) d\tau \\ \tilde{x}_{T,1}^a &= e^{At} \tilde{x}_{T,1}(0) + \textstyle\int_0^t (e^{A(t-\tau)} \Gamma\theta e^{F\tau} \tilde{z}_{wT,1}(0)) d\tau \\ \tilde{z}_{T,1}^a &= e^{Ft} \tilde{z}_{wT,1}(0) \end{aligned} \tag{3.76}$$

Now, substituting K_c^w from Design procedure 3.1.1, we find:

$$\eta_1^a = \phi_{00}\eta_1(0) + \phi_{11}\eta_1(0) = \begin{bmatrix} \phi_{00}^A & \mathbf{0} & \mathbf{0} \\ \mathbf{0} & \phi_{00}^A & \mathbf{0} \\ \mathbf{0} & \mathbf{0} & \mathbf{0} \end{bmatrix} \begin{bmatrix} x_{T,1}(0) \\ \tilde{x}_{T,1}(0) \\ \tilde{z}_{wT,1}(0) \end{bmatrix} + \begin{bmatrix} \mathbf{0} & \mathbf{0} & \phi_{11}^{13} \\ \mathbf{0} & \mathbf{0} & \phi_{11}^{23} \\ \mathbf{0} & \mathbf{0} & \phi_{11}^{33} \end{bmatrix} \begin{bmatrix} x_{T,1}(0) \\ \tilde{x}_{T,1}(0) \\ \tilde{z}_{wT,1}(0) \end{bmatrix}$$

Therefore, for the entire partitioned model (3.8), $\eta^a = \begin{bmatrix} \phi_{00} + \phi_{11} & \mathbf{0} \\ \mathbf{0} & \mathbf{0} \end{bmatrix} \eta(0)$ is satisfied. Now, let $T_b = diag\{[T \otimes I_{n_x},\ T \otimes I_{n_x},\ T \otimes I_{n_{zw}}]\}$ and $\mathcal{P}$ be the same as the one that we have used to find (3.8). Then:

$$\begin{bmatrix} x^a \\ \tilde{x}^a \\ \tilde{z}_w^a \end{bmatrix} = T_b \mathcal{P}^{-1} \begin{bmatrix} \phi_{00} + \phi_{11} & \mathbf{0} \\ \mathbf{0} & \mathbf{0} \end{bmatrix} \mathcal{P} T_b^{-1} \begin{bmatrix} x(0) \\ \tilde{x}(0) \\ \tilde{z}_w(0) \end{bmatrix}$$

is achieved for the initial augmented model (3.6) (the augmented model, right before the similarity transformation). This results in the following agreement values for the system state and observer state estimation errors:

$$\begin{bmatrix} x^a \\ \tilde{x}^a \\ \tilde{z}_w^a \end{bmatrix} = \begin{bmatrix} \Phi_{00}^A & \mathbf{0} & \Phi_{11}^{13} \\ \mathbf{0} & \Phi_{00}^A & \Phi_{11}^{23} \\ \mathbf{0} & \mathbf{0} & \Phi_{11}^{33} \end{bmatrix} \begin{bmatrix} x(0) \\ \tilde{x}(0) \\ \tilde{z}_w(0) \end{bmatrix}$$

where $\Phi_{00}^A = (\frac{1}{N}\mathbf{1} \otimes \phi_{00}^A)\ \forall i \in \{1,2,3\}$, and also $\Phi_{11}^{i3} = (\frac{1}{N}\mathbf{1} \otimes \phi_{11}^{i3})\ \forall i \in \{1,2,3\}$ where $\mathbf{1} \in \mathbb{R}^{N \times N}$ denotes a matrix of all ones. Hence, the proof is completed.

3.4.5 Proof of Theorem 3.2.1 (page 98)

We aggregate (3.54) for $i \in \{2, 3, ..., N\}$ and use (3.53) in order to find the augmented cost function (3.77):

$$J(x_{Td}(0)) = \min_{\nu_{Td},\tau} \int_0^\infty (x_{Td}^T \bar{Q} x_{Td} + \nu_{Td}^T \bar{R}_\nu \nu_{Td} + \tau^T \bar{R}_\tau \tau + w_{TdM}^T \bar{R}_\tau w_{TdM}) dt$$

where $\bar{R}_\nu = I_{N-1} \otimes R_\nu$. The augmented control signals $\nu_{Td} = \bar{K}_U x_{Td}$ and $\tau = \bar{G} x_{Td}$, where $\bar{G} = I_{N-1} \otimes G$, the augmented auxiliary system (3.52), and conditions (3.77) and (3.78) can be found similarly.

$$\bar{Q} - 2\bar{G}^T \bar{R}_\tau \bar{G} + \bar{K}_U^T \bar{R}_\nu \bar{K}_U \succ \mathbf{0} \tag{3.77}$$

$$\bar{Q} - 2\bar{G}^T \bar{R}_\tau \bar{G} \succ \mathbf{0} \tag{3.78}$$

In summary, the aggregated control signals ν_{Td} and τ minimize the augmented cost function (3.77) subjected to the augmented auxiliary system (3.52) and, also, the condition (3.77) or (3.78) is satisfied. In the rest, we prove that the uncertain disagreement dynamics (3.50) can be asymptotically stabilized using only ν_{Td} in the closed-loop configuration (i.e., without implementing the auxiliary control signal τ).

We introduce a candidate Lyapunov function:

$$V(x_{Td}(t)) = x_{Td}^T(t) \bar{P} x_{Td}(t)$$

where $\bar{P} = I_{N-1} \otimes P$ and P is the solution of ARE (3.58). We know that at time $t = 0$, the relationship $V(x_{Td}(0)) = J(x_{Td}(0))$ is satisfied for

$$J(x_{Td}(0)) = \min_{\nu_{Td},\tau} \int_0^\infty (x_{Td}^T \bar{Q} x_{Td} + \nu_{Td}^T \bar{R}_\nu \nu_{Td} + \tau^T \bar{R}_\tau \tau + w_{TdM}^T \bar{R}_\tau w_{TdM}) dt \quad (3.79)$$

Thus, the Lyapunov function (3.79) satisfies the Hamilton-Jacobi-Bellman equation (3.80) (subject to the augmented auxiliary multiagent (3.52)):

$$\min_{\nu_{Td},\tau} \{x_{Td}^T \bar{Q} x_{Td} + \nu_{Td}^T \bar{R}_\nu \nu_{Td} + \tau^T \bar{R}_\tau \tau + w_{TdM}^T \bar{R}_\tau w_{TdM} + V_{x_{Td}}^T (\bar{A}_0 x_{Td} + \bar{B}_0 \nu_{Td} + \tau)\} = 0$$

Specifically, implementing $\nu_{Td} = \bar{K}_U x_{Td}$ and $\tau = \bar{G} x_{Td}$, the triple $(x_{Td}, \nu_{Td}, \tau_{Td})$ satisfies the following equalities:

$$x_{Td}^T \bar{Q} x_{Td} + \nu_{Td}^T \bar{R}_\nu \nu_{Td} + \tau^T \bar{R}_\tau \tau + w_{TdM}^T \bar{R}_\tau w_{TdM} + V_{x_{Td}}^T (\bar{A}_0 x_{Td} + \bar{B}_0 \nu_{Td} + \tau) = 0$$

because the ARE (3.58) is satisfied (see the relation between this inequality and an ARE in Section 2.4), and

$$\begin{aligned} 2\nu_{Td}^T \bar{R}_{\nu f} + V_{x_{Td}}^T \bar{B}_0 &= \mathbf{0} \\ 2\tau^T \bar{R}_\tau + V_{x_{Td}}^T &= \mathbf{0} \end{aligned}$$

because the control gains are chosen to be $\bar{K}_U = I_{N-1} \otimes (-\lambda_2 R_{\nu f}^{-1} B_0^T P)$ and $\bar{G} = I_{N-1} \otimes (-R_\tau^{-1} P)$. Here, $V_{x_{Td}} = \frac{\partial V(x_{Td})}{\partial x_{Td}}$.

The time deviation of V along the uncertain dynamics (3.50) results in the followings:

$$\begin{aligned}\dot{V} &= -x_{Td}^T \bar{Q} x_{Td} - \nu_{Td}^T \bar{R}_\nu \nu_{Td} - (\tau + w_{Td})^T \bar{R}_\tau (\tau + w_{Td}) \\ &\quad - 2\nu_{Td}^T \bar{R}_{\nu f} \bar{E} \nu_{Td} - (w_{TdM}^T \bar{R}_\tau w_{TdM} - w_{Td}^T \bar{R}_\tau w_{Td}) + 2\tau^T \bar{R}_\tau \tau\end{aligned}$$

where $\bar{E} = \bar{E}^T \succcurlyeq \mathbf{0}$ and we have $-2\nu_{Td}^T \bar{R}_{\nu f} \bar{E} \nu_{Td} = -2(r_\nu + r_\tau^\nu)\nu_{Td}^T \bar{E} \nu_{Td} \leq 0$. Therefore, $\dot{V}$ can be written as either one of the followings:

$$\dot{V} \leq -x_{Td}^T \bar{Q} x_{Td} - \nu_{Td}^T \bar{R}_\nu \nu_{Td} + 2\tau^T \bar{R}_\tau \tau$$

$$\dot{V} \leq -x_{Td}^T \bar{Q} x_{Td} + 2\tau^T \bar{R}_\tau \tau$$

Now, by substituting ν_{Td} and τ, we find $\dot{V} \prec 0$ because (3.77) or (3.78) is satisfied. Thus, based on the Lyapunov Theorem 2.3.1, the closed-loop disagreement dynamics (3.50) are asymptotically stable for all initial values of agents (and for all non-zero λ_i). Based on Theorem 2.3.2, we can further conclude an exponential stability by letting $b = 2$, $a_1 = \lambda_{min}(P)$, $a_2 = \lambda_{max}(P)$, $a_3 = \lambda_{min}(M)$ where M can be $Q - 2G^T R_\tau G + K_U^T R_\nu K_U$ or $Q - 2G^T R_\tau G$.

3.4.6 Proof of Lemma 3.2.1 (page 99)

We know that Theorem 3.2.2 is satisfied, thus $x_{Td}^f = \lim_{t\to\infty} x_{Td}(t) = \mathbf{0}$. Based on the partitioned representation (3.49), the dynamics of (uncontrollable) agreement space are given by:

$$\dot{x}_{T1} = A_0 x_{T1} + w_{T1}(x_{T1}) \tag{3.80}$$

where we note that the (θ-dependent) uncertain function w_{T1} depends on neither ν_T nor x_{Td}. The solution of this differential equation is given by:

$$x_{T1}(t) = e^{A_0 t} x_{T1}(0) + \int_0^t e^{A_0(t-\sigma)} w_{T1}(x_{T1}(\sigma)) d\sigma \tag{3.81}$$

Therefore, we observe the following behavior for (3.49) after reaching to the agreement subspace:

$$\begin{aligned} x_T^f = \begin{bmatrix} x_{T1}^f \\ x_{Td}^f \end{bmatrix} &= \begin{bmatrix} e^{A_0 t} x_{T1}(0) + \int_0^t e^{A_0(t-\sigma)} w_{T1}(x_{T1}(\sigma)) d\sigma \\ \mathbf{0} \end{bmatrix} \\ &= \begin{bmatrix} e^{A_0 t} & \mathbf{0} \\ \mathbf{0} & \mathbf{0} \end{bmatrix} x_T(0) + \int_0^t \begin{bmatrix} e^{A_0(t-\sigma)} & \mathbf{0} \\ \mathbf{0} & \mathbf{0} \end{bmatrix} w_T(x_T(\sigma), \nu_T(\sigma)) d\sigma \end{aligned}$$

where ν_T is added as an input argument to w_T to consider its effect on w_{Td}. We further partition the similarity transformation matrix $T = [T_1 | T_d]$ where $T_1 = \frac{1}{\sqrt{N}} \mathbf{1}_N$ (corresponding to $\lambda_1 = 0$), and T_d contains all other columns of T. This transformation matrix was used to get (3.49). Now, we find:

$$\begin{aligned} x^f &= \tfrac{1}{N}(\mathbf{1} \otimes e^{A_0 t}) x(0) + \int_0^t \tfrac{1}{N}(\mathbf{1} \otimes e^{A_0(t-\sigma)}) w(x(\sigma), u(\sigma)) d\sigma \\ &= \tfrac{1}{N}(\mathbf{1}_N \otimes e^{A_0 t} \textstyle\sum_{i=1}^N x_i(0)) + \int_0^t \tfrac{1}{N}(\mathbf{1}_N \otimes e^{A_0(t-\sigma)} \textstyle\sum_{i=1}^N w_i(x_i(\sigma), u_i(\sigma))) d\sigma \end{aligned}$$

where $x^f = [x_1^{fT}, x_2^{fT}, ..., x_N^{fT}]^T$, and $\mathbf{1}$ is an $N \times N$ matrix of all ones.

3.4.7 Proof of Lemma 3.2.2 (page 100)

Based on the conditions of this lemma, we know the inequalities $||A_m x_{T1}|| \leq \sqrt{|\mu_{m,M}|}||x_{T1}||$, $||w_{mT1}|| \leq \kappa_m ||x_{T1}||$, and $||w_{T1}(x_T, \nu_T)|| \leq q||x_{T1}||$ are achieved. Using the solution (3.81) in Subsection 3.4.6, we further find:

$$||x_{T1}(t)|| \leq \alpha ||x_{T1}^0|| e^{-\beta t} + \alpha q e^{-\beta t} \int_0^t (e^{\beta\sigma} ||x_{T1}(\sigma)||) d\sigma$$

where $x_{T1}^0 \triangleq x_{T1}(0)$. Based on the Bellman-Gronwall Lemma 2.3.3, by setting $w(t) = ||x_{T1}(t)||$, $z(t) = \alpha ||x_{T1}^0|| e^{-\beta t}$, $g(t) = \alpha q e^{-\beta t}$, and $h(t) = e^{\beta t}$, we find the following inequality:

$$||x_{T1}(t)|| \leq \alpha ||x_{T1}^0|| e^{-(\beta - \alpha q)t}$$

Therefore, the condition $q < \frac{\beta}{\alpha}$ guarantees exponential stabilization of the agreement dynamics (3.80). Using the result of Theorem 3.2.1 for the disagreement space, all states of (3.49) converge to the origin that means all states of (3.44) reach to an agreement on zero. Thus, the proof is done.

3.4.8 Proof of Theorem 3.2.2 (page 103)

Aggregation of (3.70) for $i \in \{2, 3, ..., N\}$ results in the network-level nominal multiagent system in (3.66) where, for this nominal multiagent system, the control signal $\nu_{Td} = \bar{K}_M x_{Td}$ minimizes the following augmented cost function:

$$J(x_{Td}(0)) = \min_{\nu_{Td}} \int_0^\infty (x_{Td}^T \bar{Q} x_{Td} + \nu_{Td}^T \bar{R} \nu_{Td} + z_{Td\lambda M}^T \bar{R} z_{Td\lambda M}) dt$$

where $\bar{Q} = I_{N-1} \otimes Q$. In the rest, we prove that this ν_{Td} also stabilizes the entire *uncertain multiagent system* (3.66). We propose the following candidate Lyapunov function for $t \geq 0$:

$$V(x_{Td}(t)) = x_{Td}^T(t)\bar{P}x_{Td}(t)$$

where $\bar{P} = I_{N-1} \otimes P$ and P is the solution of ARE (3.71). We further notice that the boundary condition $V(x_{Td}(0)) = J(x_{Td}(0)) = \min_{\nu_{Td}} \int_0^\infty (x_{Td}^T \bar{Q} x_{Td} + \nu_{Td}^T \bar{R} \nu_{Td} + z_{Td\lambda M}^T \bar{R} z_{Td\lambda M}) ds \succ 0$ is satisfied. Thus, we write the following Hamilton-Jacobi-Bellman equation using the network-level nominal dynamics in (3.66):

$$\min_{\nu_{Td}} \{x_{Td}^T \bar{Q} x_{Td} + \nu_{Td}^T \bar{R} \nu_{Td} + z_{Td\lambda M}^T \tilde{R} z_{Td\lambda M} + V_{x_{Td}}^T (\bar{A}_0 x_{Td} + \bar{B}_0 \nu_{Td})\} = 0$$

Particularly, implementing $\nu_{Td} = \bar{K}_M x_{Td}$, the following equalities are guaranteed by the pair (x_{Td}, ν_{Td}):

$$\begin{aligned} s x_{Td}^T \bar{Q} x_{Td} + \nu_{Td}^T \bar{R} \nu_{Td} + z_{Td\lambda M}^T \tilde{R} z_{Td\lambda M} + V_{x_{Td}}^T (\bar{A}_0 x_{Td} + \bar{B}_0 \nu_{Td}) = 0 \\ 2\nu_{Td}^T \bar{R} + V_{x_{Td}}^T \bar{B}_0 = \mathbf{0} \end{aligned} \tag{3.82}$$

because the ARE (3.71) is satisfied by P, and the control gain is selected as $K_M = -\lambda_2 R^{-1} B_0^T P_m$. Now, the time deviation of the candidate Lyapunov function along the uncertain dynamics (3.66) gives the following result:

$$\begin{aligned} \dot{V} &= V_{x_{Td}}^T \dot{x}_{Td} \\ &= -x_{Td}^T \bar{Q} x_{Td} - (z_{Td\lambda M}^T \bar{R} z_{Td\lambda M} - z_{Td\lambda}^T \bar{R} z_{Td\lambda}) - 2\nu_{Td}^T \bar{R} \bar{E} \nu_{Td} \\ &\quad - (z_{Td\lambda} + \nu_{Td})^T \bar{R} (z_{Td\lambda} + \nu_{Td}) \leq -x_{Td}^T \bar{Q} x_{Td} \prec 0 \end{aligned}$$

where $\bar{E} = \bar{E}^T \succcurlyeq \mathbf{0}$, we have $-2\nu_{Td}^T \bar{R} \bar{E} \nu_{Td} = -2r\nu_{Td}^T \bar{E} \nu_{Td} \leq 0$. Thus, based on the Lyapunov Theorem 2.3.1, the disagreement uncertain dynamics (3.66) are asymptotically stable for all initial values of agent dynamics over the graph $\mathcal{G}$. Furthermore, using the Rayleigh-Ritz inequality in Fact 2.1.1, we can show that the condition of Theorem 2.3.2 are also satisfied, and the closed-loop disagreement

dynamics are exponentially stable by setting $b = 2$, $a_1 = \lambda_{min}(P)$, $a_2 = \lambda_{max}(P)$, $a_3 = \lambda_{min}(Q)$.

Chapter 4

Distributed Stationary Consensus in Multi-Vehicle/Multi-Robot Systems[1]

In Chapter 1, we discussed that various distributed algorithms have already been designed to ensure collective behavior among agents of multiagent systems. In Chapter 3, we developed an optimal control-theoretic tool that ensured consensus in multiagent systems subject to unknown disturbances or operating point-dependent modeling uncertainties. In Examples 3.1.1 and 3.1.2, we showed the proposed leaderless consensus algorithm ended in agreement on position and velocity in which all vehicles continuously increase their speed. In this chapter, we develop a dynamic output feedback leaderless stationary consensus algorithm based on the relative output information of vehicles and only a few vehicles' ab-

[1]This chapter is based on the reference [113].

solute measurements. We propose a framework to transform this dynamic output feedback problem into three low-order subproblems for disturbance rejection, consensus, and observer gain design tasks. Independently of the number of vehicles, consensus and observer gains are systematically found through two robust static state feedback formulations for low-order dynamics subject to fictitious modeling uncertainties. We further prove the proposed framework can be used to guarantee leader-follower stationary consensus in multi-vehicle systems (with a leader whose dynamics are not identical to the follower vehicles), and find analytical solutions for the consensus gains based on the design parameters and inter-vehicle communication graph. We verify the feasibility of proposed leaderless and leader-follower stationary consensus approaches in simulation.

The rest of this chapter is organized as follows. In Section 4.1, we propose a distributed leaderless stationary consensus algorithm that ensure vehicles' agreement on a fixed point in the presence of unknown persistent disturbances. In Section 4.2, we further prove the proposed framework for the leaderless scheme can be generalized to the leader-follower stationary consensus in which the agreement value is an adjustable command. In Section 4.3, we verify the effectiveness of these approaches through various simulation studies. In Section 4.4, we summarize these results and provide additional references that are related to the topic of this chapter. All proofs are gathered in Section 4.5.

4.1 Leaderless stationary consensus

In this section, we develop a systematic framework to design output feedback dynamic stationary consensus algorithm for leaderless multi-vehicle systems. The

proposed strategy is based on the relative output measurements and a few vehicles (potentially, only one vehicle) absolute output variables, and ensures agreement in the presence of various unknown persistent disturbances. For such a multi-vehicle system with limited information, we first show the relative information-based dynamic consensus task can be reformulated as a set of local stability problems using heterogeneous absolute measurements. Then, in order to have a scalable design applicable to multi-vehicle systems with a high-number of vehicles, we further recast it as three sub-problems to find disturbance cancellation, robust feedback, and robust observer gains.

4.1.1 Problem statement

We consider a group of moving vehicles modeled by the following dynamics:

$$\begin{aligned} &\dot{x}_i = v_i \qquad \dot{v}_i = u_i + d_i \\ &y_i^r = g_1(\textstyle\sum_{j\in\mathcal{N}_i}(x_i - x_j) + b_i x_i) + g_2(\sum_{j\in\mathcal{N}_i}(v_i - v_j) + b_i v_i) \end{aligned} \tag{4.1}$$

where $x_i \in \mathbb{R}$ denotes position, $v_i \in \mathbb{R}$ velocity, $u_i \in \mathbb{R}$ control input, and $y_i \in \mathbb{R}$ output measurement of the i^{th} vehicle. Also, $g_1 \neq 0, g_2 \in \mathbb{R}$ are two output-gain scalars where, e.g., when $g_2 = 0$ reduces to a partial measurement scenario for the multi-vehicle system. Moreover, whenever i^{th} vehicle has access to its absolute output measurement, we set $b_i = 1$ and, otherwise, $b_i = 0$.

Fact 4.1.1. *The triple (C, A, B) is controllable and observable where:*

$$A = \begin{bmatrix} 0 & 1 \\ 0 & 0 \end{bmatrix}, \qquad B = \begin{bmatrix} 0 \\ 1 \end{bmatrix}, \qquad C = \begin{bmatrix} g_1 & g_2 \end{bmatrix} \qquad \textit{where} \quad g_1 \neq 0$$

The effects of unknown environment, e.g., road profile or wind disturbance, on the vehicles' dynamics are modeled by a set of heterogeneous persistent disturbances $d_i \in \mathbb{R}$ (also see (3.2)):

$$\begin{aligned} \dot{z}_i &= A_d z_i, \qquad z_i(0) = z_i^0 \\ d_i &= C_d z_i \end{aligned} \tag{4.2}$$

where $z_i \in \mathbb{R}^{n_z}$ stands for the disturbance-state of i^{th} vehicle, z_i^0 *unknown* initial value of the disturbance-state, and $A_d \in \mathbb{R}^{n_z \times n_z}$ and $C_d \in \mathbb{R}^{n_d \times n_z}$ are two *known* constant matrices that determine the shape of disturbance. For this multi-vehicle system, the leaderless stationary consensus task is defined as follows which should be achieved in the presence of unknown persistent disturbances:

$$\begin{aligned} &\lim_{t\to\infty}(x_i(t) - x_j(t)) = 0 \\ &\lim_{t\to\infty} v_i(t) = 0 \end{aligned} \qquad \forall i, j \in \{1, 2, ..., N\} \tag{4.3}$$

Based on the definitions in Chapter 3, the conventional leaderless consensus for the multi-vehicle system can be defined as $\lim_{t\to\infty}(x_i(t) - x_j(t)) = 0$ and $\lim_{t\to\infty}(v_i(t) - v_j(t)) = 0$ for $i, j \in \{1, 2, ..., N\}$ (see (3.3)). This agreement can be achieved whenever the stationary consensus (4.3) is satisfied; however, the reveres direction is not necessarily true (for nonzero $v_i = v_j$). Moreover, the formulation (4.2) generates various types of disturbances as given in Table 3.1. In particular, the combination of constant and sinusoidal waveforms with unknown amplitudes can be used to model the persistently constant (dc component) and main harmonics of complicated disturbance waveforms, e.g., based on the (fast) Fourier series decomposition of road profile and wind disturbance data.

4.1.2 Main result

In order to guarantee the leaderless stationary consensus of multi-vehicle system (4.1) in the presence of heterogeneous persistent disturbances (4.2), we propose a dynamic distributed stationary consensus algorithm:

$$u_i = k_{cx} \sum_{j \in \mathcal{N}_i} (\hat{x}_i - \hat{x}_j) + k_{cv} \sum_{j \in \mathcal{N}_i} (\hat{v}_i - \hat{v}_j) - \alpha_v \hat{v}_i + K_{cd} \hat{z}_{di} \tag{4.4}$$

where $\alpha_v > 0$ is a design scalar, and $k_{cx}, k_{cv} \in \mathbb{R}$ and $K_{cd} \in \mathbb{R}^{1 \times n_z}$ are the control gains to be determined later in this section. The i^{th} vehicle's estimated position $\hat{x}_i \in \mathbb{R}$, velocity $\hat{v}_i \in \mathbb{R}$, and disturbance state variable $\hat{z}_{di} \in \mathbb{R}^{n_z}$ are found using a distributed observer:

$$\begin{aligned}
\dot{\hat{x}}_i &= \hat{v}_i + k_{ox}(y_i^r - \hat{y}_i^r) \\
\dot{\hat{v}}_i &= u_i + \hat{d}_i + k_{ov}(y_i^r - \hat{y}_i^r) \\
\dot{\hat{z}}_{di} &= A_d \hat{z}_{di} + K_{od}(y_i^r - \hat{y}_i^r) \\
\hat{y}_i^r &= g_1(\textstyle\sum_{j \in \mathcal{N}_i}(\hat{x}_i - \hat{x}_j) + b_i \hat{x}_i) + g_2(\sum_{j \in \mathcal{N}_i}(\hat{v}_i - \hat{v}_j) + b_i \hat{v}_i) \\
\hat{d}_i &= C_d \hat{z}_{di}
\end{aligned} \tag{4.5}$$

in which the observer gains $k_{ov}, k_{ox} \in \mathbb{R}$ and $K_{od} \in \mathbb{R}^{n_z \times 1}$ will be designed later in this section. Also, $\mathcal{N}_i$ denotes the neighboring set of i^{th} vehicle over an undirected graph $\mathcal{G}$ which satisfies the following assumption.

Assumption 4.1.1. *The undirected communication graph $\mathcal{G}$ is connected.*

We define observer error variables $e_{xi} = \hat{x}_i - x_i$, $e_{vi} = \hat{v}_i - v_i$, $e_{zi} = \hat{z}_{di} - z_{di}$ and find the observer error dynamics:

$$
\begin{aligned}
\dot{e}_{xi} &= e_{vi} - k_{ox}(g_1(\textstyle\sum_{j\in\mathcal{N}_i}(e_{xi}-e_{xj}) + b_i e_{xi}) + g_2(\textstyle\sum_{j\in\mathcal{N}_i}(e_{vi}-e_{vj}) + b_i e_{vi}))\\
\dot{e}_{vi} &= C_d e_{zi} - k_{ov}(g_1(\textstyle\sum_{j\in\mathcal{N}_i}(e_{xi}-e_{xj}) + b_i e_{xi}) + g_2(\textstyle\sum_{j\in\mathcal{N}_i}(e_{vi}-e_{vj}) + b_i e_{vi}))\\
\dot{e}_{zi} &= A_d e_{zi} - K_{od}(g_1(\textstyle\sum_{j\in\mathcal{N}_i}(e_{xi}-e_{xj}) + b_i e_{xi}) + g_2(\textstyle\sum_{j\in\mathcal{N}_i}(e_{vi}-e_{vj}) + b_i e_{vi}))
\end{aligned}
\tag{4.6}
$$

The augmented multi-vehicle system and observer error dynamics are modeled by:

$$
\left[\begin{array}{c}\dot{\zeta}\\ \hline \dot{e}\end{array}\right] = \left[\begin{array}{c|c}\mathbf{A}_{11} & \mathbf{A}_{12}\\ \hline \mathbf{0} & \mathbf{A}_{22}\end{array}\right]\left[\begin{array}{c}\zeta\\ \hline e\end{array}\right] + \left[\begin{array}{c}\mathbf{B}_{d1}\\ \hline \mathbf{0}\end{array}\right] z \tag{4.7}
$$

$$
\mathbf{A}_{11} = \begin{bmatrix}\mathbf{0} & I_N\\ k_{cx}\mathcal{L} & k_{cv}\mathcal{L} - \alpha_v I_N\end{bmatrix}, \qquad \mathbf{A}_{12} = \begin{bmatrix}\mathbf{0} & \mathbf{0} & \mathbf{0}\\ k_{cx}\mathcal{L} & k_{cv}\mathcal{L} - \alpha_v I_N & K_{cd}\otimes I_N\end{bmatrix}
$$

$$
\mathbf{A}_{22} = \begin{bmatrix}-g_1 k_{ox}\mathcal{H} & I_N - g_2 k_{ox}\mathcal{H} & \mathbf{0}\\ -g_1 k_{ov}\mathcal{H} & -g_2 k_{ov}\mathcal{H} & C_d\otimes I_N\\ -g_1 K_{od}\otimes\mathcal{H} & -g_2 K_{od}\otimes\mathcal{H} & A_d\otimes I_N\end{bmatrix}, \qquad \mathbf{B}_{d1} = \begin{bmatrix}\mathbf{0}\\ (K_{cd}+C_d)\otimes I_N\end{bmatrix}
$$

where $\zeta = [x^T, v^T]^T \in \mathbb{R}^{2N}$, $x = col\{x_i\} \in \mathbb{R}^N$, $v = col\{v_i\} \in \mathbb{R}^N$, $e = [e_x^T, e_v^T, e_z^T]^T \in \mathbb{R}^{2N+Nn_z}$, and $e_x = col\{e_{xi}\}, e_v = col\{e_{vi}\} \in \mathbb{R}^N$. Based on the disturbance generator model (4.2) and Table 3.1, it is evident that the dimension n_z of disturbance state variable z_i depends on the shape of persistent disturbance; thus, we define $z = col\{col\{z_{li}\}, ..., col\{z_{n_z}\}\} \in \mathbb{R}^{Nn_z}$ and $e_z = col\{col\{e_{z1i}\}, ..., col\{e_{zn_zi}\}\} \in \mathbb{R}^{Nn_z}$ where $e_{zli} = \hat{z}_{li} - z_{li}$ for all $l \in \{1, ..., n_z\}$.

We now take the diagonal blocks of (4.7) and find two sets of differential equations corresponding to multi-vehicle and observer error dynamics. In particular, $\dot{e} = \mathbf{A}_{22}e$ results in the following transformed aggregated observer dynamics:

$$\begin{bmatrix} \dot{e}_{xT} \\ \dot{e}_{vT} \\ \dot{e}_{zT} \end{bmatrix} = \begin{bmatrix} -g_1 k_{ox}\Lambda_h & I_N - g_2 k_{ox}\Lambda_h & \mathbf{0} \\ -g_1 k_{ov}\Lambda_h & -g_2 k_{ov}\Lambda_h & C_d \otimes I_N \\ -g_1 K_{od} \otimes \Lambda_h & -g_2 K_{od} \otimes \Lambda_h & A_d \otimes I_N \end{bmatrix} \begin{bmatrix} e_{xT} \\ e_{vT} \\ e_{zT} \end{bmatrix} \tag{4.8}$$

in which $e_{xT} = T_h^{-1}e_x$, $e_{vT} = T_h^{-1}e_v$, $e_{zT} = (I_{n_z} \otimes T_h^{-1})$, and $T_h \in \mathbb{R}^{N\times N}$ is a unitary transformation matrix that completely diagonalizes the symmetric matrix $\mathcal{H}$ as $T_h\mathcal{H}T_h^{-1} = \Lambda = diag\{\mu_i\}$ where $\mu_i > 0$ are eigenvalues of $\mathcal{H} \succ \mathbf{0}$ for $i \in \{1, 2, ..., N\}$. We notice that these aggregated error dynamics are in fact composed by N "networked" observer error models:

$$\begin{aligned} \dot{e}_{xTi} &= -\mu_i g_1 k_{ox} e_{xTi} + (1 - g_2\mu_i k_{ox}) e_{vTi} \\ \dot{e}_{vTi} &= -\mu_i g_1 k_{ov} e_{xTi} - \mu_i g_2 k_{ov} e_{vTi} + C_d e_{zTi} \\ \dot{e}_{zTi} &= -\mu_i g_1 K_{od} e_{xTi} - \mu_i g_2 K_{od} e_{vTi} + A_d e_{zTi} \end{aligned} \tag{4.9}$$

where μ_i result in heterogeneity of the closed-loop networked observers (with k_{ox}, k_{ov} and K_{od} in the loop).

Moreover, using the first row $\dot{\zeta} = \mathbf{A}_{11}\zeta + \mathbf{B}_{d1}z$ of (4.7), the multi-vehicle system is written as follows:

$$\begin{bmatrix} \dot{x}_T \\ \dot{v}_T \end{bmatrix} = \begin{bmatrix} \mathbf{0} & I_N \\ k_{ox}\Lambda_l & k_{cv}\Lambda_l - \alpha_v I_N \end{bmatrix} \begin{bmatrix} x_T \\ v_T \end{bmatrix} + \begin{bmatrix} \mathbf{0} \\ (K_{cd} + C_d) \otimes I_N \end{bmatrix} z_T \tag{4.10}$$

in which $x_T = T_l^{-1}x$, $v_T = T_l^{-1}v$, $z_T = (I_{n_z} \otimes T^{-1})z$ where $T_l \in \mathbb{R}^{N\times N}$ is a unitary transformation that completely diagonalizes the symmetric Laplacian matrix $\mathcal{L}$ such that $T_l\mathcal{L}T_l^{-1} = \Lambda_l = diag\{0, \lambda_2, \lambda_3, ..., \lambda_N\}$. As is seen, $\lambda_1 = 0$ in the diagonal matrix Λ_l determines the null space of graph Laplacian matrix $\mathcal{L}$, and results in a subsystem that does not satisfy the controllability condition. Therefore, we apply another transformation $\xi = \mathcal{P}\zeta$ where $\zeta = [x^T, v^T]^T$ and $\mathcal{P} \in \mathbb{R}^{2N\times 2N}$ is a row switching matrix that results in $\xi = [\xi_a, \xi_d]^T$, $\xi_a = [x_{T1}, v_{T1}]^T$, and $\xi_d = [col\{x_{Ti}\}^T, col\{v_{Ti}\}^T]^T$ for $i \in \{2, 3, ..., N\}$. The subscript $_a$ stands for agreement subspace which is uncontrollable, and $_d$ indicates disagreement controllable subspace. The transformed system can be written as follows:

$$\dot{\xi} = \left[\begin{array}{cc|cc} 0 & 1 & \mathbf{0} & \mathbf{0} \\ 0 & -\alpha_v & \mathbf{0} & \mathbf{0} \\ \hline \mathbf{0} & \mathbf{0} & \mathbf{0} & I_{N-1} \\ \mathbf{0} & \mathbf{0} & k_{cx}\Lambda_{ld} & k_{cv}\Lambda_{ld} - \alpha_v I_{N-1} \end{array}\right] \xi + \left[\begin{array}{c} 0 \\ K_{cd} + C_d \\ \hline \mathbf{0} \\ (K_{cd} + C_d) \otimes I_{N-1} \end{array}\right] z_{Tr} \quad (4.11)$$

in which the agreement and disagreement dynamics are decoupled from each other. The vector $z_{Tr} = [z_{Ta}^T, z_{Td}]^T$ is a re-arranged vector of disturbances according to the row switching rule of $\mathcal{P}^{-1}$. The unobservable agreement dynamics show their effects on the (stationary) consensus value, and will be discussed later in Corollary 4.1.1 and Lemma 4.1.1. However, the controllable disagreement dynamics are made by $N-1$ heterogeneous networked vehicle models for $i \in \{2, 3, ..., N\}$:

$$\begin{aligned} \dot{x}_{Ti} &= v_{Ti} \\ \dot{v}_{Ti} &= \lambda_i k_{cx} x_{Ti} + (\lambda_i k_{cv} - \alpha_v) v_{Ti} + (K_{cd} + C_d) z_{Ti} \end{aligned} \quad (4.12)$$

where the heterogeneity is due to the nonzero eigenvalues λ_i of $\mathcal{L}$, and the word "networked" is used with the same interpretation as in (4.9).

We now rely on the networked local dynamics (4.9) and (4.12), and characterize the relative output feedback stationary consensus problem (4.3) as output feedback stabilization task using heterogeneously-scaled absolute measurements (due to μ_i and λ_i), and establish three equivalent conditions for consensus gains to ensure stationary agreement (4.3) in multi-vehicle system (4.1) using dynamic relative output feedback algorithm (4.4)-(4.5).

Proposition 4.1.1. *The dynamic distributed algorithm* (4.4)-(4.5) *guarantees leaderless stationary consensus* (4.3) *among vehicles* (4.1) *in the presence of persistent disturbances* (4.2) *whenever Assumption 4.1.1 is satisfied and the following vehicle-level conditions are guaranteed:*

1. *The disturbance control gain K_{cd} should accommodate the effect of unknown heterogeneous disturbances on the networked vehicle dynamics* (4.12).

2. *Verifying the observability of (C_o, A_o), a single (Luenberger) observer gain $K_o = [k_{ox}, k_{ov}, K_{od}^T]^T$ should be designed for the following networked error dynamics:*

$$\begin{bmatrix} \dot{e}_{xTi} \\ \dot{e}_{vTi} \\ \dot{e}_{zTi} \end{bmatrix} = \underbrace{\begin{bmatrix} 0 & 1 & 0 \\ 0 & 0 & C_d \\ 0 & 0 & A_d \end{bmatrix}}_{A_o} \begin{bmatrix} e_{xTi} \\ e_{vTi} \\ e_{zTi} \end{bmatrix} \qquad y_{Ti} = \underbrace{\begin{bmatrix} \mu_i g_1 & \mu_i g_2 & \boldsymbol{0} \end{bmatrix}}_{C_o} \begin{bmatrix} e_{xTi} \\ e_{vTi} \\ e_{zTi} \end{bmatrix} \tag{4.13}$$

with N heterogeneous measurements where the heterogeneity is due to the positive eigenvalues μ_i of $\mathcal{H}$.

3. *For any arbitrarily selected scalar $\alpha_v > 0$, the control gain $K_c = [k_{cx}, k_{cv}]$ should stabilize the networked vehicle dynamics for $i \in \{2, ..., N\}$:*

$$\begin{aligned} &\dot{x}_{Ti} = v_{Ti} \qquad \dot{v}_{Ti} = u_{Ti} - \alpha_v v_{Ti} \qquad u_{Ti} = K_c y_{Ti} \\ &y_{Ti} = \lambda_i \begin{bmatrix} x_{Ti} \\ v_{Ti} \end{bmatrix} \end{aligned} \tag{4.14}$$

with $N-1$ heterogeneous measurements where heterogeneity is the effect of positive eigenvalues λ_i of $\mathcal{L}$. (The effect of α_v on final position of vehicles will be discussed at the end of this section.)

The proof of this proposition is immediate based on the aforementioned derivations noticing the fact that, satisfying Part 1 of proposition, separation principle holds for designing observer and controller gains (see the structure of (4.7)). Although the first part of this proposition is independent of the multi-vehicle system's dimension, we need to examine the observer gains k_{ox}, k_{ov} and K_{od} for N nonzero eigenvalues μ_i of $\mathcal{H}$, and control gains k_{cx}, k_{cv} for $N-1$ nonzero eigenvalues λ_i of $\mathcal{L}$. This fact puts question on the feasibility of using Proposition 4.1.1 for a multi-vehicle system with a high-number of vehicles.

We follow follow the ideas of Chapter 3 and, by reformulating the static output feedback problem (4.14) as a state-feedback robust control challenge for the nominal networked vehicles' model subject to fictitious uncertainties, provide a systematic approach to find appropriate control and observer gains that guaran-

tee stationary consensus in a multi-vehicle system operating in unknown environments. At first, we investigate the control design problem in Parts 1 and 3 of Proposition 4.1.1 and, later, we will discuss the observer gain design problem.

Design procedure 4.1.1. *1. Disturbance control gain K_c should minimize the norm $\|(K_c+C_d)z_{Ti}\|$ where, based on the definition of disturbance generator model (4.2), $K_{cd}=-C_d$ accommodates all persistent disturbances.*

2. Robust state feedback gains k_{cx} and k_{cv} should be designed to stabilize networked robot dynamics:

$$\begin{aligned}\dot{x}_{Ti} &= v_{Ti}\\ \dot{v}_{Ti} &= -\alpha_v v_{Ti}+\lambda_2 u_{Ti}+\underbrace{\lambda_2 E(\lambda_i)u_{Ti}}_{\textit{Modeling uncertainties}}\end{aligned} \tag{4.15}$$

where $E(\lambda_i)=\frac{\lambda_i}{\lambda_2}-1\geq 0$ are (communication graph-induced) factitious modeling uncertainties for $i\in\{2,3,...,N\}$.

We emphasize that all eigenvalues λ_i might be known due to the knowledge about communication topology $\mathcal{G}$, but we only use the algebraic connectivity λ_2 and consider the rest as the sources of modeling uncertainties in order to propose a one-step design procedure and find consensus gains in (4.4). (This is the reason to call $\lambda_2 E(\lambda_i)u_{Ti}$ "fictitious" modeling uncertainties.) Now, we define a second-order state space model $\dot{\xi}_i=A\xi_i+Bu_{Ti}$ for the nominal networked vehicle dynamics in (4.15):

$$\begin{bmatrix}\dot{x}_{Ti}\\ \dot{v}_{Ti}\end{bmatrix}=\begin{bmatrix}0 & 1\\ 0 & -\alpha_v\end{bmatrix}\begin{bmatrix}x_{Ti}\\ v_{Ti}\end{bmatrix}+\begin{bmatrix}0\\ \lambda_2\end{bmatrix}u_{Ti} \tag{4.16}$$

and let $Q_c = Q_c^T \in \mathbb{R}^{2\times 2} \succ \mathbf{0}$ be a design matrix and $r_c > 0$ be a design scalar to respectively weigh state and control input variables. In the next theorem, we systematically derive two static consensus gains k_{cx} and k_{cv} that stabilize uncertain dynamics in Step 2 of Design procedure 4.1.1 for all $i \in \{2, 3, ..., N\}$.

Theorem 4.1.1. *Let $u_{Ti} = K_c\xi_i$ be the signal that minimizes the quadratic cost function* (4.17) *where $\mathcal{U}_{Ti}$ is the set of all (admissible) stabilizing signals u_{Ti}. Then, $K_c = [k_{cx}, k_{cv}]$ is the required gain to stabilize uncertain networked-vehicle dynamics* (4.15).

$$\begin{aligned} \min_{u_{Ti}\in\mathcal{U}_{Ti}} \quad & J(\xi_i(0)) = \textstyle\int_0^\infty (\xi_i^T Q_c \xi_i + r_c u_{Ti}^2) dt \\ \textit{subject to} \quad & \dot{\xi}_i = A\xi_i + Bu_{Ti} \quad \textit{in} \quad (4.16) \end{aligned} \tag{4.17}$$

Proof. This proof is available at Subsection 4.5.1. □

Now, we introduce the networked observer's nominal dynamics:

$$\dot{\tau}_i = A_o\tau_i, \qquad y_i = C_{o\mu_1}u_{oi} \tag{4.18}$$

where A_o is defined in (4.13) and $C_{o\mu_1} = \mu_1[g_1, g_2, 0]$. Also, let $Q_o = Q_o^T \in \mathbb{R}^{(2+n_z)\times(2+n_z)} \succ \mathbf{0}$ be a design matrix and $r_o > 0$ be a design scalar. In the next theorem, we systematically find the required observer gain $K_o = [k_{ox}, k_{ov}, K_{od}^T]^T \in \mathbb{R}^{n_z+2}$ to be used in (4.5).

Theorem 4.1.2. *Let $u_{oi} = K_o^T\tau_i$ be the minimizer of* (4.19) *subject to a completely known dynamical system and $\mathcal{U}_{oi}$ denote the set of admissible control signals for u_{oi}. Then, K_o is the required observer gains for dynamical system* (4.13) *in Step 2 of Proposition 4.1.1.*

$$\begin{aligned} \min_{u_{oi}\in\mathcal{U}_{oi}} \quad & J(\tau_i(0)) = \int_0^\infty (\tau_i^T Q_o \tau_i + r_c u_{oi}^2) dt \\ \textit{subject to} \quad & \dot{\tau}_i = A_o^T \tau_i + C_{o\mu_1}^T u_{oi} \end{aligned} \tag{4.19}$$

Proof. This proof is available at Subsection 4.5.2. □

Now that the required control and observer gains of Proposition 4.1.1 are designed, we know all trajectories of the closed-loop multi-vehicle system (4.1) with consensus algorithm (4.4)-(4.5) converge to an agreement subspace which is determined by the nullity of graph Laplacian matrix $\mathcal{L}$ (e.g., the subspace created by agreement dynamics corresponding to the first row in (4.11)). In the next corollary, we find the agreement value assuming that all vehicles measure their relative variables and use the observer-free stationary consensus algorithm:

$$u_i = k_{cx} \sum_{j\in\mathcal{N}_i} (x_i - x_j) + k_{cv} \sum_{j\in\mathcal{N}_i} (v_i - v_j) - \alpha_v v_i - d_i \tag{4.20}$$

where the last term is changed from $K_{cd} z_i$ to $-d_i$ since we know d_i. Then, in Lemma 4.1.1, we generalize it to the observer-based approach of this section.

Corollary 4.1.1. *The observer-free consensus algorithm* (4.20)*, with perfect state and disturbance measurements, will result in the following stationary agreement values in multi-vehicle system* (4.1)*:*

$$\begin{aligned} \lim_{t\to\infty} x_i(t) &= \tfrac{1}{N} \textstyle\sum_{i=1}^N x_i(0) + \tfrac{1}{\alpha_v N} \sum_{i=1}^N v_i(0) \\ \lim_{t\to\infty} v_i(t) &= 0 \end{aligned} \tag{4.21}$$

Proof. This proof is given at Subsection 4.5.3. □

Lemma 4.1.1. *The observer-based output feedback stationary consensus algorithm* (4.4)-(4.5) *results in an agreement on the following point:*

$$\begin{aligned}\lim_{t\to\infty} x_i(t) = \; & \tfrac{1}{N}\sum_{i=1}^{N} x_i(0) + \tfrac{1}{\alpha_v N}\sum_{i=1}^{N} v_i(0) \\ & + \tfrac{1}{N}\int_0^\infty e^{-\alpha_v \sigma}\int_0^\sigma e^{\alpha_v \tau}\sum_{i=1}^{N}(-\alpha_v e_{vi}(\tau) + K_{cd} e_{zi}(\tau))d\tau d\sigma\end{aligned} \tag{4.22}$$

$$\lim_{t\to\infty} v_i(t) = 0$$

Proof. The proof is written at Subsection 4.5.4. □

In summary, based on the formulation (4.14) (also (4.15)), Theorem 4.1.1 guarantees that the stability of disagreement dynamics in (4.11) is achieved for any "arbitrarily" selected $\alpha_v > 0$, and Lemma 4.1.1 shows this α_v adds a level of flexibility to tune the internal behavior of multi-vehicles agreement dynamics (although they remain "cooperatively" uncontrollable according to the partitioning in (4.11)). Additionally, as expected, the last term in x_i^a indicates that the agreement value depends on the average of velocity and disturbance state estimation errors' transient behavior. This will be discussed in simulations of Section 4.3.

4.2 Leader-follower stationary consensus

We adopt the result of Section 4.1 and develop a systematic approach to design a leader-follower stationary consensus algorithm. Furthermore, we analytically find the solution for consensus gains based on the design variables.

4.2.1 Problem statement

In this section, we consider a multi-vehicle system where the followers are modeled by second-order dynamics for $i \in \{1, 2, ..., N\}$:

$$\begin{aligned} &\dot{x}_i = v_i \qquad \dot{v}_i = u_i + d_i \\ &y_i^r = g_1(\textstyle\sum_{j=1}^{N}(x_i - x_j) + b_i(x_i - x_0)) + g_2(\sum_{j=1}^{N}(v_i - v_j) + b_i v_i) \end{aligned} \tag{4.23}$$

Here, $b_i = 1$ whenever the i^{th} vehicle can is aware of its relative distance to the reference position and is potentially aware of its absolute velocity (depending on g_2), and $b_i = 0$ otherwise. All variables $x_i, v_i, u_i, y_i^r, d_i, g_1, g_2 \in \mathbb{R}$ are defined similar to the leaderless consensus problem in Section 4.1, and we emphasize that $g_1 \neq 0$. The reference point is commanded by a stationary leader:

$$\dot{x}_0 = 0 \tag{4.24}$$

which, unlike followers, is described by a first-order model and its adjustable initial state value $x_0(t) = x_0(t_0)$ denotes the desired position for all $t \geq t_0$. Now, we define the leader-follower stationary consensus as follows:

$$\lim_{t\to\infty} x_i(t) = x_0(t_0) \qquad \textit{and} \qquad \lim_{t\to\infty} v_i(t) = 0 \tag{4.25}$$

where $t_0 \geq 0$ denotes the time of change in the reference command. Before proposing the main result of this section, we make an assumption on the leader-follower communication graph topology $\mathcal{G}_{lf}$.

Assumption 4.2.1. *The leader-follower graph $\mathcal{G}_{lf}$ has a spanning tree with the leader node $i = 0$ as the root.*

4.2.2 Main result

In this subsection, we propose a dynamic distributed leader-follower stationary consensus algorithm in order to ensure agreement (4.25) in a multi-vehicle system (4.23)-(4.24):

$$u_i = k_{cx}(\sum_{j=1}^{N}(\hat{x}_i - \hat{x}_j) + b_i(\hat{x}_i - x_0)) + k_{cv}(\sum_{j=1}^{N}(\hat{v}_i - \hat{v}_j) + b_i\hat{v}_i) + K_{cd}\hat{z}_i \quad (4.26)$$

where $\hat{x}_i, \hat{v}_i \in \mathbb{R}$ respectively denote position and velocity of the i^{th} vehicle estimated by the following distributed observer:

$$\begin{aligned}
&\dot{\hat{x}}_i = \hat{v}_i + k_{ox}(y_i^r - \hat{y}_i^r) \qquad\qquad \dot{\hat{v}}_i = u_i + \hat{d}_i + k_{ov}(y_i^r - \hat{y}_i^r)\\
&\dot{\hat{z}}_i = A_d\hat{z}_i + K_{od}(y_i^r - \hat{y}_i^r)\\
&\hat{y}_i^r = g_1(\textstyle\sum_{j=1}^{N}(\hat{x}_i - \hat{x}_j) + b_i(\hat{x}_i - x_0)) + g_2(\sum_{j=1}^{N}(\hat{v}_i - \hat{v}_j) + b_i\hat{v}_i)\\
&\hat{d}_i = C_d\hat{z}_i
\end{aligned} \quad (4.27)$$

We define observer error variables $e_{xi} = \hat{x}_i - x_i$, $e_{vi} = \hat{v}_i - v_i$, $e_{zi} = \hat{z}_i - z_i$, and find observer error dynamics:

$$\begin{aligned}
\dot{e}_{xi} &= e_{vi} - k_{ox}(g_1(\textstyle\sum_{j=1}^{N}(e_{xi} - e_{xj}) + b_ie_{xi}) + g_2(\sum_{j=1}^{N}(e_{vi} - e_{vj}) + b_ie_{vi}))\\
\dot{e}_{vi} &= C_de_{zi} - k_{ov}(g_1(\textstyle\sum_{j=1}^{N}(e_{xi} - e_{xj}) + b_ie_{xi}) + g_2(\sum_{j=1}^{N}(e_{vi} - e_{vj}) + b_ie_{vi}))\\
\dot{e}_{zi} &= A_de_{zi} - K_{od}(g_1(\textstyle\sum_{j=1}^{N}(e_{xi} - e_{xj}) + b_ie_{xi}) + g_2(\sum_{j=1}^{N}(e_{vi} - e_{vj}) + b_ie_{vi}))
\end{aligned} \quad (4.28)$$

Furthermore, the leader-follower tracking error dynamics are written as:

$$\begin{aligned}
\dot{\epsilon}_{xi} = \;& v_i\\
\dot{v}_i = \;& k_{cx}(\textstyle\sum_{j=1}^{N}(\epsilon_{xi} - \epsilon_{xj}) + b_i\epsilon_{xi}) + k_{cv}(\sum_{j=1}^{N}(v_i - v_j) + b_iv_i)\\
&+k_{cx}(\textstyle\sum_{j=1}^{N}(e_{xi} - e_{xj}) + b_ie_{xi}) + k_{cv}(\sum_{j=1}^{N}(e_{vi} - e_{vj}) + b_ie_{vi})\\
&+K_{cd}e_{zi}
\end{aligned} \quad (4.29)$$

where $\epsilon_{xi} = x_i - x_0 \in \mathbb{R}$ is the leader-follower position tracking error (recall that the leader is modeled as a first-order system). Thus, the aggregated leader-follower tracking and observation error dynamics are represented as follows:

$$\left[\begin{array}{c}\dot{\zeta}\\ \hline \dot{e}\end{array}\right] = \left[\begin{array}{c|c}\mathbf{A}_{11} & \mathbf{A}_{12}\\ \hline \mathbf{0} & \mathbf{A}_{22}\end{array}\right]\left[\begin{array}{c}\zeta\\ \hline e\end{array}\right] + \left[\begin{array}{c}\mathbf{B}_{d1}\\ \hline \mathbf{0}\end{array}\right] z \tag{4.30}$$

where $\zeta = [\epsilon_x^T, v^T]^T \in \mathbb{R}^{2N}$, $\epsilon_x = col\{\epsilon_{xi}\} \in \mathbb{R}^N$, $v = col\{v_i\} \in \mathbb{R}^N$, $e = [e_x^T, e_v^T, e_z^T]^T \in \mathbb{R}^{2N+Nn_z}$, $e_x = col\{e_{xi}\} \in \mathbb{R}^N$, $e_v = col\{e_{vi}\} \in \mathbb{R}^N$, $e_z = col\{e_{zi}\} \in \mathbb{R}^{Nn_z}$, and $z = col\{z_i\} \in \mathbb{R}^{Nn_z}$ for all $i \in \{1, 2, ..., N\}$, and the sub-matrices are as follows:

$$\mathbf{A}_{11} = \begin{bmatrix} \mathbf{0} & I_N \\ k_{cx}\mathcal{H} & k_{cv}\mathcal{H} \end{bmatrix} \qquad \mathbf{A}_{12} = \begin{bmatrix} \mathbf{0} & \mathbf{0} & \mathbf{0} \\ k_{cx}\mathcal{H} & k_{cv}\mathcal{H} & K_{cd} \otimes I_d \end{bmatrix}$$

$$\mathbf{A}_{22} = \begin{bmatrix} -g_1 k_{ox}\mathcal{H} & -g_2 k_{ox}\mathcal{H} & \mathbf{0} \\ -g_1 k_{ov}\mathcal{H} & -g_2 k_{ov}\mathcal{H} & C_d \otimes I_N \\ -g_1 K_{od} \otimes \mathcal{H} & -g_2 K_{od} \otimes \mathcal{H} & A_d \otimes I_N \end{bmatrix} \qquad \mathbf{B}_{d1} = \begin{bmatrix} \mathbf{0} \\ (K_{cd} + C_d) \otimes I_N \end{bmatrix}$$

Based on the augmented system (4.30), we conclude the separation principle holds and, thus, consensus and observer gains can be designed independent of each other. For the observer design purpose, we find the following networked observer dynamics:

$$\begin{aligned} \dot{e}_{xTi} &= -\mu_i g_1 k_{ox} e_{xTi} + (1 - \mu_i g_2 k_{ox}) e_{vTi} \\ \dot{e}_{vTi} &= -\mu_i g_1 k_{ov} e_{xTi} - \mu_i g_2 k_{ov} e_{vTi} + C_d e_{zTi} \\ \dot{e}_{zTi} &= -\mu_i g_1 K_{od} e_{xTi} - \mu_i g_2 K_{od} e_{vTi} + A_d e_{zTi} \end{aligned} \tag{4.31}$$

which show the proposed leader-follower stationary consensus algorithm (4.26)-(4.27) has resulted in the same problem as the leaderless consensus scenario in (4.13). For the control gain design problem, since $\mathcal{H}$ is a symmetric positive-definite matrix, we find a completely controllable diagonal representation:

$$\begin{bmatrix} \dot{\epsilon}_{xT} \\ \dot{v}_T \end{bmatrix} = \begin{bmatrix} \mathbf{0} & I_N \\ k_{cx}\Lambda_h & k_{cv}\Lambda_h \end{bmatrix} \begin{bmatrix} \epsilon_{xT} \\ v_T \end{bmatrix} + \begin{bmatrix} \mathbf{0} \\ (K_{cd} + C_d) \otimes I_N \end{bmatrix} z_T \tag{4.32}$$

based on $\epsilon_{xT} = T_h^{-1}\epsilon_x$, $v_T = T_h^{-1}v$, and $z_T = (I_{n_z} \otimes T_h^{-1})z$ where $T_h \in \mathbb{R}^{N\times N}$ is defined such that $T_h\mathcal{H}T_h^{-1} = \Lambda_h = diag\{\mu_i\}$ for $i \in \{1, 2, ..., N\}$. The transformed dynamics (4.32) are in fact composed by N heterogeneous networked leader-follower tracking error systems:

$$\begin{aligned} \dot{\epsilon}_{xTi} &= v_{Ti} \\ \dot{v}_{Ti} &= \mu_i k_{cx}\epsilon_{Ti} + \mu_i k_{cv} v_{Ti} + (K_{cd} + C_d) z_{Ti} \end{aligned} \tag{4.33}$$

in which $\mu_i > 0$ for all $i \in \{1, 2, ..., N\}$. Therefore, the following proposition holds in this section.

Proposition 4.2.1. *Suppose Assumption 4.2.1 is satisfied by communication graph $\mathcal{G}_{lf}$. The dynamic distributed algorithm* (4.26)-(4.27) *ensures leader-follower stationary agreement* (4.25) *in a multi-vehicle system* (4.23) *in the presence of unknown disturbances* (4.2) *whenever, in addition to Steps 1 and 2 of Proposition 4.1.1, the control gain $K_c = \begin{bmatrix} k_{cx} & k_{cv} \end{bmatrix}$ stabilizes the networked leader-follower tracking error dynamics:*

$$
\begin{aligned}
&\dot{\epsilon}_{xTi} = v_{Ti}, \qquad \dot{v}_{Ti} = u_{Ti} \\
&u_{Ti} = K_c y_i \\
&y_i = \begin{bmatrix} \mu_i & 0 \\ 0 & \mu_i \end{bmatrix} \begin{bmatrix} \epsilon_{xTi} \\ v_{Ti} \end{bmatrix}
\end{aligned} \qquad \forall i \in \{1, 2, ..., N\} \tag{4.34}
$$

where $\mu_i > 0$ *are the eigenvalues of reduced-order Laplacian matrix* $\mathcal{H}$ *for all* $i \in \{1, 2, ..., N\}$.

This proposition, along with the observer dynamics (4.31) and disturbance component in (4.33), formulates the distributed stationary leader-follower algorithm (4.26)-(4.27) such that the disturbance control gain can be found following Step 1 in Design procedure 4.1.1, and the observer gain can be designed using Theorem 4.1.2 in Section 4.1. In the next design procedure, we propose a systematic framework to find the consensus gains k_{cx} and k_{cv} based on a robust control formulation for modified networked leader-follower tracking error dynamics with a homogeneous nominal part and heterogeneous fictitious modeling uncertainties.

Design procedure 4.2.1. *Design state feedback gains* $k_{cx}, k_{cv} \in \mathbb{R}$ *that stabilize the networked vehicle dynamics with homogeneous nominal model and heterogeneous fictitious modeling uncertainties:*

$$
\begin{aligned}
\dot{x}_{Ti} &= v_{Ti} \\
\dot{v}_{Ti} &= \mu_1 u_{Ti} + \mu_1 E(\mu_i) u_{Ti} \\
u_{Ti} &= k_{cx} x_{Ti} + k_{cv} v_{Ti}
\end{aligned} \tag{4.35}
$$

where $E(\mu_i) = \frac{\mu_i}{\mu_1} - 1 \geq 0$ *are the sources of heterogeneous modeling uncertainties.*

Note that we originally proposed a dynamic output feedback stationary consensus algorithm (4.26)-(4.27) using relative measurements; converted it to three sub-

problems to design consensus, observer, and disturbance gains in Proposition 4.2.1 where the consensus gains k_{cx} and k_{cv} were the stabilizing solutions for N static "output feedback" networked vehicles using N scaled absolute measurements; and, eventually, reformulated the problem as N static "state feedback" robust stabilization tasks using vehicles' absolute state measurements (Design procedure 4.2.1). Now, we introduce a second-order state space realization $\dot{\xi}_i = A\xi_i + Bu_{Ti}$ which models the nominal dynamics of (4.35):

$$\begin{bmatrix} \dot{x}_{Ti} \\ \dot{v}_{Ti} \end{bmatrix} = \begin{bmatrix} 0 & 1 \\ 0 & 0 \end{bmatrix} \begin{bmatrix} x_{Ti} \\ v_{Ti} \end{bmatrix} + \begin{bmatrix} 0 \\ \mu_1 \end{bmatrix} u_{Ti} \tag{4.36}$$

Furthermore, we define $Q_c = Q_c^T \in \mathbb{R}^{2\times 2} \succ \mathbf{0}$ as the state weighting, and $r_c > 0$ as the control input weighting design matrices. In the next theorem, we propose a systematic framework to find the required consensus gains as a single robust state feedback problem.

Theorem 4.2.1. *The solution $u_{Ti} = K_c\xi_i$ to the minimization problem* (4.37)*, where $\mathcal{U}_{Ti}$ denotes the set of all stabilizing state feedback controllers u_{Ti}, stabilizes the heterogeneous networked vehicle dynamics* (4.35) *for all $i \in \{1, 2, ..., N\}$.*

$$\begin{aligned} \min_{u_{Ti}\in\mathcal{U}_{Ti}} \quad & J(\xi_i(0)) = \textstyle\int_0^\infty (\xi_i^T Q_c \xi_i + r_c u_{Ti}^2) dt \\ \textit{subject to} \quad & \dot{\xi}_i = A\xi_i + Bu_{Ti} \quad \textit{in} \quad (4.36) \end{aligned} \tag{4.37}$$

Proof: We mention that, although system matrices (A, B) in (4.37) is different from (4.17), the minimization problems are structurally the same such that the fundamental properties (4.39) are still valid for any pairs ξ_i, u_{Ti} of this leader-

follower control theorem. Therefore, a detailed proof can be found by following the steps of proof in Theorem 4.1.1 which is omitted for brevity. □

As discussed earlier, the leader-follower approach is formulated such the disturbance control gain and observer gain design problems can be solved using the ideas in leaderless stationary consensus of Section 4.1. However, due to the special structure of (A, B) in (4.36), the 2×2 nonlinear matrix equation $A^T P_c + P_c A + Q_c - \frac{1}{r_c} P_c B B^T P_c = \mathbf{0}$ can be reduced to three scalar equations:

$$\frac{\mu_1^2}{r_c} p_{12}^2 = q_{11}, \qquad \frac{\mu_1^2}{r_c} p_{22}^2 = q_{22} + 2p_{12}, \qquad \frac{\mu_1^2}{r_c} p_{12} p_{22} = q_{12} + p_{11}$$

As a result, we find the following closed-form solution for the unique positive-definite stabilizing matrix P:

$$P_c = \begin{bmatrix} \sqrt{2q_{11} + q_{22}\sqrt{\frac{\mu_1^2}{r_c} q_{11}}} - q_{12} & \sqrt{\frac{r_c}{\mu_1^2} q_{11}} \\ \sqrt{\frac{r_c}{\mu_1^2} q_{11}} & \sqrt{2\frac{r_c}{\mu_1^2}\sqrt{\frac{r_c}{\mu_1^2} q_{11}} + \frac{r_c}{\mu_1^2} q_{22}} \end{bmatrix}$$

Consequently, we find closed-form solutions for the consensus gains k_{cx} and k_{cv} explicitly based on the design matrix Q_c, scalar r_c, and smallest eigenvalue of reduced-order Laplacian matrix μ_1 of $\mathcal{H}$:

$$k_{cx} = -\sqrt{\frac{1}{r_c} q_{11}} \qquad k_{cv} = -\sqrt{-\frac{2}{\mu_1} k_{cx} + \frac{1}{r_c} q_{22}}$$

using the optimal gain formula $K_c = [k_{cx}, k_{cv}] = -\frac{\mu_1}{r_c}[p_{12}, p_{22}] = -\frac{1}{r_c} B^T P$. We note that $P_c(1,1) > 0$ is guaranteed based on the observability and stabilizability of $(Q_c^{1/2}, A, B)$. As is seen, the position consensus gain k_{cx} is independent of the

communication network $\mathcal{G}$ (or μ_1); however, a network-dependent fraction of it appears in the velocity consensus gain k_{cv} (i.e., see $-\frac{2}{\mu_1}k_{cx}$ that is added to $\frac{1}{r_c}q_{22}$). These closed-form solutions can be used in tuning of weighting matrices Q_c and r_c, and also for the communication topology design purpose. We mention that the tuning process can be further simplified by letting $q_{12} = q_{21} = 0$ or using $Q_c = q_c I_2$ for a scalar tuning parameter $q_c > 0$.

4.3 Simulation verification

In this section, we verify the feasibility of the proposed theoretical results through various numerical simulations. The challenges of using conventional consensus algorithms have been discussed in Examples 3.1.1, 3.1.2, and 3.1.5. However, we rebuild the setup for the sake of readability.

4.3.1 Problem setup

In the leaderless problem, we consider a group of 5 vehicles modeled by (4.1) with $g_1 = 1$ and $g_2 = 0$, and assume nodes 1 and 2 have access to their absolute position information (i.e., $b_1 = b_2 = 1$). Vehicles are at initial conditions $x_1(0) = [-10, 20]^T$, $x_2(0) = [15, -15]^T$, $x_3(0) = [10, 15]^T$, $x_4(0) = [-30, 20]^T$, and $x_5(0) = [20, -30]^T$ (which are unknown to the designer). Moreover, vehicles are subject to heterogeneous constant disturbances $d_1 = 2, d_2 = 5, d_3 = 3, d_4 = 9$ and $d_5 = 4$. We let vehicles to exchange information over the leaderless graph in Figure 4.1.

In the leader-follower scenario, we add a leader agent v_0 modeled by (4.24) where its initial value can be commanded globally (and we will use a square

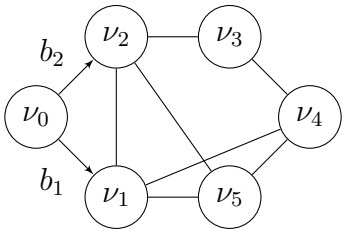

Figure 4.1: *Leaderless communication:* By removing node v_0 and edges originating from it, nodes v_1-v_5 and the associated edges represent an undirected leaderless communication topology $\mathcal{G}$ with graph Laplacian matrix $\mathcal{L}$. We assume agents v_1 and v_2 have access to their absolute measurements. *Leader–Follower communication:* v_1-v_5 communicate over undirected graph $\mathcal{G}$, v_1 and v_2 are aware of their relative distances to v_0, v_0-v_5 build a leader-follower communication graph $\mathcal{G}_{lf}$ with reduced-order Laplacian matrix $\mathcal{H} = \mathcal{L} + \mathcal{B}$ where $\mathcal{B} = diag\{1, 1, 0, 0, 0\}$.

wave input in simulation), and let vehicles to communicate over $\mathcal{G}_{lf}$ in Figure 4.1, and vehicles are subject to unknown sinusoidal disturbances: $d_1 = 7sin(0.5t)$, $d_2 = 5.5sin(0.5t)$, $d_3 = 6sin(0.5t)$, $d_4 = 2sin(0.5t)$, and $d_5 = 4sin(0.5t)$.

4.3.2 Leaderless stationary consensus

At first, in Figure 4.2, we consider an observer-free algorithm and verify that vehicles reach to zero and agree on the unknown position $x_i^a = 2$ as expected by Corollary 4.1.1. In Figure 4.3, we use the proposed observer-based algorithm (4.4)-(4.5) where all observers are at initial rest condition, and show all vehicles reach to a fixed-position agreement at $x_i^a = 2.9$. Moreover, unlike the conventional leaderless scenario of Example 3.1.2, all estimations are the same as actual position and velocity variables of vehicles. We further note that the difference in agreement position values of Figures 4.2 and 4.3 is expected based on Lemma 4.1.1.

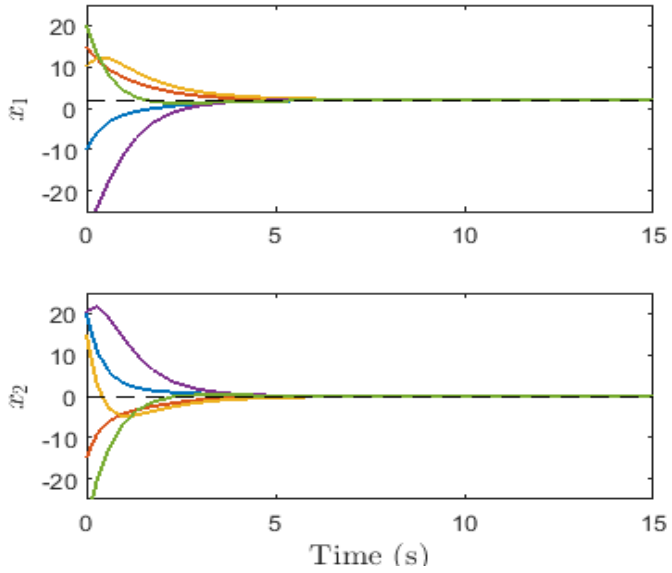

Figure 4.2: Observer-free stationary consensus algorithm to verify the result of Corollary 4.1.1 in the presence of constant disturbances. All vehicles agree on $x_i^a = 2$.

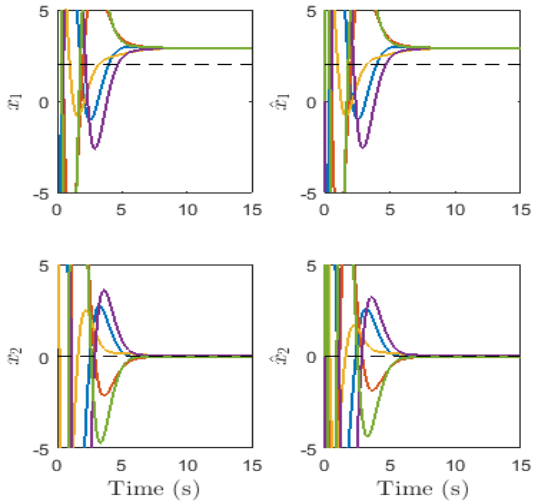

Figure 4.3: Leaderless stationary consensus algorithm of Section 4.1 where all observers are at initial rest condition and the agreement is on $x_i^a = 2.9$. The dashed line show the agreement value of Figure 4.2. This new agreement value is expected based on Lemma 4.1.1.

In Figure 4.4, we initialize the second observer at $\hat{x}_2(0) = [-10, 15, 0]^T$ and show the effect of observer error (trajectories) on the consensus value where, compared to Figures 4.3, the agreement is on $x_i^a = 2.4$. Finally, based on Theorem 4.1.2, we redesign observer gains by setting the state weighting matrix to be 10^3 greater than the first design (see Figure 4.3), and find a new agreement on $x_i^a = 0.078$ as is shown in Figure 4.5. In all of these simulation scenarios, disturbances are eventually estimated precisely as is depicted in Figure 4.6.

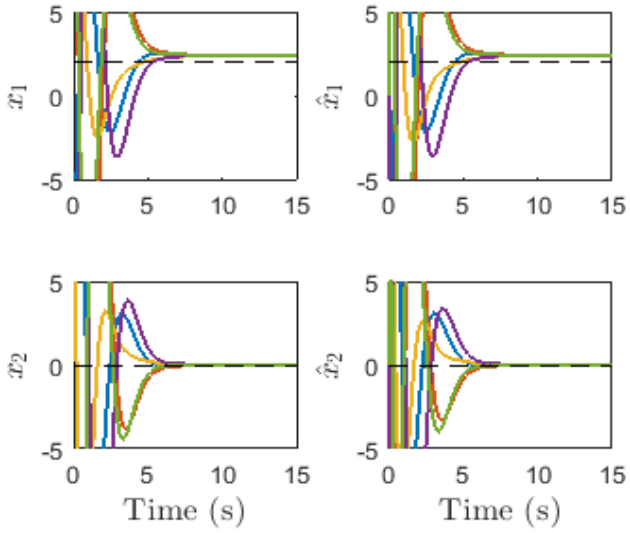

Figure 4.4: Leaderless stationary consensus algorithm of Section 4.1. All observers are at initial rest condition except $\hat{x}_2(0)$. Different from Figure 4.3, $x_i^a = 2.4$ which shows the effect of observer error trajectories on the agreement value (see Lemma 4.1.1).

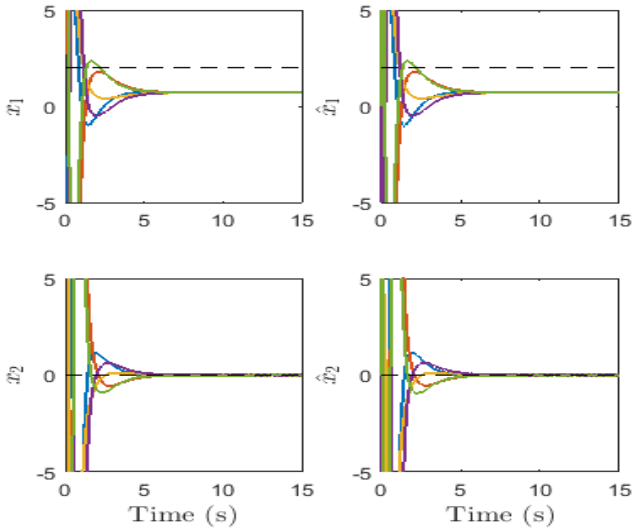

Figure 4.5: Leaderless stationary consensus algorithm of Section 4.1 with re–tuned observer design matrices compared to Figure 4.3. All observers are at initial rest condition. This verifies the effect of observer dynamics (error trajectories) on the stationary agreement value.

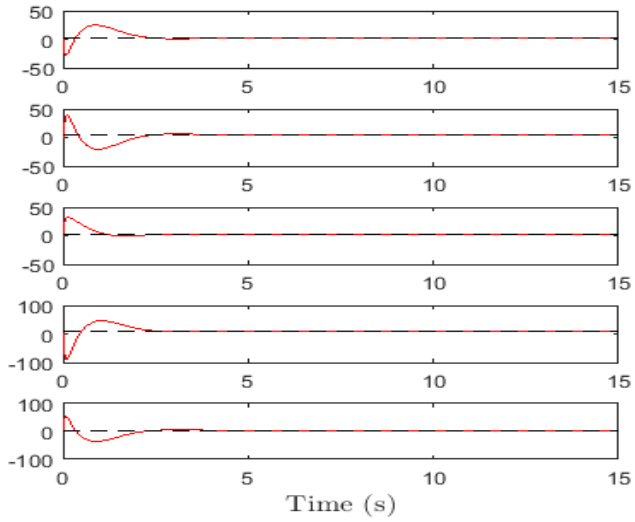

Figure 4.6: In all leaderless stationary consensus simulations, disturbances are estimated precisely (with some differences in transient behavior). Top to bottom are d_1 to d_5 (black) and their estimations (red).

4.3.3 Leader-follower stationary consensus

In this subsection, we investigate the effectiveness of leader-follower stationary algorithm (4.26)-(4.27) in ensuring a stationary consensus on a (desirable) position with minimum information about the leader (as discussed in Section 4.2). We now consider a leader-follower setup as introduced in Subsection 4.3.1 subject to sinusoidal disturbances. For this setup, we use a square wave command to determine the desired position of vehicles. As is shown in Figures 4.7 and 4.8, all vehicles precisely estimate their positions and velocities, and agree on the commanded stationary point while only a two vehicles are aware of their relative distances to the desired reference point.

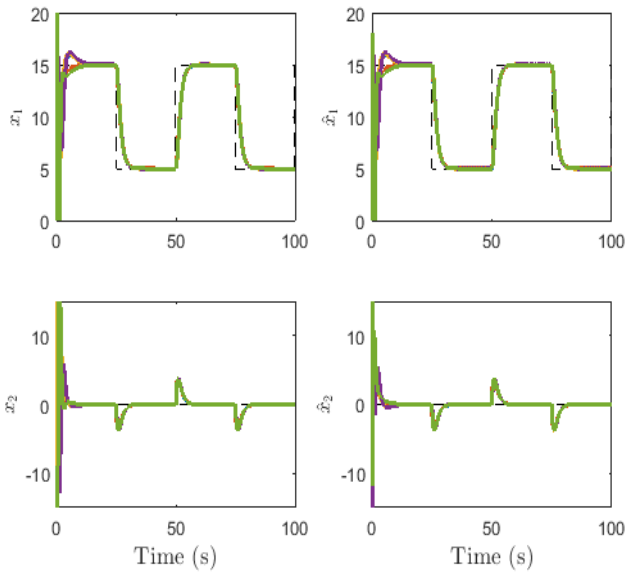

Figure 4.7: Leader-follower stationary consensus: State variables and their estimations. The dashed back waves represent the leader's command.

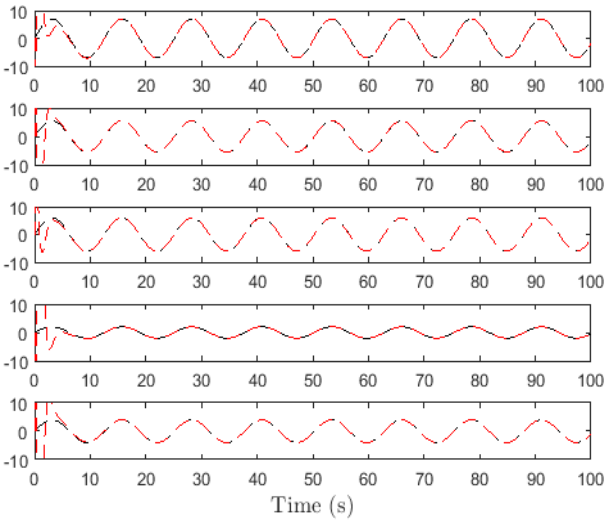

Figure 4.8: Leader-Follower stationary consensus: Top to bottom are d_1 to d_5 (black) and their estimations (red).

4.4 Summary and bibliography

In this chapter, we propose leaderless and leader-follower stationary consensus algorithms which ensure all vehicles' agreement on a fixed point in the presence of unknown persistent disturbances and using only a few vehicles' absolute measurements. In both leaderless and leader-follower scenarios, we provide a systematic framework that transform the high-order dynamic relative-output feedback stationary consensus challenge to three low-order subproblems to design disturbance, consensus, and observer gains. We formulate the consensus and observer gain design tasks as two robust static feedback problems for modified vehicle dynamic subject to fictitious modeling uncertainties which are induced by communication graph topology. In simulation, we discuss the challenges of applying non-stationary disturbance rejection algorithms to multi-vehicle systems, and verify

the feasibility of using proposed strategies for multi-vehicle systems in unknown environments where vehicles might be subject to road profile and wind disturbances.

Control of vehicular systems has received a significant attention among policy makers and researchers during the past two decades due to the increased demand in transportation systems, advances in wireless communication devices, embedded sensing and computation technologies (see [14] and [125]) such that the market of autonomous vehicular systems will expectedly hit $42B by 2025 and, shortly after that, $85B by 2030 [126].

Cooperative analysis and control of multi-vehicle systems have been done from both the systems-theoretic and graph-theoretic viewpoints. In the first, the multi-vehicle system is usually considered over a standard string or mesh topology ([6] and [12]). Along with the advances in wireless and embedded technologies, graph-theoretic tools have created a promising alternative viewpoint in which the behavior of a multi-vehicle system can be analyzed over graphs where nodes represent vehicles and edges indicate inter-vehicle communication. This approach allows to consider more complicated topologies than the standard string or mesh multi-vehicle system [127], and design the multi-vehicle cooperative algorithm independently of the vehicle-level controllers.

Reference [44] developed a feedback linearization-like scheme to transform a moving robot's nonlinear dynamics to a double integrator model with the goal of cooperative formation; [128] used double integrator models for the formation of unmanned vehicles; single integrators were used in [11] to model a multi-robot system, [127] proposed double integrators to study the relationship between com-

munication topology and the stability of coordination algorithm, and [129] designed vehicle level controllers for linear models of vehicles and a filtering-based cooperative algorithm for multi-vehicle system.

Motivated by their wide applications in the cooperation of multi-vehicle and multi-robot systems, significant theoretical research work has been devoted to the distributed control of single and double integrators [30], [42] and [130]. Other than multi-agent system of single integrators, it is known that distributed consensus algorithms usually result in a dynamic agreement in which all trajectories evolve during the time (e.g., see [127] for dynamic agreement in multi-vehicle systems). References [131]-[134] introduced leaderless stationary consensus problem in which agents agree to stop at the same (fixed) position. Nevertheless, multi-vehicle systems are subject to unknown disturbances such as road profile [135]-[136] or wind [137]-[139] which may degrade the performance of consensus algorithm or destabilize it.

The conventional distributed disturbance rejection algorithms have been discussed in Section 3.3, and we do not review its literature for brevity. We mention that, because persistent disturbances continuously excite the uncontrollable and unobservable agreement dynamics, the leaderless disturbance rejection algorithms are not able to guarantee stationary consensus in the multi-vehicle systems.

Additionally, note that the disturbance-free stationary leaderless consensus algorithms of [131]-[134] require all vehicles' access to their absolute velocity measurements. However, in the proposed algorithm (4.4)-(4.5), depending on g_2 and b_i, only a few vehicles have access to their absolute output measurements. Moreover, we know the definition of adjacency (Laplacian) matrix does not admit

self loops in the communication graph. Thus, we use the reduced-order (leader-follower) Laplacian matrix $\mathcal{H}$ to analytically handle this situation in the leaderless scenario (4.7).

4.5 Appendix: proofs

The proofs for theoretical results of this chapter are gathered in section.

4.5.1 Proof of Theorem 4.1.1 (page 131)

We first note that the control gain $K_c = \frac{\lambda_2}{r_c} B^T P_c$ results in the minimum cost function $J(\xi_i(0)) = \xi_i^T(0) P_c \xi_i(0)$ where $P_c \in \mathbb{R}^{2\times 2}$ is the unique positive-definite stabilizing solution of ARE (4.38) (existence and uniqueness of a stabilizing $P_c \succ \mathbf{0}$ can be guaranteed by verifying controllability and observability of $(Q_c^{1/2}, A, \lambda_2 B)$ for the networked vehicle's nominal dynamics (4.16) and $Q_c^{T/2} Q_c^{1/2} = Q_c$).

$$A^T P_c + P_c A + Q_c - \frac{\lambda_2^2}{r_c} P_c B B^T P_c = \mathbf{0} \tag{4.38}$$

Furthermore, implementing $u_{Ti} = K_c \xi_i$, we know any pairs (ξ_i, u_{Ti}) satisfy two fundamental properties of optimal control theory:

$$\begin{aligned} \xi_i^T Q_c \xi_i^T + r_c u_{Ti}^2 + J_{\xi_i}^T (A\xi_i + B u_{Ti}) = &\quad 0 \\ 2 r_c u_{Ti} + \lambda_2 J_{\xi_i}^T B = &\quad \mathbf{0} \end{aligned} \tag{4.39}$$

where $J_{\xi_i} = \frac{\partial J}{\partial \xi_i}$ for all $i \in \{2, 3, ..., N\}$. Now, in order to prove this theorem, we introduce a candidate Lyapunov function:

$$V(\xi_i) = \xi_i^T P_c \xi_i \succ \mathbf{0}$$

which satisfies $V(\xi_i(0)) = J(\xi_i(0))$ for any initial conditions, and find its time deviation along the uncertain trajectories in (4.15):

$$\dot{V} = V_{\xi_i}^T \dot{\xi}_i = -\xi_i^T Q_c \xi_i - r_c u_{Ti}^2 - 2 r_c E(\lambda_i) u_{Ti}^2 \prec 0$$

where we have used the fundamental properties (4.39) replacing J by V, $E(\lambda_i) = \frac{\lambda_i}{\lambda_2} - 1 \geq 0$, and negative definiteness of Q_c. Therefore, asymptotic stability of origin in the networked vehicle model (4.15) is proved using two static control gains that are designed based on homogeneous networked vehicle dynamics in (4.16). Based on the Rayleigh-Ritz inequality, we further find:

$$\lambda_{min}(P_c)\|\xi_i\|^2 \leq V(\xi_i) \leq \lambda_{max}(P_c)\|\xi_i\|^2$$
$$\dot{V}(\xi_i) \leq -\lambda_{min}(Q_{\dot{V}})\|\xi_i\|^2$$

that proves exponential stability of the origin for networked vehicle systems (4.15).

4.5.2 Proof of Theorem 4.1.2 (page 131)

A sketch of this poof can be given by noticing that the dynamical system in (4.19) is dual to (4.18). We can similarly find the dual representation for (4.13). Then, this theorem is proved following the steps in the proof of Theorem 4.1.1 for the dual problem and based on the next ARE:

$$A_o P_o + P_o A_o^T + Q_o - \frac{\mu_1^2}{r_o} P_o C_{o\mu_1}^T C_{o\mu_1} P_o = \mathbf{0}$$

where the unique stabilizing $P_o \in \mathbb{R}^{(2+n_z)\times(2+n_z)} \succ \mathbf{0}$ exists by verifying observability and controllability of $(Q_o^{1/2}, A_o^T, C_{o\mu_1}^T)$ for $Q_o^{T/2} Q_o^{1/2} = Q_o$.

4.5.3 Proof of Corollary 4.1.1 (page 132)

Based on (4.11), we know agreement dynamics are decoupled from the disagreement dynamics (respectively determined by ξ_a and ξ_d). The agreement dynamics are modeled by $\dot{x}_{T1} = v_{T1}$ and $\dot{v}_{T1} = -\alpha_v v_{T1}$, and we write the solution of these differential equations as $x_{T1}(t) = x_{T1}(0) - \frac{1}{\alpha_v}(e^{-\alpha_v t} - 1)v_{T1}(0)$ and $v_{T1} = e^{-\alpha_v t} v_{T1}(0)$ which result in the following limit behavior:

$$\begin{bmatrix} x^a_{T1} \\ v^a_{T1} \end{bmatrix} = \begin{bmatrix} 1 & \frac{1}{\alpha_v} \\ 0 & 0 \end{bmatrix} \begin{bmatrix} x_{T1}(0) \\ v_{T1}(0) \end{bmatrix} =: \phi_d \begin{bmatrix} x_{T1}(0) \\ v_{T1}(0) \end{bmatrix}$$

because $\alpha_v > 0$ and $e^{-\alpha_v t} \to 0$ as $t \to \infty$ (this α_v is a design scalar and can be tuned to achieve desirable consensus behavior). Note that the superscript ^{a} denotes the "agreement" value as $t \to \infty$. Let $T_b = I_2 \otimes T_l$ where $T_l = [\frac{1_N}{\sqrt{N}}, T_d]$ is the diagonalizing unitary transformation such that $\mathcal{L} = T_l^{-1} \Lambda_l T_l$. We rewrite this result based on the agreement and disagreement variables and use the fact $\lim_{t\to\infty} \xi_d(t) = \mathbf{0}$ (based on Theorem 4.1.1) and find:

$$\begin{bmatrix} x^a \\ v^a \end{bmatrix} = T_b \mathcal{P}^{-1} \left[\begin{array}{c|c} \phi_d & \mathbf{0} \\ \hline \mathbf{0} & \mathbf{0} \end{array}\right] \mathcal{P} T_b^{-1} \begin{bmatrix} x(0) \\ v(0) \end{bmatrix} = T_b \left[\begin{array}{cc|cc} 1 & \mathbf{0} & \frac{1}{\alpha_v} & \mathbf{0} \\ \mathbf{0} & \mathbf{0} & \mathbf{0} & \mathbf{0} \\ \hline 0 & \mathbf{0} & 0 & \mathbf{0} \\ \mathbf{0} & \mathbf{0} & \mathbf{0} & \mathbf{0} \end{array}\right] T_b^{-1} \begin{bmatrix} x(0) \\ v(0) \end{bmatrix}$$

$$= \left[\begin{array}{c|c} \frac{1}{N} 1_N 1_N^T & \frac{1}{\alpha_v N} 1_N 1_N^T \\ \hline \mathbf{0} & \mathbf{0} \end{array}\right] \begin{bmatrix} x(0) \\ v(0) \end{bmatrix}$$

which completes the proof noticing that $x(0) = col\{x_i(0)\}$, $v(0) = col\{v_i(0)\}$, $x^a = \lim_{t\to\infty} col\{x_i(t)\}$, and $v^a = \lim_{t\to\infty} col\{v_i(t)\}$.

4.5.4 Proof of Lemma 4.1.1 (page 132)

We begin from the augmented multi-vehicle and observer error dynamics (4.7), substitute K_{cd} by $-C_d$, and find:

$$\left[\begin{array}{c}\dot{\zeta}_{T_l}\\ \hline \dot{e}_{T_l}\end{array}\right] = \left[\begin{array}{c|c}\mathbf{D}_{11} & \mathbf{D}_{12}\\ \hline \mathbf{0} & (I_{2+n_z}\otimes T_l^{-1})\mathbf{A}_{22}(I_{2+n_z}\otimes T_l)\end{array}\right]\left[\begin{array}{c}\zeta_{T_l}\\ \hline e_{T_l}\end{array}\right]$$

$$\mathbf{D}_{11} = \begin{bmatrix}\mathbf{0} & I_N\\ k_{cx}\Lambda_l & k_{cv}\Lambda_l - \alpha_v I_N\end{bmatrix}, \qquad \mathbf{D}_{12} = \begin{bmatrix}\mathbf{0} & \mathbf{0} & \mathbf{0}\\ k_{cx}\Lambda_l & k_{cv}\Lambda_l - \alpha_v I_N & K_{cd}\otimes I_N\end{bmatrix}$$

in which $\zeta_{T_l} = (I_2 \otimes T_l^{-1})\zeta$ and $e_{T_l} = (I_{2+n_z} \otimes T_l^{-1})e$. Based on a row switching transformation $\mathcal{P}_l = diag\{\mathcal{P}, I_{2N+Nn_z}\} \in \mathbb{R}^{(4N+Nn_z)\times(4N+Nn_z)}$ where $\mathcal{P} \in \mathbb{R}^{2n\times 2N}$ is defined in (4.11), we write the disagreement dynamics as follows:

$$\begin{bmatrix}\dot{x}_{T1}\\ \dot{v}_{T1}\end{bmatrix} = \begin{bmatrix}0 & 1\\ 0 & -\alpha_v\end{bmatrix}\begin{bmatrix}x_{T1}\\ v_{T1}\end{bmatrix} + \begin{bmatrix}0 & 0 & 0\\ 0 & -\alpha_v & K_{cd}\end{bmatrix}\begin{bmatrix}e_{xT1}\\ e_{vT1}\\ e_{zT1}\end{bmatrix}$$

The solution of second equation is as follows:

$$v_{T1}(t) = e^{-\alpha_v t}v_{T1}(0) + e^{-\alpha_v t}\int_0^t e^{\alpha_v \tau}(-\alpha_v e_{vT1}(\tau) + K_{cd}e_{zT1}(\tau))d\tau$$

where, as $t \to \infty$, the integral converges to a constant $\beta_I \in \mathbb{R}$ (because the error variables go to zero). Thus, $\alpha_v > 0$ results in $v_{T1}^a = \lim_{t\to\infty} v_{T1}(t) = \mathbf{0}$. Furthermore, we have the following position response $x_{T1}(t) = x_{T1}(0) - \frac{1}{\alpha_v}(e^{-\alpha_v t} - 1)v_{T1}(0) + \int_0^t e^{-\alpha_v \sigma}\int_0^\sigma e^{\alpha_v \tau}(-\alpha_v e_{vT1}(\tau) + K_{cd}e_{zT1}(\tau))d\tau d\sigma$.

We follow the steps of Corollary 4.1.1 to find:

$$\begin{bmatrix} x^a \\ v^a \end{bmatrix} = \begin{bmatrix} \frac{1}{N}1_N 1_N^T & \frac{1}{\alpha_v N}1_N 1_N^T \\ \mathbf{0} & \mathbf{0} \end{bmatrix} \begin{bmatrix} x(0) \\ v(0) \end{bmatrix} + \lim_{t\to\infty} \int_0^t e^{-\alpha_v \sigma} \int_0^\sigma e^{\alpha_v \tau} \begin{bmatrix} \mathbf{0} & -\frac{\alpha_v}{N}1_N 1_N^T & \frac{K_{cd}}{N}1_N 1_N^T \\ \mathbf{0} & \mathbf{0} & \mathbf{0} \end{bmatrix} \begin{bmatrix} e_x(\tau) \\ e_v(\tau) \\ e_z(\tau) \end{bmatrix} d\tau d\sigma$$

which results in equation (4.22). Now, we let $t_\star$ be the time that both errors converges to zero. We introduce $\beta_I(t_\star) = \sum_{i=1}^N \int_0^{t_\star} e^{\alpha_v \tau}(-\alpha_v e_{vi}(\tau) + K_{cd} e_{zi}(\tau))d\tau$ and find $\int_0^\infty e^{-\alpha_v \sigma} \int_0^{t_\star} e^{\alpha_v \tau} \sum_{i=1}^N (-\alpha_v e_{vi}(\tau) + K_{cd} e_{zi}(\tau))d\sigma d\tau = \frac{\beta_I(t_\star)}{\alpha_v}$ which is a constant. Thus, the position agreement

$$x_i^a = \frac{1}{N}\sum_{i=1}^N x_i(0) + \frac{1}{\alpha_v N}\sum_{i=1}^N v_i(0) + \frac{\beta_I}{\alpha_v}(\star)$$

will be a constant value as well.

Chapter 5

Distributed Stabilization of Physically Coupled Multiagent Systems with Known Coupling Structures[1]

In Chapter 3, we established a framework to study distributed control problems. Particularly, we considered the consensus problem in a multiagent system of dynamical agents that were described by linear state space models under modeling uncertainties. We proposed a modified LQR-based formulation enabling us to find appropriate consensus gains without being worried about the selection of coupling strength (see Subsection 1.2.2, page 24). In Section 3.1, we proposed

[1]Part of the introductory materials has been reported in [140]. The theoretical developments are based on the results of [141] and [142]. Each section has its own parameters and variables which are (re-) defined appropriately.

a linear time-invariant multiagent system subject to persistent disturbances. In Section 3.2, we proposed another scenario by introducing an (unknown) operating point-dependent linear model of a multiagent system. This scenario resulted in a multiagent systems where the modeling uncertainty of each agent was a function of its own state and input variables. For this case, we proved the unknown agreement value will depend on all agents' initial values as well as the modeling uncertainties. We further showed that an agreement on zero could be guaranteed whenever an additional sufficient condition is satisfied. Motivated by this (theoretical) observation, we propose a different scenario which is distributed stabilization (agreement on zero) of physically coupled (interconnected) multiagent systems where the modeling uncertainty of each agent is a function of that agent's as well as its physical neighbors' variables.

In this chapter, we propose two classes of these systems: *1)* parameter-varying physically coupled linear multiagent system which is an extension to the proposed model in Subsection 3.2, and *2)* Lur'e multiagent system with nonlinear physical couplings. Both scenarios result in heterogeneous multiagent systems and, with appropriate modified LQR formulations, we prove that the optimal control concepts of Section 2.4 can be used to find the required static feedback gains in order to address the distributed stabilization problems.

This chapter is organized as follows: in Section 5.1, we introduce the distributed stabilization and decoupling problems for an interconnected multiagent system. In Section 5.2, we address the distributed decoupling problem for an operating point-dependent physically coupled heterogeneous linear multiagent system based on a leaderless consensus approach. The result of this section enables us to

guarantee a level of convergence rate. In Section 5.3, we address the same problem for Lur'e-type physically coupled nonlinear multiagent systems based on a leader-follower consensus approach. In Section 5.4, we summarize the result and provide some references for this chapter. Finally, we gather all proofs in Section 5.5.

5.1 Distributed stabilization in physically coupled multiagent systems: revisiting a problem

In many applications, linear time-invariant model of a large-scale system, composed by N subsystems, is realized by the following state space model:

$$\begin{aligned} \dot{x} &= \mathbf{A}x + \mathbf{B}u \\ y &= \mathbf{C}x \end{aligned} \tag{5.1}$$

where, for $i \in \{1, 2, ..., N\}$, $x = col\{x_i\}$ denotes the aggregated state vector, $u = col\{u_i\}$ represents the aggregated control input, $y = col\{y_i\}$ stands for the aggregated output vector; and $x_i \in \mathbb{R}^{n_x}$, $u_i \in \mathbb{R}^{n_u}$, and $y_i \in \mathbb{R}^{n_y}$ respectively indicate state, input, and output vectors of i^{th} subsystem. For a *symmetric* large-scale system, $\mathbf{A}$, $\mathbf{B}$, and $\mathbf{C}$ are defined as follows:

$$\mathbf{A} = \begin{bmatrix} A' & A_c & ... & A_c \\ A_c & A' & ... & A_c \\ \vdots & \vdots & \ddots & \vdots \\ A_c & A_c & ... & A' \end{bmatrix} \quad \mathbf{B} = \begin{bmatrix} B' & B_c & ... & B_c \\ B_c & B' & ... & B_c \\ \vdots & \vdots & \ddots & \vdots \\ B_c & B_c & ... & B' \end{bmatrix} \quad \mathbf{C} = \begin{bmatrix} C' & C_c & ... & C_c \\ C_c & C' & ... & C_c \\ \vdots & \vdots & \ddots & \vdots \\ C_c & C_c & ... & C' \end{bmatrix}$$

In the literature of large-scale systems, two approaches have been proposed to control (5.1). The first approach is the *centralized control* where a central processor gathers information from all subsystems, calculates a global control signal, and sends an appropriate control command back to each subsystem. The practicality of this approach depends on several factors. Of those, we point to *1)* the required computational complexity for the central processor, and *2)* implementation cost.

Regarding the first potential limitation, there are several research studies where the central processor's task is limited to some simple calculations. For example, calculating the average of all subsystems' state and input variables does not impose any computation problems for the central processor and, also, does not require a very high-bandwidth communication channel; thus, can be viewed as a cost efficient approach for implementation. However, centralized schemes are usually inefficient considering the cost of communication and, furthermore, the delay in receiving the measurements, calculating an appropriate global control command using a central processor, and sending the (sub-) commands back to subsystems maybe significant (particularly, when subsystems are geographically located far from each others).

As the second approach, *decentralized control* has been proposed to handle these difficulties. In fact, this is a semi-local controller that *1)* only uses the corresponding subsystems' measurements and, in this sense, operates similar to a local controller, and *2)* different from a (purely) local control approach, it is designed based on our knowledge about the global requirements (e.g., whenever the stability of an interconnected system is the control objective, we use our knowledge about the effect of interconnection on each subsystem, and design a controller to

handle it). In summary, we use our knowledge about the physical couplings and design a set of decentralized controllers which will be implemented locally. Since each individual controller uses only its own subsystem's information, the computation and implementation costs can be significantly less than the centralized approach (potentially, at the expense of reduced performance). Figure 5.1 shows centralized and decentralized control structures for a typical large-scale system with non all-to-all physical couplings.

Stabilization of a large-scale system is a global objective and can be achieved using global knowledge about all subsystems' measurements in a centralized manner. On the other hand, decentralized control techniques prove this objective can be achieved by only sending local absolute measurements to each subsystem's controller. However, we need to notice two points:

1. The performance of a closed-loop large-scale system with a centralized controller can be theoretically higher than a closed-loop system with a set of decentralized controllers. (The word "theoretically" refers to a scenario without any long unknown communication delays.)

2. A large-scale system might be characterized by some "decentralized fixed modes" that cannot be changed using any linear time-invariant decentralized controllers. Additionally, we know that "quotient fixed modes" of a large-scale system are not controllable by any decentralized controllers (including the time-varying and nonlinear approaches). There are several methods to handle the problem of these (potentially unstable) fixed modes and stabilize a large-scale system. In particular interest of this dissertation, we mention

the structured control systems which can be designed following these steps: find the fixed modes, impose a special structure to share a few (additional) measurements among subsystems, transform the structured control design problem to a decentralized control problem, use a suitable decentralized control design technique, and find the structured controller by transferring back to the original coordinate. (See [146].)

Thus, based on the literature of large-scale system, we know sharing information might be required to stabilize a large-scale system. On the other hand, based on our knowledge about distributed consensus in multiagent systems, we note that a large-scale system can be stabilized by cooperatively sharing agents' information in some neighborhoods (e.g., see the agreement on zero in a physically decoupled multiagent systems of Section 3.2). Thus, we propose the stabilization of large-scale systems as another team-based objective that could exist in Section 1.1. Here, the neighboring sets can be defined in different manners. Based on the literature of network design, they can be found based on some optimization criteria (see Section 1.3). However, using the literature of large-scale systems, a minimum number of communications (and their locations) can be established to deal with decentralized or quotient fixed modes of the system. Also, based on the literature of multiagent system, we impose some connectedness requirements on the communication graph topology[2].

[2]Finding fixed modes of a large-scale system can be a tedious task. Thus, we follow a multiagent systems viewpoint to define the communication graphs in Chapters 4 and 5. Also, by imposing a connectedness requirement, we will be able to stabilize both linear time invariant and Lur'e nonlinear time-varying interconnected multiagent systems using LQR-based linear time-invariant (static feedback) controllers.

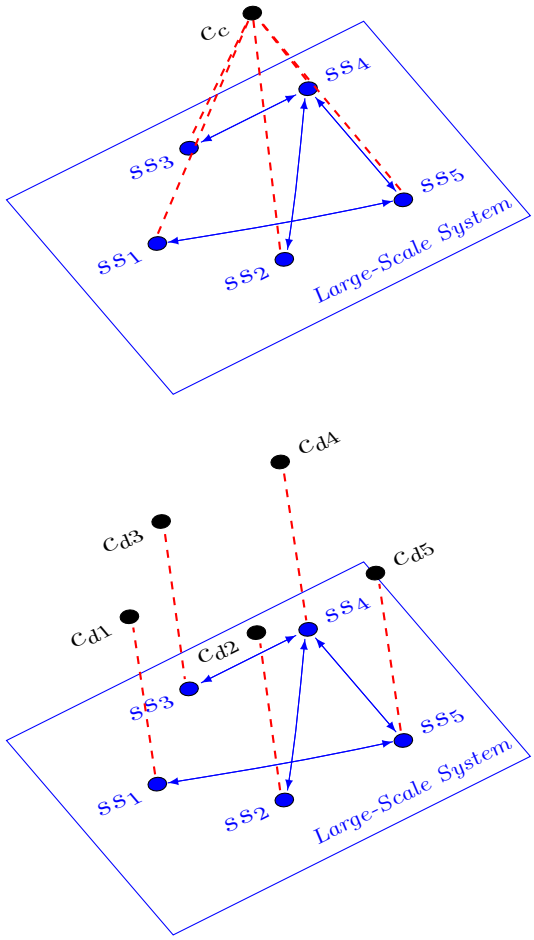

Figure 5.1: The main existing control approaches in the literature of large-scale systems: *Top)* centralized, and *Bottom)* decentralized controls. The letters ss and c respectively stand for subsystem and controller. Subsystems are numbered from 1 to 5, and controllers are specified by the subscript $_c$ which represents centralized, and $_{di}$ where d denotes decentralized and $i \in \{1, 2, ..., 5\}$ specifies the controller's number. The blue circles indicate subsystems, and blue arrows show the physical coupling between them. The black circles indicate the control systems, and dashed red lines represent the subsystem-controller communication which, in the decentralized scenario, is implemented at the corresponding subsystem's location.

Having this background knowledge, we use our graph-theoretic modeling ideas, and rewrite the elements of state space matrices in (5.1) as follows:

$$\begin{aligned} A' &= A + |\mathcal{N}_i^a| A_0, \qquad A_{c,ij} = -a_{ij}^a A_0 \\ B' &= B_m + |\mathcal{N}_i^a| B_0, \quad B_{c,ij} = -a_{ij}^a B_0 \\ C' &= C + |\mathcal{N}_i^a| C_0, \qquad C_{c,ij} = -a_{ij}^a C_0 \end{aligned}$$

where $|\mathcal{N}_i^a|$ denotes the in-degree of i^{th} subsystem, and a_{ij}^a represents $(i,j)^{th}$ component of the adjacency matrix over an agent-layer coupling graph $\mathcal{G}_a$; $A, A_0 \in \mathbb{R}^{n_x \times n_x}$, $B_m, B_0 \in \mathbb{R}^{n_x \times n_u}$, and $C, C_0 \in \mathbb{R}^{n_y \times n_x}$. Note that there exists a freedom in choosing $a_{ij}^a \in \{0,1\}$. When all $a_{ij}^a = 1$ for $i,j \in \{1,2,...,N\}$, we can convert it to a complete undirected graph which is equal to all-to-all physical couplings in (5.1).

This new graph-theoretic formulation realizes a class of multiagent systems where agents, individually, are modeled by *homogeneous* linear time-invariant dynamics; and, cooperatively, are subjected to *homogeneous* state, input, and output linear interconnections over an agent-layer coupling graph $\mathcal{G}_a$:

$$\begin{aligned} \dot{x}_i &= Ax_i + A_0 \textstyle\sum_{j \in \mathcal{N}_i^a} (x_i - x_j) + B_m u_i + B_0 \sum_{j \in \mathcal{N}_i^a} (u_i - u_j) \\ y_i &= Cx_i + C_0 \textstyle\sum_{j \in \mathcal{N}_i^a} (x_i - x_j) \end{aligned} \tag{5.2}$$

In the rest of this chapter and also in Chapter 5, inspired by this discussion, we introduce different types of the physically coupled multiagent system (5.2), propose a (global) stabilization problem, reformulate it as leaderless and leader-follower consensus tasks, and show this objective can be systematically guaranteed based on appropriate linear quadratic regulator formulations using some relative

measurements. In fact, we consider two different scenarios that are indirectly related to the availability of local measurements:

1. Without interconnections, agents can be described by some stable dynamics. However, the instability may arise due to the physical coupling terms. For example, in (5.2), A is Hurwitz but $A_0 \sum_{j\in\mathcal{N}_i^a}(x_i - x_j)$ and $B_0 \sum_{j\in\mathcal{N}_i^a}(u_i - u_j)$ can result in an unstable behavior. Thus, we need to design a *distributed decoupling control system* to cancel the de-stabilization effects of the coupling terms on each agent, and globally stabilize the physically coupled multiagent system using some *relative measurements* in each neighborhood.

2. Without interconnections, agents' dynamics are unstable. In this case, the control system should deal with both local and global (interconnected) unstable behavior of a physically coupled multiagent system. We call it a *distributed stabilization* problem which includes the distributed decoupling as a special case.

By further thinking about the required measurements for an (locally and globally) unstable multiagent system, we prove that the distributed stabilization problem can be solved whenever at least one agent provides its absolute measurement to the distributed stabilization system (this will be discussed in Chapter 5). As a special case, when all agents provide their absolute measurements, we locally stabilize agents using them, and design a distributed decoupling system based on some relative measurements.

We can also think about the structure of controllers based on the required information. For clarity, we do it through an example.

Example 5.1.1. *Assume there is a large scale system with four subsystems. Then, the structure of static feedback centralized and decentralized controllers can be described by the following matrices:*

$$\boldsymbol{K}_c = \begin{bmatrix} 1 & 1 & 1 & 1 \\ 1 & 1 & 1 & 1 \\ 1 & 1 & 1 & 1 \\ 1 & 1 & 1 & 1 \end{bmatrix}, \quad \boldsymbol{K}_d = \begin{bmatrix} 1 & \boldsymbol{0} & \boldsymbol{0} & \boldsymbol{0} \\ \boldsymbol{0} & 1 & \boldsymbol{0} & \boldsymbol{0} \\ \boldsymbol{0} & \boldsymbol{0} & 1 & \boldsymbol{0} \\ \boldsymbol{0} & \boldsymbol{0} & \boldsymbol{0} & 1 \end{bmatrix}, \quad \boldsymbol{K}_{sc} = \begin{bmatrix} 1 & \boldsymbol{0} & \boldsymbol{0} & 1 \\ \boldsymbol{0} & 1 & \boldsymbol{0} & \boldsymbol{0} \\ 1 & \boldsymbol{0} & 1 & \boldsymbol{0} \\ \boldsymbol{0} & \boldsymbol{0} & \boldsymbol{0} & 1 \end{bmatrix}$$

where, based on the literature of large-scale systems, each entry 1 *indicates the presence of the* j^{th} *subsystem's absolute measurement in the* i^{th} *subsystem's control signal for* $i, j \in \{1, 2, 3, 4\}$*. The subscripts* $_c$*,* $_d$*, and* $_{sc}$ *respectively denote centralized, decentralized, and structurally constrained (to control fixed modes of a large-scale system). In the distributed approaches of this chapter, based on the notation of graph theory, we show the available information's structure using adjacency matrix:*

$$\mathcal{A}_{dd} = \begin{bmatrix} 1 & 1 & 0 & 0 \\ 1 & 1 & 1 & 0 \\ 0 & 1 & 1 & 1 \\ 0 & 0 & 1 & 1 \end{bmatrix}, \quad \mathcal{A}_{ds} = \begin{bmatrix} 1 & 1 & 0 & 0 \\ 1 & 0 & 1 & 0 \\ 0 & 1 & 0 & 1 \\ 0 & 0 & 1 & 0 \end{bmatrix}$$

where the off diagonal terms indicate the presence of relative information between corresponding agents, and diagonal terms represent self-loops[3]*. The subscripts* $_{dd}$

[3]Each self-loop indicates an agent is a neighbor of itself. Based on the preliminary discussed in Section 2.2, we need to avoid this situation in our graph-theoretic designs. In the rest of this dissertation, we address self loops by proposing a hierarchical framework in distributed

and $_{ds}$ stand for distributed decoupling and distributed stabilization, respectively. Looking at these structures, it is clear that the distributed decoupling system has access to all information that are required to design a decentralized control system[4]*. However, this is not true about the distributed stabilization system. At the same time, compared to a centralized controller, both of these distributed algorithms can be designed with a set of fewer measurements.*

5.2 Distributed decoupling of linear multiagent systems with state and output couplings

In this section, we investigate our distributed decoupling control ideas for a group of interconnected parameter-dependent agents.

5.2.1 Problem statement

We consider the following heterogeneous parameter-dependent model of a physically coupled multiagent system:

$$\begin{aligned} \dot{x}_i(t) &= A(\theta_i(t))x_i(t) + B(\theta_i(t))u_i(t) + F(\theta_i(t))\textstyle\sum_{j\in\mathcal{N}_i}(x_i(t) - x_j(t)) \\ y_i(t) &= Cx_i + C_0\textstyle\sum_{j\in\mathcal{N}_i}(x_i(t) - x_j(t)) \end{aligned} \tag{5.3}$$

decoupling problem, or adding a virtual leader in distributed stabilization problem.

[4]In this example, the same thing happens with the structurally constrained controller K_{sc}, however it is not required. Also, in K_{sc}, the communication is disconnected and the shared information is an absolute measurement.

where, compared to the linear time-invariant model (5.2), we have changed: $A \leftarrow A(\theta_i)$, $B_m \leftarrow B(\theta_i)$, and $A_0 \leftarrow F(\theta_i)$. Here, $i \in \{1, 2, ..., N\}$ denotes the agent's number; $x_i \in \mathbb{R}^{n_x}$ represents the i^{th} agent's state variable deviation and $u_i \in \mathbb{R}^{n_u}$ indicates the control input deviation from an operating point[5]; $A \in \mathbb{R}^{n_x \times n_x}$ stands for the state matrix, $B \in \mathbb{R}^{n_x \times n_u}$ represents the input gain matrix, $F \in \mathbb{R}^{n_x \times n_x}$ denotes the state-coupling matrix, and $C \in \mathbb{R}^{n_y \times n_x}$ gives the output gain matrix. In this state space realization, $A(\theta_i(t))$, $B(\theta_i(t))$, and $F(\theta_i(t))$ are functions of an independent time-varying parameter $\theta_i(t)$ that can uniquely characterize the i^{th} agent's operating condition. For $m \in \{0, 1\}$, these matrices are modeled by $A(\theta_i(t)) = A_0 + A_1\theta_i(t)$ where $A_m \in \mathbb{R}^{n_x \times n_x}$, $B(\theta_i(t)) = B_0 + B_1\theta_i(t)$ where $B_m \in \mathbb{R}^{n_x \times n_u}$, and $F(\theta_i(t)) = F_0 + F_1\theta_i(t)$ where $F_m \in \mathbb{R}^{n_x \times n_x}$. The matrices C and C_0 model a set of sensors, and are independent of $\theta_i(t)$. Furthermore, the following assumptions are satisfied:

Assumption 5.2.1. *For $i \in \{1, 2, ..., N\}$, the unknown independent parameters $\theta_i(t)$ satisfy $\theta_i \in [\theta_m, \theta_M]$ with a known lower-bound θ_m and a known upper-bound θ_M. Also, A_m, B_m, C, and C_0 are some known matrices for $m \in \{0, 1\}$.*

Assumption 5.2.2. *The fixed graph $\mathcal{G}$ is known and connected.*

Remark 5.2.1. *As a result of Assumption 5.2.1, a group of agents* (5.3) *represents a "partially-unknown" heterogeneous interconnected multiagent system where both agent-level matrices $A(\theta_i)$ and $B(\theta_i)$ with known A_m and B_m, and multiagent system-level interconnection matrix $F(\theta_i)$ with a known F_m vary in time depending*

[5]These deviation variables are defined as difference variables $x_i = x_i^{act} - x_i^{opt}$ and $u_i = u_i^{act} - u_i^{opt}$ where (x_i^{act}, u_i^{act}) denotes the actual value and (x_i^{opt}, u_i^{opt}) represents the value at a given operating point.

on the i^{th} agent's unknown parameters θ_i. The term $F(\theta_i)\sum_{j\in\mathcal{N}_i}(x_i-x_j)$ indicates a physical state coupling, and $\sum_{j\in\mathcal{N}_i}(y_i-y_j)=C_0\sum_{j\in\mathcal{N}_i}(x_i-x_j)$ represents either a physical output coupling or a lumped relative-output measurement for i^{th} agent. While we assume completely known C and C_0, the results of this section can be modified to include parameter-dependent version of these output gain matrices.

We consider a hierarchical control structure for uncertain interconnected multiagent system (5.3) where a lower-level controller stabilizes the *decoupled residual* agents using local output measurements Cx_i (or a lookup-table-based scheduling system enforces agents to operate at a desired operating point). The residual dynamics are given by:

$$\dot{x}_i = A_\star x_i + B_\star u_i \tag{5.4}$$

where $A_\star$ and $B_\star$ are two constant matrices to be determined using our partial knowledge about the operating point-dependent uncertainties. Then, a higher-level controller decouples agents using only coupled-state or -output measurements.

We only focus on designing the higher-level decoupling system, and skip the lower-level local control system by proposing an assumption on stability of the residual system (5.4) (note that the local controller can be designed using any static feedback control techniques for a single agent). The following assumption holds true in the rest of this section:

Assumption 5.2.3. *a) The matrix $A_\star$ is Hurwitz, b) the pair $(A_\star, B_\star)$ is controllable, and c) the pair $(C_0, A_\star)$ is observable.*

Remark 5.2.2. *Note that the assumption on having a Hurwitz $A_\star$ is made without loss of generality. Whenever this condition is not satisfied, we can take the local control design procedure into account and introduce $\dot{x}_i = A_{lc}x_i + B_\star u_i$ instead of (5.4). Here, $A_{lc} = A_\star + B_\star K_l$ is (by design) a Hurwitz matrix that has been obtained by locally closing a static feedback loop around each residual system using a local control gain K_l. Then, we also rewrite Assumption 5.2.3 based on a controllable $(A_{lc}, B_\star)$ and an observable (C_0, A_{lc}). Since the results of this section are based on the "properties" of a Hurwitz matrix $A_\star$, they will remain valid by switching to another Hurwitz matrix A_{lc}.*

Based on these discussion and assumption, from this point, we consider the following model for the (higher-level) decoupling control design purpose:

$$\begin{aligned} \dot{x}_i(t) &= A(\theta_i(t))x_i(t) + B(\theta_i(t))u_i(t) + F(\theta_i(t))\textstyle\sum_{j\in\mathcal{N}_i}(x_i(t) - x_j(t)) \\ y_i(t) &= C_0 \textstyle\sum_{j\in\mathcal{N}_i}(x_i(t) - x_j(t)) \end{aligned} \tag{5.5}$$

where we mention that, using some coupled measurements (relative-output measurements), the control objective is exponentially mitigating the effect of agents' partially-known state-couplings such that a multiagent system of agents (5.5) behaves as a multiagent system of N decoupled agents (5.4). Since, by definition, x_i and u_i are some deviation variables; from each (locally stabilized) interconnected agent's point of view, the effect of interconnections are damped whenever (5.6) is guaranteed for all $i \in \{1, 2, ..., N\}$:

$$\lim_{t\to\infty} x_i(t) = \mathbf{0} \tag{5.6}$$

An immediate idea is designing a centralized decoupling control scheme that uses the information about all agents. However, as discussed earlier, we are interested in "distributed" algorithms where this objective can be achieved using some coupled (relative) measurements in each neighborhood. Thus, we propose the following distributed decoupling problems:

Problem 5.2.1. *(State feedback decoupling) Design a distributed decoupling control algorithm that solves* (5.6) *based on coupled-state measurements in* (5.5) *with* $C_0 = I_{n_x}$.

Problem 5.2.2. *(Output feedback decoupling) Address Problem 5.2.1 using the coupled-output measurements in* (5.5).

Now, we reformulate (5.6) as a *leaderless consensus* task:

$$\lim_{t\to\infty}(x_i(t) - x_j(t)) = \mathbf{0} \tag{5.7}$$

where we need to ensure an agreement on zero by designing a state-agreement protocol for heterogeneous agents in (5.5). This objective should be achieved in the presence of operating point-dependent (time-varying) physical interconnections and under any initial conditions. Note that, in general, as found in Chapter 3, consensus protocols just guarantee *an agreement* that depends on the initial conditions of agents.

Before proposing any decoupling control systems that address Problems 5.2.1 and 5.2.1, we use our partial knowledge about varying operating points of agents, and find $A_\star$ and $B_\star$. Let $\theta_i(t)$ be rewritten as follows:

$$\theta_i(t) = \bar{\theta} + p_\theta \delta_i(t) \tag{5.8}$$

with

$$\bar{\theta} = \frac{\theta_M + \theta_m}{2}, \quad p_\theta = \frac{\theta_M - \theta_m}{2}, \quad |\delta_i(t)| \leq 1$$

where $\bar{\theta}$ and p_θ are two known constant scalars, and $\delta_i(t)$ are unknown scalar variables for $i \in \{1, 2, ..., N\}$. As a result, we find:

$$\begin{aligned} \dot{x}_i = \; & A_{avg} x_i + B_{avg} u_i + F_{avg} \textstyle\sum_{j \in \mathcal{N}_i} (x_i - x_j) \\ & + A_\delta \delta_i x_i + B_\delta \delta_i u_i + F_\delta \delta_i \textstyle\sum_{j \in \mathcal{N}_i} (x_i - x_j) \end{aligned} \tag{5.9}$$

where

$$A_{avg} = A(\bar{\theta}) = A_0 + A_1 \bar{\theta} \quad B_{avg} = B(\bar{\theta}) = B_0 + B_1 \bar{\theta} \quad F_{avg} = F(\bar{\theta}) = F_0 + F_1 \bar{\theta}$$

$$A_\delta = A(p_\theta) = A_1 p_\theta \qquad B_\delta = B(p_\theta) = B_1 p_\theta \qquad F_\delta = F(p_\theta) = F_1 p_\theta$$

Referring to Assumption 5.2.3, we emphasize that $A_{avg} =: A_\star$ and $B_{avg} =: B_\star$ represent a controllable pair (A_{avg}, B_{avg}) and an observable pair (A_{avg}, C_0) (this is valid in its general sense, including $C_0 = I_{n_x}$), and A_{avg} is Hurwitz. (Also, see Remark 5.2.2.) Now we are ready to discuss the main results of this section.

5.2.2 Leaderless consensus-based decoupling: main results

5.2.2.1 State Feedback Distributed Decoupling

In this subsection, we address Problem 5.2.1 using some coupled (relative-) state measurements. In this subsection, we further consider a structural assumption $F_{avg} = B_{avg} G_{avg}$ on agent's dynamics. Thus, we find:

$$\begin{aligned} \dot{x}_i = \; & A_{avg} x_i + B_{avg} (u_i + G_{avg} \textstyle\sum_{j \in \mathcal{N}_i} (x_i - x_j)) \\ & + A_\delta \delta_i x_i + B_\delta \delta_i u_i + F_\delta \delta_i \textstyle\sum_{j \in \mathcal{N}_i} (x_i - x_j) \end{aligned} \tag{5.10}$$

and, furthermore, propose the distributed decoupling signal:

$$u_i = K_c y_i = K_c \sum_{j \in \mathcal{N}_i} (x_i - x_j) \tag{5.11}$$

where $K_c \in \mathbb{R}^{n_u \times n_x}$ denotes a static distributed decoupling gain. Now, the aggregated multiagent system's dynamics over $\mathcal{G}$ are given by:

$$\begin{aligned} \dot{x} = \quad & ((I_N \otimes A_{avg}) + (\mathcal{L} \otimes B_{avg} G_{avg}))x + (I_N \otimes B_{avg})u \\ & + ((\Delta \otimes A_\delta) + (\Delta\mathcal{L} \otimes F_\delta))x + (\Delta \otimes B_\delta)u \end{aligned} \tag{5.12}$$

where $\Delta = diag\{\delta_i\}$ and $u = (\mathcal{L} \otimes K_c)x$. Therefore, the closed-loop multiagent system dynamics are written as follows:

$$\underbrace{\dot{x}(t) = \tilde{A}_c x(t)}_{\text{Closed-loop nominal dynamics}} \quad + \quad \underbrace{\tilde{A}_\Delta(t) x(t)}_{\text{Closed-loop modeling uncertainty}} \tag{5.13}$$

where $\tilde{A}_c = ((I_N \otimes A_{avg}) + (\mathcal{L} \otimes B_{avg}(G_{avg} + K_c)))$, $\tilde{A}_\Delta(t) = (\Delta(t) \otimes I_{n_x})\tilde{A}_N$, and $\tilde{A}_N = (I_N \otimes A_\delta) + (\mathcal{L} \otimes (F_\delta + B_\delta K_c))$. We rewrite the closed-loop nominal dynamics as follows (We distinguish the effect of uncertainty on the closed-loop multiagent system by using closed-loop "nominal dynamics" and "modeling uncertainty."):

$$\dot{x} = (I_N \otimes A_{avg})x + (I_N \otimes B_{avg})u + (\mathcal{L} \otimes B_{avg} G_{avg})x \tag{5.14}$$

with the aggregated decoupling control (consensus) signal $u = (\mathcal{L} \otimes K_c)x$ that should be designed. Here, u is a coupled signal of all agents' control signals u_i due to the presence of $\mathcal{L}$. We decomposing it to a coupled part $u = (\mathcal{L} \otimes I_{n_u})\nu$ and a decoupled part $\nu = (I_N \otimes K_c)x$, and pass the coupled component to the dynamics of multiagent system: $\dot{x} = (I_N \otimes A_{avg})x + (\mathcal{L} \otimes B_{avg})\nu + (\mathcal{L} \otimes B_{avg} G_{avg})x$. Now, using a transformation matrix T as defined in Fact 2.2.1, we find:

$$\dot{x}_T = (I_N \otimes A_{avg})x_T + (\Lambda \otimes B_{avg})\nu_T + (\Lambda \otimes B_{avg} G_{avg})x_T \tag{5.15}$$

where $x_T = (T^{-1} \otimes I_{n_x})x$, $\nu_T = (T^{-1} \otimes I_{n_u})\nu$, and T and $\Lambda \triangleq diag\{[0, \Lambda_d]\}$ with $\Lambda_d \triangleq diag\{[\lambda_2, ..., \lambda_N]\}$. (We can find $\nu_T = (I_N \otimes K_c)x_T$.) Hence, we have the following partitioned representation:

$$\begin{aligned}\begin{bmatrix}\dot{x}_{Ta}\\ \dot{x}_{Td}\end{bmatrix} = \begin{bmatrix}A_{avg} & \mathbf{0}\\ \mathbf{0} & \bar{A}_{avg}\end{bmatrix}\begin{bmatrix}x_{Ta}\\ x_{Td}\end{bmatrix} &+ \begin{bmatrix}\mathbf{0} & \mathbf{0}\\ \mathbf{0} & \Lambda_d \otimes B_{avg}\end{bmatrix}\begin{bmatrix}\nu_{Ta}\\ \nu_{Td}\end{bmatrix}\\ &+ \begin{bmatrix}\mathbf{0} & \mathbf{0}\\ \mathbf{0} & \Lambda_d \otimes B_{avg}G_{avg}\end{bmatrix}\begin{bmatrix}x_{Ta}\\ x_{Td}\end{bmatrix}\end{aligned} \tag{5.16}$$

where $\bar{A}_{avg} = I_{N-1} \otimes A_{avg}$; $x_{Ta} = x_{T1} \in \mathbb{R}^{n_x}$ and $\nu_{Ta} = \nu_{T1} \in \mathbb{R}^{n_u}$ respectively denote state variable and control input of the agreement dynamics, and $x_{Td} = col\{x_{Ti}\} \in \mathbb{R}^{(N-1)n_x}$ and $\nu_{Td} = col\{\nu_{Ti}\} \in \mathbb{R}^{(N-1)n_u}$ respectively stand for state variable and control input of the disagreement dynamics[6] for $i \in \{2, 3, ..., N\}$. Note that $\nu_{Td} = (I_{N-1} \otimes K_c)x_{Td}$.

This representation gives uncontrollable agreement dynamics:

$$\dot{x}_{Ta} = A_{avg}x_{Ta}$$

and controllable disagreement dynamics:

$$\dot{x}_{Td} = \bar{A}_{avg}x_{Td} + (\Lambda_d \otimes B_{avg})\nu_{Td} + (\Lambda_d \otimes B_{avg}G_{avg})x_{Td}$$

In order to design a consensus gain K_c (or distributed decoupling control gain), we rewrite the disagreement dynamics as follows:

$$\underbrace{\dot{x}_{Td} = \bar{A}_{avg}x_{Td} + \bar{B}_{avg}\nu_{Td}}_{\text{Network-level nominal dynamics}} + \underbrace{\bar{B}_{avg}(\bar{E}\nu_{Td} + \bar{G}_{avg}x_{Td})}_{\text{Network-level modeling uncertainty}} \tag{5.17}$$

[6]See the footnote at page 67 for a discussion on agreement and disagreement dynamics.

where $\bar{B}_{avg} = I_{N-1} \otimes \lambda_2 B_{avg}$, $\bar{E} = \bar{E}^T = ((\frac{\Lambda_d}{\lambda_2} - I_{N-1}) \otimes I_{n_u}) \succcurlyeq \mathbf{0}$, and $\bar{G}_{avg} = \frac{\Lambda_d}{\lambda_2} \otimes G_{avg}$. Note that, although Λ_d is completely known, we consider it as a fictitious source of modeling uncertainties in order to find a homogeneous network-level nominal model for all agents (with heterogeneous modeling uncertainties), and find a "single" decoupling gain K_c that works for all agents[7]. Similarly, we consider the known $\bar{G}_{avg}$ as another fictitious source of modeling uncertainties to find known *homogeneous* network-level nominal dynamics.

Now, we propose the network-level shifted dynamics:

$$\underbrace{\dot{x}_{Td} = \bar{A}_\gamma x_{Td} + \bar{B}_{avg}\nu_{Td}}_{\text{Network-level shifted nominal dyn}} + \underbrace{\bar{B}_{avg}(\bar{E}\nu_{Td} + \bar{G}_{avg}x_{Td})}_{\text{Network-level modeling uncertainty}} \tag{5.18}$$

where $\bar{A}_\gamma = I_N \otimes A_\gamma$, $A_\gamma = A_{avg} + \gamma I_{n_x}$, and $\gamma \geq 0$ is a design parameter. Before designing a consensus gain K_c, let P_s be the solution of an algebraic Riccati equation (ARE):

$$A_\gamma^T P_s + P_s A_\gamma + Q_s - \lambda_2^2 P_s B_{avg} R^{-1} B_{avg}^T P_s = \mathbf{0} \tag{5.19}$$

where $Q_s = Q + R_x$, $R_x = \frac{\lambda_N^2}{\lambda_2^2} G_{avg}^T R G_{avg}$, and $Q = Q^T \succ \mathbf{0}$ and $R = R^T \succ \mathbf{0}$ are two design matrices. Since the pair (A_γ, B_{avg}) is controllable due to the controllability of (A_{avg}, B_{avg})[8], existence of the stabilizing P_s is guaranteed for

[7]See Remark 3.1.2 at page 70 about the network-level modeling uncertainty. Also, note that the known Λ_d acts as a source of heterogeneity, thus we pass G_{avg} to the uncertain (unwanted) part of (5.17).

[8]Based on the controllability Definition 2.3.2 at page 48, a pair (A_γ, B_{avg}) is controllable if and only if there exist no nonzero complex vector z and scalar λ_γ such that both $z^* A_\gamma = \lambda_\gamma z^*$ and $z^* B_{avg} = 0$ are simultaneously satisfied. Substituting A_γ by $A_{avg} + \gamma I_{n_x}$, we need to check whether a nonzero z and a λ exist to satisfy $z^* A_{avg} = \lambda z^*$ and $z^* B_{avg} = 0$ or not (here, $\lambda = \lambda_\gamma - \gamma$). This is in fact the controllability condition of a pair (A_{avg}, B_{avg}).

any observable pairs $(Q_s^{\frac{1}{2}}, A)$ where we have used $Q_s = Q_s^{\frac{1}{2}T} Q_s^{\frac{1}{2}}$. Furthermore, let $\sigma_c \triangleq \sqrt{|\lambda_{max}(\tilde{A}_N^T \tilde{A}_N)|}$ where $\tilde{A}_N$ is defined in (5.13).

Using these preliminary derivations, we now propose a systematic approach to design a K_c that ensures distributed decoupling in a multiagent system of partially-unknown heterogeneous interconnected agents (5.10).

Theorem 5.2.1. *Let $\nu_{Ti} = K_c x_{Ti} = -\lambda_2 R^{-1} B_{avg}^T P_s x_{Ti}$ be the control signal that achieves the minimum of a linear quadratic regulatory cost function* (5.20) *subject to the networked agent dynamics* (5.21) *for $i \in \{2, ..., N\}$*[9]*. Then, the leaderless consensus problem* (5.7) *is solved for the multiagent system dynamics* (5.14) *with a state-agreement on zero. If there exist α_c and β_c such that the inequality $\sigma_c < \frac{\beta_c}{\alpha_c}$ is satisfied for $\|e^{\tilde{A}_c t}\| \leq \alpha_c e^{-\beta_c t}$, then the state feedback distributed decoupling problem 5.2.1 is also solved for a partially-unknown interconnect multiagent system of agents* (5.10)*.*

$$J_i(x_{Ti}(0)) = \min_{\nu_{Ti}} \int_0^\infty (x_{Ti}^T Q_s x_{Ti} + \nu_{Ti}^T R \nu_{Ti}) dt \tag{5.20}$$

$$\dot{x}_{Ti} = A_\gamma x_{Ti} + \lambda_2 B_{avg} \nu_{Ti} \tag{5.21}$$

Proof. This proof is given at Subsection 5.5.1. □

Note that the design parameter γ can be used either as a degree of freedom in order to find a K_c that satisfies the exponential decoupling condition $\sigma_c < \frac{\beta_c}{\alpha_c}$ or as a tuning parameter to adjust the *convergence rate*. Note that Theorem 5.2.1

[9]Due to the presence of λ_2, we use the word "networked" in order to distinguish this system from the single agent dynamics.

addresses a scenario based on heterogeneous $\theta_i(t)$ while the formulation of Section 3.2 was only able to deal with a homogeneous $\theta(t)$ for all agents.

5.2.2.2 Observer-Based Output Feedback Distributed Decoupling

In this subsection, we address Problem 5.2.2 using some coupled-output measurements (or relative-output measurements). We still use our partial-knowledge about the operating point parameter, as given by (5.8), and find a similar result to (5.9) without any restrictions on F_{avg}. We propose a dynamic distributed decoupling system:

$$u_i = K_c \hat{y}_i \tag{5.22}$$

where $\hat{y}_i$ is the estimated output of multiagent system (5.5), and is found by a state- and output-coupled Luenberger observer:

$$\begin{aligned}
\dot{\hat{x}}_i &= A_{avg}\hat{x}_i + B_{avg}u_i + F_{avg}\textstyle\sum_{j\in\mathcal{N}_i}(\hat{x}_i - \hat{x}_j) + K_o(y_i - \hat{y}_i) \\
\hat{y}_i &= C_0 \textstyle\sum_{j\in\mathcal{N}_i}(\hat{x}_i - \hat{x}_j)
\end{aligned}$$

where $K_o \in \mathbb{R}^{n_x \times n_y}$ indicates the observer gain. We define $e_i \triangleq x_i - \hat{x}_i$ as the observer error and, substituting u_i by (5.22), we find:

$$\begin{aligned}
\dot{e}_i &= A_{avg}e_i + (F_{avg} - K_oC_0)\textstyle\sum_{j\in\mathcal{N}_i}(e_i - e_j) + A_\delta\delta_i x_i \\
&\quad + (F_\delta + B_\delta K_c)\delta_i \textstyle\sum_{j\in\mathcal{N}_i}(x_i - x_j) - B_\delta K_c \delta_i \textstyle\sum_{j\in\mathcal{N}_i}(e_i - e_j) \\
\dot{x}_i &= A_{avg}x_i + (F_{avg} + B_{avg}K_c)\textstyle\sum_{j\in\mathcal{N}_i}(x_i - x_j) - B_{avg}K_c\textstyle\sum_{j\in\mathcal{N}_i}(e_i - e_j) \\
&\quad + A_\delta\delta_i x_i + (F_\delta + B_\delta K_c)\delta_i \textstyle\sum_{j\in\mathcal{N}_i}(x_i - x_j) - B_\delta K_c\delta_i \textstyle\sum_{j\in\mathcal{N}_i}(e_i - e_j)
\end{aligned}$$

Now, we define $\xi = [x^T, e^T]^T$ and find the aggregated system dynamics over $\mathcal{G}$:

$$\underbrace{\dot{\xi}(t) = \tilde{A}_c\xi(t)}_{\text{Closed-loop nominal dynamics}} \quad + \quad \underbrace{\tilde{A}_\Delta(t)\xi(t)}_{\text{Closed-loop modeling uncertainty}} \tag{5.23}$$

$$\tilde{A}_c = \begin{bmatrix} \tilde{A}_{c11} & \tilde{A}_{c12} \\ \mathbf{0} & \tilde{A}_{c22} \end{bmatrix}, \qquad \tilde{A}_{c11} = (I_N \otimes A_{avg}) + (\mathcal{L} \otimes (F_{avg} + B_{avg}K_c))$$
$$\tilde{A}_{c12} = -(\mathcal{L} \otimes B_{avg}K_c), \quad \tilde{A}_{c22} = (I_N \otimes A_{avg} + (\mathcal{L} \otimes (F_{avg} - K_oC_0)))$$

$$\tilde{A}_\Delta = \begin{bmatrix} \Delta(t) \otimes I_{n_x} & \mathbf{0} \\ \mathbf{0} & \Delta(t) \otimes I_{n_x} \end{bmatrix} \tilde{A}_N, \qquad \tilde{A}_N = \begin{bmatrix} \tilde{A}_{N11} & \tilde{A}_{N12} \\ \tilde{A}_{N21} & \tilde{A}_{N22} \end{bmatrix}$$
$$\tilde{A}_{N11} = (I_N \otimes A_\delta) + (\mathcal{L} \otimes (F_\delta + B_\delta K_c)), \quad \tilde{A}_{N12} = -(\mathcal{L} \otimes B_\delta K_c)$$
$$\tilde{A}_{N21} = \tilde{A}_{N11}, \quad \tilde{A}_{N22} = \tilde{A}_{N12}$$

In the rest, based on the principle of separation Lemma 2.3.2, we design a control gain K_c and an observer gain K_o for the decoupled nominal multiagent system's dynamics $\dot{\xi} = \tilde{A}_c\xi$; and, later, we establish a sufficient condition in order to address the output feedback decoupling Problem 5.2.2. Based on the Fact 2.2.1, we define $x_T = (T^{-1} \otimes I_{n_x})x$ and $e_T = (T^{-1} \otimes I_{n_x})e$, and rewrite the closed-loop nominal dynamics of (5.23) as follows:

$$\dot{x}_T = ((I_N \otimes A_{avg}) + (\Lambda \otimes (F_{avg} + B_{avg}K_c)))x_T - (\Lambda \otimes B_{avg}K_c)e_T \tag{5.24}$$

$$\dot{e}_T = (I_N \otimes A_{avg} + (\Lambda \otimes (F_{avg} - K_oC_0)))e_T \tag{5.25}$$

or in the following partitioned form:

$$\left[\begin{array}{c} \dot{\xi}^T_{Tx} \\ \hline \dot{\xi}^T_{Te} \end{array}\right] = \left[\begin{array}{cc|cc} \tilde{A}^{11}_c & \mathbf{0} & \mathbf{0} & \mathbf{0} \\ \mathbf{0} & \tilde{A}^{22}_c & \mathbf{0} & \tilde{A}^{24}_c \\ \hline \mathbf{0} & \mathbf{0} & \tilde{A}^{33}_c & \mathbf{0} \\ \mathbf{0} & \mathbf{0} & \mathbf{0} & \tilde{A}^{44}_c \end{array}\right] \left[\begin{array}{c} \xi^T_{Tx} \\ \hline \xi^T_{Te} \end{array}\right] \tag{5.26}$$

$$\tilde{A}_c^{11} = A_{avg} \quad \tilde{A}_c^{22} = (I_{N-1} \otimes A_{avg}) + (\Lambda_d \otimes (F_{avg} + B_{avg}K_c))$$
$$\tilde{A}_c^{24} = -(\Lambda_d \otimes B_{avg}K_c) \quad \tilde{A}_c^{33} = A_{avg}$$
$$\tilde{A}_c^{44} = (I_{N-1} \otimes A_{avg}) + (\Lambda_d \otimes (F_{avg} - K_o C_0))$$

Note that we have partitioned $\xi_T = [\xi_{Tx}^T | \xi_{Te}^T]^T = [x_{Ta}^T, x_{Td}^T | e_{Ta}^T, e_{Td}^T]^T$ where the subscripts $_a$ and $_d$ respectively stand for agreement and disagreement. There exists a row permutation matrix $\mathcal{P}$ such that the transformation $\xi_P = \mathcal{P}\xi_T$ results in:

$$\left[\begin{array}{c} \dot{\xi}_a \\ \hline \dot{\xi}_d \end{array}\right] = \left[\begin{array}{cc|cc} \tilde{A}_c^{11} & \mathbf{0} & \mathbf{0} & \mathbf{0} \\ \mathbf{0} & \tilde{A}_c^{33} & \mathbf{0} & \mathbf{0} \\ \hline \mathbf{0} & \mathbf{0} & \tilde{A}_c^{22} & \tilde{A}_c^{24} \\ \mathbf{0} & \mathbf{0} & \mathbf{0} & \tilde{A}_c^{44} \end{array}\right] \left[\begin{array}{c} \xi_a \\ \hline \xi_d \end{array}\right] \tag{5.27}$$

where $\xi_P = [\xi_a^T | \xi_d^T]^T = [x_{Ta}^T, e_{Ta}^T | x_{Td}^T, e_{Td}^T]^T$, and we have the following partitions:

$$\underbrace{\dot{\xi}_a = \begin{bmatrix} \tilde{A}_c^{11} & \mathbf{0} \\ \mathbf{0} & \tilde{A}_c^{33} \end{bmatrix} \xi_a}_{\text{Unobservable agreement dynamics}} \qquad \underbrace{\dot{\xi}_d = \begin{bmatrix} \tilde{A}_c^{22} & \tilde{A}_c^{24} \\ \mathbf{0} & \tilde{A}_c^{44} \end{bmatrix} \xi_d}_{\text{Observable disagreement dynamics}}$$

We limit the design of our observer-based strategy to the second (observable) partition. Since all $\tilde{A}_c^{22}$, $\tilde{A}_c^{24}$, and $\tilde{A}_c^{44}$ are block-diagonal matrices, we find the following networked agent dynamics for $i \in \{2, 3, ..., N\}$:

$$\dot{x}_{Ti} = (A_{avg} + \lambda_i(F_{avg} + B_{avg}K_c))x_{Ti} - \lambda_i B_{avg}K_c e_{Ti} \tag{5.28}$$

and networked observer error dynamics:

$$\dot{e}_{Ti} = (A_{avg} + \lambda_i(F_{avg} - K_o C_{avg}))e_{Ti} \tag{5.29}$$

At this point, We find a control-gain K_c such that $\nu_{Ti} = K_c x_{Ti}$ stabilize (5.30):

$$\dot{x}_{Ti} = (A_{avg} + \lambda_i F_{avg})x_{Ti} + \lambda_i B_{avg}\nu_{Ti} \tag{5.30}$$

and design an observer-gain K_o to be used in (Luenberger) observers (5.31) for $i \in \{2, 3, ..., N\}$:

$$\begin{aligned} \dot{x}_{Ti} &= (A_{avg} + \lambda_i F_{avg})x_{Ti} \\ y_{Ti} &= \lambda_i C_0 x_{Ti} \end{aligned} \tag{5.31}$$

We first rewrite (5.30) as follows:

$$\dot{x}_{Ti} = A_{avg}x_{Ti} + \lambda_2 B_{avg}\nu_{Ti} + \lambda_2 B_{avg}(\frac{\lambda_i}{\lambda_2} - 1)\nu_{Ti} + \lambda_i F_{avg}x_{Ti}$$

and aggregate them for $i \in \{2, 3, ..., N\}$:

$$\underbrace{\dot{x}_{Td} = \bar{A}_{avg}x_{Td} + \bar{B}_{avg}\nu_{Td}}_{\text{Network-level nominal dynamics}} + \underbrace{\bar{B}_{avg}\bar{E}\nu_{Td} + \bar{F}_{avg}x_{Td}}_{\text{Network-level modeling uncertainty}} \tag{5.32}$$

where $\bar{A}_{avg}$, $\bar{B}_{avg}$, and $\bar{E}$ are defined as in (5.17); and $\bar{F}_{avg} = (\Lambda_d \otimes F_{avg})$. We introduce the following shifted dynamics:

$$\underbrace{\dot{x}_{Td} = \bar{A}_{\gamma_c}x_{Td} + \bar{B}_{avg}\nu_{Td}}_{\text{Network-level shifted nominal dyn}} + \underbrace{\bar{B}_{avg}\bar{E}\nu_{Td} + \bar{F}_{avg}x_{Td}}_{\text{Network-level modeling uncertainty}} \tag{5.33}$$

where $\bar{A}_{\gamma_c} = I_{N-1} \otimes A_{\gamma_c}$, $A_{\gamma_c} = A_{avg} + \gamma_c I_{n_x}$, and the non-negative scalar $\gamma_c \geq 0$ is a design parameter. Let $\bar{F}_{avg} = \bar{F}_\tau \bar{\Lambda}_d$ where $\bar{F}_\tau = I_{N-1} \otimes F_{avg}$ and $\bar{\Lambda}_d = \Lambda_d \otimes I_{n_x}$.

Now, we propose the following auxiliary multiagent system model:

$$\dot{x}_{Td} = \bar{A}_{\gamma_c}x_{Td} + \bar{B}_{avg}\nu_{Td} + \bar{F}_\tau \tau \tag{5.34}$$

where the fictitious control signal $\tau = col\{\tau_i\}$, for $i \in \{2, 3, ..., N\}$, is added to handle the fictitious modeling uncertainty $\bar{\Lambda}_d x_{Td}$. We should mention that the numbering of τ matches the numbering of x_{Td} (or ν_{Td}), and, in fact, τ_1 does not exist. Also, using Rayleigh-Ritz inequality Lemma 2.1.1 and proper-

ties of the Kronecker product in Section 2.1, we find the quadratic upper bound $x_{Td}^T \bar{\Lambda}_d \bar{W}_c \bar{\Lambda}_d x_{Td} \leq x_{Td}^T (\lambda_N^2 \bar{W}_c) x_{Td}$ on $\bar{\Lambda}_d x_{Td}$ where $\bar{W}_c = I_{N-1} \otimes W_c$, and $W_c = W_c^T \succ \mathbf{0}$ is a design matrix.

As another preliminary definition for this section, let P_c denote the solution of the following ARE:

$$A_{\gamma_c}^T P_c + P_c A_{\gamma_c} + Q_c - P_c B_c \begin{bmatrix} R_c^{-1} & \mathbf{0} \\ \mathbf{0} & W_c^{-1} \end{bmatrix} B_c^T P_c = \mathbf{0} \tag{5.35}$$

where $B_c = \begin{bmatrix} \lambda_2 B_{avg} & F_{avg} \end{bmatrix}$, $Q_c = Q + \lambda_N^2 W_c$, and $Q = Q^T \succ \mathbf{0}$, $R_c = R_c^T \succ \mathbf{0}$ are two design matrices. (Existence of the stabilizing P_c can be discussed similar to the ARE (5.19) in Subsection 5.2.2.1.)

Next theorem characterizes the required conditions to systematically find a control-gain K_c (for all agents).

Theorem 5.2.2. *Let $\nu_{Ti} = K_c x_{Ti} = -\lambda_2 R_c^{-1} B_{avg}^T P_c x_{Ti}$ and $\tau_i = H_c x_{Ti} = -W_c^{-1} F_{avg}^T P_c x_{Ti}$ respectively be the control signal and fictitious control signal that results in the minimum of a cost function* (5.36) *subject to the auxiliary agent dynamics* (5.37) *for $i \in \{2, ..., N\}$. Then, the aggregated agents in* (5.24) *reach a state-agreement if* (5.38) *is satisfied.*

$$J_i(x_{Ti}(0)) = \min_{\nu_{Ti}, \tau_i} \int_0^\infty (x_{Ti}^T Q_c x_{Ti} + \nu_{Ti}^T R_c \nu_{Ti} + \tau_i^T W_c \tau_i) dt \tag{5.36}$$

$$\dot{x}_{Ti} = A_{\gamma c} x_{Ti} + \lambda_2 B_{avg} \nu_{Ti} + F_{avg} \tau_i \tag{5.37}$$

$$Q + K_c^T R_c K_c - 2 H_c^T W_c H_c \succ \boldsymbol{0} \tag{5.38}$$

Proof. This proof is given at Subsection 5.5.2. □

Now that we have designed a control gain, we start designing an observer gain. We introduce:

$$\dot{x}_{Ti} = (A_{\gamma_o} + \lambda_i F_{avg})x_{Ti} \quad and \quad y_{Ti} = \lambda_i C_0 x_{Ti}$$

as the shifted dynamics of (5.31), where $A_{\gamma_o} = A_{avg} + \gamma_o I_{n_x}$, and $\gamma_o \geq 0$ is a design parameter. We further propose the following Luenberger observer dynamics:

$$\begin{aligned} \dot{\hat{x}}_{Ti} &= (A_{\gamma_o} + \lambda_i F_{avg})\hat{x}_{Ti} + K_o(y_{Ti} - \hat{y}_{Ti}) \\ \hat{y}_{Ti} &= \lambda_i C_0 \hat{x}_{Ti} \end{aligned} \tag{5.39}$$

Also, let P_o be the solution of ARE:

$$A_{\gamma_o}P_o + P_o A_{\gamma_o}^T + Q_o - P_o B_o^T \begin{bmatrix} R_o^{-1} & \mathbf{0} \\ \mathbf{0} & W_o^{-1} \end{bmatrix} B_o P_o = \mathbf{0} \tag{5.40}$$

where $B_o = [\lambda_2 C_0^T, F_{avg}^T]^T$, $Q_o = Q + \lambda_N^2 W_o$, and $Q = Q^T \succ \mathbf{0}$ and $W_o = W_o^T \succ \mathbf{0}$ are two design matrices (The discussion on existence of the stabilizing solution P_o is similar to that of ARE (5.19)).

In the next theorem, we characterize a systematic (LQR-based) procedure to design an observer-gain K_o.

Theorem 5.2.3. *Let $\omega_{Ti} = K_o^T x_{Ti} = -\lambda_2 R_o^{-1} C_0 P_o x_{Ti}$ be the control signal and $\eta_i = H_o^T x_{Ti} = -W_c^{-1} F_{avg} P_o x_{Ti}$ be the fictitious control signal that achieves the minimum of a cost function* (5.41) *subject to* (5.42) *such that the condition* (5.43)

is satisfied for $i \in \{2, ..., N\}$. Then, the required observer gain K_o for the consensus purpose is found.

$$J_i(x_{Ti}(0)) = \min_{\nu_{Ti}, \tau_i} \int_0^\infty (x_{Ti}^T Q_o x_{Ti} + \omega_{Ti}^T R_o \omega_{Ti} + \eta_i^T W_o \eta_i) dt \tag{5.41}$$

$$\dot{x}_{Ti} = A_{\gamma_o}^T x_{Ti} + \lambda_2 C_0^T \nu_{Ti} + F_{avg}^T \eta_i \tag{5.42}$$

$$Q + K_o R_o K_o^T - 2 H_o W_o H_o^T \succ \boldsymbol{0} \tag{5.43}$$

Proof. A sketch of the proof is provided at Subsection 5.5.3. □

Based on the results of Theorems 5.2.2 and 5.2.3, we propose Lemma 5.2.1 in order to address Problem 5.2.2. In this Lemma, $\sigma_c \triangleq \sqrt{|\lambda_{max}(\tilde{A}_N^T \tilde{A}_N)|}$ where $\tilde{A}_N$ is defined in (5.23).

Lemma 5.2.1. *Using K_c of Theorem 5.2.2 and K_o of Theorem 5.2.3, the closed-loop nominal dynamics in* (5.23) *reach an agreement on zero. Furthermore, Problem 5.2.2 is solved if there exist positive scalars α_c and β_c such that $\|e^{\tilde{A}_c t}\| \leq \alpha_c e^{\beta_c t}$ and $\sigma_c < \frac{\beta_c}{\alpha_c}$ are satisfied.*

Proof: This proof follows Steps 2 and 3 of Theorem 5.2.1 for an output feedback problem.

5.3 Distributed decoupling of linear multiagent systems with state-coupled nonlinearities

In this section, we propose two distributed decoupling control algorithms for a group of Lur'e nonlinear multiagent systems with (multiagent system-level) nonlinear coupling terms.

5.3.1 Problem statement

We already have discussed that a (conventional consensus-based) distributed controller, which is designed based on the decoupled nominal linear models of agents, does not necessarily guarantee the stabilization of entire multiagent system in the presence of modeling uncertainties or interconnections of agents. At the beginning of this chapter, we modeled a linear time-invariant large-scale system using graph-theoretic ideas (see (5.2)), and named it an interconnected or a physically coupled multiagent system. Based on a hierarchical framework, in Section 5.2, we designed two graph-theoretic ideas to systematically find distributed decoupling systems. In this section, we propose a Lur'e nonlinear version of physically coupled multiagent system:

$$\dot{x}_i = Ax_i + B_m u_i + w_i(x_i, \mathcal{N}_i^a) \tag{5.44}$$

where, now, the effect of physical couplings appear through an (partially-) unknown nonlinearities w_i which are functions of state variables x_i in neighborhoods $\mathcal{N}_i^a$ over an agent-layer graph $\mathcal{G}_a$. In this section, we assume that the coupling

structure is completely known, and the communication happens over the same topology. Thus, we consider a single graph $\mathcal{G}_a$ with neighboring sets $\mathcal{N}_i$.

We focus on two scenarios: *1)* the nonlinearity w_i is in the range space of the input matrix B_m, we write $w_i = B_m\phi_i$, and call ϕ_i a matched nonlinearity or nonlinear modeling uncertainty; and *2)* this w_i is not in the range space of B_m, we write is as $w_i = B_u\psi_i$, and name ψ_i an unmatched nonlinearity (B_u is not in the range of B_m). Note that we have introduced B_u without loss of generality as it can be the identity matrix which results in $\psi_i = w_i$. We are interested in modifying our state-feedback distributed control ideas in Subsection 5.2, systematically find new static state feedback linear time-invariant algorithms which use relative-state measurements agents' neighborhoods, and decouple physically (state) coupled Lur'e nonlinear multiagent systems[10]. We emphasize that, although each model includes a homogeneous linear part, we deal with a class of heterogeneous nonlinear multiagent systems due to the presence of a set of heterogeneous nonlinearities w_i. The following definitions are used in this section:

Definition 5.3.1. *For a vector $x = [x_1, x_2, ..., x_n]^T \in \mathbb{R}^n$, an entry-wise absolute-value is defined to be $|x| = [|x_1|, |x_2|, .., |x_n|]^T$ where $|x_i|$ indicates the absolute-value of $x_i \in \mathbb{R}$ for $i \in \{1, 2, ..., n\}$.*

Definition 5.3.2. *For any vectors x and $y \in \mathbb{R}^n$, we define the inequality $|x| \leq |y| \Leftrightarrow |x_i| \leq |y_i| \ \forall \ i \in \{1, 2, ..., n\}$.*

[10]For simplicity, we confine this section to time-invariant nonlinear scenarios. However, the same results are valid for time-varying nonlinearities (assuming piecewise continuous time-dependency). This fact will be clarified in Chapter 6.

5.3.1.1 Lur'e multiagent systems with matched nonlinear interconnection

We rewrite (5.44) as a multiagent system with homogeneous linear dynamics and matched heterogeneous nonlinear interconnections over an undirected graph $\mathcal{G}$ (we refer to (5.45) as the i^{th} follower's dynamics):

$$\begin{aligned} \dot{x}_i &= Ax_i + B_m(u_i + \phi_i(z_i)) \\ z_i &= C_z \sum_{j\in\mathcal{N}_i}(x_i - x_j) \end{aligned} \tag{5.45}$$

where $x_i \in \mathbb{R}^{n_x}$ stands for the state deviation from the operating-point and $u_i \in \mathbb{R}^{n_u}$ indicates the control input deviation from the operating-point; and $A \in \mathbb{R}^{n_x\times n_x}$ and $B_m \in \mathbb{R}^{n_x\times n_u}$. Also, $z_i \in \mathbb{R}^{n_u}$ denotes the input to the i^{th} follower's nonlinearity $\phi_i \in \mathbb{R}^{n_u}$, and $C_z \in \mathbb{R}^{n_u\times n_x}$ indicates the coupling matrix.

Assumption 5.3.1. *The nonlinear functions $\phi_i(z_i) : \mathbb{R}^{n_u} \to \mathbb{R}^{n_u}\ \forall\ i \in \{1, ..., N\}$ satisfy the followings:*

1. *Each function $\phi_i(z_i)$ is composed by separate nonlinearities:*

$$\phi_i(z_i) \triangleq col\{\phi_{im}(z_{im})\}$$

   in which $\phi_{im}(z_{im}) : \mathbb{R} \to \mathbb{R}$ and $z_i = col\{z_{im}\}$ for $m = \{1, 2, ..., n_u\}$.

2. *Each separate nonlinearity $\phi_{im}(z_i)$ satisfies a sector condition:*

$$-\gamma_{im}|z_{im}| \leq \phi_{im}(z_{im}) \leq \gamma_{im}|z_{im}|$$

   where $\gamma_{im} \geq 0$ such that $-\Gamma_{ui}|z_i| \leq \phi_i(z_i; t) \leq \Gamma_{ui}|z_i|$ where $\Gamma_{ui} = diag\{\gamma_{im}\}$.

Remark 5.3.1. *The Assumption 5.3.1 will be specifically used in this section. However, we further need to assume that the nonlinearities ϕ_i satisfy the Lipschitz condition. While we do not use the Lipschitz inequality* (2.7) *in derivations of equations, it is inherently required to prove the results based the statement of Lyapunov Theorem 2.3.1.*

5.3.1.2 Lur'e multiagent systems with unmatched nonlinear interconnection

In this scenario, we introduce the (follower) agents' dynamics with unmatched heterogeneous nonlinear interconnections:

$$\begin{aligned} \dot{x}_i &= Ax_i + B_m u_i + B_u \psi_i(y_i) \\ y_i &= C_y \textstyle\sum_{j\in\mathcal{N}_i}(x_i - x_j) \end{aligned} \tag{5.46}$$

where $B_u \in \mathbb{R}^{n_x \times n_\psi}$ and $C_y \in \mathbb{R}^{n_\psi \times n_x}$; and $y_i \in \mathbb{R}^{n_\psi}$ and $\psi_i(y_i) \in \mathbb{R}^{n_\psi}$.

Assumption 5.3.2. *The nonlinear functions $\psi_i(y_i) : \mathbb{R}^{n_\psi} \to \mathbb{R}^{n_\psi}\ \forall\ i \in \{1, ..., N\}$ satisfy similar conditions to the Assumption 5.3.1 substituting ϕ_i by ψ_i, n_u by n_ψ, and Γ_{ui} by $\Gamma_{\psi i}$ (also see Remark 5.3.1).*

5.3.1.3 Leader-Follower Consensus Formulation

Briefly, we want to design a (distributed) decoupling controller in order to exponentially mitigate the effect of interconnected unknown nonlinearities in (5.45) or (5.46) such that they behave as a group of N decoupled agents[11]:

[11] Here, we exactly know these nominal dynamics. Thus, compared to the results of Section 5.2, these residual dynamics are the same as the homogeneous nominal part of the interconnected agents.

$$\dot{x}_i = Ax_i + B_m u_i \tag{5.47}$$

This global decoupling objective should be achieved using only relative-state measurements. We already have discussed that, because the variables x_i and u_i are defined as state and control input deviations from the operating-point values of the i^{th} agent, this decoupling task is achieved whenever the following condition is satisfied under any initial conditions and over a fixed-graph $\mathcal{G}$:

$$\lim_{t\to\infty} x_i(t) = 0 \tag{5.48}$$

In each matched or unmatched scenario, we further assume that there exists one agent that is not physically affected by other agents (but may have some physical effects on others). We call this special agent a leader. We introduce a leader agent (5.49) for the matched case:

$$\begin{aligned} \dot{x}_0 &= Ax_0 + B_m(u_0 + \phi_0(z_0)) \\ z_0 &= C_z x_0 \end{aligned} \tag{5.49}$$

and a leader agent (5.50) for the unmatched scenario:

$$\begin{aligned} \dot{x}_0 &= Ax_0 + B_m u_0 + B_u \psi_0(y_0) \\ y_0 &= C_y x_0 \end{aligned} \tag{5.50}$$

where $x_0 \in \mathbb{R}^{n_x}$ and $u_0 \in \mathbb{R}^{n_u}$ are defined similar to the variables in (5.45). The functions $\phi_0(z_0) \in \mathbb{R}^{n_u}$ and $\psi_0(y_0) \in \mathbb{R}^{n_\psi}$ satisfy the Assumption 5.3.1 and Assumption 5.3.2 for $i = 0$, respectively. We further adopt the follower models (5.45) and (5.46) as (5.51) and (5.52), respectively:

$$\begin{aligned} \dot{x}_i &= Ax_i + B_m(u_i + \phi_i(z_i)) \\ z_i &= C_z(\textstyle\sum_{j\in\mathcal{N}_i}(x_i - x_j) + b_i(x_i - x_0)) \end{aligned} \tag{5.51}$$

$$\begin{aligned} \dot{x}_i &= Ax_i + B_m u_i + B_u\psi_i(y_i) \\ y_i &= C_y(\textstyle\sum_{j\in\mathcal{N}_i}(x_i - x_j) + b_i(x_i - x_0)) \end{aligned} \tag{5.52}$$

Now, the distributed decoupling task (5.48) for (5.45) or (5.46) is accomplished when the leader-follower consensus problem (5.53) is solved for (5.49) and (5.51), or (5.50) and (5.52):

$$\lim_{t\to\infty}(x_i(t) - x_0(t)) = 0 \tag{5.53}$$

by setting a new *control objective* to be finding the control signals u_0 and u_i that simultaneously stabilize the uncertain leader dynamics (5.49) (or (5.50)) and derive the followers' states x_i in (5.51) (or (5.52)) to the leader state x_0, under any initial state conditions and over a fixed graph $\mathcal{G}_{lf}$.

The following assumptions are satisfied in this section:

Assumption 5.3.3. *The matrix A is Hurwitz, (A, B) characterizes a stabilizable model, there exists a direct path from the leader to each follower over $\mathcal{G}_{lf}$, and x_0 is known but u_0 is unknown to the followers connected to the leader.*

Assumption 5.3.4. *Nonlinear functions $\phi_i(z_i)$ and $\psi_i(y_i)$ are unknown, Γ_{ui} in Assumption 5.3.1 and $\Gamma_{\psi i}$ in Assumption 5.3.2 are known matrices, there exists a local (agent-level) lookup-table scheduling system or feedback tracking controller such that each agent's nominal model* (5.47) *operates at the desired operating-point (x_i^{opt}, u_i^{opt}), and the distributed controller does not have access to (x_i^{opt}, u_i^{opt}).*

5.3.2 Leader-follower consensus-based decoupling: main results

5.3.2.1 Matched nonlinear interconnection

In order to achieve the consensus in a multiagent system of (5.49) and (5.51), we propose the following control signals u_0 and u_i:

$$u_0 = K_0 x_0 \quad \textit{and} \quad u_i = K(\sum_{j\in\mathcal{N}_i}(x_i - x_j) + b_i(x_i - x_0)) \tag{5.54}$$

where $K_0 \in \mathbb{R}^{n_u\times n_x}$ represents the leader's control gain and $K \in \mathbb{R}^{n_u\times n_x}$ stands for the followers' control gain. By introducing the leader-follower tracking error $\epsilon_i \triangleq x_i - x_0$, we find the leader-follower tracking error dynamics:

$$\dot{\epsilon}_i = A\epsilon_i + B_m u_i + B_m\Phi_i(u_0, z_0, z_i)$$

and

$$\begin{aligned}\Phi_i(u_0, z_0, z_i) &= \phi_i(z_i) - \phi_0(z_0) - u_0\\ z_i &= C_z(\textstyle\sum_{j\in\mathcal{N}_i}(\epsilon_i - \epsilon_j) + b_i(\epsilon_i - \epsilon_0))\\ u_i &= K(\textstyle\sum_{j\in\mathcal{N}_i}(\epsilon_i - \epsilon_j) + b_i\epsilon_i)\end{aligned}$$

where $b_i \in \{0, 1\}$ is defined based on a special type of leader-follower digraphs in page 80.

We further define $\epsilon = col\{\epsilon_i\}$ as the aggregated tracking error vector, $u = col\{u_i\}$ be the aggregated control-input, $\Phi = col\{\Phi_i\} = \phi(z) - (\mathbf{1}_N \otimes I_{n_u})\phi_0(z_0) - (\mathbf{1}_N \otimes I_{n_u})u_0$ be the aggregated unknown matched nonlinearity, $\phi(z) = col\{\phi_i(z_i)\}$, and $i \in \{1, 2, ...N\}$. Now, over $\mathcal{G}_{lf}$, we have:

$$z = (\mathcal{H} \otimes C_z)\epsilon$$

$$u_0 = K_0 x_0 \quad \textit{and} \quad u = (\mathcal{H} \otimes K)\epsilon$$

where the reduced order Laplacian matrix $\mathcal{H}$ is defined in Subsection 3.1.2.1 at page 79. We decompose the followers' aggregated control signal as follows:

$$u = (\mathcal{H} \otimes I_{n_u})\nu \qquad and \qquad \nu = \bar{K}\epsilon = (I_N \otimes K)\epsilon$$

and pass the communication-induced (relative measurement-induced) coupling term $\mathcal{H} \otimes I_{n_u}$ to the augmented leader-follower multiagent system dynamics:

$$\underbrace{\dot{\xi} = \tilde{A}\xi + \tilde{B}_u\tau}_{\text{Networked nominal dynamics}} \quad + \underbrace{\tilde{B}_u\tilde{E}\tau + \tilde{B}_u\eta(u_0, z_0, z)}_{\text{Modeling uncetainty}} \tag{5.55}$$

where $\xi = [x_0^T, \epsilon^T]^T$, $\tau = [u_0^T, \nu^T]^T = \tilde{K}\xi$, $\tilde{K} = diag\{[K_0, \bar{K}]\}$, $\eta = [\phi_0^T, \Phi_\mu^T]$, and $\Phi_\mu = \frac{1}{\mu_1}\Phi$. Also, $\tilde{A} = diag\{[A, \bar{A}]\}$, $\bar{A} = I_N \otimes A$, $\tilde{B}_m = diag\{[B_u, \bar{B}_u]\}$, $\bar{B}_u = I_N \otimes \mu_1 B_u$, $\tilde{E} = diag\{[\mathbf{0}, \bar{E}]\}$, and $\bar{E} = \bar{E}^T = ((\frac{1}{\mu_1}\mathcal{H} - I_N) \otimes I_{n_u}) \succcurlyeq \mathbf{0}$. We further define $\Gamma_u \triangleq diag\{[\gamma_{u1}, \gamma_{u2}, ..., \gamma_{un_u}]\}$ where $\gamma_{um} \triangleq \max_i\{\gamma_{im}\}$ for $m \in \{1, ..., n_u\}$ and $i \in \{1, 2, ..., N\}$.

We know that $\Phi_\mu(u_0, z_0, z) \leq \frac{1}{\mu_1}\Phi_M(u_0, z_0, z)$ where the upper bound function Φ_M is given by (5.56):

$$\Phi_M \triangleq (I_N \otimes \Gamma_u)|z| + (\mathbf{1}_N \otimes \Gamma_{u0})|z_0| + (\mathbf{1}_N \otimes I_{n_u})|u_0| \tag{5.56}$$

Moreover, using the Rayleigh-Ritz inequality Lemma 2.1.1 and Fact 2.2.1, a quadratic upper bound on the unknown nonlinearity η is given by:

$$\eta^T\tilde{R}\eta \leq \epsilon^T\bar{R}^\epsilon\epsilon + x_0^T R^{x_0}x_0 + u_0^T R^{u_0}u_0 =: \eta_M^T\tilde{R}\eta_M \tag{5.57}$$

where $\tilde{R} = \tilde{R}^T = diag\{[R_l, \bar{R}_f]\}$, $R_l = R_l^T \succ \mathbf{0}$, $\bar{R}_f = I_N \otimes R_f$, $R_f = R_f^T = r_f I_{n_u} \succ \mathbf{0}$, $\bar{R}^\epsilon = I_N \otimes R^\epsilon$, $R^\epsilon = R_f^\epsilon = 2r_f\frac{\mu_N^2}{\mu_1^2}C_z^T\Gamma_u^2C_z$, $R^{x_0} = R_l^{x_0} + R_f^{x_0} = C_z^T\Gamma_{u0}R_l\Gamma_{u0}C_z + 4Nr_f\frac{1}{\mu_1^2}C_z^T\Gamma_{u0}^2C_z$, and $R^{u_0} = R_f^{u_0} = 4Nr_f\frac{1}{\mu_1^2}I_{n_u}$. (Note that

$\eta_M^T \tilde{R} \eta_M$ is a symbol to specify the upper-bound on $\eta^T \tilde{R} \eta$. In fact, it is a function x_0, u_0, and ϵ. We may read it as $\eta_M^T \tilde{R} \eta_M(x_0, u_0, \epsilon)$.)

Now, in next Theorem, we provide a sufficient condition to achieve the leader-follower consensus (5.53) using (5.55), and, consequently, to solve (5.48) for a multiagent system of (5.45).

Theorem 5.3.1. *Let* $u_0 = K_0 x_0 = -R_{1l}^{-1} B_m^T P_{1l} x_0$ *be the control signal that achieves the minimum cost* (5.58) *subject to* (5.59) *satisfying a condition* (5.60)*, where* P_{1l} *denotes solution of the ARE* (5.61)*,* $Q_{1l} = Q_l + R^{x_0}$*,* $R^{x_0} = R_l^{x_0} + R_f^{x_0}$*,* $R_{1l} = R_l + R^{u_0}$*,* $R^{u_0 x_0} = C_z^T \Gamma_{u0} R^{u_0} \Gamma_{u0} C_z = 4N r_f \frac{1}{\mu_1^2} C_z^T \Gamma_{u0}^2 C_z$*, and* $Q_l = Q_l^T \succ \boldsymbol{0}$ *and* $R_l = R_l^T \succ \boldsymbol{0}$ *are two design matrices.*

$$J_0(x_0(0)) = \min_{u_0} \int_0^\infty (x_0^T Q_{1l} x_0 + u_0^T R_{1l} u_0) dt \tag{5.58}$$

$$\dot{x}_0 = A x_0 + B_m u_0 \tag{5.59}$$

$$Q_l - R^{u_0 x_0} - K_0^T R^{u_0} K_0 \succ \boldsymbol{0} \tag{5.60}$$

$$A^T P_{1l} + P_{1l} A + Q_{1l} - P_{1l} B_m R_{1l}^{-1} B_m^T P_{1l} = \boldsymbol{0} \tag{5.61}$$

Also, let $\nu_i = K \epsilon_i = -\mu_1 R_{1f}^{-1} B_m^T P_{1f} \epsilon_i \ \forall i \in \{1, 2, ..., N\}$ *be the* i^{th} *follower's control signal that achieves the minimum cost* (5.62) *subject to* (5.63)*, where* P_{1f} *represents solution of the ARE* (5.64)*,* $Q_{1f} = Q_f + R^\epsilon$*,* $R_{1f} = R_f$*, and* $Q_f = Q_f^T \succ \boldsymbol{0}$ *and* $R_f = R_f^T = r_f I_{n_u} \succ \boldsymbol{0}$ *for* $r_f > 0$ *are two design matrices.*

$$J_i(\epsilon_i(0)) = \min_{\nu_i} \int_0^\infty (\epsilon_i^T Q_{1f} \epsilon_i + \nu_i^T R_{1f} \nu_i) dt \tag{5.62}$$

$$\dot{\epsilon}_i = A \epsilon_i + \mu_1 B_m \nu_i \tag{5.63}$$

$$A^T P_{1f} + P_{1f} A + Q_{1f} - \mu_1^2 P_{1f} B_m R_{1f}^{-1} B_m^T P_{1f} = \boldsymbol{0} \tag{5.64}$$

Then, the closed-loop system (5.55) *is exponentially stable and the distributed decoupling problem* (5.48) *is solved in the presence of heterogeneous matched interconnected nonlinear modeling uncertainties.*

Proof. This proof is given at Subsection 5.5.4 □

5.3.2.2 Unmatched nonlinear interconnection

In this subsection, we consider the unmatched nonlinear uncertainty scenario. We only introduce new variables and the rest can be found in Subsection 5.3.2.1.

We propose the control signals u_0 and u_i:

$$u_0 = G_0 x_0 \qquad and \qquad u_i = G(\sum_{j\in\mathcal{N}_i}(x_i - x_j) + b_i(x_i - x_0)) \tag{5.65}$$

where, for a leader-follower tracking error $\epsilon_i = x_i - x_0$, the followers' control signal can be rewritten as:

$$u_i = G(\sum_{j\in\mathcal{N}_i}(\epsilon_i - \epsilon_j) + b_i\epsilon_i)$$

Here, $G_0 \in \mathbb{R}^{n_u\times n_x}$ denotes the leader's control gain, and $G \in \mathbb{R}^{n_u\times n_x}$ indicates the followers' control gain. Also, the leader-follower tracking error dynamics are given by:

$$\dot{\epsilon}_i = A\epsilon_i + B_m u_i - B_m u_0 + B_u\Psi_i(y_0, y_i)$$

where the unknown nonlinear functions $\Psi_i(y_0, y) = \psi_i(y_i) - \psi_0(y_0)$ satisfy:

$$\Psi_i(y_0, z) \leq \Gamma_\psi|y_i| + \Gamma_{\psi 0}|y_0|$$

for a Γ_ψ that is defined similar to Γ_u in Subsection 5.3.2.1.

Over $\mathcal{G}_{lf}$, the augmented leader-follower dynamics are as follows:

$$\underbrace{\dot{\zeta} = \tilde{A}\zeta + \tilde{B}_u\sigma}_{\text{Networked nominal dyn.}} \quad \underbrace{+\tilde{B}_u\tilde{E}\sigma + \tilde{B}_{u_0}\underline{u}_0 + \tilde{B}_\psi\Psi_t(y_0, y)}_{\text{Modeling uncertainty}} \tag{5.66}$$

where $\zeta = [x_0^T, \epsilon^T]^T$, $\sigma = [u_0^T, \nu^T]^T = \tilde{G}\zeta = diag\{G_0, \bar{G}\}\zeta$, $\bar{G} = I_N \otimes G$, $\underline{u}_0 = -(\mathbf{1}_N \otimes I_{n_u})u_0 \in \mathbb{R}^{Nn_u}$, $\Psi_t = [\psi_0^T, \Psi^T]^T$, $\Psi(y_0, y) = col\{\Psi_i(y_i)\} = \psi(y) - (\mathbf{1}_N \otimes I_{n_u})\psi_0(y_0)$, $\psi(y) = col\{\psi_i(y_i)\}$, and $y = (\mathcal{H} \otimes C_y)\epsilon$. Also, $\tilde{B}_{u_0} = [\mathbf{0}^T, \bar{B}_{u_0}^T]^T$, $\bar{B}_{u_0} = I_N \otimes B_m$, $\tilde{B}_u = diag\{B_u, \bar{B}_u\}$, and $\bar{B}_u = I_N \otimes B_u$.

We further find that the following inequality is satisfied:

$$\Psi \leq (I_N \otimes \Gamma_\psi)|y| + (\mathbf{1}_N \otimes \Gamma_{\psi 0})|y_0|$$

Now, we define the following *auxiliary leader-follower multiagent system's dynamics*:

$$\dot{\zeta} = \tilde{A}\zeta + \tilde{B}_u\sigma + \tilde{B}_{u_0}\theta + \tilde{B}_\psi\beta \tag{5.67}$$

where $\theta = [\theta_1^T, ..., \theta_N^T]^T \in \mathbb{R}^{Nn_u}$ and $\beta = [\beta_0^T, \beta_1^T, ..., \beta_N^T]^T \in \mathbb{R}^{(N+1)n_\psi}$ are two auxiliary control inputs corresponding to two unmatched uncertainties $\underline{u}_0$ (unknown to followers) and $\Psi_t(y_0, y)$, respectively. The quadratic (upper) bounds on these uncertainties are given by (5.68) and (5.69), respectively:

$$\underline{u}_0^T \bar{S} \underline{u}_0^T = u_0^T (NS) u_0 \tag{5.68}$$

$$\Psi_t^T \tilde{W} \Psi_t \leq \epsilon^T \bar{W}^\epsilon \epsilon + x_0^T W^{x_0} x_0 =: \Psi_{tM}^T \tilde{W} \Psi_{tM} \tag{5.69}$$

where $\bar{S} = I_N \otimes S$, $S = S^T \succ \mathbf{0}$, $\tilde{W} = diag\{W_l, \bar{W}_f\}$, $W_l = W_l^T \succ \mathbf{0}$, $\bar{W}_f = I_N \otimes W_f$, $W_f = W_f^T \succ \mathbf{0}$, $\bar{W}^\epsilon = \bar{W}_f^\epsilon = I_N \otimes W_f^\epsilon$, $W_f^\epsilon = 2\mu_N^2 C_y^T \Gamma_\psi W_f \Gamma_\psi C_y$, and $W^{x_0} = W_l^{x_0} + W_f^{x_0} = C_y^T \Gamma_{\psi_0} W_l \Gamma_{\psi_0} C_y + 2N C_y^T \Gamma_{\psi_0} W_f \Gamma_{\psi_0} C_y$.

In the next theorem, we systematically find the required control gains in (5.65) and characterize some sufficient conditions for stabilization of (5.66). Equivalently, we guarantee the leader-follower consensus (5.53) for (5.50) and (5.52) or, equivalently, solve (5.48) for (5.46).

Theorem 5.3.2. *Let* $\begin{bmatrix} u_0 \\ \beta_0 \end{bmatrix} = \begin{bmatrix} G_0 \\ L_0 \end{bmatrix} x_0 = \begin{bmatrix} -R_{2l}^{-1} B_m^T P_{2l} \\ -W_l^{-1} B_u^T P_{2l} \end{bmatrix} x_0$ *be the control signal that achieves the minimum cost* (5.70) *subject to the auxiliary system* (5.71) *where the condition* (5.72) *or* (5.73) *is satisfied. The matrix* P_{2l} *denotes solution of the ARE* (5.74)*;* $Q_{2l} = Q_l + W^{x_0}$*,* $R_{2l} = R_l + NS$*;* $Q_l = Q_l^T \succ \boldsymbol{0}$*,* $R_l = R_l^T \succ \boldsymbol{0}$*, and* $W_l = W_l^T = \boldsymbol{0}$ *are three design matrices,* $B_{Ul} = [B_m, B_u]$*, and* $R_{Ul} = diag\{[R_{2l}, W_l]\}$*.*

$$J_0(x_0(0)) = \min_{u_0, \beta_0} \int_0^\infty (x_0^T Q_{2l} x_0 + u_0^T R_{2l} u_0 + \beta_0^T W_l \beta_0) dt \tag{5.70}$$

$$\dot{x}_0 = A x_0 + B_m u_0 + B_u \beta_0 \tag{5.71}$$

$$Q_l - 2L_0^T W_l L_0 \succ \boldsymbol{0} \tag{5.72}$$

$$Q_l + G_0^T R_l G_0 - 2L_0^T W_l L_0 \succ \boldsymbol{0} \tag{5.73}$$

$$A^T P_{2l} + P_{2l} A + Q_{2l} - P_{2l} B_{Ul} R_{Ul}^{-1} B_{Ul}^T P_{2l} = \boldsymbol{0} \tag{5.74}$$

Also, let $\begin{bmatrix} \nu_i \\ \beta_i \\ \theta_i \end{bmatrix} = \begin{bmatrix} G \\ L \\ H \end{bmatrix} \epsilon_i = \begin{bmatrix} -\mu_1 R_{2f}^{-1} B_u^T P_{2f} \\ -W_f^{-1} B_\psi^T P_{2f} \\ -S^{-1} B_u^T P_{2f} \end{bmatrix} \epsilon_i$ *be the control signal that achieves the minimum cost* (5.75) *subject to the auxiliary system* (5.76) *where the condition* (5.77) *or* (5.78) *is satisfied. The matrix* P_{2f} *stands for the solution of the ARE* (5.79)*,* $Q_{2f} = Q_f + W^\epsilon$*, and* $R_{2f} = R_f$*. Also,* $Q_f = Q_f^T \succ \boldsymbol{0}$*,* $R_f = R_f^T = r_f I_{n_u} \succ \boldsymbol{0}$ *for* $r_f \in \mathbb{R}^+$*,* $W_f = W_f^T \succ \boldsymbol{0}$*, and* $S = S^T \succ \boldsymbol{0}$ *are four design matrices. Moreover,* $B_{Uf} = [\mu_1 B_m, B_u, B_m]$ *and* $R_{Uf} = diag\{[R_{2f}, W_f, S]\}$*.*

$$J_i(\epsilon_i(0)) = \min_{\nu_i, \beta_i, \theta_i} \int_0^\infty (\epsilon_i^T Q_{2f} \epsilon_i + \nu_i^T R_{2f} \nu_i + \beta_i^T W_f \beta_i + \theta_i^T S \theta) dt \tag{5.75}$$

$$\dot{\epsilon}_i = A \epsilon_i + \mu_1 B_m \nu_i + B_u \beta_i + B_m \theta_i \tag{5.76}$$

$$Q_f - 2L^T W_f L - 2H^T S H \succ \boldsymbol{0} \tag{5.77}$$

$$Q_f + G^T R_f G - 2L^T W_f L - 2H^T S H \succ \boldsymbol{0} \tag{5.78}$$

$$A^T P_{2f} + P_{2f} A + Q_{2f} - P_{2f} B_{Uf} R_{Uf}^{-1} B_{Uf}^T P_{2f} = \boldsymbol{0} \tag{5.79}$$

Then, the closed-loop system (5.66) *is exponentially stable and the distributed decoupling problem* (5.48) *is solved.*

Proof. This proof is provided at Subsection 5.5.5. □

Remark 5.3.2. *The condition* (5.73) *is essentially an alternative version of* (5.72) *with an added term* $G_0^T R_l G_0$ *(similarly, see* (5.78) *and* (5.77)*).*

5.3.3 Simulation Verification

In this section, we investigate the feasibility of our ideas through simulation studies over a coupling and control graph topology $\mathcal{G}_{lf}$ that is depicted in Fig. 5.2. The follower's graph Laplacian matrix $\mathcal{L}$ corresponding to $\mathcal{G}$, the pinning vector b (to find $\mathcal{B}$), and the reduced-order graph Laplacian matrix $\mathcal{H}$ are given below:

$$\mathcal{L} = \begin{bmatrix} 3 & -1 & 0 & -1 & -1 \\ -1 & 3 & -1 & 0 & -1 \\ 0 & -1 & 2 & -1 & 0 \\ 0 & 0 & -1 & 2 & -1 \\ -1 & -1 & 0 & -1 & 3 \end{bmatrix}, \quad b = \begin{bmatrix} 1 \\ 1 \\ 0 \\ 0 \\ 0 \end{bmatrix}, \quad \mathcal{H} = \begin{bmatrix} 4 & -1 & 0 & -1 & -1 \\ -1 & 4 & -1 & 0 & -1 \\ 0 & -1 & 2 & -1 & 0 \\ 0 & 0 & -1 & 2 & -1 \\ -1 & -1 & 0 & -1 & 3 \end{bmatrix}$$

Let agents be described by a stable nominal local part in the state space domain, specified by the following pair of matrices:

$$A = \begin{bmatrix} 0 & 1 \\ -5 & -3 \end{bmatrix} \quad and \quad B_m = \begin{bmatrix} 0 \\ 1 \end{bmatrix}$$

and be initialized as follows where $x_i^0 = x_i(0)$ for $i \in \{0, 1, ..., 5\}$:

$$x_0^0 = \begin{bmatrix} 15 \\ 15 \end{bmatrix} \quad x_1^0 = \begin{bmatrix} -10 \\ 20 \end{bmatrix} \quad x_2^0 = \begin{bmatrix} 15 \\ -15 \end{bmatrix} \quad x_3^0 = \begin{bmatrix} 10 \\ 15 \end{bmatrix} \quad x_4^0 = \begin{bmatrix} -30 \\ 20 \end{bmatrix} \quad x_5^0 = \begin{bmatrix} 20 \\ -30 \end{bmatrix}$$

5.3.3.1 Matched nonlinear modeling uncertainty

In the matched scenario, we let $C_z = [0, 1.5]$, and use the following nonlinearities in simulation (unknown in design process):

$$\phi_0(z_0) = 0.1sin(z_0), \quad \phi_1(z_1) = 0.7z_1, \quad \phi_2(z_2) = -0.2sin(z_2),$$
$$\phi_3(z_3) = 0.5tanh(z_3), \quad \phi_4(z_4) = -0.5tanh(z_4), \quad \phi_5(z_5) = -0.3sin(z_5)$$

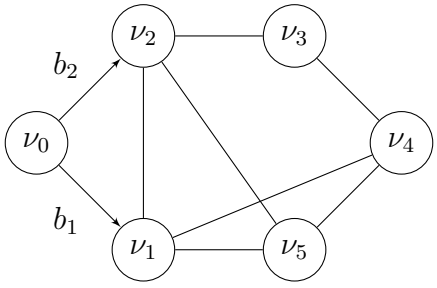

Figure 5.2: The (physical) coupling and communication topology $\mathcal{G}_{lf}$. The followers' undirected graph $\mathcal{G}$ can be found by removing the node v_0 and directed edges originating from that.

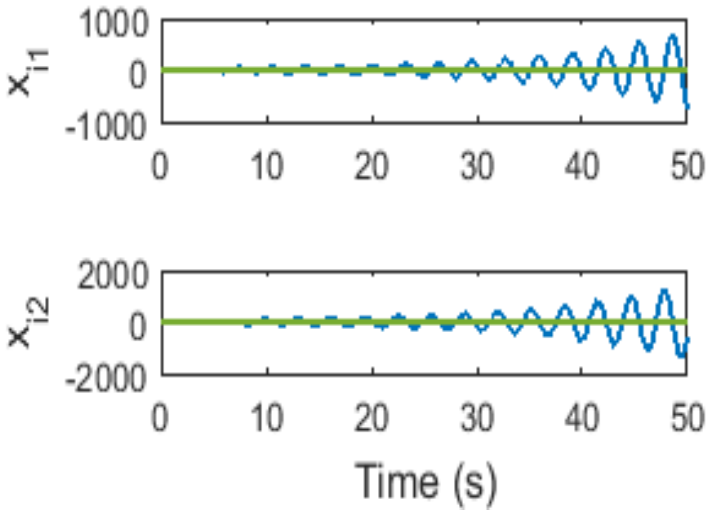

Figure 5.3: Matched scenario: State deviation variables of all agents without the distributed decoupling controller (see the definition in (5.45)) where x_{i1} and x_{i2} denote the first and second state deviation variables of the i^{th} agent, respectively.

where $tanh(.)$ refers to the hyperbolic tangent. By removing the node ν_0 and its edges in Figure 5.2, we first simulate the open-loop interconnected multiagent system over the leaderless graph $\mathcal{G}$ without the distributed decoupling controller of Subsection 5.3.2.1. The unstable behavior of the interconnected multiagent system in Figure 5.3 indicates the need for a (distributed) decoupling controller. Figure 5.4 represents the stable closed-loop multiagent system behavior using the controllers of Theorem 5.3.1, in terms of the state variables' deviations from the operating-point.

5.3.3.2 Unmatched nonlinear modeling uncertainty

In this subsection, we implement the controllers of Theorem 5.3.2 for a multiagent system with $C_y = [0.5, 1.5]$ and $B_u = [0.2, 1]^T$. Substituting z_i variables

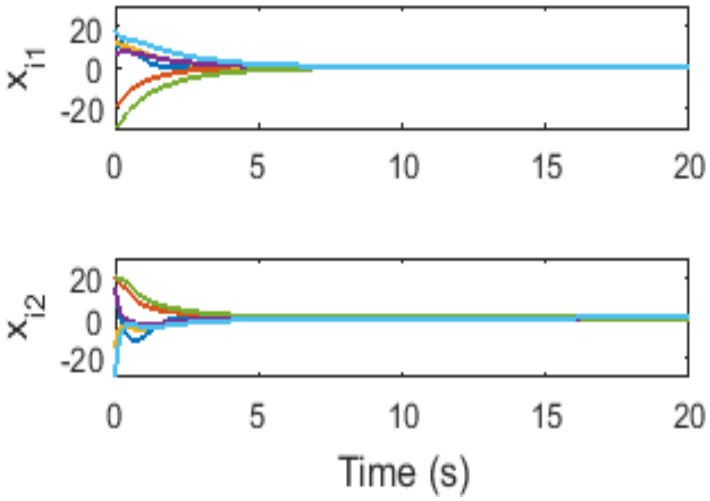

Figure 5.4: Matched scenario: State deviation variables of all agents with distributed decoupling controller, respectively.

by y_i, the nonlinear functions are the same as Subsection 5.3.3.1. The unstable open-loop behavior of the multiagent system over $\mathcal{G}$ is depicted in Fig. 5.5. The simulation result of a closed-loop multiagent system with controllers of Theorem 5.3.2 is shown in Figure 5.6 which indicates that agents can independently operate at their desired operating points.

5.4 Summary and bibliography

In this chapter, we overview the main approaches in the control of large-scale systems along with a brief discussion on their disadvantages with respect to each others. We propose graph-theoretic ideas as intermediate approaches to model and stabilize physically interconnected multiagent systems (large-scale systems). We need to mention that the change from "large-scale" to "physically interconnect multiagent" systems is made to convey that our approaches are based on graph-

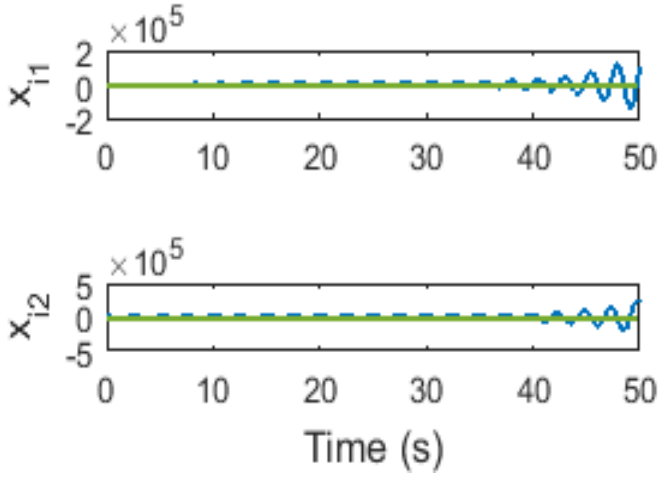

Figure 5.5: Unmatched scenario: State deviation variables of all agents without distributed decoupling controller.

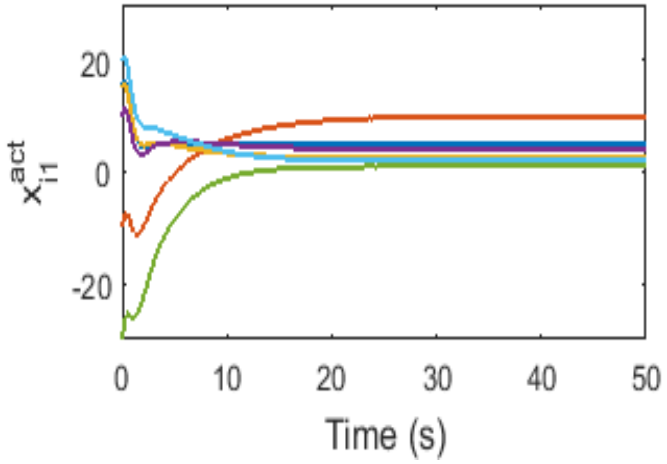

Figure 5.6: Unmatched scenario: The first actual state variables x_{i1}^{act} of all agents with distributed decoupling controller.

theoretic ideas and the availability of relative-measurements. We acknowledge that the symmetric linear time-invariant large-scale model is taken from [143], and the discussion on control of large-scale systems can be inspired by any standard references such as [2]-[3]. In our opinion, [144] provides a good example of

"practical" centralized control approaches that have been reported in the literature. The notion of decentralized fixed mode was introduced in [145]. Thereafter, many research studies have been done to find decentralized fixed modes, and to control a large-scale system with decentralized fixed modes (e.g., see the structurally constrained control approach in [146]). By further walking through the literature of large-scale systems, we mention that the models that we introduce in this chapter are sometimes called "large-scale systems with strong interconnections" (e.g., see [147] with a single-input single-output model of subsystems in a large-scale system).

Regarding the topic of this chapter, we further clarify that the word "decoupling" in the distributed decoupling problems emphasizes on the fact that the control protocol is using relative measurements to damp the (adverse) effects of physical couplings while the residual (local) dynamics of agents are stabilized using some local measurements in a hierarchical manner.

In Section 5.2, we generalize the model of Section 3.2 to a heterogeneously (operating point) parameter-dependent physically coupled uncertain multiagent system, and propose both state and output feedback distributed decoupling problems. The distributed stabilization problem is addressed via a leaderless consensus (re-) formulation. We use the well-known parametric robust control ideas of the reference [148] to deal with the unknown operating point parameters of agents. Importantly, we mention that the structural (simplification) assumptions on the state-feedback model of Subsection 5.2.2.1 are made based on the results of [77] which was limited to the constant homogeneous state space matrices. Specifically, using our notation, that reference was assuming a state coupling matrix

$F_{avg} = B_{avg}K_c$ with K_c denoting the consensus gain (our research work proposes a more realistic scenario because G_{avg} can be different from the control gain K_c). This structural assumption is relaxed in the output feedback decoupling of Subsection 5.2.2.2. Moreover, in the output feedback case, our formulation allows using the separation principle Lemma 2.3.2 in the presence of modeling uncertainties. Although we do not focus on any special applications, these distributed decoupling ideas can be used to damp the inter-area oscillation in a multi-machine power system.

In Section 5.3, we propose Lur'e models of multiagent systems with unknown physically coupled nonlinear terms. We assume that the nonlinearities are separable. This is in fact a common assumption in the literature and, specifically, we borrow it from [149] (it can also be referred to the materials of [106]). In this section, we propose a leader-follower viewpoint to address the distributed stabilization problem under two different scenarios: the matched and unmatched nonlinear interconnections. We design two linear time-invariant static distributed decoupling algorithms in order to cancel the adverse effects of these unknown nonlinear interconnections on physically coupled agents. Based on the simulation verification results, a decoupling system enables agents to operate at their desired operating-points using their own local control systems, and independent of their neighbors.

Finally, we mention that the proposed distributed decoupling challenges include many of the distributed consensus problems as special cases (see the literature survey in Section 1.2 to find about the existing results on the distributed consensus of multiagent systems). For example, regarding the results of Sec-

tion 5.3, we could simply assume a leader with no control input and no modeling uncertainties $\dot{x}_0 = Ax_0$ (as is usually the case in the literature), and propose a leader-follower consensus problem for a set of physically coupled Lur'e nonlinear followers. However, we assume that the leader is a new physical agent such that u_0 and ϕ_0 (or ψ_0) appear in (5.49) (or (5.50)). The case where the leader has a bounded control input, without any modeling uncertainties and physical interconnections, has been addressed in the literature via adaptive control techniques (e.g., see [94] for a set of linear time-invariant agents) whereas our solutions provide fixed-gain LQR-based distributed consensus algorithms.

5.5 Appendix: proofs

We have proposed the main results of this chapter through several theorems. For the sake of readability, we have not discussed their proofs within the main body of this chapter, and, instead, have collected all of them in this Appendix section.

5.5.1 Proof of Theorem 5.2.1 (page 174)

We prove this theorem in 3 steps: *1)* K_c ensures a state-agreement, *2)* the agreement is on zero, and *3)* the distributed decoupling problem of uncertain interconnected multiagent system is solved whenever $\sigma_c < \frac{\beta_c}{\alpha_c}$ is satisfied by a closed-loop multiagent system with a static decoupling feedback gain K_c.

Step 1) We aggregate the control signals ν_{Ti}, cost functions (5.20), and dynamics (5.21) for $i \in \{2, 3, ..., N\}$ and find that ν_{Td} achieves the minimum of following aggregated cost function:

$$J(x_{Td}(0)) = \min_{\nu_{Td}} \int_0^\infty (x_{Td}^T \bar{Q}_s x_{Td} + \nu_{Td}^T \bar{R} \nu_{Td}) dt$$

subject to the network-level shifted nominal dynamics in (5.18) where $\bar{Q}_s = I_{N-1} \otimes Q_s$ and $\bar{R} = (I_{N-1} \otimes R)$.

By optimality of $\nu_{Td} = \nu_{Td}^\star$ and thus $x_{Td} = x_{Td}^\star$, we have the following results satisfied for the aggregated closed-loop system:

$$\begin{aligned} x_{Td}^T \bar{Q}_s x_{Td} + \nu_{Td}^T \bar{R} \nu_{Td} + J_{x_{Td}}^T (\bar{A}_\gamma x_{Td} + \bar{B}_{avg} \nu_{Td}) = 0 \\ 2\nu_{Td}^T \bar{R} + J_{x_{Td}}^T \bar{B}_{avg} = \mathbf{0} \end{aligned} \tag{5.80}$$

where $J_{x_{Td}}(x_{Td}) = \frac{\partial J(x_{Td})}{\partial x_{Td}}$. Although the optimal control gain K_c is designed subject to the shifted "nominal" dynamics in (5.18), in the rest of this step, we prove that ν_{Td} stabilizes the entire uncertain non-shifted multiagent system (5.17). We introduce a candidate Lyapunov function:

$$V(x_{Td}(t)) = x_{Td}^T(t) \bar{P}_s x_{Td}(t) \succ 0$$

where $\bar{P}_s = I_{N-1} \otimes P_s$, and P_s is the solution of ARE (5.19). Also, we find that the following is satisfied:

$$V(x_{Td}(0)) = J(x_{Td}(0)) = \min_{\nu_{Td}} \int_t^\infty (x_{Td}^T \bar{Q} x_{Td} + \nu_{Td}^T \bar{R} \nu_{Td} + x_{Td}^T \bar{R}_x x_{Td}) dt' \succ 0$$

where $\bar{Q} = I_{N-1} \otimes Q$ and $\bar{R}_x = I_{N-1} \otimes R_x$. Since the control gain $K_c = -\lambda_2 R^{-1} B_{avg}^T P_s$ is implemented and algebraic Riccati equation (5.19) is satisfied, we know that the conditions (5.80) are satisfied by this candidate Lyapunov function substituting $J_{x_{Td}}$ by $V_{x_{Td}}$. Now, along the uncertain dynamics of the shifted multiagent system (5.18), we find:

$$\begin{aligned}\dot{V}(x_{Td}) &= V_{x_{Td}}^T \dot{x}_{Td} = V_{x_{Td}}^T (\bar{A}_{avg} x_{Td} + \bar{B}_{avg} \nu_{Td} + \bar{B}_{avg}(\bar{E}\nu_{Td} + \bar{G}_{avg} x_{Td})) \\ &= -x_{Td}^T \bar{Q} x_{Td} - 2\nu_{Td}^T \bar{R}\bar{E}\nu_{Td} - (\nu_{Td} + \bar{G}_{avg} x_{Td})^T \bar{R}(\nu_{Td} + \bar{G}_{avg} x_{Td}) \\ &\quad - (x_{Td}^T \bar{R}_x x_{Td} - x_{Td}^T \bar{G}_{avg}^T \bar{R} \bar{G}_{avg} x_{Td}) \leq -x_{Td}^T \bar{Q} x_{Td} \prec 0\end{aligned}$$

Based on the Lyapunov Theorem 2.3.1, the shifted linear disagreement dynamics (5.18) are asymptotically stable. Also, based on the Rayleigh-Ritz inequality 2.1.1, we find $\lambda_{min}(P_s)\|x_{Td}\|^2 \leq V(x_{Td}) \leq \lambda_{max}(P_s)\|x_{Td}\|^2$ and $\dot{V} \leq -\lambda_{min}(Q)\|x_{Td}\|^2$. Thus, based on the exponential stability Theorem 2.3.2, we conclude that the origin is exponentially stable.

Now, we know that all eigenvalues of $(\bar{A}_\gamma + (\Lambda_d \otimes B_{avg}(K_c + G_{avg})))$ are in the open left half plane (LHP). Consequently, the solutions of $det(sI_{(N-1)n_x} - \bar{A}_\gamma - (\Lambda_d \otimes B_{avg}(K_c + G_{avg})) = 0$ satisfy $\Re\{s\} < 0$ for $s \in \mathbb{C}$. Thus, we further conclude that the solutions of $det(s' I_{(N-1)n_x} - \bar{A}_{avg} - (\Lambda_d \otimes B_{avg}(K_c + G_{avg})) = 0$ satisfy $\Re\{s'\} < -\gamma$ where $s' \triangleq s - \gamma$. In other words, in addition to exponential stability of the disagreement dynamics, the LQR-gain K_c ensures a (desired) level of consensus rate for the non-shifted disagreement dynamics (5.17).

Step 2) Based on the partitioned model (5.16) of multiagent system, agreement dynamics are decoupled from disagreement dynamics. Then, based on Assump-

tion 5.2.3.a and Step 1 of this proof, we conclude $\lim_{t\to\infty} x(t) = \lim_{t\to\infty} x_T(t) = \mathbf{0}$ which proves the state-agreement on zero (for a model of multiagent system excluding the uncertainty $\tilde{A}_\Delta(t)x(t)$ in (5.13)).

Step 3) The solution of differential equation (5.13) is given by:

$$x(t) = e^{\tilde{A}_c t}x(0) + \int_0^t (e^{\tilde{A}_c(t-s)}\tilde{A}_\Delta(s)x(s)ds$$

Hence, whenever $\|e^{\tilde{A}_c t}\| \leq \alpha_c e^{-\beta_c t}$, we can rewrite this state response as follows:

$$\|x(t)\| \leq \alpha_c e^{-\beta_c t}\|x(0)\| + \int_0^t (\alpha_c \sigma_c e^{-\beta_c(t-s)}\|x(s)\|)ds$$

where we have used $\|\tilde{A}_\Delta x(t)\| \leq \sigma_c\|x(t)\|$. Now, based on the Bellman-Gronwall Lemma 2.3.3, we find:

$$\|x(t)\| \leq \alpha_c e^{-(\beta_c - \sigma_c\alpha_c)t}\|x(0)\|$$

which indicates that $x(t) \in \mathbb{R}^{Nn_x}$ exponentially converges to zero whenever $\sigma_c < \frac{\beta_c}{\alpha_c}$ is satisfied. Thus, the distributed decoupling problem 5.2.1 is also solved in this condition.

5.5.2 Proof of Theorem 5.2.2 (page 179)

By augmenting ν_{Ti}, τ_i, and also (5.36)-(5.37) for all $i \in \{2, 3, , ..., N\}$; we know that ν_{Td} and τ achieves the minimum aggregated cost function value:

$$J(x_{Td}(0)) = \min_{\nu_T, \tau} \int_0^\infty (x_{Td}^T \bar{Q}_c x_{Td} + \nu_{Td}^T \bar{R}_c \nu_{Td} + \tau^T \bar{W}_c \tau)dt$$

subject to (5.34), where $\bar{Q}_c = I_{N-1} \otimes Q_c$ and $\bar{R}_c = I_{N-1} \otimes R_c$. The aggregated version of (5.38) is also found as follows:

$$\bar{Q} + \bar{K}_c^T \bar{R}_c \bar{K}_c - 2\bar{H}_c^T \bar{W}_c \bar{H}_c \succ \mathbf{0} \tag{5.81}$$

where $\bar{K}_c = I_{N-1} \otimes K_c$ and $\bar{H}_c = I_{N-1} \otimes H_c$.

Similar to Step 1 in Theorem 5.2.1, we know the triple (x_{Td}, ν_{Td}, τ) satisfies:

$$\begin{aligned} x_{Td}^T \bar{Q}_c x_{Td} + \nu_{Td}^T \bar{R}_c \nu_{Td} + \tau^T \bar{W}_c \tau + J_{x_{Td}}^T (\bar{A}_{\gamma_c} x_{Td} + \bar{B}_{avg} \nu_{Td} + \bar{F}_\tau \tau) = 0 \\ 2\nu_{Td}^T \bar{R}_c + J_{x_{Td}}^T \bar{B}_{avg} = \mathbf{0} \\ 2\tau^T \bar{W}_c + J_{x_{Td}}^T \bar{F}_\tau = \mathbf{0} \end{aligned} \tag{5.82}$$

In the rest of this proof, we show that the uncertain non-shifted multiagent system dynamics (5.32) are also stabilized using only the control signal ν_{Td} (i.e., without implementing τ). We propose a candidate Lyapunov function:

$$V(x_{Td}(t)) = x_{Td}^T(t) \bar{P}_c x_{Td}(t) \succ 0$$

where $\bar{P}_c = I_{N-1} \otimes P_c$, and P_c is the solution of ARE (5.35). This candidate Lyapunov function satisfies:

$$V(x_{Td}(0)) = \min_{\nu_{Td}, \tau} \int_t^\infty (x_{Td}^T \bar{Q} x_{Td} + \nu_{Td}^T \bar{R}_c \nu_{Td} + \tau^T \bar{W}_c \tau + x_{Td}^T (\lambda_N^2 \bar{W}_c) x_{Td}) dt' \succ 0$$

Since the ARE (5.35) is satisfied by implementing the optimal control (and fictitious control) gains of this theorem, the conditions (5.82) are hold true by this

candidate Lyapunov function substituting $J_{x_{Td}}$ by $V_{x_{Td}}$. Now, along the uncertain shifted multiagent system's dynamics (5.33), we find:

$$\begin{aligned}
\dot{V} &= V_{x_{Td}}^T \dot{x}_{Td} \leq -x_{Td}^T(\bar{Q} + \bar{K}_c^T \bar{R}_c \bar{K}_c - 2\bar{H}_c^T \bar{W}_c \bar{H}_c) x_{Td} \\
&= -x_{Td}^T \bar{Q} x_{Td} - \nu_{Td}^T \bar{R}_c \nu_{Td} - 2\nu_{Td}^T \bar{R}_c \bar{E} \nu_{Td} + 2\tau^T \bar{W}_c \tau - \tau^T \bar{W}_c \tau - 2\tau^T \bar{W}_c \bar{\Lambda}_d x_{Td} \\
&\quad - x_{Td}^T \bar{\Lambda}_d \bar{W}_c \bar{\Lambda}_d x_{Td} - (x_{Td}^T (\lambda_N^2 \bar{W}_c) x_{Td} - x_{Td}^T \bar{\Lambda}_d \bar{W}_c \bar{\Lambda}_d x_{Td}) \\
&\leq -x_{Td}^T(\bar{Q} + \bar{K}_c^T \bar{R}_c \bar{K}_c - 2\bar{H}_c^T \bar{W}_c \bar{H}_c) x_{Td}
\end{aligned}$$

which indicates $\dot{V} \prec 0$ whenever (5.81) is satisfied. Thus, based on the Lyapunov stability Theorem 2.3.1, the shifted uncertain disagreement dynamics (5.33) are asymptotically stable. Moreover, setting $a_1 \leftarrow \lambda_{min}(P_c)$, $a_2 \leftarrow \lambda_{max}(P_c)$, $a_3 \leftarrow \lambda_{min}(Q + K_c^T R_c K_c - 2H_c^T W_c H_c)$, and $b \leftarrow 2$ in Theorem 2.3.2, we are able to guarantee exponential stability of the system which is a stronger result than asymptotic stability.

Similar to Step 1 of Theorem 5.2.1, we further conclude that the design parameter γ_c ensures a minimum level of consensus convergence rate for the non-shifted uncertain multiagent system's dynamics (5.32).

5.5.3 Proof of Theorem 5.2.3 (page 180)

A dual form to the observer design problem (5.39) is designing a control signal $\omega_{Ti} = K_o^T x_{Ti}$ for

$$\dot{x}_{Ti} = (A_{\gamma_o} + \lambda_i F_{avg})^T x_{Ti} + \lambda_i C^T \omega_{Ti}$$

which can be rewritten as follows:

$$\dot{x}_{Ti} = A_{\gamma_o}^T x_{Ti} + \lambda_2 C^T \omega_{Ti} + \lambda_2 C^T (\frac{\lambda_i}{\lambda_2} - 1)\omega_{Ti} + \lambda_i F_{avg}^T x_{Ti}$$

that, for $i \in \{2, 3, ..., N\}$, results in the following aggregated dynamics:

$$\dot{x}_{Td} = (I_N \otimes A_{\gamma_o}^T)x_{Td} + (I_N \otimes \lambda_2 C^T)\omega_{Td} + (I_N \otimes \lambda_2 C^T)((\tfrac{\Lambda_d}{\lambda_2} - I_{N-1}) \otimes I_{n_y})\omega_{Td} + (I_N \otimes F_{avg}^T)(\Lambda_d \otimes I_{n_x})x_{Td}$$

where $\omega_{Td} = col\{\omega_{Ti}\}$ for $i \in \{2, 3, ..., N\}$. We further propose an auxiliary shifted multiagent system:

$$\dot{x}_{Td} = (I_{N-1} \otimes A_{\gamma_o}^T)x_{Td} + (I_{N-1} \otimes \lambda_2 C^T)\omega_{Td} + (I_{N-1} \otimes F_{avg})\eta$$

where $\eta = col\{\eta_i\}$ for $i \in \{2, 3, ..., N\}$ denotes a fictitious control signal corresponding to the uncertainty $(\Lambda_d \otimes I_{n_x})x_{Td}$. Now, the rest follows the proof of Theorem 5.2.2 (see Subsection 5.5.2).

5.5.4 Proof of Theorem 5.3.1 (page 190)

Using (5.58) and (5.62) for $i \in \{1, 2, ..., N\}$, we find an aggregated cost function:

$$J(\xi(0)) = \min_{\tau} \int_0^\infty (\xi^T \tilde{Q} \xi + \tau^T \tilde{R} \tau + \eta_M^T \tilde{R} \eta_M) dt$$

where $\tilde{Q} = diag\{[Q_l, \bar{Q}_f]\}$ and $\bar{Q}_f = I_N \otimes Q_f$. Using (5.59) and (5.63) for $i \in \{1, 2, ..., N\}$, we find the networked nominal dynamics in (5.55). Hence, the control signals $u_0 = K_0 x_0$ and $\nu = \bar{K}\epsilon$ achieves the minimum aggregated leader-follower cost function $J(\xi(0))$ subject to the networked nominal dynamics

in (5.55). We need to show that the static feedback $\tau = \tilde{K}\xi$ stabilizes the uncertain dynamics (5.55). We propose the following Lyapunov candidate function:

$$V(\xi(t)) = \xi^T(t)\tilde{P}_1\xi(t) \succ 0$$

where $\tilde{P}_1 = diag\{P_{1l}, \bar{P}_{1f}\}$, $\bar{P}_{1f} = I_N \otimes P_{1f}$, and P_{1l} and P_{1f} are the positive definite solutions of algebraic Riccati equations (5.61) and (5.64), respectively.

$$V(\xi(0)) = J(\xi(0)) = \min_{\tau} \int_0^{\infty} (\xi^T\tilde{Q}\xi + \tau^T\tilde{R}\tau + \eta_M^T\tilde{R}\eta_M)dt' \succ 0$$

We also have the following Hamilton-Jacobi-Bellman equation:

$$\min_{\tau}\{\xi^T\tilde{Q}\xi + \tau^T\tilde{R}\tau + \eta_M^T\tilde{R}\eta_M + V_\xi^T(\tilde{A}\xi + \tilde{B}_u\tau)\} = 0$$

In fact, implementing the gains K_0 and K of this theorem, the pair (ξ, τ) satisfies the following equalities:

$$\begin{aligned} \xi^T\tilde{Q}\xi + \tau^T\tilde{R}\tau + \eta_M^T\tilde{R}\eta_M + V_\xi^T(\tilde{A}\xi + \tilde{B}_u\tau) &= 0 \\ 2\tau^T(\tilde{R} + \tilde{R}^\tau) + V_\xi^T\tilde{B}_u &= \mathbf{0} \end{aligned}$$

where $\tilde{R}^\tau = diag\{[R^{u_0}, \mathbf{0}]\}$. Now, we are ready to calculate the time deviation of $V(\xi(t))$ along the uncertain dynamics (5.55):

$$\begin{aligned} \dot{V} &= V_\xi^T\dot{\xi} = -\xi^T\tilde{Q}\xi - \tau^T\tilde{R}\tau - \eta_M^T\tilde{R}\eta_M - 2\tau^T(\tilde{R} + \tilde{R}^\tau)\tilde{E}\tau - 2\tau^T(\tilde{R} + \tilde{R}^\tau)\eta \\ &\leq -\xi^T\tilde{Q}\xi + x_0^TR^{u_0x_0}x_0 + u_0^TR^{u_0}u_0 - (\eta_M^T(\tilde{R} + \tilde{R}^\tau)\eta_M - \eta^T(\tilde{R} + \tilde{R}^\tau)\eta) \\ &\quad - (\eta + \tau)^T(\tilde{R} + \tilde{R}^\tau)(\eta + \tau) \\ &\leq -x_0^TQ_lx_0 - \epsilon^T\bar{Q}_f\epsilon + x_0^TR^{u_0x_0}x_0 + u_0^TR^{u_0}u_0 \\ &\leq -x_0^T(Q_l - R^{u_0x_0} - K_0^TR^{u_0}K_0)x_0 - \epsilon^T\bar{Q}_f\epsilon \prec 0 \end{aligned}$$

where the first inequality is found based on the completion of squares by adding and subtracting $x_0^T R^{u_0 x_0} x_0 + u_0^T R^{u_0} u_0 + \eta^T(\tilde{R} + \tilde{R}^\tau)\eta$. We further mention that $\bar{E} = \bar{E}^T \succcurlyeq \mathbf{0}$ such that $-2\tau^T(\tilde{R} + \tilde{R}^\tau)\tilde{E}\tau = -2r_f \nu^T \bar{E}\nu \leq 0$ and $\eta^T(\tilde{R} + \tilde{R}^\tau)\eta \leq \eta_M^T \tilde{R}\eta_M + x_0^T R^{u_0 x_0} x_0 =: \eta_M^T(\tilde{R} + \tilde{R}^\tau)\eta_M$.

Based on the Lyapunov theorem 2.3.1, the leader-follower multiagent system's dynamics (5.55) are asymptotically stable for all initial state values and over the fixed-graph $\mathcal{G}_{lf}$. We further show that the conditions of Theorem 2.3.2 are satisfied by $b \leftarrow 2$, $a_1 = \min\{\lambda_{min}(P_{1l}), \lambda_{min}(P_{1f})\}$, $a_2 = \min\{\lambda_{max}(P_{1l}), \lambda_{max}(P_{1f})\}$, and $a_3 = \min\{\lambda_{min}(Q_f), \lambda_{min}(Q_l - R^{u_0 x_0} - K_0^T R^{u_0} K_0)\}$. Thus, using a static feedback gain, we are able to guarantee exponential stability of the origin for an uncertain Lur'e nonlinear multiagent system. Now, based on the reformulation in Subsection 5.3.1.3, the distributed decoupling of agents is also achieved.

5.5.5 Proof of Theorem 5.3.2 (page 192)

We find (5.67) using (5.71) and (5.76). Also, based on (5.70) and (5.75), we find an aggregated leader-follower cost function:

$$J(\zeta(0)) = \min_{\sigma,\theta,\beta} \int_0^\infty \{\zeta^T \tilde{Q}\zeta + \sigma^T \tilde{R}\sigma + \theta^T \bar{S}\theta + \beta^T \tilde{W}\beta + \underline{u}_0^T \bar{S}\underline{u}_0 + \Psi_{tM}^T \tilde{W}\Psi_{tM}\}dt$$

The optimal control signals σ, θ, and β achieves the minimum $J(\zeta(0))$ subject to (5.67). We need to show that the uncertain closed-loop system (5.66) will be stabilized using σ (i.e., there is no need for θ and β for the implementation purpose). We propose the following Lyapunov candidate function for $t \geq 0$:

$$V(\zeta(t)) = \zeta^T(t)\tilde{P}_2\zeta(t) \succ 0$$

where $\tilde{P}_2 = diag\{P_{2l}, \bar{P}_{2f}\}$, $\bar{P}_{2f} = I_N \otimes P_{2f}$, and P_{2l} and P_{2f} are respectively the positive definite solutions of AREs in (5.74) and (5.79). Also, we observe that the equality $V(\zeta(0)) = J(\zeta(0)) = \min_{\sigma,\theta,\beta} \int_0^\infty \{\zeta^T\tilde{Q}\zeta + \sigma^T\tilde{R}\sigma + \theta^T\bar{S}\theta + \beta^T\tilde{W}\beta + \underline{u}_0^T\bar{S}\underline{u}_0 + \Psi_{tM}^T\tilde{W}\Psi_{tM}\}dt' \succ 0$ is satisfied subject to the augmented auxiliary system (5.67) for which the Hamilton-Jacobi-Bellman equation $\min_{\sigma,\theta,\beta}\{\zeta^T\tilde{Q}\zeta + \sigma^T\tilde{R}\sigma + \theta\bar{S}\theta + \underline{u}_0^T\bar{S}\underline{u}_0 + \beta^T\bar{W}\beta + \Psi_{tM}^T\tilde{W}\Psi_{tM} + V_\zeta^T(\tilde{A}\zeta + \tilde{B}_u\sigma + \tilde{B}_{u_0}\theta + \tilde{B}_\psi\beta)\} = 0$ holds.

We further know that implementing the control and fictitious control gains G_0, L_0, G, L, and H of this theorem, the quadruple $(\xi, \sigma, \theta, \beta)$ satisfies $\zeta^T\tilde{Q}\zeta + \sigma^T\tilde{R}\sigma + \theta^T\bar{S}\theta + \beta^T\tilde{W}\beta + \underline{u}_0^T\bar{S}\underline{u}_0^T + \Psi_{tM}^T\tilde{W}\Psi_{tM} + V_\zeta^T(\tilde{A}\zeta + \tilde{B}_u\sigma + \tilde{B}_{u_0}\theta + \tilde{B}_\psi\beta) = 0$ and

$$\begin{aligned} 2\sigma^T(\tilde{R} + \tilde{R}^\sigma) + V_\zeta^T\tilde{B}_u &= \mathbf{0} \\ 2\theta^T\bar{S} + V_\zeta^T\tilde{B}_{u_0} &= \mathbf{0} \\ 2\beta^T\tilde{W} + V_\zeta^T\tilde{B}_\psi &= \mathbf{0} \end{aligned}$$

where $\tilde{R}^\sigma = diag\{[NS, \mathbf{0}]\}$. Using these equalities, we calculate $\dot{V}$ along the uncertain trajectory (5.66):

$$\begin{aligned} \dot{V}(\zeta) &\leq -\zeta^T\tilde{Q}\zeta - \sigma^T\tilde{R}\sigma + 2\beta^T\tilde{W}\beta + 2\theta^T\bar{S}\theta \\ &\leq -\zeta^T(\tilde{Q} + \tilde{G}^T\tilde{R}\tilde{G} - 2\tilde{L}^T\tilde{W}\tilde{L} - 2\tilde{H}^T\tilde{S}\tilde{H})\zeta \end{aligned}$$

Alternatively, we can find:

$$\dot{V}(\zeta) \leq -\zeta^T\tilde{Q}\zeta + 2\beta^T\tilde{W}\beta + 2\theta^T\bar{S}\theta \leq -\zeta^T(\tilde{Q} - 2\tilde{L}^T\tilde{W}\tilde{L} - 2\tilde{H}^T\tilde{S}\tilde{H})\zeta$$

where $\tilde{L} = diag\{L_0, I_N \otimes L\}$, $\tilde{H} = diag\{\mathbf{0}, I_N \otimes H\}$, and $\tilde{S} = diag\{\mathbf{0}, I_N \otimes S\}$.

Based on the conditions (5.72)-(5.73) and (5.77)-(5.78), we find $\dot{V} \prec 0$. Hence, using the Lyapunov Theorem 2.3.1, the closed-loop multiagent system (5.66) is asymptotically stable. Furthermore, it is straightforward to see that the conditions of Theorem 2.3.2 are also satisfied by $a_3 = \min\{\lambda_{min}(\tilde{Q}+\tilde{G}^T\tilde{R}\tilde{G}-2\tilde{L}^T\tilde{W}\tilde{L}-2\tilde{H}^T\tilde{S}\tilde{H}), \lambda_{min}(\tilde{Q}-2\tilde{L}^T\tilde{W}\tilde{L}-2\tilde{H}^T\tilde{S}\tilde{H})\}$. Thus, the origin is exponentially stable which, equivalently, indicates exponential distributed decoupling of an interconnected Lur'e multiagent system (with nonlinear modeling uncertainty).

Chapter 6

Distributed Stabilization of Physically Coupled Multiagent Systems with Unknown Coupling Structures[1]

Based on the introduction in Chapter 1, we know that graph-theoretic distributed control algorithms have been widely designed to accomplish cooperative tasks using a group of individual agents. We further are aware of some references that, following the same viewpoint on achieving agreement on unknown values, consider multiagent systems with interconnected agents via linear state-coupling terms (over known coupling graph). Also, based on the results of Chapter 3, we know that the agreement on zero (independent of agents' initial values) may

[1]A major part of this chapter has been published in [140] and [150]. Each section has its own parameters and variables which are (re-) defined appropriately.

need sanctification of additional conditions in an agreed multiagent system (after reaching agreement in multiagent system).

In Chapter 5, we interpreted achieving "agreement on zero independent of agents' initial conditions" as a "distributed stabilization" problem. Then, inspired by the literature of both large-scale and multiagent systems, we introduced some models of "physically interconnected multiagent systems" using graph-theoretic ideas which were equivalent to the large-scale systems' models. In each scenario, we assumed a known (connected) physical coupling structure, and designed a distributed control algorithm over the same graph topology. Assuming a known coupling structure and designing a distributed controller with exactly the same communication topology as the coupling structure could restrict the applicability of ideas in Chapter 5.

In this chapter, we assume agents are physically coupled over *unknown "agent-layer coupling graphs"*, and design distributed protocols over a second graph layer to share agents' information in their neighborhood. We name it *control-layer communication graph*. In Section 6.1, we mix the models of Section 5.3 and propose a fixed-gain fully distributed decoupling strategy for a Lur'e multiagent system with mixed matched and unmatched time-varying interconnected nonlinearities. While the decoupling allows agents to operate in their stand-alone modes, availability of all agents' absolute measurements could bea restrictive assumption in ensuring the stability of interconnected multiagent system. Therefore, in Section 6.2, we propose a distributed stabilization problem where we only a few agents provide their absolute measurements to the control-layer operator (potentially, only one agent shares its absolute information).

The rest of this Chapter is organized as follows. In Section 6.1 we propose a multi-layer distributed decoupling structure. This is essentially an extension to the results of 5.3 by proposing a Lur'e multiagent system with mixed matched and unmatched state-coupled time-varying nonlinear uncertainties over an unknown coupling graph. In this section, we further introduce a fixed-gain fully-distributed decoupling approach which can be designed without any global knowledge about coupling and communication graphs. In Section 6.2, we assume a limited access to the absolute state information for a set of only few agents, and propose a multi-layer distributed stabilization problem. In fact, this is based on our two-layer viewpoint in Section 6.1 where the agent-layer coupling graph is further modeled by two subgraphs for state and input coupling terms. In Section 6.3, we discuss the fully distributed alternatives to the decoupling algorithms of Chapter 4. We summarize this chapter and provide some references in Section 6.4. Finally, We collect all proofs in Section 6.5.

6.1 Distributed decoupling of multiagent systems with mixed matched and unmatched nonlinear state couplings

In this section, we propose a class of Lur'e nonlinear multiagent systems with homogeneous linear nominal dynamics subject to heterogeneous state-dependent time-varying nonlinear couplings. Compared to the results of Section 5.3, from the modeling aspect, we assume that these nonlinearities appear as mixed matched

and unmatched modeling uncertainties, and the coupling graph is unknown and possibly disconnected (i.e., with a less restrictive structural assumption compared to Chapter 4); and from the control aspect, we propose a multi-layer structure.

This new viewpoint enables us to overcome the lack of knowledge about the physical coupling graph and, mainly, provides an additional degree of freedom to design a control-layer graph in order to guarantee some further (optimization-based) criteria for a closed-loop physically coupled multiagent system. Since our fully distributed decoupling algorithm allows post-designing the control-layer network at a later time, we do not go through the communication graph design problem.

We consider a group of $N+1$ linear time-invariant agents which are coupled to each other over a graph $\mathcal{G}_a$ through some heterogeneous time-varying nonlinear uncertainty functions which, all together, build a heterogeneous Lur'e time-varying nonlinear multiagent system:

$$\dot{x}_i = A'x_i + B_m u_i' + \underbrace{B_m f_i(z_i;t) + B_u g_i(y_i;t)}_{\phi_i(z_i,y_i;t)} \tag{6.1}$$

where $i \in \{0,1,2,...,N\}$ denotes the agent number; $x_i \in \mathbb{R}^{n_x}$ represents the state variable and $u_i \in \mathbb{R}^{n_z}$ indicates the control input; and $A' \in \mathbb{R}^{n_x \times n_x}$, $B_m \in \mathbb{R}^{n_x \times n_z}$, and $B_u \in \mathbb{R}^{n_x \times n_y}$ are some known constant matrices. The nonlinear functions $\phi_i(z_i, y_i; t)$ are written as sum of two unknown nonlinearities. The terms $B_m f_i(z_i;t)$ are in the range space of B_m and we call $f_i(z_i;t) \in \mathbb{R}^{n_z}$ the *matched* nonlinearities, and the terms $B_u g_i(y_i;t) \in \mathbb{R}^{n_y}$ do not satisfy this condition and we name $g_i(y_i;t)$ the *unmatched* nonlinearities. The input vectors $z_i \in \mathbb{R}^{n_z}$ and

$y_i \in \mathbb{R}^{n_y}$ into these nonlinear functions are the following lumped state-dependent signals:

$$\begin{aligned} z_i &= C_z \sum_{j \in \mathcal{N}_i^a} (x_i - x_j) \\ y_i &= C_y \sum_{j \in \mathcal{N}_i^a} (x_i - x_j) \end{aligned} \tag{6.2}$$

where $C_z \in \mathbb{R}^{n_z \times n_x}$ and $C_y \in \mathbb{R}^{n_y \times n_x}$, and $\mathcal{N}_i^a$ denotes the i^{th} agent's neighboring set over $\mathcal{G}_a$. The following assumptions are satisfied in this section. In theses assumptions, $\mathbb{R}^+$ denotes the set of positive real numbers, and $\mathbb{R}^{0+}$ represents the set of non-negative real numbers.

Assumption 6.1.1. *The pair (A', B_m) represents a stabilizable state space realization $\dot{x}_i = A'x + B_m u_i'$.*

Assumption 6.1.2. *The nonlinear functions $f_i : \mathbb{R}^{n_z} \times \mathbb{R}^{0+} \to \mathbb{R}^{n_z}$ $\forall$ $i \in \{0, 1, ..., N\}$ are not exactly known, but satisfy the quadratic upper-bound:*

$$f_i^T(z_i; t) R f_i(z_i; t) \leq z_i^T (\alpha_i R) z_i$$

where $R = R^T \succ \boldsymbol{0}$ for $R \in \mathbb{R}^{n_z \times n_z}$, and $\alpha_i \in \mathbb{R}^+$. Moreover, $f_i(\boldsymbol{0}; t) = \boldsymbol{0}$, and $\alpha \triangleq \max_i\{\alpha_i\}$ $\forall i \in \{1, 2, ..., N\}$ is a known constant.

Assumption 6.1.3. *The nonlinear functions $g_i : \mathbb{R}^{n_y} \times \mathbb{R}^{0+} \to \mathbb{R}^{n_y}$ $\forall$ $i \in \{0, 1, ..., N\}$ satisfy the Assumption 6.1.2 substituting R by $S \in \mathbb{R}^{n_y \times n_y}$, and α by $\beta \in \mathbb{R}^+$.*

Remark 6.1.1. *Since these findings are proved based on the Lyapunov Theorem 2.3.1, we also need the nonlinearities f_i and g_i be piecewise continuous in time and globally Lipschitz (if they are locally Lipschitz, the result will be valid in*

a neighborhood around the origin). However, we do not directly use the Lipschitz inequality (2.7) *in the derivations of this chapter.*

Regarding the (unknown) agent-layer coupling graph $\mathcal{G}_a$, we assume:

Assumption 6.1.4. *There exists at least one connected component over $\mathcal{G}_a$ (at least two agents are coupled to each other).*

We need to note that the disconnected graph $\mathcal{G}_a$ represents a decoupled multiagent system which is preferred (reduces to the existing results in Section 1.2). However, we propose Assumption 6.1.4 in order to have meaningful "decoupling" ideas. In this section, we introduce a multi-layer (two-layer) control structure:

- An undirected *agent-layer coupling graph* $\mathcal{G}_a$ with $\mathcal{L}_a = \mathcal{L}_a^T \succcurlyeq \mathbf{0}$ as its graph Laplacian matrix. We define a leader indexed by subscripts $_0$, and let others be some followers. We further define $\mathcal{G}_{af}$ as an undirected agent-layer coupling graph among N followers with $\mathcal{L}_{af} = \mathcal{L}_{af} \succcurlyeq \mathbf{0}$ as its graph Laplacian matrix. Furthermore, we let $b_a = [b_{a1}, b_{a2}, ..., b_{aN}]^T$ be such that $b_{ai} = 1$ whenever the leader and the i^{th} follower communicate over an undirected edge, and $b_{ai} = 0$ otherwise. We also define a diagonal matrix $\mathcal{B}_a = diag\{b_a\}$ in order to lump all leader-followers' physical coupling information. We partition the agent-layer Laplacian matrix as follows:

$$\mathcal{L}_a = \begin{bmatrix} \sum_{i=1}^{N} b_{ai} & -b_a^T \\ -b_a & \mathcal{H}_a \end{bmatrix}$$

  where $\mathcal{H}_a = \mathcal{H}_a^T \in \mathbb{R}^{N \times N}$ is defined by $\mathcal{H}_a = \mathcal{L}_{af} + \mathcal{B}_a$.

- A directed *control-layer communication graph* $\mathcal{G}_c$ with a graph Laplacian matrix $\mathcal{L}_c$. Similar to the agent-layer graph, we define $\mathcal{G}_{cf}$ and $\mathcal{L}_{cf} = \mathcal{L}_{cf} \succcurlyeq \mathbf{0}$ for the *undirected* control-layer communication graph *among N followers*. However, over $\mathcal{G}_c$, the leader agent does not receive information from followers. Thus, $b_c = [b_{c1}, b_{c2}, ..., b_{cN}]^T$ is defined such that $b_{ci} = 1$ when the i^{th} follower receives information from the leader *over a directed edge*, and $b_{ai} = 0$ otherwise. Also, we let $\mathcal{B}_c = diag\{b_c\}$ be a diagonal matrix that provides information about leader-to-follower communication. As a result, the following partitioning is valid for the control-layer Laplacian matrix:

$$\mathcal{L}_c = \begin{bmatrix} 0 & \mathbf{0} \\ -b_c & \mathcal{H}_c \end{bmatrix}$$

  where $\mathcal{H}_c = \mathcal{H}_c^T \in \mathbb{R}^{N \times N}$ is defined by $\mathcal{H}_c = \mathcal{L}_{cf} + \mathcal{B}_c$.

The control-layer communication graph satisfies the following assumption:

Assumption 6.1.5. *The control-layer communication graph $\mathcal{G}_c$ has a directed spanning tree with the node $i = 0$ as the root.*

As a result of Assumption 6.1.5, we know that $\mathcal{H}_c \succ \mathbf{0}$ such that $0 < \mu_{c1} \leq \mu_{c2} \leq ... \leq \mu_{cN}$ where μ_{cl} denote eigenvalues of $\mathcal{H}_c$ for $l \in \{1, 2, ..., N\}$.

We now clarify our multi-layer viewpoint in Figure 6.1 for a typical physically interconnected multiagent system. In this figure, the black rectangle represents the agent-layer multiagent system, and the blue rectangle shows the control-layer communication.

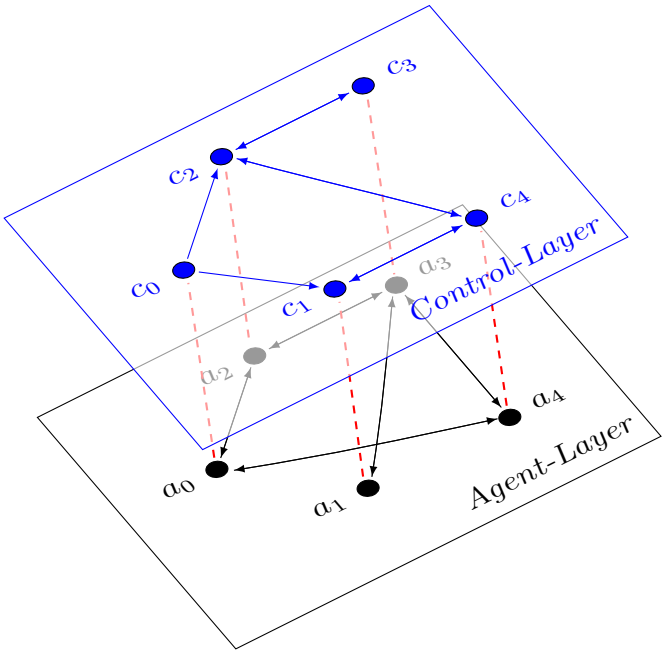

Figure 6.1: An example of the proposed structure where all agents and agent-layer physical coupling are shown in black; all decoupling control systems and control-layer communication are given in blue; letters a and c stand for agent and controller; and agent-controller correspondence are clarified by dashed red lines.

Similar to the results of Chapter 4, we consider a hierarchical control structure where a local controller stabilizes the i^{th} agent's local model, and a global decoupling controller cancels the adverse effects of the nonlinear modeling uncertainties ϕ_i in (6.1). We first write $u_i' = u_{il} + u_i$ where the local control signal u_{il} can be designed using any control techniques such that, for example by using the optimal LQR strategy, $u_{il} = K_l x_i$ results in a new model:

$$\dot{x}_i = Ax_i + B_m u_i + B_m f_i(z_i; t) + B_u g_i(y_i; t) \tag{6.3}$$

where $A = A' + B_m K_l \in \mathbb{R}^{n_x \times n_x}$ denotes a Hurwitz matrix (see Assumption 6.1.1). In the rest of this section, we only focus on designing the global control signal u_i

such that a multiagent of agents (6.3) asymptotically behaves as $N+1$ decoupled dynamical systems:

$$\dot{x}_i = Ax_i + B_m u_i \tag{6.4}$$

We are interested in distributed decoupling controllers (vs. centralized and decentralized control systems). Thus, we reformulate this decoupling task and propose a leader-follower consensus problem:

$$\lim_{t\to\infty} (x_i(t) - x_0(t)) = 0 \tag{6.5}$$

where the new control objective is finding the control signals u_0 and u_i that simultaneously stabilize the uncertain leader dynamics, i.e., $x_0 \to \mathbf{0}$ (leader is coupled to followers over $\mathcal{G}_a$), and derive all followers' states x_i to the leader state x_0, i.e., $x_i \to x_0$ as $t \to \infty$ (followers are coupled to each other and to the leader over $\mathcal{G}_a$). This objective should be achieved under any initial state conditions while the fixed graph $\mathcal{G}_c$ can be different from the fixed graph $\mathcal{G}_a$.

Remark 6.1.2. *While A denotes a Hurwitz matrix by itself (e.g., after using a local controller): (a) the Assumption 6.1.1 indicates a stabilizable pair (A, B_m) as well, and (b) the entire multiagent system of* (6.3) *can be unstable due to the state-dependent coupling terms.*

6.1.1 Distributed decoupling based on the smallest positive eigenvalue of the control-layer graph

In order to achieve the objective (6.5) in a multiagent system of (6.3), we propose the following control signals u_0 and u_i:

$$u_0 = K_0 x_0 \qquad u_i = K(\sum_{j \in \mathcal{N}_i^{cf}} (x_i - x_j) + b_i(x_i - x_0)) \tag{6.6}$$

where $K_0 \in \mathbb{R}^{n_z \times n_x}$ denotes the leader's control gain, $K \in \mathbb{R}^{n_z \times n_x}$ represents the followers' control gain, and $\mathcal{N}_i^{cf}$ indicates the neighboring set of i^{th} follower over $\mathcal{G}_{cf}$. We introduce the leader-follower tracking error $e_i \triangleq x_i - x_0$ and find the following error dynamics:

$$\dot{e}_i = Ae_i + B_m u_i + B_m F_i(u_0, z_0, z_i; t) + B_u G_i(y_0, y_i; t)$$

where for $i \in \{1, 2, ..., N\}$. Now, the followers' control signals can be rewritten as follows:

$$u_i = K(\sum_{j \in \mathcal{N}_i^{cf}} (e_i - e_j) + b_i e_i)$$

Here, we have defined:

$$F_i \ = f_i(z_i; t) - f_0(z_0; t) - u_0 \quad \textit{and} \quad G_i(y_0, y_i; t) = g_i(y_i; t) - g_0(y_0; t)$$

Furthermore, let $e = col\{e_i\}$ be the augmented leader-follower tracking error, $u = col\{u_i\}$ augmented control input, $F(u_0, \bar{z}; t) = col\{F_i\} = f(z; t) - (\mathbf{1}_N \otimes I_{n_z}) f_0(z_0; t) - (\mathbf{1}_N \otimes I_{n_z}) u_0$ the augmented matched uncertainty where $\bar{z} = [z_0^T, z^T]^T$ for $z = col\{z_i\}$, and $G(\bar{y}; t) = col\{G_i\} = g(y; t) - (\mathbf{1}_N \otimes I_{n_y}) g_0(y_0; t)$ the augmented unmatched uncertainty where $\bar{y} = [y_0^T, y^T]^T$ for $y = col\{y_i\}$. Thus, we find an augmented multiagent system with some physically coupled terms F and G over $\mathcal{G}_a$:

$$\dot{e} = (I_N \otimes A)e + (I_N \otimes B_m)u + (I_N \otimes B_m)F + (I_N \otimes B_u)G$$

We also decompose the control signal $u = (\mathcal{H}_c \otimes K)e$ as follows:

$$u = (\mathcal{H}_c \otimes I_{n_z})\nu, \quad and \quad \nu = (I_N \otimes K)e.$$

Now, we find a revised version of the augmented error dynamics:

$$\dot{e} = (I_N \otimes A)e + (\mathcal{H}_c \otimes B_m)\nu + (I_N \otimes B_m)F + (I_N \otimes B_u)G \tag{6.7}$$

where, in this new model, the coupling appears due to both $\mathcal{G}_a$ and $\mathcal{G}_c$. We rewrite these error dynamics as follows:

$$\dot{e} = \bar{A}e + \bar{B}_m\nu + \bar{B}_m\bar{E}\nu + \bar{B}_m F_\mu + \bar{B}_u G \tag{6.8}$$

where $\bar{A} = I_N \otimes A$, $\bar{B}_m = I_N \otimes \mu_{c1}B_m$, $\bar{B}_u = I_N \otimes B_u$, and $\bar{E} = \bar{E}^T = (\frac{1}{\mu_{c1}}\mathcal{H}_c - I_N) \otimes I_{n_z} \succcurlyeq \mathbf{0}$ is satisfied; and $F_\mu = \frac{1}{\mu_{c1}}F$.

Now, we introduce an augmented model that includes all leader and leader-follower tracking error dynamics:

$$\dot{\xi} = \tilde{A}\xi + \tilde{B}_m\tau + \tilde{B}_m\tilde{E}\tau + \tilde{B}_m F_t + \tilde{B}_u G_t \tag{6.9}$$

where $\xi = [x_0^T, e^T]^T$, $\tau = [u_0^T, \nu^T]^T$, $F_t = [f_0^T, F_\mu^T]^T$, and $G_t = [g_0^T, G^T]^T$; and $\tilde{A} = Diag_b\{[A, \bar{A}]\}$, $\tilde{B}_m = Diag_b\{[B_m, \bar{B}_m]\}$, $\tilde{E} = \tilde{E}^T = Diag_b\{[\mathbf{0}, \bar{E}]\} \succcurlyeq \mathbf{0}$, and $\tilde{B}_u = Diag_b\{[B_u, \bar{B}_u]\}$.

We mention that f_i and g_i are such that the origin is an equilibrium point of the unforced (6.9) setting $\tau = \mathbf{0}$. Moreover, along with the partitioning of $\mathcal{L}_a$ in this section, (6.2) can be rewritten as follows:

$$z_0 = -(b_a^T \otimes C_z)e \qquad z = (\mathcal{H}_a \otimes C_z)e$$
$$y_0 = -(b_a^T \otimes C_y)e \qquad y = (\mathcal{H}_a \otimes C_y)e$$

Therefore, we find the following quadratic upper bounds on the nonlinear functions F_t and G_t in (6.9):

$$\begin{aligned} F_t^T \tilde{R} F_t &\leq e^T \bar{R}^e e + u_0^T R^{u_0} u_0 =: F_{tM}^T \tilde{R} F_{tM} \\ G_t^T \tilde{S} G_t &\leq e^T \bar{S}^e e =: G_{tM}^T \tilde{S} G_{tM} \end{aligned} \tag{6.10}$$

where we emphasize that $F_{tM}^T \tilde{R} F_{tM}$ is a quadratic function of u_0 and e, and $G_{tM}^T \tilde{S} G_{tM}$ is a quadratic function of e. Also, $\tilde{R} = Diag_b\{[R_0, \bar{R}]\}$, $R_0 = R_0^T \succ \mathbf{0}$, $\bar{R} = (I_N \otimes R)$, $\bar{R}^e = (I_N \otimes R^e)$, $R^e = R_0^e + R_f^e + R_{f_0}^e$, $R_0^e = \alpha_0 \lambda_{max}(b_a b_a^T) C_z^T R_0 C_z$, $R_f^e = \frac{4\alpha \mu_{aN}^2}{\mu_{c1}^2} C_z^T R C_z$, $R_{f_0}^e = \frac{2\alpha_0 N \lambda_{max}(b_a b_a^T)}{\mu_{c1}^2} C_z^T R C_z$, and $R^{u_0} = \frac{4N}{\mu_{c1}^2} R$. Moreover, $\tilde{S} = Diag_b\{[S_0, \bar{S}]\}$, $S_0 = S_0^T \succ \mathbf{0}$, $\bar{S} = (I_N \otimes S)$, $\bar{S}^e = (I_N \otimes S^e)$ where $S^e = S_0^e + S_g^e + S_{g0}^e$, $S_0^e = \beta_0 \lambda_{max}(b_a b_a^T) C_y^T S_0 C_y$, $S_g^e = 2\beta \mu_{aN}^2 C_y^T S C_y$, and $S_{g0}^e = 2N\beta_0 \lambda_{max}(b_a b_a^T) C_y^T S C_y$. (See Assumptions 6.1.2 and 6.1.3, Fact 2.1.1, and properties of Kronecker product.)

We propose an *auxiliary leader-follower multiagent system*:

$$\dot{\xi} = \tilde{A}\xi + \tilde{B}_m \tau + \tilde{B}_u \sigma \tag{6.11}$$

where the fictitious control signal $\sigma = [\sigma_0^T, \sigma_1^T, ..., \sigma_N^T]^T \in \mathbb{R}^{(N+1)n_y}$ deals with the augmented unmatched uncertainty $G_t(y;t)$. In the rest of this subsection, we provide some basic results and definitions, and propose Theorem 6.1.1.

Let $K_0 = -R_{1l}^{-1} B_m^T P_{1l}$ and $L_0 = -S_{1l}^{-1} B_u^T P_{1l}$ be the leader's control and fictitious control gains, respectively, where P_{1l} denotes the positive definite solution of an algebraic Riccati equation (ARE):

$$A^T P_{1l} + P_{1l} A + Q_{1l} - P_{1l}(B_m^T R_{1l}^{-1} B_m + B_u^T S_{1l}^{-1} B_u) P_{1l} = \mathbf{0} \tag{6.12}$$

where $Q_{1l} = Q_0 = Q_0^T \succ \mathbf{0}$, $R_{1l} = R_0 + R^{u_0}$, and $S_{1l} = S_0$. We use Q_0, R_0, and S_0 as three design matrices.

Also, let $K = -\mu_{c1} R_{1f}^{-1} B_m^T P_{1f}$ and $L = -S_{1f}^{-1} B_u^T P_{1f}$ be followers' control and fictitious control gains, respectively, where P_{1f} denotes the positive definite solution of another ARE:

$$A^T P_{1f} + P_{1f} A + Q_{1f} - P_{1f}(\mu_{c1}^2 B_m R_{1f}^{-1} B_m^T + B_u^T S_{lf}^{-1} B_u) P_{1f} = \mathbf{0} \tag{6.13}$$

in which $Q_{1f} = Q + R^e + S^e$, $R_{1f} = R$, and $S_{1f} = S$. Similar to the previous paragraph, $Q = Q^T \succ \mathbf{0}$, R, and S are three design matrices.

In order to ensure the existence of a positive definite stabilizing solution for each ARE, the pair $(C_{1\star}, A)$ should be observable where $C_{1\star}^T C_{1\star} =: Q_{1\star}$ and $\star \in \{l, f\}$. Note that Assumption 6.1.5 and Remark 6.1.2.a already imply stabilizable pairs $(A, [B_m, B_u])$ and $(A, [\mu_{c1} B_m, B_u])$. We further define $R^{\tau e} = \alpha_0 \lambda_{max}(b_a b_a^T) C_z^T R^{u_0} C_z$, $\tilde{R}^\tau = Diag_b\{[R^{u_0}, \mathbf{0}]\}$, and $\tilde{Q} = Diag_b\{[Q_0, I_N \otimes Q]\}$. Now, we characterize some sufficient conditions in order to achieve the distributed decoupling in a physically coupled multiagent system of agents described by (6.3).

Theorem 6.1.1. *Let $u_0 = K_0 x_0$ and $\sigma_0 = L_0 x_0$ be such that the minimum cost* (6.14) *is achieved subject to an auxiliary system* (6.15) *while satisfying the condition* (6.16)*. Also, for $i \in \{1, 2, ..., N\}$, let $\nu_i = K e_i$ and $\sigma_i = L e_i$ be such that the minimum cost* (6.17) *is achieved subject to auxiliary systems* (6.18) *while the condition* (6.19) *is satisfied. Then, the exponential distributed decoupling problem is solved implementing two static feedback gains K_0 and K.*

$$J_0(x_0(0)) = \min_{u_0, \sigma_0} \int_0^\infty (x_0^T Q_{1l} x_0 + u_0^T R_{1l} u_0 + \sigma_0^T S_{1l} \sigma_0) dt \tag{6.14}$$

$$\dot{x}_0 = Ax_0 + B_m u_0 + B_u \sigma_0 \tag{6.15}$$

$$Q_0 - K_0^T R^{u_0} K_0 - 2L_0^T S_0 L_0 \succ \boldsymbol{0} \tag{6.16}$$

$$J_i(e_i(0)) = \min_{\nu_i, \sigma_i} \int_0^\infty (e_i^T Q_{1f} e_i + \nu_i^T R_{1f} \nu_i + \sigma_i^T S_{1f} \sigma_i) dt \tag{6.17}$$

$$\dot{e}_i = Ae_i + \mu_{c1} B_m \nu_i + B_u \sigma_i \tag{6.18}$$

$$Q - R^{\tau e} - 2L^T SL \succ \boldsymbol{0} \tag{6.19}$$

Proof. This proof is given at Subsection 6.5.1. □

6.1.2 Distributed decoupling based on the largest positive eigenvalue of the control-layer graph

We start this subsection from (6.7) for the proposed decoupling control algorithms in (6.6). However, now, we define $F_\mu = \frac{1}{\mu_{cN}} F$ and rewrite the augmented multiagent system's dynamics as follows:

$$\dot{e} = \bar{A}e + \bar{B}_m \nu + \bar{B}_m \bar{E} \nu + \bar{B}_m F_\mu + \bar{B}_u G$$

where $\bar{B}_m = I_N \otimes \mu_{cN} B_m$. Also, $\bar{E} = \bar{E}^T = (\frac{\mathcal{H}_c}{\mu_{cN}} - I_N) \otimes I_{n_z} \preccurlyeq \mathbf{0}$ where eigenvalues of $\bar{E}$ belong to the interval $(-1, 0]$ using the properties of Kronecker product in Chapter 1. We introduce the augmented leader-follower dynamics:

$$\dot{\xi} = \tilde{A}\xi + \tilde{B}_m \tau + \tilde{B}_m \tilde{E} \tau + \tilde{B}_m F_t + \tilde{B}_u G_t \tag{6.20}$$

where $F_t = [f_0^T, F_\mu^T]^T$ with a new F_μ that hs been introduced in this Subsection, and $Diag_b\{[\mathbf{0}, -I_{Nn_z}]\} \preccurlyeq \tilde{E} = \tilde{E}^T = Diag_b\{[\mathbf{0}, \bar{E}]\} \preccurlyeq \mathbf{0}$ where eigenvalues of $\tilde{E}$ belong to $(-1, 0]$. Also, we find two quadratic upper-bounds similar

to (6.10) with some new matrices $R^e = \alpha_0 \lambda_{max}(b_a b_a^T) C_z^T R_0 C_z + \frac{2}{\mu_{cN}^2}(2\alpha\mu_{aN}^2 + \alpha_0 N \lambda_{max}(b_a b_a^T)) C_z^T R C_z$, $R^{u_0} = \frac{4N}{\mu_{cN}^2} R$.

We propose the following leader-follower auxiliary multiagent system model:

$$\dot{\xi} = \tilde{A}\xi + \tilde{B}_m \tau + \tilde{B}_u \theta \tag{6.21}$$

where the fictitious control signal $\theta = [\theta_0^T, \theta_1^T, ..., \theta_N^T]^T \in \mathbb{R}^{(N+1)n_y}$ handles the effect of G_t.

Before proposing the main result of this subsection, let $K_0 = -R_{2l}^{-1} B_m^T P_{2l}$, $L_0 = -S_{2l}^{-1} B_u^T P_{2l}$, $Q_{2l} = Q_0 = Q_0^T \succ \mathbf{0}$ be a design matrix, $R_{2l} = R_0 + R^{u_0}$ where $R_0 = R_0^T \succ \mathbf{0}$ is a design matrix, $S_{2l} = S_0 = S_0^T \succ \mathbf{0}$ be a design matrix, and P_{2l} be the positive definite solution of an ARE:

$$A^T P_{2l} + P_{2l} A + Q_{2l} - P_{2l}(B_m^T R_{2l}^{-1} B_m + B_u^T S_{2l}^{-1} B_u) P_{2l} = \mathbf{0}$$

Also, let $K = -\mu_{cN}^T R_{2f}^{-1} B_m^T P_{2f}$, $L = -S_{2f}^{-1} B_u^T P_{2f}$, $Q_{2f} = Q + R^e + S^e$ where $Q = Q^T \succ \mathbf{0}$, $R_{2f} = R = R^T \succ \mathbf{0}$ be a design matrix, $S_{2f} = S = S^T \succ \mathbf{0}$ be a design matrix, and P_{2f} be the positive definite solution of the following ARE:

$$A^T P_{2f} + P_{2f} A + Q_{2f} - P_{2f}(\mu_{cN}^2 B_m^T R_{2f}^{-1} B_m + B_u^T S_{2f}^{-1} B_u) P_{2f} = \mathbf{0}$$

Existence of a stabilizing solution for each ARE follows the discussion in Subsection 6.1.1 (e.g., for the pair $(A, [\mu_{cN} B_m, B_u])$. Note that the matrices $R^{\tau e} = \alpha_0 \lambda_{max}(b_a b_a^T) C_z^T R^{u_0} C_z$ and $\tilde{R}^\tau = Diag_b\{[R^{u_0}, \mathbf{0}]\}$ were defined previously. Next theorem provides the main result of this subsection.

Theorem 6.1.2. *Let the leader's control signal $u_0 = K_0 x_0$ and the fictitious control signal $\theta_0 = L_0 x_0$ be such that achieved the minimum cost* (6.22) *subject to the*

auxiliary system (6.23) *while the condition* (6.24) *is satisfied. For* $i \in \{1, 2, ..., N\}$, *let the followers' control signals* $\nu_i = Ke_i$ *and fictitious control signals* $\theta_i = Le_i$ *be such that the minimum costs* (6.25) *are obtained subject to the auxiliary systems* (6.26) *while satisfying the condition* (6.27). *Then, the exponential distributed decoupling problem is solved implementing two static feedback gains* K_0 *and* K.

$$J_0(x_0(0)) = \min_{u_0,\theta_0} \int_0^\infty (x_0^T Q_{2l} x_0 + u_0^T R_{2l} u_0 + \theta_0^T S_{2l} \theta_0) dt \tag{6.22}$$

$$\dot{x}_0 = Ax_0 + B_m u_0 + B_u \theta_0 \tag{6.23}$$

$$Q_0 - K_0^T R^{u_0} K_0 - 2L_0^T S_0 L_0 \succ \boldsymbol{0} \tag{6.24}$$

$$J_i(e_i(0)) = \min_{\nu_i,\theta_i} \int_0^\infty (e_i^T Q_{2f} e_i + \nu_i^T R_{2f} \nu_i + \theta_i^T S_{2f} \theta_i) dt \tag{6.25}$$

$$\dot{e}_i = Ae_i + \mu_{cN} B_m \nu_i + B_u \theta_i \tag{6.26}$$

$$Q - R^{\tau^e} - 2K^T RK - 2L^T SL \succ \boldsymbol{0} \tag{6.27}$$

Proof. This proof is provided at Subsection 6.5.2. □

6.1.3 Fully distributed decoupling algorithm

Up to this point, although these distributed algorithms can be locally implemented, all designs depend on the availability of global knowledge about the multiagent system. To clarify the word "global knowledge", we note that smallest and largest positive eigenvalues of a graph Laplacian are unknown unless after being aware of the entire graph topology (which is a global knowledge). Thus, we propose the next corollary to have a fixed-gain fully distributed decoupling system

based on the result of Subsection 6.1.2. This way, we are able to independently design the distributed decoupling system and control-layer communication graph and, independently, take the advantages of both control and optimization ideas in Figure 1.1.

Corollary 6.1.1. *Based on Theorem 6.1.2, a distributed decoupling system is achieved whenever* μ_{aN} *is substituted by* $2N-1$*,* μ_{cN} *by* $2N-1$*, and* $\lambda_{max}(b_a b_a^T)$ *by* N *where* $N+1$ *denotes the number of agents in the coupled multiagent system.*

Proof. This proof is given at Subsection 6.5.3. □

Remark 6.1.3. *In Corollary 6.1.1, we do not need any global information about* $\mathcal{G}_a$ *and* $\mathcal{G}_c$ *other than the number of agents* $N+1$*. In the rare case of an unknown number of agents, as can bee seen in the proof of this corollary, we can substitute* N *by an estimated upper-bound* $\bar{N}$ *(i.e.,* $\bar{N} \geq N$*).*

6.2 Distributed stabilization of linear multiagent systems with state and input couplings

The results on the distributed decoupling algorithms are based on the availability of agents' absolute measurements (in hierarchical manners). This might be unrealistic in some circumstances, particularly, while agents might be willing to cooperatively contribute toward a common global task completion (by providing some relative information) they could be worried about their own privacy (by do not sharing their absolute measurements to any control operator). Therefore, in this section, we assume having access to the absolute measurements of a set of

only few agents (possibly just one agent), and address the distributed stabilization problem through a revised formulation. Compared to the previous sections, now we also consider the potential physical coupling terms in the control input gain matrix $\mathbf{B}$ of the model (5.1). Thus, in this section, we introduce a linear time-invariant multiagent system with heterogeneous coupled state and input terms:

$$\dot{x}_i = Ax_i + B_m u_i + B_u D_i \sum_{j \in \mathcal{N}_i^{au}} (u_i - u_j) + B_x F_i \sum_{j \in \mathcal{N}_i^{ax}} (x_i - x_j) \tag{6.28}$$

where $\mathcal{N}_i^{au}$ and $\mathcal{N}_i^{ax}$ denote the neighboring set of i^{th} agent over agent-layer coupling graphs $\mathcal{G}_{au}$ and $\mathcal{G}_{ax}$, respectively; $A \in \mathbb{R}^{n_x}$, $B_m^{n_u}$, $B_x \in \mathbb{R}^{n_x \times n_u}$, and $B_u \in \mathbb{R}^{n_x \times n_u}$; and $F_i \in \mathbb{R}^{n_u \times n_x}$ and $D_i \in \mathbb{R}^{n_u \times n_u}$ uniquely characterize i^{th} agent[2]. We assume that B_u and B_x are not in the range space of B_m.

In this section, we focus on heterogeneous coupling terms over directed agent-layer coupling graphs $\mathcal{G}_{ax}$ and $\mathcal{G}_{au}$ that can be different from each other (i.e., $\mathcal{N}_i^a \in \{\mathcal{N}_i^{ax}, \mathcal{N}_i^{au}\}$). We assume that at least one agent is providing its local state information to the distributed control system, and only lumped relative-state information is measurable for all other agents. Moreover, for the control design purpose, the following Assumption is satisfied in the rest of this section:

Assumption 6.2.1. *The pair (A, B_m) is stabilizable. Matrices D_i and F_i are unknown, but satisfy $\max_i \|D_i\|_2 =: \|D\|_M$ and $\max_i \|F_i\|_2 =: \|F\|_M$ for $i \in \{1, 2, ..., N\}$. Also, both graphs $\mathcal{G}_{ax}$ and $\mathcal{G}_{au}$ are unknown, directed in the general*

[2]We only need to assume that $B_{0i} = B_u D_i \in \mathbb{R}^{n_x \times n_u}$ and $A_{0i} = B_x F_i \in \mathbb{R}^{n_x \times n_x}$. Other than this, without loss of generality, we have selected n_u as the internal dimension for both of these matrix products in order to minimize the number of new parameters and symbols.

sense, and each one includes at least one connected component; $\max_i \|\mathcal{L}_{ax}\|_2 =: \|\mathcal{L}_{ax}\|_M$ *and* $\max_i \|\mathcal{L}_{au}\|_2 =: \|\mathcal{L}_{au}\|_M$ *are known.*

Now, for a *partially-heterogeneous asymmetrically interconnected multiagent system* of agents (6.28), the distributed stabilization problem is formulated as exponentially achieving (6.29) using some lumped relative-state information:

$$\lim_{t\to 0} x = 0 \tag{6.29}$$

which also indicates $\lim_{t\to 0} x_i = 0$ for agents $i \in \{1, 2, ..., N\}$.

6.2.1 Main Result

In order to achieve the distributed exponential stability (6.29) for a multiagent system of agents (6.28), we add a virtual leader to the interconnected multiagent system (6.28) (this name is taken from [152]):

$$\dot{x}_0 = Ax_0 + B_m u_0 \tag{6.30}$$

that is indexed by $i = 0$; and $x_0 \in \mathbb{R}^{n_x}$, $u_0 \in \mathbb{R}^{n_u}$, and (A, B_m) realizes the nominal dynamics of (6.28). We refer to this virtual leader as "leader" and to all agents $i \in \{1, 2, ..., N\}$ as "followers", and propose the following distributed control algorithm over the control-layer communication graph $\mathcal{G}_c$:

$$\begin{aligned} u_0 &= K_0 x_0 \\ u_i &= K(\textstyle\sum_{j\in\mathcal{N}_i^{cf}}(x_i - x_j) + b_i^c(x_i - x_0)) \end{aligned} \tag{6.31}$$

where $\mathcal{N}_i^{cf}$ denotes the neighboring set of i^{th} agent over $\mathcal{G}_c^f$ corresponding to all followers. Note that $\mathcal{G}_c$ denotes a special directed graph where all followers com-

municate over an undirected graph $\mathcal{G}_c^f$, that is a subgraph of $\mathcal{G}_c$ and can be found by removing the leader and all directed edges originating from that node. Now, we need to design a $K_0 \in \mathbb{R}^{n_u \times n_x}$ that stabilizes the leader, and a $K \in \mathbb{R}^{n_u \times n_x}$ that ensures the leader-follower tracking errors $e_i \triangleq x_i - x_0$ exponentially converge to zero for all $i \in \{1, 2, ..., N\}$. We also emphasize that $\mathcal{G}_c$ can be different from $\mathcal{G}_{au}$ and $\mathcal{G}_{ax}$ which are unknown. Moreover, note that the (virtual) leader should be connected to those followers that provide their local state information, and those particular followers should make a leader-follower graph $\mathcal{G}_c$ which includes a directed spanning tree. Since the control-layer graph $\mathcal{G}_c$ can be arbitrarily designed, this connectedness requirement does not restrict the applicability of our design. We rewrite (6.28) as follows:

$$\dot{x}_i = Ax_i + B_m u_i + B_u \delta_{ui}(u) + B_x \delta_{xi}(x) \tag{6.32}$$

where $\delta_{ui}(u) = D_i \sum_{j \in \mathcal{N}_i^{au}} (u_i - u_j)$ and $\delta_{xi}(x) = F_i \sum_{j \in \mathcal{N}_i^{ax}} (x_i - x_j)$. Figure 6.2 shows an example for the final closed-loop multiagent system (6.30)-(6.32).

We now find the leader-follower tracking error dynamics:

$$\begin{aligned} \dot{e}_i &= Ae_i + B_m u_i + B_u \delta_{ui}(u) + B_x \delta_{xi}(e) + B_m \delta_{u_0 i}(u_0) \\ \delta_{ui}(u) &= D_i \textstyle\sum_{j \in \mathcal{N}_i^{au}} (u_i - u_j) \\ \delta_{xi}(e) &= F_i \textstyle\sum_{j \in \mathcal{N}_i^{ax}} (e_i - e_j) \\ \delta_{u_0 i}(u_0) &= -u_0 \end{aligned} \tag{6.33}$$

and control signals:

$$\begin{aligned} u_0 &= K_0 x_0 \\ u_i &= K(\textstyle\sum_{j \in \mathcal{N}_i^{cf}} (e_i - e_j) + b_i^c e_i) \end{aligned} \tag{6.34}$$

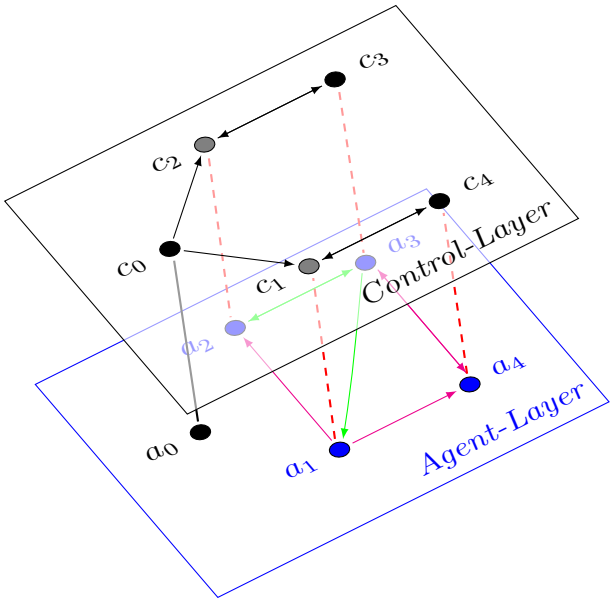

Figure 6.2: An example for the proposed two-layer structure by (6.30)-(6.32). Letters a and c stand for agent and controller, respectively. *Blue*: agent-layer items, *green arrows* input couplings, and *magenta arrows* state couplings; *Black*: control-layer items (note that the virtual leader agent a_0 is part of the control-layer communication graph and is shown in black). *Dashed red lines*: agent-controller correspondence. Moreover, the *gray* nodes c_1 and c_2 provide their absolute state information to the distributed control algorithm.

where we should mention that the subscript $_i$ is added to $\delta_{u_0 i}(u_0)$ only for the purpose of consistency in notation. We also change the input argument of δ_{xi} from x to e in order to simply emphasize this change of variables while the subscript $_x$ shows the origin of this "state coupling" term $\delta_{xi}(e)$.

We define $e = col\{e_i\}T$ and find the coupled term $u = (\mathcal{H}_c \otimes K)e$ as followers' control signals where this coupling appears because of having a "distributed" control algorithm in (6.34), and $\mathcal{H}_c$ denotes the reduced-order Laplacian matrix of $\mathcal{G}_c$. We propose the next decomposition:

$$u = (\mathcal{H}_c \otimes I_{n_u})\nu \qquad \nu = (I_N \otimes K)e \tag{6.35}$$

where $\nu = col\{\nu_i\} \in \mathbb{R}^{Nn_u}$. Now, we find an augmented tracking error model that includes the effect of $\mathcal{G}_c$ as well as $\mathcal{G}_{au}$ and $\mathcal{G}_{ax}$:

$$\begin{aligned}
\dot{e} &= \bar{A}e + \bar{B}_m\nu + \bar{B}_m\bar{E}_m\nu + \bar{B}_u\delta_u + \bar{B}_x\delta_x + \bar{B}_{u0}\delta_{u0} \\
\delta_u &= D(\mathcal{L}_{au}\mathcal{H}_c \otimes I_{n_u})\nu \\
\delta_x &= F(\mathcal{L}_{ax} \otimes I_{n_x})e \\
\delta_{u_0} &= -(\mathbf{1}_N \otimes I_{n_u})u_0
\end{aligned}$$

where $\bar{A} = I_N \otimes A$, $\bar{B}_m = I_N \otimes \mu_{c1}B_m$, $\bar{E}_m = (\frac{\mathcal{H}_c}{\mu_{c1}} - I_N) \otimes I_{n_u}$, $\bar{B}_u = I_N \otimes B_u$, $\bar{B}_x = I_N \otimes B_x$, $D = diag\{D_1, ..., D_N\}$, and $F = diag\{F_1, ..., F_N\}$. Also, $\delta_u = col\{\delta_{ui}\}$, $\delta_x = col\{\delta_{xi}\}$, and $\delta_{u_0} = col\{\delta_{u_0 i}\} = -(\mathbf{1}_N \otimes I_{n_u})u_0$; and $\mathcal{L}_{au}$ and $\mathcal{L}_{ax}$ denote the Laplacian matrices of $\mathcal{G}_{au}$ and $\mathcal{G}_{ax}$, respectively.

We further propose an augmented dynamical system of all leader and followers:

$$\underbrace{\dot{\xi} = \tilde{A}\xi + \tilde{B}_m\sigma}_{\text{Nominal decoupled dynamics}} + \underbrace{\tilde{B}_m\tilde{E}_m\sigma + \tilde{B}_u\delta_u + \tilde{B}_x\delta_x + \tilde{B}_{u_0}\delta_{u_0}}_{\text{Coupling term}} \tag{6.36}$$

where $\tilde{A} = diag\{A, \bar{A}\}$, $\tilde{B}_m = diag\{B_m, \bar{B}_m\}$, $\tilde{E}_m = diag\{\mathbf{0}, \bar{E}_m\}$, $\tilde{B}_u = [\mathbf{0}, \bar{B}_u^T]^T$, $\tilde{B}_x = [\mathbf{0}, \bar{B}_x^T]^T$, and $\tilde{B}_{u_0} = [\mathbf{0}, \bar{B}_{u_0}^T]^T$; and $\xi = [x_0^T, e^T]^T$, and $\sigma = [u_0^T, \nu^T]^T$. This model is divided into a *decoupled* part and a *coupled* part. The decoupled term is partially affected by $\mathcal{G}_c$ due to the presence of μ_{c1} in $\bar{B}_m$. The coupling term includes E_m that interconnects followers to each other and to the leader over $\mathcal{G}_c$; δ_u and δ_x that couple some followers to each others over $\mathcal{G}_{au}$ and $\mathcal{G}_{ax}$, respectively; and δ_{u_0} that couples all followers to the leader and appears after introducing the leader-follower error dynamics. Some properties of these coupling terms are explained as follows:

Property 6.2.1. *The following properties hold by multiagent system* (6.36)*:*

- $\tilde{E}_m = \tilde{E}_m^T = diag\{\boldsymbol{0}, (\frac{\mathcal{H}_c}{\mu_{c1}} - I_N) \otimes I_{n_u}\}$ *is a "positive semidefinite" matrix,*

- δ_u, δ_x, *and* δ_{u_0} *satisfy the following inequalities with known quadratic upper bounds* $\delta_u^T \bar{S} \delta_u \leq \nu^T \bar{S}^\nu \nu =: \delta_{uM}^T \bar{S} \delta_{uM}$, $\delta_x^T \bar{W} \delta_x \leq e^T \bar{W}^e e =: \delta_{xM}^T \bar{W} \delta_{xM}$, *and* $\delta_{u_0}^T \bar{V} \delta_{u_0} \leq u_0^T V^{u_0} u_0 =: \delta_{u_0 M}^T \bar{V} \delta_{u_0 M}$ *where* $\bar{X} = I_N \otimes X$ *and* $X \in \{S, W, V, S^\nu, W^e\}$. *We introduce* $S = sI_{n_u}$ *for* $s > 0$, $W = wI_{n_x}$ *for* $w > 0$, *and* $V = V^T \succ \boldsymbol{0}$ *as three design matrices. Additionally, we find* $S^v = \mu_{cN}^2 \|D\|_M^2 \|\mathcal{L}_{au}\|_M^2 sI_{n_u}$, $W^e = \|F\|_M^2 \|\mathcal{L}_{ax}\|_M^2 wI_{n_x}$, *and* $V^{u_0} = NV$.

In the rest of this section, we focus on finding an augmented control signal σ that stabilizes (6.36) (i.e., solves (6.29)). At first, we propose an augmented auxiliary model:

$$\dot{\xi} = \tilde{A}\xi + \tilde{B}_m \sigma + \tilde{B}_u \tau + \tilde{B}_x \theta + \tilde{B}_{u_0} \rho \tag{6.37}$$

where the fictitious control signals $\tau = col\{\tau_i\} \in \mathbb{R}^{Nn_u}$, $\theta = col\{\theta_i\} \in \mathbb{R}^{Nn_x}$, and $\rho = col\{\rho_i\} \in \mathbb{R}^{Nn_u}$ are added to respectively handle the coupled modeling uncertainties δ_u, δ_x, and δ_{u_0}. Now, in Design procedure 6.2.1, we provide a systematic approach to find σ, τ, θ, and ρ.

Design procedure 6.2.1. *Find the LQR control signal* $u_0 = K_0 x_0$ *that achieves the minimum value* J_0 *in* (6.38) *(subject to* (6.39)*), where* $R_{0f} = R_0 + V^{u_0}$*; and* $Q_0 = Q_0^T \succ \boldsymbol{0}$ *and* $R_0 = R_0^T \succ \boldsymbol{0}$ *are two design matrices:*

$$J_0(x_0(0)) = \min_{u_0} \int_0^\infty (x_0^T Q_0 x_0 + u_0^T R_{0f} u_0) dt \tag{6.38}$$

$$\dot{x}_0 = Ax_0 + B_m u_0. \tag{6.39}$$

Also, find $\gamma_i = K_{all} e_i$ *that result in* (6.40) *(subject to* (6.41)*) for* $i \in \{1, 2, ..., N\}$, *where* $\gamma_i = [\nu_i^T, \tau_i^T, \theta_i^T, \rho_i^T]^T$; $R_f = R + S^\nu$, *and* $Q_f = Q + W^e$; *and* $Q = Q^T \succ \mathbf{0}$ *and* $R = R^T = rI_{n_u} \succ \mathbf{0}$ *for* $r > 0$ *are two design matrices in addition to* $S = S^T \succ \mathbf{0}$, $W = W^T \succ \mathbf{0}$, *and* $V = V^T \succ \mathbf{0}$ *in Property 6.2.1:*

$$J_i(e_i(0)) = \min_{\beta_i} \int_0^\infty (e_i^T Q_f e_i + \gamma_i^T Y \gamma_i) dt \tag{6.40}$$

$$\dot{e}_i = A e_i + B \gamma_i \tag{6.41}$$

As a result, we find $K_0 = -R_{0f}^{-1} B_m^T P_0 x_0$, *and* $K_{all} = -Y^{-1} B^T P$ *for the aggregated matrices* $B = [\mu_{c1} B_m, B_u, B_x, B_m]$ *and* $Y = diag\{R_f, S, W, V\}$. *Equivalently,* $\nu_i = Ke_i$, $\tau_i = Ge_i$, $\theta_i = He_i$, *and* $\rho_i = Le_i$; *with* $K = -\mu_{c1} R_f^{-1} B_m^T P$, $G = -S^{-1} B_u^T P$, $H = -W^{-1} B_x^T P$, *and* $L = -V^{-1} B_m^T P$. *The matrices* $P_0 = P_0^T \succ \mathbf{0}$ *and* $P = P^T \succ \mathbf{0}$ *are the solutions of the algebraic Riccati equations* (6.42) *and* (6.43), *respectively:*

$$A^T P_0 + P_0 A - P_0 B_m R_{0f}^{-1} B_m^T P_0 + Q_0 = \mathbf{0} \tag{6.42}$$

$$A^T P + P A - P B Y^{-1} B^T P + Q_f = \mathbf{0} \tag{6.43}$$

Stability and optimality of this design for an auxiliary multiagent system model (6.37) are guaranteed based on the LQR optimal control formulation (with respect to a global cost function that will be shown in Property 6.2.2). Note that the pair (A, B_m) represents a stabilizable state space realization (6.39). Thus, existence of the stabilizable solution P_0 in (6.42) is guaranteed whenever the pair $(Q_0^{\frac{1}{2}}, A)$ is observable where $Q_0 = Q_0^{\frac{1}{2}T} Q_0^{\frac{1}{2}}$. Furthermore, due to stabilizability of (A, B_m) and because $\mu_{c1} \neq 0$, the pair (A, B) provides a stabilizable state space

realization (6.41). Hence, existence of the stabilizable solution P in (6.43) can be similarly discussed for a state weighting matrix Q_f.

Let us rewrite (6.37) as follows:

$$\dot{\xi} = \tilde{A}\xi + \tilde{B}\beta \tag{6.44}$$

where $\beta = [\sigma^T, \beta_\delta^T]^T$ denotes a vector of all control signal σ and fictitious control signals $\beta_\delta = [\tau^T, \theta^T, \rho^T]^T$; and $\tilde{B} = [\tilde{B}_m, \tilde{B}_\delta]$ and $\tilde{B}_\delta = [\tilde{B}_u, \tilde{B}_x, \tilde{B}_{u_0}]$. Moreover, let $\tilde{Q}_f = diag\{Q_0, \bar{Q}_f\}$ where $\bar{Q}_f = I_N \otimes Q_f$, $\tilde{Y} = diag\{\tilde{R}_f, \bar{S}, \bar{W}, \bar{V}\}$, $\tilde{R}_f = diag\{R_{0f}, \bar{R}_f\}$, and $\bar{R}_f = I_N \otimes R_f$. Now, we characterize some main properties of the closed-loop auxiliary system (6.37) using the control and fictitious control gains of Design procedure 6.2.1.

Property 6.2.2. *Let $\beta = \beta^\star$ be the aggregated control signal that results in the minimum augmented cost function $J(\xi(0))$ in* (6.45) *subject to* (6.44)*:*

$$J(\xi(0)) = \min_{\beta} \int_0^\infty (\xi^T \tilde{Q}_f \xi + \beta^T \tilde{Y} \beta) dt. \tag{6.45}$$

The corresponding Hamiltonian function to this LQR cost function minimization problem is defined by:

$$\boldsymbol{H} = \xi^T \tilde{Q}_f \xi + \beta^T \tilde{Y} \beta + (\frac{\partial J}{\partial \xi})^T (\tilde{A}\xi + \tilde{B}\beta). \tag{6.46}$$

Then, the equalities in (6.47) *and* (6.48) *are satisfied as optimality conditions for the infinite horizon LQR control problem* (6.45) *subject to LTI dynamics* (6.44) *by setting $\boldsymbol{H} = 0$ and $\frac{\partial \boldsymbol{H}}{\partial \beta} = \boldsymbol{0}$, respectively (see Sec. 3.11 in [109]):*

$$\xi^T \tilde{Q}_f \xi + \beta^T \tilde{Y} \beta + (\frac{\partial J}{\partial \xi})^T (\tilde{A}\xi + \tilde{B}\beta) = 0 \tag{6.47}$$

$$2\beta^T \tilde{Y} + (\frac{\partial J}{\partial \xi})^T \tilde{B} = \boldsymbol{0} \tag{6.48}$$

Remark 6.2.1. *We rewrite* (6.47) *as:*

$$\begin{aligned}\xi^T \tilde{Q} \xi + \sigma^T \tilde{R} \sigma + \tau^T \bar{S} \tau + \quad & \theta^T \bar{W} \theta + \rho^T \bar{V} \rho + \delta_u^T \bar{S} \delta_u + \delta_x^T \bar{W} \delta_x + \delta_{u_0}^T \bar{V} \delta_{u_0} \\ & + (\tfrac{\partial J}{\partial \xi})^T (\tilde{A}\xi + \tilde{B}_m \sigma + \tilde{B}_u \tau + \tilde{B}_x \theta + \tilde{B}_{u_0} \rho) = 0\end{aligned}$$

Also, based on (6.48)*, we find the following four equalities:*

$$\begin{aligned} 2\sigma^T \tilde{R}_f + (\tfrac{\partial J}{\partial \xi})^T \tilde{B}_m &= \boldsymbol{0} \\ 2\tau^T \bar{S} + (\tfrac{\partial J}{\partial \xi})^T \bar{B}_u &= \boldsymbol{0} \\ 2\theta^T \bar{W} + (\tfrac{\partial J}{\partial \xi})^T \bar{B}_x &= \boldsymbol{0} \\ 2\rho^T \bar{V} + (\tfrac{\partial J}{\partial \xi})^T \bar{B}_{u_0} &= \boldsymbol{0} \end{aligned}$$

Now, we provide a sufficient condition that ensures the global exponential stabilization of an interconnected multiagent system of agents (6.28) with state- and input-coupled modeling uncertainties using the distributed algorithm (6.31).

Theorem 6.2.1. *The distributed control algorithm* (6.31) *solves the exponential stabilization problem* (6.29) *for a multiagent system of agents* (6.28) *with asymmetric heterogeneous state- and input-coupled modeling uncertainties, if the control gain K and fictitious control gains G, H, and L of Design procedure 6.2.1 satisfy the following condition:*

$$Q + K^T R K - 2G^T S G - 2H^T W H - 2L^T V L \succ \boldsymbol{0} \tag{6.49}$$

Proof. This proof is provided at Subsection 6.5.4. □

Remark 6.2.2. *Note that the communication graph $\mathcal{G}_c$ has the same topology as that of Section 6.1. Thus, a fully distributed version of Theorem 6.2.1 can be established following the ideas of Section 6.1.*

6.2.2 Simulation Verification

In this section, we verify the feasibility of our virtual leader-based distributed control algorithm to achieve (6.29) for a multiagent system of four agents in Fig 6.2 (these agents are shown by blue circles). Each agent is modeled by a state space realization (6.28) with the following state and input matrices:

$$A = \begin{bmatrix} 0 & 1 \\ 2 & -1 \end{bmatrix}, \quad B_m = \begin{bmatrix} 0 \\ 1 \end{bmatrix}, \quad B_u = \begin{bmatrix} 0.02 \\ 0 \end{bmatrix}, \quad B_x = \begin{bmatrix} 0.01 \\ 0.9 \end{bmatrix}$$

where A is a non-Hurwitz matrix. In simulation, we assume that all agents are in initial rest condition. However, at time $t_\star = 25s$, a perturbation in 3^{rd} agent changes its state variables to $x_3(t_\star) = [10, 15]^T$.

We first assume that there is no distributed controller (i.e., remove all black symbols in Fig 6.2) and local state information is available to each agent. We design a local LQR control gain K_{local} such that each closed-loop local agent has a stable state space realization with a Hurwitz matrix $A_{cl} = A + B_m K_{local}$. Without any agent-layer couplings, the 3^{rd} agent should damp this state perturbation, and, furthermore, we expect no reactions in other agents because $x_i(t_\star) = \mathbf{0}\ \forall i \neq 3$. In order to show the insufficiency of this blind local design for the global stabilization purpose, interconnection parameters and matrices D_i and F_i for $i \in \{1, 2, 3, 4\}$ are

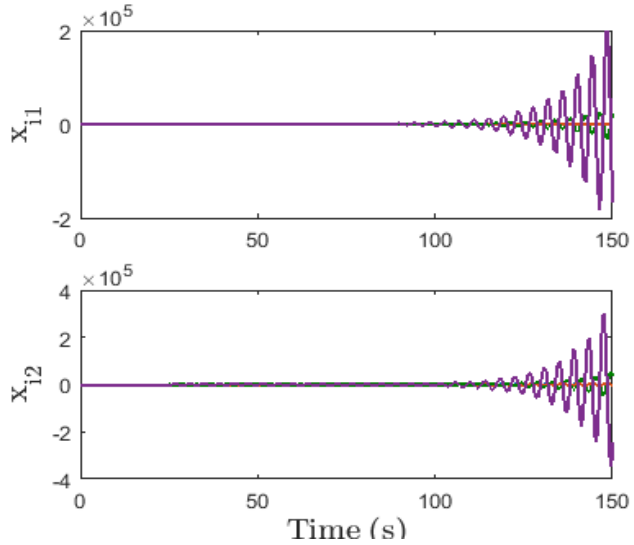

Figure 6.3: Simulation result over the agent-layer coupling graph of Fig. 6.2 with 4 agents, where x_{i1} and x_{i2} stand for the first and second state variables of agents (6.28) locally equipped with LQR controllers $u_i = K_{local}x_i$ to stabilize the local (decoupled) dynamics $\dot{x}_i = Ax_i + B_m u_i$ for $i \in \{1, 2, 3, 4\}$. We do implement the block control-layer symbols in Fig. 6.2 since we do not use any distributed stabilizing systems.

chosen such that the interconnected multiagent system of locally stabilized agents has two eigenvalues in the right half plane. As is depicted in Fig. 6.3, while only the 3^{rd} agent is nominally perturbed, the entire multiagent system's response is unbounded due to the presence of agent-layer physical couplings. This indicates the need for a multiagent system-level (distributed) stabilizing system.

Now, we assume that the previously designed local control gain K_{local} does not exist any more (i.e., we deal with locally unstable agents). Based on the Design procedure 6.2.1, we design the control gain K together with all virtual and fictitious control gains K_0, G, H, and L satisfying the sufficient condition (6.49). The simulation result is presented in Fig. 6.4 assuming the same interconnection matrices and excitation scenario as Fig. 6.3. It shows the entire multiagent system

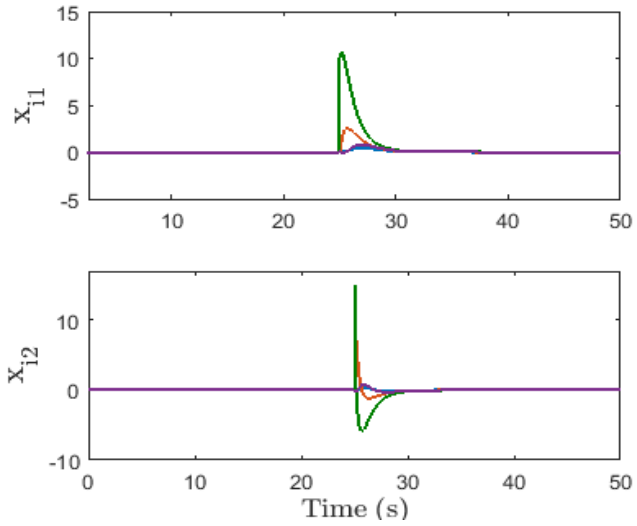

Figure 6.4: Simulation result after using the distributed stabilizing algorithm in Design procedure 6.2.1 and Theorem 6.2.1 over the proposed structure of Fig. 6.2. The simulation scenario is the same as Fig. 6.3; however, we no longer use the locally stabilizing control gain K_{local}.

has a stable behavior in response to the 3^{rd} agent's perturbation at time $t_\star = 25s$. This verifies the claim of Theorem 6.2.1.

6.3 Revisiting the results of Chapter 4

In Chapter 4, we designed two distributed decoupling algorithms for physically coupled multiagent systems. In those designs, the control-layer communication graphs were the same as the agent-layer coupling graphs. In Section 5.2, the coupling (also communication) was described over an undirected graph. In Section 5.3, we designed two distributed algorithms over a special type of directed leader-follower graph. In Section 6.1, we discussed the need for a global knowledge

in the distributed decoupling strategies of Chapter 4, and proposed a fixed-gain fully distributed decoupling strategy in order to relax this requirement.

By following the steps of Section 6.1, it is possible to revise the results of Section 5.3 and find two fixed-gain fully distributed decoupling algorithms. In next corollary, we address the fully distributed problem for the state and output feedback scenarios in Section 5.2 over an undirected (leaderless) graph:

Corollary 6.3.1. *Based on the leaderless state and output feedback algorithms of Section 5.2, the fixed-gain fully distributed decoupling problem is solved whenever* λ_2 *is substituted by* $2(1 - cos(\frac{\pi}{N}))$*, and* λ_N *by* $2(N-1)$.

Proof. This proof is available at Subsection 6.5.5. □

6.4 Summary and bibliography

In this Chapter, we propose multi-layer distributed control structures for two classes of physically interconnected multiagent systems. In Section 6.1, we consider a class of partially-unknown Lur'e time-varying nonlinear multiagent systems where agents are coupled to each other by some state-dependent nonlinear functions. These nonlinear functions are unknown but satisfy some known norm bounded conditions, and the state-dependent interconnection is explained by an (unknown) agent-layer coupling graph. Controllers are allowed to communicate over a control-layer communication graph that can be different from the agent-layer physical coupling graph. We propose two modified LQR-based formulations and design some distributed decoupling systems using only relative-state measurements. Furthermore, we re-think about the proposed formulation and develop

a fixed-gain fully distributed LQR-based decoupling system without any global information about graph topologies. This enables us using the network design techniques to optimize the communication topology independent of the control protocol at a later time (and also, in each start, replace the control-layer communication network without being worried about its effect on the distributed control algorithm's gains).

In the distributed decoupling control, we assume that agents' absolute information is measurable. This is not an unrealistic assumption as has been justified in [11], [58], [66], [79], and [151]. However, in some instances, agents might not be willing to share their absolute information to the distributed control-layer while participating in a cooperative task completion by sharing their (lumped) relative information in each neighborhood. In Section 6.2, we propose a class of multiagent systems with unknown physical interconnections that appear through some heterogeneous coupled-state and coupled-input terms in the state space model which are described over two different unknown coupling graphs. In fact, this class of multiagent systems resembles the asymmetric large-scale systems with unknown coupling terms. We assume that only a few agents provide their absolute state information, introduce a distributed stabilization problem, add a virtual leader (this name is taken from [152]), re-state the problem as a leader-follower consensus task, and systematically design the distributed control gain using the modified LQR approach for an auxiliary multiagent system model. We show that the global exponential stability of the closed-loop system is guaranteed if a sufficient condition is satisfied.

6.5 Appendix: proofs

We have proposed the main results of this chapter through several theorems and corollaries. For the sake of readability, we have not discussed their proofs within the main body of this chapter. In this Appendix section, we go through these proofs.

6.5.1 Proof of Theorem 6.1.1 (page 224)

We aggregate (6.15) and (6.18) for $i \in \{1, 2, ..., N\}$, and find (6.11). Moreover, an aggregated leader-follower cost function can be obtained based on (6.14) and (6.17):

$$J(\xi(0)) = \int_0^\infty \{\xi^T \tilde{Q} \xi + \tau^T \tilde{R} \tau + \sigma^T \tilde{S} \sigma + F_{tM}^T \tilde{R} F_{tM} + G_{tM} \tilde{S} G_{tM}\} dt$$

The optimal control signal $\tau = \tau^\star$ and fictitious control signal $\sigma = \sigma^\star$ of this theorem achieves the minimum cost $J(\xi(0))$ subject to (6.11). We need to show the exponential stability of the closed-loop system (6.9) in the presence of modeling uncertainties by implementing only τ (i.e., without the fictitious control signal σ). We introduce the following candidate Lyapunov function for $t \geq 0$:

$$V(\xi(t)) = \xi^T(t) \tilde{P} \xi(t) \succ 0$$

where $\tilde{P} = diag\{P_{1l}, \bar{P}_{1f}\}$, $\bar{P}_{1f} = I_N \otimes P_{1f}$, and P_{1l} and P_{1f} are respectively the positive definite solutions of AREs (6.12) and (6.13). We notice that $V(\xi(0)) = J(\xi(0)) = \min_{\tau,\sigma} \int_t^\infty \{\xi^T \tilde{Q} \xi + \tau^T \tilde{R} \tau + \sigma^T \tilde{S} \sigma + F_{tM}^T \tilde{R} F_{tM} + G_{tM} \tilde{S} G_{tM}\} dt' \succ 0$ is sat-

isfied subject to the augmented auxiliary system (6.11). The following Hamilton-Jacobi-Bellman equation holds substituting J_ξ by $V_\xi = \frac{\partial V(\xi)}{\partial \xi}$:

$$\min_{\tau,\sigma}\{\xi^T\tilde{Q}\xi + \tau^T\tilde{R}\tau + \sigma^T\tilde{S}\sigma + F_{tM}^T\tilde{R}F_{tM} + G_{tM}\tilde{S}G_{tM} + V_\xi^T(\tilde{A}\xi + \tilde{B}_m\tau + \tilde{B}_u\sigma)\} = 0$$

Consequently, implementing the optimal gains K_0 and K, and fictitious gains L_0 and L, the followings are satisfied by triple (ξ, τ, σ):

$$\begin{aligned}\xi^T\tilde{Q}\xi + \tau^T\tilde{R}\tau + \sigma^T\tilde{S}\sigma + F_{tM}^T\tilde{R}F_{tM} + G_{tM}\tilde{S}G_{tM} + V_\xi^T(\tilde{A}\xi + \tilde{B}_m\tau + \tilde{B}_u\sigma) &= 0\\ 2\tau^T(\tilde{R} + \tilde{R}^\tau) + V_\xi^T\tilde{B}_m &= \mathbf{0}\\ 2\sigma^T\tilde{S} + V_\xi^T\tilde{B}_u &= \mathbf{0}\end{aligned}$$

Now, the time deviation of this candidate Lyapunov function along the uncertain trajectory (6.9) results in the following inequality:

$$\begin{aligned}\dot{V}(\xi) &\leq -\xi^T\tilde{Q}\xi + 2\sigma^T\tilde{S}\sigma + u_0^T R^{F_t u_0}u_0 + e^T\bar{R}^{\tau e}e\\ &\leq -x_0^T(Q_0 - K_0^T R^{u_0}K_0 - 2L_0^T S_0 L_0)x_0 - \textstyle\sum_{i=1}^N\{e_i^T(Q - R^{\tau e} - 2L^T SL)e_i\}\end{aligned}$$

where, in order to find this upper-bound on $\dot{V}$, we need to use $-2\tau^T(\tilde{R}+\tilde{R}^\tau)\tilde{E}\tau = -2\nu^T\bar{R}\bar{E}\nu \leq 0$ and $F_t^T(\tilde{R} + \tilde{R}^\tau)F_t \leq F_{tM}^T\tilde{R}F_{tM} + e^T(I_N \otimes R^{\tau e})e$.

Because (6.16) and (6.19) are satisfied, we find $\dot{V} \prec 0$. Now, based on the Lyapunov Theorem 2.3.1, the closed-loop Lur'e nonlinear multiagent system (6.9) (subject to the modeling uncertainties) is globally asymptotically stable[3]. We know $a_1 = \min(\lambda_{min}(P_{1l}), \lambda_{min}(P_{1f}))$, $a_2 = max(\lambda_{max}(P_{1l}), \lambda_{max}(P_{1f}))$,

[3]Note that, since there is no hidden "undamped" mode in the sense of Kalman decomposition, asymptotic stability around the equilibrium point origin is achievable for this type of systems. (See Figure 2.2.)

$a_3 = \min(\lambda_{min}(Q_0 - K_0^T R^{u_0} K_0 - 2L_0^T S_0 L_0), \lambda_{min}(Q - R^{\tau e} - 2L^T SL))$, and $b = 2$ to prove the exponential stability based on Theorem 2.3.2. Finally, based on the proposed reformulation of this section, we conclude that the distributed decoupling of agents (6.3) in the presence of mixed matched and unmatched unknown nonlinear couplings is achieved over two fixed graphs $\mathcal{G}_a$ and $\mathcal{G}_c$, and using two static gains K_0 and K.

6.5.2 Proof of Theorem 6.1.2 (page 226)

We aggregate (6.23) and (6.26) $\forall i \in \{1, 2, ..., N\}$, and find (6.21). Moreover, the aggregated leader-follower cost function can be obtained based on (6.22) and (6.25):

$$J(\xi(0)) = \int_0^\infty \{\xi^T \tilde{Q} \xi + \tau^T \tilde{R} \tau + \theta^T \tilde{S} \theta + F_{tM}^T \tilde{R} F_{tM} + G_{tM}^T \tilde{S} G_{tM}^T\} dt$$

We know that the optimal control and fictitious control signals $\tau = \tau^\star$ and $\theta = \theta^\star$ achieves the minimum $J(\xi(0))$ subject to (6.21) such that the Hamilton-Jacobi-Bellman equation $\min_{\tau,\theta}\{\xi^T \tilde{Q} \xi + \tau^T \tilde{R} \tau + \theta^T \tilde{S} \theta + F_{tM}^T \tilde{R} F_{tM} + G_{tM}^T \tilde{S} G_{tM}^T\} + J_\xi^T (\tilde{A}\xi + \tilde{B}_m \tau + \tilde{B}_u \theta)\} = 0$ is satisfied where $J_\xi = \frac{\partial J(\xi)}{\partial \xi}$. In the rest, we show that, in the presence of nonlinearly interconnected modeling uncertainties, the closed-loop system (6.20) will be stabilized using only τ (i.e., without implementing the fictitious control signal θ).

We introduce a candidate Lyapunov function for $t \geq 0$:

$$V(\xi(t)) = \xi^T(t) \tilde{P}_2 \xi(t) \succ 0$$

$$V(\xi(0)) = J(\xi(0)) = \min_{\tau,\theta} \int_0^\infty \{\xi^T \tilde{Q} \xi + \tau^T \tilde{R} \tau + \theta^T \tilde{S} \theta + F_{tM}^T \tilde{R} F_{tM} + G_{tM}^T \tilde{S} G_{tM}^T\} dt'$$

subject to (6.21) (where $V(\xi(0)) = J(\xi(0))$). Hence, the control and fictitious control gains of this theorem are such that the triple (ξ, τ, θ) satisfies the following three equalities:

$$\begin{aligned} \xi^T \tilde{Q} \xi + \tau^T \tilde{R} \tau + \theta^T \tilde{S} \theta + F_{tM}^T \tilde{R} F_{tM} + G_{tM}^T \tilde{S} G_{tM}^T + V_\xi^T (\tilde{A}\xi + \tilde{B}_m \tau + \tilde{B}_u \theta) &= 0 \\ 2\tau^T (\tilde{R} + \tilde{R}^\tau) + V_\xi^T \tilde{B}_m &= \mathbf{0} \\ 2\theta^T \tilde{S} + V_\xi^T \tilde{B}_u &= \mathbf{0} \end{aligned}$$

Now, along the uncertain trajectory (6.20), we find:

$$\begin{aligned} \dot{V}(\xi) \quad &\leq -x_0^T (Q_0 - K_0^T R^{u_0} K_0 - L_0^T S_0 L_0) x_0 \\ &\quad - \textstyle\sum_{i=1}^N e_i^T (Q - R^{\tau e} - 2K^T R K - 2L^T S L) e_i \end{aligned}$$

where we have used the definition of $\tilde{E}$, given by (6.20), to find $-2\tau^T(\tilde{R}+\tilde{R}^\tau)\tilde{E}\tau \leq 2\nu^T \bar{R} \nu$.

We know that $\dot{V}(\xi) \prec 0$ whenever the conditions (6.24) and (6.27) are satisfied. Therefore, based on the Lyapunov Theorem 2.3.1, and recalling the fact that there is no hidden undamped mode (see the proof of Theorem 6.5.1), the origin of closed-loop multiagent system (6.20) (with interconnected nonlinear modeling uncertainties) is asymptotically stable. If we set $a_1 = \min(\lambda_{min}(\lambda_{min}(P_{2l}), \lambda_{min} P_{2f}))$, $a_2 = \max(\lambda_{max}(P_{2l}), \lambda_{max}(P_{2f}))$, $a_3 = \min(\lambda_{min}(Q_0 - K_0^T R^{u_0} K_0 - L_0^T S_0 L_0), \lambda_{min}(Q - R^{\tau e} - 2K^T R K - 2L^T S L))$, and $b = 2$ in theorem 2.3.2, we can prove the exponential stability of the origin. Equivalently, based on the proposed reformulation of this section, we conclude that the distributed decoupling of agents (6.3) is also

guaranteed in the presence of mixed matched and unmatched unknown nonlinear couplings is achieved over two fixed graphs $\mathcal{G}_a$ and $\mathcal{G}_c$, and using two static gains K_0 and K.

6.5.3 Proof of Corollary 6.1.1 (page 228)

Based on the Gershgorin disk Theorem 2.1.1 we know that $\mu_{aN} \leq 2N-1$, $\mu_{cN} \leq 2N-1$, and $\lambda_{max}(b_a b_a^T) \leq N$. Still all eigenvalues of the symmetric matrix $\bar{E} = \bar{E}^T = ((\frac{\mathcal{H}_c}{2N-1} - I_N) \otimes I_{n_z})$ in (6.20) belong to the interval $(-1, 0]$ (a zero eigenvalue exists only if $\mu_{cN} = 2N-1$). Therefore, in the proof of Theorem 6.1.2, the inequality $V_\xi^T \tilde{B}_m \tilde{E} \tau \leq 2\nu^T \bar{R} \nu$ is still satisfied. Thus, the rest remains valid.

6.5.4 Proof of Theorem 6.2.1 (page 237)

We already have designed the required control gain K in (6.31) for a multiagent system of (6.28). Moreover, we do not need to "physically" implement the leader's controller u_0, because it is a virtual agent. Thus, the main claim of this theorem is about globally achieving exponential stability of the closed-loop multiagent system in the presence of coupled modeling uncertainties δ_u and δ_x in (6.28), without implementing the fictitious controllers τ, θ, and ρ as either physical or virtual controllers. In order to prove this claim, we propose a candidate Lyapunov function:

$$\Omega(\xi) = \xi^T(t) \tilde{P} \xi(t) \succ 0 \tag{6.50}$$

where $\tilde{P} = diag\{P_0, \bar{P}\}$, $\bar{P} = I_N \otimes P$, and P_0 and P are positive definite solutions of AREs in Design procedure 6.2.1.

In order to use (6.50) as the required Lyapunov function, we need to find its time deviation along the uncertain trajectory (6.36). We use the fact that $\Omega(\xi(0)) = J(\xi(0))$ is satisfied as a boundary condition and $J(\xi(0))$ is given in Property 6.2.2. Thus, using the gains in Design procedure 6.2.1, the triple the conditions of Remark 6.2.1 are satisfied, and we find:

$$\xi^T\tilde{Q}\xi+\sigma^T\tilde{R}\sigma+\tau^T\bar{S}\tau+\theta^T\bar{W}\theta+\rho^T\bar{V}\rho+\delta_{uM}^T\bar{S}\delta_{uM}+\delta_{xM}^T\bar{W}\delta_{xM}+\delta_{u_0M}^T\bar{V}\delta_{u_0M}+\Omega_\xi^T\dot{\xi}=0 \tag{6.51}$$

where $\Omega_\xi = \frac{\partial\Omega}{\partial\xi}$, and $\dot{\xi} = \tilde{A}\xi + \tilde{B}_m\sigma + \tilde{B}_u\tau + \tilde{B}_x\theta + \tilde{B}_{u_0}\rho$ based on the auxiliary dynamics (6.37) (we re-emphasize that Property 6.2.2 is satisfied for the auxiliary model (6.44) that is the same as (6.37)). Also, we know:

$$\begin{aligned} 2\sigma^T\tilde{R}_f + \Omega_\xi^T\tilde{B}_m = \mathbf{0}, \qquad 2\tau^T\bar{S} + \Omega_\xi^T\bar{B}_u = \mathbf{0} \\ 2\theta^T\bar{W} + \Omega_\xi^T\bar{B}_x = \mathbf{0}, \qquad 2\rho^T\bar{V} + \Omega_\xi^T\bar{B}_{u_0} = \mathbf{0} \end{aligned} \tag{6.52}$$

Consequently, along the uncertain trajectory (6.36), we write $\dot{\Omega}(\xi)$ as follows:

$$\begin{aligned} \dot{\Omega}(\xi) \;&\leq -\xi^T\tilde{Q}\xi - \sigma^T\tilde{R}\sigma + 2\tau^T\bar{S}\tau + 2\theta^T\bar{W}\theta + 2\rho^T\bar{V}\rho \\ &\quad - (\tau+\delta_u)^T\bar{S}(\tau+\delta_u) - (\delta_{uM}^T\bar{S}\delta_{uM} - \delta_u^T\bar{S}\delta_u) \\ &\quad - (\theta+\delta_x)^T\bar{W}(\theta+\delta_x) - (\delta_{xM}^T\bar{W}\delta_{xM} - \delta_x^T\bar{W}\delta_x) \\ &\quad - (\rho+\delta_{u_0})^T\bar{V}(\rho+\delta_{u_0}) - (\delta_{u_0M}^T\bar{V}\delta_{u_0M} - \delta_{u_0M}^T\bar{V}\delta_{u_0M}) \\ &\leq -x_0^TQ_0x_0 - \textstyle\sum_{i=1}^N e_i^T(Q + K^TRK - 2G^TSG - 2H^TWH - 2L^TVL)e_i \end{aligned}$$

which has been found based on some manipulations using (6.51) and (6.52), and noting that $-2\sigma^T\tilde{R}_f\tilde{E}_m\sigma = -2\nu^T\bar{R}\bar{E}_m\nu \leq 0$ (see Property 6.2.1.a and recall

that $\bar{R}_f = I_N \otimes R_f \succ \mathbf{0}$). Thus, whenever (6.49) is satisfied, we can show that the exponential stability is achieved for a multiagent system agents (6.28) with state- and input-coupled modeling uncertainties, and independent of the agents' initial state values. (In Theorem 2.3.2, set $a_3 = \min(\lambda_{min}(Q_0), \lambda_{min}(Q + K^T R K - 2G^T S G - 2H^T W H - 2L^T V L))$. Other parameters are easy to find.)

6.5.5 Proof of Corollary 6.3.1 (page 241)

We use Gershgorin disk Theorem 2.1.1 to find that the maximum eigenvalue of an undirected graph's Laplacian matrix satisfies $\lambda_N \leq 2(N-1)$. Additionally, we know that its smallest positive eigenvalue satisfies $\lambda_2 \geq 2\eta(\mathcal{G})(1 - cos(\frac{\pi}{N}))$ (see Section III in [79] about the spectrum of graphs[4]). Here, $\eta(\mathcal{G})$ denotes the edge connectivity of $\mathcal{G}$ which is the minimum number of edges whose removal results in a disconnected graph. For an unknown graph, we take $\eta(\mathcal{G}) = 1$ and substitute λ_2 by $2(1 - cos(\frac{\pi}{N}))$ to find a fixed-gain fully distributed algorithm. We note that $\bar{E} = ((\frac{\Lambda_d}{2(1-cos(\frac{\pi}{N}))} - I_{N-1}) \otimes I_{n_u}) \succcurlyeq ((\frac{\Lambda_d}{\lambda_2} - I_{N-1}) \otimes I_{n_u}) \succcurlyeq \mathbf{0}$. Thus, the results of Section 5.2 are still valid.

[4]This is a standard property of undirected graphs and was taken from Bollobas B, *Modern Graph Theory*, Springer, 2002. However, we have found it in [79].

Chapter 7

Distributed Tracking in Physically Coupled Multiagent Systems with Unknown Coupling Structures

In Chapters 3, we proposed a one-step control-theoretic strategy to design distributed consensus algorithms ensuring leaderless and leader-follower collective behavior in multiagent systems in the presence of various sources of modeling mismatch. While agents could reach agreement, in simulation, we showed that ensuring leaderless consensus was not sufficient for the control of multi-vehicle and multi-robot systems in the presence of (road profile or wind) disturbances which, by persistently exciting the null space of multi-agent system's collective dynamics (agreement subspace), resulted in continuous increase in the vehicle's speed. To

overcome this issue using the same tool, in Chapter 4, we further developed stationary consensus algorithms by which all vehicles or robots could reach agreement on velocity and position, and stop at a fixed point. In Chapter 5, we used this tool for the distributed stabilization purpose in multiagent systems with linear interconnected modeling uncertainties. In Chapter 6, we further generalized this approach for the stabilization problem in multiagent systems with interconnected nonlinear modeling uncertainties. The ideas of Chapter 6 could be viewed as the two-layer distributed control of multiagent systems with uncertain agent-layer model and a-priori known control-layer communication topology among agents. In fact, although we did not use it, this latter layer provided a design degree of freedom to improve the closed-loop interconnected multiagent systems' behavior.

In this chapter, we consider robust *cooperative tracking* problem (vs. the stability problem in Chapters 5 and 6) for three classes of heterogeneous nonlinear multiagent systems: first-, second-, and mixed first- and second-order agents in which each subsystem is equipped with appropriate sensing, computation, and communication technologies. Based on a cyber-physical viewpoint where assuming a completely-known system is unrealistic, we propose a multi-layer framework in which the physical agent-layer's interconnected dynamics are described by partially-known time-varying nonlinearities, and the control-layer should be designed to track a reference command that is sent to only a few agents. We propose three linear cooperative tracking problems and, by treating each inter-agent communication link as a proportional gain (controller), reformulate them as control-layer topology and communication strength co-design challenges to be addressed based on the modified LQR problems with globally coupled cost functions. At

first, we use matrix-algebraic tools and derive analytical solution for the control-layer communication topology of multiagent systems with first-order agent-layer interconnected dynamics. Then, for multiagent systems with physically-coupled second- or mixed-order agents, we use this result and find closed-form solutions for the multi-layer communication topology design challenges. In particular, we show that each communication (sub-) topology of the control-layer can be designed based on a nonlinear matrix equation that has the same structure as in the first-order problem.

We also provide several algorithms to systematically find the structurally non-symmetric graph topologies to be used in the proposed linear cooperative tracking protocols. In addition to robust tracking, we prove the proposed multi-layer linear distributed protocols guarantee an upper-bound on quadratic cost functions and provide degrees of freedom to adjust tracking convergence rate as performance criteria. For the existing (known) communication digraphs, we further unify these results and propose systematic approaches to find bounds on the maximum tolerable nonlinear uncertainties in the agent-layer dynamics. We also investigate guaranteed-cost control-layer design problems relying on the results of this chapter.

The rest of this chapter is organized as follows. In Section 7.1, although we rely on the preliminaries of Chapter 2, we introduce a few definitions and symbols which are devoted to only this chapter. In Section 7.2, we propose the main results of this chapter on multi-layer distributed tracking for first-, second-, and mixed-order interconnected multiagent systems. In Section 7.3, we verify the feasibility of these theoretical results through simulation studies. In Section 7.4, along with

some relevant references from the literature, we provide concluding remarks on the proposed viewpoint of this chapter.

7.1 Notation

The symbol $[A]_{sym} = \frac{A+A^T}{2}$ represents the symmetric component of matrix A, and *exp* denotes exponential function. For vector $x \in \mathbb{R}^n$, the element-wise inequality $x > \mathbf{0}$ means all entries of x are positive scalars, and $x \geq \mathbf{0}$ represents a vector with non-negative entries and at least one positive value. A nonsingular M-matrix $A = [a_{ij}] \in \mathbb{R}^{n\times n}$ is defined by the property $A = sI_n - B$ where $s > \rho(B)$ and ρ is the spectral radius of $B \geq \mathbf{0}$ (all entries of B are non-negative real numbers). Inverse of an M-matrix A satisfies $A^{-1} \geq \mathbf{0}$. The principal square root of matrix $A \in \mathbb{R}^{n\times n}$, that has no eigenvalue in the left-hand side of complex plane, is denoted by $A^{1/2}$ with all eigenvalues in the right half of complex plane. The principal square root of a nonsingular M-matrix is a nonsingular M-matrix with positive eigenvalues.

This chapter is based on the weighted digraph $\mathcal{G}(\mathcal{V}, \mathcal{E}, \mathcal{A})$ with a node set $\mathcal{V}$, edge set $\mathcal{E}$, and weighted adjacency matrix $\mathcal{A} = [a_{ij}]$ where $a_{ij} \geq 0$ denotes the weight of edge $(j, i) \in \mathcal{E}$ for $i, j \in \mathcal{V}$, and $a_{ii} = 0$ (this definition does not admit self loops). A weighted digraph $\mathcal{G}$ is *structurally symmetric* whenever the corresponding $0-1$ adjacency matrix is symmetric. A $0-1$ adjacency matrix can be found if we replace $a_{ij} > 0$ by 1 in the adjacency matrix $\mathcal{A}$. A *graph Laplacian matrix* $\mathcal{L} \in \mathbb{R}^{N_{nodes}\times N_{nodes}}$ is determined by $\mathcal{L}_{ij} = -a_{ij}$ and $\mathcal{L}_{ii} = \sum_{j=1}^{N_{nodes}} a_{ij}$. In particular, based on the reference-agent tracking problem of this chapter with

$N_{nodes} = N_a + 1$ and N_a agents, $\mathcal{G}^{ra}$ is abstracted by graph Laplacian matrix $\mathcal{L}^{ra} \in \mathbb{R}^{(N_a+1)\times(N_a+1)}$ which is partitioned as follows:

$$\mathcal{L}^{ra} = \begin{bmatrix} 0 & \mathbf{0} \\ -b^a & \mathcal{H}^a \end{bmatrix}, \quad \mathcal{H}^a = \mathcal{L}^a + \mathcal{B}^a, \quad \mathcal{B}^a = diag\{b^a\}$$

where the first row corresponds to the reference generator, $\mathcal{L}^a \in \mathbb{R}^{N_a \times N_a}$ denotes the inter-agent graph Laplacian matrix, $b^a = col\{b_i^a\} \in \mathbb{R}^{N_a}$, and b_i^a represents the directed edge from reference generator to i^{th} agent. Since, the condition $\mathcal{L}\mathbf{1}_{N_\star} = \mathbf{0}$ holds in any graphs with $N_\star$ nodes, we can completely characterize $\mathcal{G}^{ra}$ based on our knowledge about $\mathcal{H}^a \in \mathbb{R}^{N_a \times N_a}$ and, therefore, we name $\mathcal{H}^a$ a *reduced-order Laplacian matrix* (note that $\mathcal{H}_a \mathbf{1}_N = b^a$).

Remark 7.1.1. *We consider two agent- and control-layer graphs which are specified by sub- or super-script a and c, respectively. Each layer may include various graphs for the agents' first and second state variables x and v that are respectively distinguished by sub- or super-script x and v. Let $\star \in \{x, v\}$. We do not need to completely know the topologies of $\mathcal{G}_{a\star}$ in the proposed algorithms; however, we assume the induced 2-norms $\|\mathcal{L}_{a\star}\|_2 \geq 0$ are known scalars in which $\mathcal{L}_{a\star} \in \mathbb{R}^{N\times N}$ denotes the Laplacian matrix corresponding to $\mathcal{G}_{a\star}$ and N is the total number of agents. The agent-layer graph $\mathcal{G}_{a\star}$ visualizes interconnection in multiagent systems and the physical neighboring set $\mathcal{N}_i^{a\star}$ includes the list of agents that share their variables with the i^{th} agent. The control-layer digraphs $\mathcal{G}_{c\star}$ are initially unknown and left to be determined.* □

7.2 Main results

In this section, we first investigate first- and second-order distributed cooperative tracking problems in physically coupled heterogeneous multiagent systems with unknown time-varying nonlinear agent-layer dynamics. Then, we generalize these results to the cooperative tracking for mixed-order interconnected multiagent systems. In each scenario, we first propose a control-theoretic approach to design fixed control-layer communication digraph $\mathcal{G}_{cx}$ or $\mathcal{G}_{cv}$ with structurally symmetric topologies. We then extend the result and systematically design structurally non-symmetric fixed digraphs that guarantee robust stability and performance of the closed-loop multiagent system. Finally, we discuss the maximum tolerable interconnected time-varying nonlinear uncertainties by the given communication digraph to be used in the proposed linear distributed tracking algorithms, and also investigate guaranteed-cost design challenges for the given upper-bound on the linear quadratic cost function.

7.2.1 First-order cooperative tracking

In this subsection, we consider a multiagent system of N physically coupled first-order agents with heterogeneous time-varying nonlinear agent-layer dynamics:

$$\dot{x}_i(t) = f_i(z_i(t), t) + u_{xi}(t), \qquad z_i(t) = C_{xi} \sum_{j=1}^{N} a_{ij}^{ax}(x_i(t) - x_j(t)) \tag{7.1}$$

where $i \in \{1, 2, ..., N\}$ denotes agent number, and $a_{ij}^{ax} \geq 0$ represents $(i, j)^{th}$ entry of the adjacency matrix corresponding to the agent-layer x-variable (physical) coupling digraph $\mathcal{G}_{ax}$; $x_i \in \mathbb{R}$ indicates the i^{th} agent's state variable, $u_{xi} \in \mathbb{R}$ control input, and $z_i \in \mathbb{R}$ coupling variable. The nonlinear functions f_i and coupling matrices C_{xi} are unknown but satisfy the following conditions.

Assumption 7.2.1. *The nonlinear functions $f_i : \mathbb{R} \times \mathbb{R} \to \mathbb{R}$ are piecewise continuous in time and Lipschitz in state variable*[1]*, satisfy norm-bounded conditions $f_i^2(z_i, t) \leq \alpha_i z_i^2(t)$ where $\alpha_i \geq 0$ are known real-valued scalars, and $f_i(0, t) = 0$ are satisfied such that the origin is an equilibrium point of agents' unforced nonlinear dynamics. Moreover, $C_{xi} \leq \gamma_{cxi}$ for known real-valued scalars $\gamma_{cxi} \geq 0$.*

We consider a constant reference tracking problem for $i \in \{1, 2, ..., N\}$:

$$\lim_{t \to \infty} (x_i(t) - r) = 0 \tag{7.2}$$

where the reference signal $r \in \mathbb{R}$ is sent to only a few agents. This reference r can be generated by a command generator or virtual leader:

$$\dot{x}_0(t) = 0 \tag{7.3}$$

which is initialized at $x_0(0) = r$, and $x_0 \in \mathbb{R}$ denotes the command generator's state variable. We need to design a communication algorithm such that all agents cooperatively track the reference signal or, equivalently, agree on the command generator's state variable: $\lim_{t \to \infty}(x_i(t) - x_0(t)) = 0$.

[1]We do not directly use Lipschitz condition in this chapter's derivations. But it is required to ensure the existence and uniqueness of solutions.

We propose a cooperative tracking algorithm:

$$u_{xi}(t) = -(\sum_{j=1}^{N} a_{ij}^{cx}(x_i(t) - x_j(t)) + b_i^{cx}(x_i(t) - x_0(t))) \tag{7.4}$$

where $a_{ij}^{cx}, b_i^{cx} \geq 0$ denote the weights of control-layer x-variable communication (information exchange) graph, and should be designed to ensure robust first-order tracking (7.2) with a guaranteed upper-bound on the following quadratic cost function[2]:

$$\mathcal{J}_1(e_x(0)) = \int_0^{\infty} (e_x^T(t)Q_x e_x(t) + u_x^T(t)R_x u_x(t))dt \leq e_x^T(0)\mathcal{P}_1 e_x(0) \tag{7.5}$$

where $e_x = col\{e_{xi}\} \in \mathbb{R}^N$ and $e_{xi} = x_i - x_0$ denotes the i^{th} agent's x-variable reference tracking error, and $u_x = col\{u_{xi}\} \in \mathbb{R}^N$. Also, the $M-$matrix $Q_x = Q_x^T \in \mathbb{R}^{N\times N} \succ \mathbf{0}$ and $R_x = R_x^T = diag\{r_{xi}\} \in \mathbb{R}^{N\times N} \succ \mathbf{0}$ (with real-valued scalars $r_{xi} > 0$) are two design matrices to respectively weight the state tracking error and control input variables. The constant matrix $\mathcal{P}_1 = \mathcal{P}_1^T \in \mathbb{R}^{N\times N} \succ \mathbf{0}$ is either unknown (to be found) or given a-priori as will be discussed later in this subsection. We drop the time variable t for the sake of readability.

Remark 7.2.1. *In this subsection, we seek robust cooperative tracking and performance in time-varying nonlinear multiagent systems of first-order interconnected agents based on the linear protocol* (7.4)*. This is a multiagent system-level design problem and includes conventional node-wise consensus algorithm*

[2]Due to the presence of coupled modeling uncertainties, we cannot explicitly find the exact minimum value of this cost. Thus, we propose a guaranteed cost problem.

$u'_{xi}(t) = -k_{cx}(\sum_{j=1}^{N} a'_{ij}(x_i(t) - x_j(t)) + b'_i(x_i(t) - x_0(t)))$ *as a special case (with known* $a'_{ij}, b'_i \geq 0$ *and unknown consensus gain* k_{cx} *to be designed).* □

In order to design a control-layer graph topology $\mathcal{G}_{cx}$, we first rewrite the agent's dynamics (7.1) based on the x-variable tracking error:

$$\dot{e}_{xi} = f_i(z_i) + u_{xi} \quad and \quad z_i = C_{xi} \sum_{j=1}^{N} a_{ij}^{ax}(e_{xi} - e_{xj})$$

and, similarly, find a new representation for the cooperative tracking protocol (7.4):

$$u_{xi} = -(\sum_{j=1}^{N} a_{ij}^{cx}(e_{xi} - e_{xj}) + b_i^{cx} e_{xi})$$

Over the agent-layer coupling digraph $\mathcal{G}_{ax}$, we find the aggregated tracking error dynamics:

$$\dot{e}_x = f(z) + u_x \quad and \quad z = C_x \mathcal{L}_{ax} e_x \tag{7.6}$$

where $z = col\{z_i\}$, $f(z) = col\{f_i(z_i)\}$, and $C_x = diag\{C_{xi}\}$. We also find the aggregated cooperative tracking signal over $\mathcal{G}_{cx}$:

$$u_x = -\mathcal{H}_{cx} e_x \tag{7.7}$$

in which $\mathcal{H}_{cx}$ denotes the reduced-order Laplacian matrix corresponding to $\mathcal{G}_{cx}$ which should be appropriately designed.

In the following design procedure, we propose a control-theoretic approach and find candidate communication graph topology $\mathcal{G}_{cx}$ to be used in distributed tracking algorithm (7.4). Let $Q_{xm} = Q_{xm}^T = Q_x + R_{xf} \succ \mathbf{0}$ be an M-matrix, $R_{xf} = r_{xf} I_N$, and $r_{xf} = \max_i\{r_{xi}\alpha_i\gamma_{cxi}^2\}\|\mathcal{L}_{ax}\|^2$ for $i \in \{1, 2, ..., N\}$.

Design procedure 7.2.1. *Let $\mathcal{U}_{1m}$ be the set of all admissible stabilizing control signals for a completely known dynamical system in the modified LQR problem* (7.8)*, and $u_x = K_x e_x$ be the control signal that minimizes this quadratic cost function. The reduced-order Laplacian matrix $\mathcal{H}_{cx} = -K_x = R_x^{-1}P$ characterizes the candidate communication-layer graph topology $\mathcal{G}_{cx}$ for first-order tracking problem* (7.2) *if the solution $P = P^T \in \mathbb{R}^{N\times N} \succ \boldsymbol{0}$ of $N \times N$ nonlinear matrix equation* (7.9) *satisfies the condition* (7.10)*.*

$$\begin{aligned} \min_{u_x \in \mathcal{U}_{1m}} \quad & J_{1m}(e_x(0)) = \textstyle\int_0^\infty (e_x^T Q_{xm} e_x^T + u_x^T R_x u_x) dt \\ \textit{subject to} \quad & \dot{e}_x = u_x \end{aligned} \tag{7.8}$$

$$Q_{xm} - P R_x^{-1} P = \boldsymbol{0} \tag{7.9}$$

$$P \boldsymbol{1}_N \geq 0 \tag{7.10}$$

The reason to impose an additional condition (7.10) on the positive definite $M-$matrix P will be clarified later in this subsection. In the next remark, we explain a few facts about Design procedure 7.2.1.

Remark 7.2.2. *In the standard LQR problem* (2.23)*, both state and input weighting matrices can be arbitrarily tuned as two design degrees of freedom. We name the minimization* (7.8) *a "modified LQR" problem because, although $Q_x \succ \boldsymbol{0}$ and $R_x \succ \boldsymbol{0}$ are still two design matrices, we should necessarily use a modified state weighting matrix Q_{xm} which depends on R_x and our partial knowledge about interconnected nonlinearities (see Remark 7.1.1 and Assumption 7.2.1). Furthermore, note that the quadratic cost function* (7.8) *is minimized subject to a completely*

known physically "decoupled" multiagent system of integrators, although the original cost function (7.5) *is given based on the unknown trajectories of interconnected agents* (7.1)*. This modified LQR problem can be solved based on the nonlinear matrix equation* (7.9) *that is a "standard" ARE for which powerful numerical solvers exist. Finally, the existence of a unique stabilizing* $P \succ \boldsymbol{0}$ *depends on observability and stabilizability of the triple* $(C_{xm}, \boldsymbol{0}, I_N)$ *where* $C_{xm}^T C_{xm} = Q_{xm}$. □

It is possible to directly solve ARE (7.9) using existing software packages and recommend a candidate $\mathcal{H}_{cx}$. However, we further propose an analytical representation for the candidate $\mathcal{G}_{cx}$ which handles computational complexities in solving this ARE for multiagent systems with a high number of agents. This closed-form solution can also be used to appropriately select state and input weighting matrices Q_x and R_x that ensure robust cooperative tracking (7.2) with a desired-level of robust performance in (7.5). From a matrix-algebraic viewpoint, the unique symmetric positive definite stabilizing solution of nonlinear matrix equation (7.9) can be written as follows:

$$P = R_x^{1/2}(R_x^{-1/2}Q_{xm}R_x^{-1/2})^{1/2}R_x^{1/2} \tag{7.11}$$

where $R_x^{1/2} = diag\{\sqrt{r_{xi}}\}$, and the principal square root of $R_x^{-1/2}Q_{xm}R_x^{-1/2}$ can be calculated using the approach in Subsection 7.1 and necessarily is a positive definite symmetric M-matrix. Thus, based on Design procedure 7.2.1, we suggest the following reduced-order Laplacian matrix as the candidate graph topology $\mathcal{G}_{cx}$ of this subsection:

$$\mathcal{H}_{cx} = R_x^{-1/2}(R_x^{-1/2}Q_{xm}R_x^{-1/2})^{1/2}R_x^{1/2} \tag{7.12}$$

This candidate $\mathcal{H}_{cx}$ is obtained based on a non-diagonal $N \times N$ matrix Q_x which corresponds to a global coupled cost function J_{1m} in (7.8). Alternatively, we may consider a set of N decoupled cost functions by letting $Q_x = diag\{q_{xi}\}$ with $q_{xi} > 0$ and, consequently, $Q_{xm} = diag\{q_{xmi}\}$ with $q_{xmi} = q_{xi} + r_f$ for $i \in \{1, 2, ..., N\}$. We define $A = \mathbf{0}$ and $B = I_N$, and use the matrix differential equation (2.29) to decompose the optimal control signal u_x of Design procedure 7.2.1 into a set of N decoupled control gains $K_x = diag\{\frac{P_i}{r_i}\}$ where $P_i = \sqrt{r_i q_{xmi}} \in \mathbb{R} > 0$ are the solutions of N scalar AREs $q_{xmi} - r_i P_i^2 = 0$. Then, we find:

$$\mathcal{H}_{cx} = diag\{\sqrt{\frac{q_{xmi}}{r_{xi}}}\} \tag{7.13}$$

Indeed, in the sense of the modified LQR problem in Design procedure 7.2.1, this proves our initial guess that $J_{1m}(e(0)) = \sum_1^N J_{1mi}(e_{xi}(0))$ subject to $\dot{x} = u_x$ with a set of N local cost functions $J_{1mi}(e_{xi}(0)) = \int_0^\infty (q_{xmi} e_{xi}^2 + r_{xi} u_{xi}^2) dt$ (subject to completely known decoupled integrators $\dot{x}_i = u_{xi}$) could be minimized independently using N scalar modified LQR problems. By the definition of reduced order Laplacian matrix in Subsection 7.1 , we know $\mathcal{H}_{cx} = \mathcal{L}_{cx} + \mathcal{B}_{cx}$. Since the off-diagonal terms of $\mathcal{H}_{cx}$ in (7.13) are equal to zero, we conclude the inter-agent graph Laplacian matrix $\mathcal{L}_{cx}$ is zero. Thus, $\mathcal{H}_{cx} = \mathcal{B}_{cx} = diag\{b_{xi}^c\}$ where $b_{xi}^c \in \mathbb{R}^N$ represents directed edge from the command generator to i^{th} agent weighed by $\sqrt{\frac{q_{xmi}}{r_{xi}}}$ for $i \in \{1, 2, ..., N\}$.

Independent of the structure of Q_{xm} and R_x in Design procedure 7.2.1, we know $\mathcal{G}_{cx}$ satisfies the next property which is adapted based on the fundamental properties of infinite horizon optimal control design.

Property 7.2.1. *The candidate graph topology $\mathcal{G}_{cx}$ in Design procedure 7.2.1, formulated by the reduced-order Laplacian matrix $\mathcal{H}_{cx}$, results in a pair (e_x, u_x) with $u_x = -\mathcal{H}_{cx} e_x$ that satisfies the following equalities:*

$$\begin{aligned} e_x^T Q_{xm} e_x + u_x^T R_x u_x + J_{1m,e_x}^{\star T} u_x &= 0 \\ 2u_x^T R_x + J_{1m,e_x}^{\star T} &= \boldsymbol{0} \end{aligned}$$

where $J_{1m}^{\star T}$ is the optimal cost in (7.8)*, and $J_{1m,e_x}^{\star} = \frac{\partial J_{1m}^{\star}}{\partial e_x}$.*

We now need to discuss the feasibility of these analytical solutions as reduced-order graph Laplacian matrix by verifying that $\mathcal{H}_{cx}$ is an M-matrix, all of its eigenvalues are in the right half plane, and it has non-negative row sums with at least one positive entry (i.e., $\mathcal{H}_{cx}\mathbf{1}_N \geq \mathbf{0}$). The reduced-order Laplacian matrix (7.13) satisfies all requirements and is necessarily a feasible star topology for the control-layer communication graph whenever all agents have access to the reference command. Regarding the candidate topology (7.12), we note that the unique solution of ARE (7.9) can be "represented" in various equivalent manners: $P = Q_{xm}(R_x^{-1}Q_{xm})^{-1/2}$ and $P = (Q_{xm}R_x^{-1})^{-1/2}Q_{xm}$ in addition to the apparently symmetric representation (7.11). We choose the design M-matrices Q_x and R_x such that all eigenvalues of $R_x^{-1}Q_{xm}$ are in the right half plane. Then $P = Q_{xm}(R_x^{-1}Q_{xm})^{-1/2}$ results in $\mathcal{H}_{cx} = (R_x^{-1}Q_{xm})^{1/2}$ which is necessarily an M-matrix with all eigenvalues in right-half plane (by definition of principal square root for M-matrices). The third requirement on row sums is already guaranteed by condition (7.10) and noticing the fact $\mathcal{H}_{cx} = R_x^{-1}P$. Based on this discussion, we can discuss the effect of design matrices on the candidate topology $\mathcal{G}_{cx}$ based

on the closed-form solution of ARE (7.9). We first use $P = (Q_{xm}R_x^{-1})^{-1/2}Q_{xm}$ and find $\mathcal{H}_{cx} = R_x^{-1}(Q_{xm}R_x^{-1})^{-1/2}Q_{xm}$ that indicates $\mathcal{H}_{cx}\mathbf{1}_N > \mathbf{0}$ for any M-matrices that satisfy $Q_{xm}\mathbf{1}_N > \mathbf{0}$ because $(Q_{xm}R_x^{-1})^{-1/2} \geq \mathbf{0}$ (a property of M-matrices); nevertheless, this means a directed communication link exists between the reference generator to each agent. On the other hand, we can look at $P\mathbf{1}_N = (Q_{xm}R_x^{-1})^{-1/2}(Q_{xm}\mathbf{1}_N) \geq \mathbf{0}$ as a non-negative matrix times a vector with "a few negative entries" and iteratively search for a positive definite M-matrix Q_x that results in the row-sum vector of modified state weighting matrix Q_{xm} has a few zero or negative values as its entries. Although we can follow this idea and iteratively search for an $\mathcal{H}_{cx} = R_x^{-1}P$ with a few reference-to-agent connections, it is still a heuristic approach rather than a systematic one and, further, is limited to structurally symmetric control-layer topology $\mathcal{G}_{cx}$. In the next algorithm, we address these issues by proposing a systematic framework to design structurally non-symmetric weighted digraph $\mathcal{G}_{cx}$ to be used in the first-order cooperative tracking algorithm (7.4). We further find the associated cost function in modified LQR problem (7.8).

Algorithm 7.2.1. *Select an arbitrary symmetric reduced-order Laplacian matrix $\mathcal{H}_x^{alg} \in \mathbb{R}^{N\times N}$ and a diagonal input weighting matrix $R_x \in \mathbb{R}^{N\times N}$. Then,*

1. *Structurally symmetric control-layer: $\mathcal{H}_{cx}^{alg} = R_x^{-1}\mathcal{H}_x^{alg}$ minimizes quadratic cost function (7.8) with weighting matrices $Q_{xm} = (\mathcal{H}_{cx}^{alg})^T R_x \mathcal{H}_{cx}^{alg}$ and R_x. If the modified state weighting matrix can be decomposed as $Q_{xm} = Q_x + R_{xf}$ with $Q_x = Q_x^T \succ \boldsymbol{0}$, then $\mathcal{H}_{cx} = \mathcal{H}_{cx}^{alg}$ represents the required candidate graph topology $\mathcal{G}_{cx}$ of this subsection associated to quadratic cost function (7.8) with a pair (Q_{xm}, R_x). This candidate topology satisfies Property 7.2.1.*

2. *Structurally non-symmetric control-layer: define the modification matrix* $\mathcal{H}_{cx}^{algm} \in \mathbb{R}^{N\times N}$ *with non-zero elements at entries corresponding to these undesirable edges such that* $\mathcal{H}_{cx} = \mathcal{H}_{cx}^{alg} + \mathcal{H}_{cx}^{algm}$ *characterizes the desirable communication graph topology*[3]. *Then, the matrix* $\mathcal{H}_{cx}$ *represents structurally non-symmetric candidate communication graph* $\mathcal{G}_{cx}$ *if the condition* $Q_x + 2[(\mathcal{H}_{cx}^{alg})^T R_x \mathcal{H}_{cx}^{algm}]_{sym} \succ \boldsymbol{0}$ *is satisfied. Note that Property 7.2.1 is satisfied by only* $\mathcal{H}_{cx}^{alg}$ *of Step 1.* □

The candidate $\mathcal{G}_{cx}$ of this subsection has been designed based on a completely-known multiagent system of integrators. In the next theorem, we prove the proposed cooperative tracking protocol (7.4) over the fixed structurally non-symmetric candidate communication digraph $\mathcal{G}_{cx}$ of Algorithm 7.2.1 ensures first-order robust cooperative tracking (7.2) with an exponential behavior, and guarantees an upper-bound on quadratic cost function (7.5) subject to a multiagent system of first-order agents (7.1) with unknown coupled time-varying nonlinear agent-layer dynamics. We define $\kappa = \sqrt{\frac{\lambda_{max}(P)}{\lambda_{min}(P)}}$ and $\sigma = \frac{\lambda_{min}(Q_x + 2[(\mathcal{H}_{cx}^{alg})^T R_x \mathcal{H}_{cx}^{algm}]_{sym})}{2\lambda_{max}(P)}$ in $e_x(t) \leq \kappa\, exp^{-\sigma t} e_x(0)$, and:

$$\mathcal{P}_1 = P + \frac{\kappa^2}{2\sigma}(\lambda_{max}[(\mathcal{H}_{cx}^{alg})^T R_x \mathcal{H}_{cx}^{alg} + (\mathcal{H}_{cx}^{algm})^T R_x \mathcal{H}_{cx}^{algm}])I_N \succ \mathbf{0}.$$

Theorem 7.2.1. *Let Assumption 7.2.1 be satisfied by agents* (7.1). *The structurally non-symmetric candidate topology* $\mathcal{G}_{cx}$, *with static weights given by* $\mathcal{H}_{cx}$ *in*

[3]As an example, we might be interested in implementing a one-way communication from node i to j. In this case, edge (j,i) should be removed by letting all entries of $\mathcal{H}_{cx}^{algm}$ be zero except $\mathcal{H}_{cx}^{algm}(i,j) = -\mathcal{H}_{cx}^{alg}(i,j) > 0$ and $\mathcal{H}_{cx}^{algm}(i,j) = \mathcal{H}_{cx}^{alg}(i,j) < 0$.

Step 2 of Algorithm 7.2.1, ensures robust exponential cooperative tracking (7.2) *and performance* (7.5) *specified by* κ, σ, *and* $\mathcal{P}_1$.

Proof. The proof is available at Subsection 7.5.1. □

This proof remains valid for structurally symmetric topology $\mathcal{G}_{cx}$ of Design procedure 7.2.1 or Algorithm 7.2.1-Step 1 by setting $\mathcal{H}_{cx}^{algm} = \mathbf{0}$ and $\mathcal{H}_{cx}^{alg} \leftarrow \mathcal{H}_{cx}$ (i.e., $\tau_{xm} = \mathbf{0}$ and $u_x = \tau_x$ in the proof at Subsection 7.5.1).

Remark 7.2.3. *In this subsection, the matrix* $\mathcal{P}_1$ *is found purely based on the design matrices* Q_x *and* R_x, *and our partial knowledge about nonlinearities and physical coupling graphs. A similar discussion holds for the exponential convergence parameters* κ *and* σ. *This provides a guideline to systematically choose a set of design matrices that guarantee a desired level of performance in terms of "quadratic cost function minimization" and "exponential convergence rate maximization". In fact, using this latter case as a performance criterion, we address a similar challenge to that of [153]-[156] for first-order multiagent systems, yet in the presence of unknown time-varying interconnected nonlinearities.* □

Remark 7.2.4. *Whenever the topology of agent-layer coupling graph* $\mathcal{G}_{ax}$ *is known (see Remark 7.1.1), we can incorporate* $R_{xf} = R_{xf}^T = \max_i\{r_{xi}\alpha_i\gamma_{cxi}^2\}\mathcal{L}_{ax}^T\mathcal{L}_{ax} \succcurlyeq \boldsymbol{0}$ *in Design procedure 7.2.1, rewrite the results of this subsection based on a new* $Q_{xm} = Q_x + R_{xf} \succ \boldsymbol{0}$, *and follow the discussion in this subsection in order to find an appropriate control-layer communication graph. (Regarding the first inequality, we know* $x^T\mathcal{L}_{ax}^T\mathcal{L}_{ax}x = \|\mathcal{L}_{ax}x\|^2 \geq 0$ *and, regarding the second inequality, note that* $Q_x \succ \boldsymbol{0}$.*)* □

In the literature, distributed control of nonlinear multiagent systems has usually been addressed based on nonlinear techniques [50]. However, we have proposed a modified LQR problem which ensures agreement solely by sharing information over appropriately designed fixed control-layer communication topology with static weights. At this point, a question may arise about the ability of finding a bound on maximum tolerable time-varying interconnected nonlinearities f_i in (7.1) by the given fixed communication digraph $\mathcal{G}_{cx}$ to be used in linear static cooperative protocol (7.4). In the next corollary, we unify the results of this subsection and find such a bound in terms of R_{xf} defined in Design procedure 7.2.1. For a special scenario, based on the quadratic cost function (7.5), we further propose a sufficient condition to be used in performance-oriented (guaranteed-cost) communication topology design problem.

Corollary 7.2.1. *Let the structurally non-symmetric leader-follower communication digraph $\mathcal{G}_{cx}$ be represented by a constant reduced-order Laplacian matrix $\mathcal{H}_{cx}$. The time-varying interconnected nonlinearities f_i in multiagent system* (7.1) *are tolerable by information exchange algorithm* (7.4) *if the reduced-order Laplacian matrix of communication topology $\mathcal{G}_{cx}$ can be decomposed as $\mathcal{H}_{cx} = \mathcal{H}_{cx,s} + \mathcal{H}_{cx,r}$, and there exists a diagonal $R_x \succ \boldsymbol{0}$ such that the structurally symmetric reduced-order Laplacian matrix $\mathcal{H}_{cx,s}$ and residual matrix $\mathcal{H}_{cx,r}$ satisfy the following conditions:*

1. *$R_x\mathcal{H}_{cx,s}$ is a symmetric positive definite matrix,*
2. *$\mathcal{H}_{cx,s}^T R_x \mathcal{H}_{cx,s} - R_{xf} + 2[\mathcal{H}_{cx,s}^T R_x \mathcal{H}_{cx,r}]_{sym} \succ \boldsymbol{0}$,*
3. *$\mathcal{H}_{cx,s}^T R_x \mathcal{H}_{cx,s} \succ R_{xf}$ where R_{xf} is defined in Design procedure 7.2.1.*

Furthermore, for a given upper-bound matrix $\mathcal{P}_1$ *in* (7.5)*, a guaranteed-cost communication digraph* $\mathcal{G}_{cx}$ *with* $\mathcal{H}_{cx} = \mathcal{H}_{cx,s} + \mathcal{H}_{cx,r}$ *can be designed by searching for* $\mathcal{H}_{cx,s}$ *and* $\mathcal{H}_{cx,r}$ *that satisfy the aforementioned robust tracking and one robust performance conditions:*

4. $R_x\mathcal{H}_{cx,s} + \frac{\kappa^2}{2\sigma}\lambda_{max}(\mathcal{H}_{cx,s}^T R_x \mathcal{H}_{cx,s} + \mathcal{H}_{cx,r}^T R_x \mathcal{H}_{cx,r}) I_N \preccurlyeq \mathcal{P}_1$

for the exponential tracking convergence $e_i(t) \leq \kappa exp^{-\sigma t} e_i(0)$ *with constant scalars* $\kappa, \sigma > 0$ *and* $i \in \{1, 2, ..., N\}$. □

The proof is immediate based on the analyses in this subsection. We further mention that κ and σ can be conservatively estimated based on the results of Theorem 7.2.1 for any $\mathcal{H}_{cx,s}$ and $\mathcal{H}_{cx,r}$. Moreover, in addition to the degrees of freedom in decomposing $\mathcal{H}_{cx}$ into $\mathcal{H}_{cx,s}$ and $\mathcal{H}_{cx,r}$, the design matrix R_x can be used to find a higher tolerable bound in terms of R_{xf}. This observation indicates the sufficiency of conditions in this corollary and can be viewed as a foundation for future work on this topic.

7.2.2 Second-order cooperative tracking

In this subsection, we generalize the result of Subsection 7.2.1 to the second-order distributed cooperative tracking problem. For brevity, unless it is unclear from the text, we only introduce new variables and the rest can be found in the previous subsection.

We consider a multiagent system with interconnected time-varying nonlinear agent-layer dynamics:

$$\begin{aligned} \dot{x}_i(t) = v_i(t), \qquad \dot{v}_i(t) = g_i(y_i(t), t) + u_{vi}(t) \\ y_i(t) = C_{xi} \sum_{j=1}^{N} a_{ij}^{ax}(x_i(t) - x_j(t)) + C_{vi} \sum_{j=1}^{N} a_{ij}^{av}(v_i(t) - v_j(t)) \end{aligned} \tag{7.14}$$

where $a_{ij}^{vx} \geq 0$ denotes the $(i,j)^{th}$ entry of adjacency matrix corresponding to the v-variable coupling digraph $\mathcal{G}_{av}$; $v_i \in \mathbb{R}$ indicates the second state variable, and $u_{vi} \in \mathbb{R}$ represents the control input of i^{th} agent; and nonlinear functions g_i, and coupling matrices C_{xi} and C_{vi} satisfy the next assumption.

Assumption 7.2.2. *The unknown nonlinear functions $g_i : \mathbb{R} \times \mathbb{R} \to \mathbb{R}$ satisfy the same conditions as in Assumption 7.2.1 replacing f_i by g_i, α_i by β_i, and z_i by y_i. Similarly, we consider the replacement of γ_{cxi} by γ_{cvi} for the unknown coupling matrices C_{vi}. Moreover, $C_{xi} \leq \gamma_{cxi}$ is also satisfied.*

We consider two types of reference commands $r_{cx}(t)$ and r_v with constant and ramp waveforms, and propose the following cooperative reference tracking problem:

$$\lim_{t\to\infty}(x_i(t) - r_{cx}(t)) = 0 \quad \textit{and} \quad \lim_{t\to\infty}(v_i(t) - r_{cv}) = 0 \tag{7.15}$$

that should be satisfied by all agent $i \in \{1, 2, ..., N\}$, although each command might be sent to only a few agents over its own control-layer communication graph. We note that these commands can be generated by the reference generator (virtual leader):

$$\dot{x}_0(t) = v_0(t) \quad \textit{and} \quad \dot{v}_0(t) = 0 \tag{7.16}$$

in which the initial state values are two manipulable variables: $v_0(t) = v(t_0) = r_v$ and $x_0(t) = r_{cx}(t) = x_0(t_0) + r_v[t - t_0]$ for any initial time $t_0 \geq 0$. We propose the following distributed tracking algorithm based on the state variables of (virtual) reference generator:

$$\begin{aligned} u_{vi}(t) = \; & -(\textstyle\sum_{j=1}^{N} a_{ij}^{cx}(x_i(t) - x_j(t)) + b_i^{cx}(x_i(t) - x_0(t))) \\ & -(\textstyle\sum_{j=1}^{N} a_{ij}^{cv}(v_i(t) - v_j(t)) + b_i^{cv}(v_i(t) - v_0(t))) \end{aligned} \tag{7.17}$$

Now, in addition to the x-variable communication topology $a_{ij}^{cx}, b_i^{cx} \geq 0$, we need to determine a v-variable graph by $a_{ij}^{cv}, b_i^{c} \geq 0$ to ensure robust second-order cooperative tracking (7.15) with guaranteed upper-bound on the following quadratic cost function:

$$\mathcal{J}_2(e(0)) = \int_0^{\infty} (e^T(t)Qe(t) + u_v^T(t)R_v u_v(t))dt \leq e^T(0)\mathcal{P}_2 e(0) \tag{7.18}$$

where $e = col\{e_x, e_v\} \in \mathbb{R}^{2N}$, $e_v = col\{e_{vi}\} \in \mathbb{R}^N$, and $e_{vi} = v_i - v_0$ denotes the i^{th} agent's second state variable's tracking error. Here, the positive-definite $Q = Q^T = [Q_{lk}] \in \mathbb{R}^{2N \times 2N}$ is an M-matrix, $Q_{lk} \in \mathbb{R}^{N \times N}$, $Q_{21} = Q_{12}^T$, and $l, k \in \{1, 2\}$. Also, $R_v = diag\{r_{vi}\} \in \mathbb{R}^{N \times N} \succ \mathbf{0}$ is a diagonal matrix with real-valued scalars $r_{vi} > 0$. The constant matrix $\mathcal{P}_2 = \mathcal{P}_2^T \in \mathbb{R}^{2N \times 2N} \succ \mathbf{0}$ will be discussed later in this subsection. We drop the time variable t for the sake of readability.

Over two sub-layers $\mathcal{G}_{ax}$ and $\mathcal{G}_{av}$, we find the aggregated the agent-layer tracking error dynamics:

$$\begin{gathered} \dot{e}_x = e_v, \quad \textit{and} \quad \dot{e}_v = g(y) + u_v \\ y = C_x \mathcal{L}_{ax} e_x + C_v \mathcal{L}_{av} e_v \end{gathered} \tag{7.19}$$

where $y = col\{y_i\} \in \mathbb{R}^N$, $g = col\{g_i\} \in \mathbb{R}^N$, and $C_v = diag\{C_{vi}\} \in \mathbb{R}^{N \times N}$. Also, we find the aggregated control signal over control-layer graphs $\mathcal{G}_{cx}$ and $\mathcal{G}_{cv}$ (to be designed):

$$u_v = -\mathcal{H}_{cx} e_x - \mathcal{H}_{cv} e_v \tag{7.20}$$

Now, we propose a control-theoretic design procedure and find two fixed candidate graph topologies $\mathcal{G}_{cx}$ and $\mathcal{G}_{cv}$ to be used in multi-layer linear cooperative protocol (7.17). Let $Q_m = [Q_{mlk}] = Q + R_f \succ \mathbf{0}$ where $R_f = diag\{R_{xf}, R_{vf}\}$, $R_{xf} = r_{xf} I_N$ and $r_{xf} = 2 \max_i(r_{vi} \beta_i \gamma_{cxi}^2) \|\mathcal{L}_{ax}\|^2$, and $R_{vf} = r_{vf} I_N$ and $r_{vf} = 2 \max_i(r_{vi} \beta_i \gamma_{cvi}^2) \|\mathcal{L}_{av}\|^2$.

Design procedure 7.2.2. *Design $u = Ke = [K_x, K_v]e$ that solves modified LQR problem* (7.21) *subject to a multiagent system of N double-integrator dynamics. Then, $\mathcal{H}_{cx} = K_x = R_v^{-1} P_{12}^T$ and $\mathcal{H}_{cv} = K_v = R_v^{-1} P_{22}$ characterize two candidate control-layer communication topologies $\mathcal{G}_{cx}$ and $\mathcal{G}_{cv}$, respectively, if condition* (7.22) *is satisfied. The matrix $P = [P_{lk}] \in \mathbb{R}^{2N \times 2N} \succ \boldsymbol{0}$ with $l, k \in \{1, 2\}$ is the solution of ARE* (7.23) *where $P_{21} = P_{12}^T$.*

$$\begin{aligned} \min_{u \in \mathcal{U}_{2m}} \quad & J_{2m}(e(0)) = \textstyle\int_0^\infty (e^T Q_m e + u_v^T R_v u_v) dt \\ \textit{subject to} \quad & \dot{e}_x = e_v \quad \dot{e}_v = u_v \end{aligned} \tag{7.21}$$

$$P_{12}^T \mathbf{1}_N \geq \mathbf{0} \quad \text{and} \quad P_{22}\mathbf{1}_N \geq \mathbf{0} \tag{7.22}$$

$$\begin{bmatrix} are(1,1) & are(1,2) \\ are(2,1) & are(2,2) \end{bmatrix} = \mathbf{0} \tag{7.23}$$

$$\begin{aligned} are(1,1) &= Q_{m11} - P_{12}R_v^{-1}P_{12}^T \\ are(1,2) &= Q_{m12} + P_{11} - P_{12}R_v^{-1}P_{22} \\ are(2,1) &= Q_{m12}^T + P_{11} - P_{22}R_v^{-1}P_{12}^T \\ are(2,2) &= P_{12} + P_{12}^T + Q_{m22} - P_{22}R_v^{-1}P_{22} \end{aligned}$$

The reason to name (7.21) a "modified" LQR problem can be explained similar to Remark 7.2.2. Also, it is straightforward to discuss the existence of a unique positive definite stabilizing $P \succ \mathbf{0}$ in ARE (7.23) based on a joint stabilizability and observability condition for the completely-known LTI multiagent system of double integrators and the modified state weighting matrix in (7.21).

An advantage of this approach is that the two candidate graphs are obtained independent of the time-varying nonlinearly coupled agent-layer dynamics. However, this requires solving $2N \times 2N$ ARE (7.23) for a multiagent system of N agents. Noticing the fact that P_{11} does not directly appear in the candidate reduced-order Laplacian matrices $\mathcal{H}_{cx}$ and $\mathcal{H}_{cv}$, we use $are(1,2)$-$are(2,1)$ and find $P_{12} = P_{12}^T$ whenever $Q_{12} = Q_{12}^T$. Based on $are(1,1)$ and $are(2,2)$, we transform the original $2N \times 2N$ ARE (7.23) to two reduced-order $N \times N$ (sub-) AREs:

$$Q_{m11} - P_{12}R_v^{-1}P_{12} = \mathbf{0} \quad \text{and} \quad (2P_{12} + Q_{m22}) - P_{22}R_v^{-1}P_{22} = \mathbf{0} \tag{7.24}$$

in order to find two candidate graph topologies $\mathcal{G}_{cx}$ and $\mathcal{G}_{cv}$. Note that P_{12} can be found using the first ARE at the left side of (7.24); thus, we treat it as a

known matrix in the second ARE at right-hand side. Since these AREs have the same structure as ARE (7.9) in first-order tracking problem, we use the result of Subsection 7.2.1 as the main foundation and propose the following apparently symmetric analytical solutions:

$$\begin{aligned} P_{12} &= R_v^{1/2}(R_v^{-1/2}Q_{m11}R_v^{-1/2})^{1/2}R_v^{1/2} \\ P_{22} &= R_v^{1/2}(R_v^{-1/2}(2P_{12}+Q_{m22})R_v^{-1/2})^{1/2}R_v^{1/2} \end{aligned} \tag{7.25}$$

which result in two candidate reduced-order Laplacian matrices:

$$\begin{aligned} \mathcal{H}_{cx} &= R_v^{-1/2}(R_v^{-1/2}Q_{m11}R_v^{-1/2})^{1/2}R_v^{1/2} \\ \mathcal{H}_{cv} &= R_v^{-1/2}(R_v^{-1/2}(2P_{12}+Q_{m22})R_v^{-1/2})^{1/2}R_v^{1/2} \end{aligned} \tag{7.26}$$

These representations enable us to describe the candidate $\mathcal{G}_{cx}$ and $\mathcal{G}_{cv}$ explicitly based on the modified state and input weighting matrices in Design procedure 7.2.2. Equivalent formulations $\mathcal{H}_{cx} = (R_v^{-1}Q_{m11})^{1/2}$ and $\mathcal{H}_{cv} = (R_v^{-1}(2P_{12} + Q_{m22}))^{1/2}$ are also valid for the x- and v-variable control-layer communication graphs, respectively (see Subsection 7.2.1).

In a special case, if we are able to send the reference commands r_x and r_v to all agents, we may consider a set of N decoupled local cost functions with $Q = diag\{Q_x, Q_v\}$, $Q_x = diag\{q_{xi}\}$ and $Q_v = diag\{q_{vi}\}$ for $q_{xi} > 0$ and $q_{vi} > 0$, and recommend two diagonal candidate reduced-order Laplacian matrices:

$$\mathcal{H}_{cx} = diag\{\sqrt{\frac{q_{xmi}}{r_{vi}}}\} \qquad \mathcal{H}_{cv} = diag\{\sqrt{2\sqrt{\frac{q_{xmi}}{r_{vi}}} + \frac{q_{vmi}}{r_{vi}}}\} \tag{7.27}$$

where $q_{xmi} = q_{xi} + r_{xf}$ and $q_{vmi} = q_{vi} + r_{vf}$, and r_{xf} and r_{vf} are defined before Design procedure 7.2.2. Based on the diagonal structure of these candidates, we know $\mathcal{H}_{cx}$ corresponds to a candidate star graph $\mathcal{G}_{cx}$ with N weighted directed edges from the command generator's first state variable to all agents' first state

variables, and $\mathcal{H}_{cv}$ models another candidate star topology $\mathcal{G}_{cv}$ with a set of N weighted directed edges from the second state variable of reference generator to that of all agents. In fact, this star topology indicates that additional inter-agent communications are unnecessary whenever all of them have access to the reference signal to be tracked.

For both coupled (7.26) and decoupled (7.27) scenarios, the fundamental property of optimal control systems is satisfied.

Property 7.2.2. *The following equalities are satisfied by any fixed candidate graphs $\mathcal{G}_{cx}$ and $\mathcal{G}_{cv}$ in Design procedure 7.2.2:*

$$e^T Q_m e + u_v^T R_v u_v + J_{2m,e}^{\star T} \begin{bmatrix} e_v \\ u_v \end{bmatrix} = 0$$

$$2u_v^T R_v + J_{2m,e}^{\star T} \begin{bmatrix} \boldsymbol{0} \\ I_N \end{bmatrix} = \boldsymbol{0}$$

where $J_{2m}^\star$ is the optimal cost in (7.21)*, $J_{2m,e}^\star = \frac{\partial J_{2m}^\star}{\partial e}$, and $e = [e_x^T, e_v^T]^T$.*

Since each ARE in (7.24) is similar to ARE (7.9) in Design procedure 7.2.1, we can generalize the discussion after Property 7.2.1 to second-order tracking problem. In particular, we know the candidate topologies $\mathcal{G}_{cx}$ and $\mathcal{G}_{cv}$ are structurally symmetric for any feasible choices of state and input weighting matrices in Design procedure 7.2.2. We now propose a systematic approach to design control-layer communication topologies with structurally non-symmetric weighted topologies. The algorithm is of particular interests when we want to incorporate a-priori

knowledge and impose a special structure on the communication layer in multi-area multiagent systems where areas are geographically far from each others.

Algorithm 7.2.2. *Select two arbitrary symmetric reduced-order Laplacian matrices* $\mathcal{H}_x^{alg} \in \mathbb{R}^{N\times N}$ *and* $\mathcal{H}_v^{alg} \in \mathbb{R}^{N\times N}$*, and a diagonal input weighting matrix* $R_v \in \mathbb{R}^{N\times N} \succ \boldsymbol{0}$ *such that* $(\mathcal{H}_x^{alg})^T R_v^{-1} \mathcal{H}_v^{alg}$ *is a symmetric matrix and the following condition is satisfied:*

$$\begin{bmatrix} (\mathcal{H}_x^{alg})^T R_v^{-1} \mathcal{H}_v^{alg} & H_x^{alg} \\ H_x^{alg} & H_v^{alg} \end{bmatrix} \succ \boldsymbol{0} \tag{7.28}$$

1. *If two structurally symmetric communication graphs* $\mathcal{G}_{cx}$ *and* $\mathcal{G}_{cv}$ *are acceptable: Reduced-order Laplacian matrices* $\mathcal{H}_{cx}^{alg} = R_v^{-1}\mathcal{H}_x^{alg}$ *and* $\mathcal{H}_{cv}^{alg} = R_v^{-1}\mathcal{H}_v^{alg}$ *minimize the quadratic cost function in Design procedure 7.2.2 with* $Q_{m11} = \mathcal{H}_{cx}^{algT} R_v \mathcal{H}_{cx}^{alg}$ *and* $Q_{m22} = \mathcal{H}_{cv}^{algT} R_v \mathcal{H}_{cv}^{alg} - 2\mathcal{H}_x^{alg}$ *if they can be decomposed as* $Q_{m11} = Q_{11} + R_{xf}$ *and* $Q_{m22} = Q_{22} + R_{vf}$ *with positive definite* $Q_{11}, Q_{22} \in \mathbb{R}^{N\times N}$ *and* $Q_{12} = \boldsymbol{0}$*. Then,* $\mathcal{H}_{cx} = \mathcal{H}_{cx}^{alg}$ *and* $\mathcal{H}_{cv} = \mathcal{H}_{cv}^{alg}$ *represent the required candidate topologies of this subsection, and satisfy Property 7.2.2.*

2. *To propose structurally non-symmetric graph topologies: Let* $\mathcal{H}_{cx}^{algm} \in \mathbb{R}^{N\times N}$ *and* $\mathcal{H}_{cv}^{algm} \in \mathbb{R}^{N\times N}$ *be two modification matrices such that* $\mathcal{H}_{cx} = \mathcal{H}_{cx}^{alg} + \mathcal{H}_{cx}^{algm}$ *and* $\mathcal{H}_{cv} = \mathcal{H}_{cv}^{alg} + \mathcal{H}_{cv}^{algm}$ *represent two structurally non-symmetric digraphs. These are the two candidate topologies to be used in* (7.18) *if* $Q + 2[(\mathcal{H}_c^{alg})^T R_v \mathcal{H}_c^{algm}]_{sym} \succ \boldsymbol{0}$ *is satisfied where* $\mathcal{H}_c^{alg} = [\mathcal{H}_{cx}^{alg}, \mathcal{H}_{cv}^{alg}]$*,* $\mathcal{H}_c^{algm} = [\mathcal{H}_{cx}^{algm}, \mathcal{H}_{cv}^{algm}]$*, and* Q *is defined in Step 1.* □

In this algorithm, we have considered a special case with $Q_{12} = \mathbf{0} \in \mathbb{R}^{N\times N}$ which results in two scenarios: $\mathcal{H}_x^{alg} = \mathcal{H}_v^{alg}$ or one of them is equal to cR_v where c is a positive scalar. Alternatively, we can select two different structurally non-symmetric $\mathcal{H}_x^{alg}$ and $\mathcal{H}_v^{alg}$, and find a sign-indefinite $Q_{12} \neq \mathbf{0}$ for which $-Q_{12}+(\mathcal{H}_x^{alg})^T R_v^{-1}\mathcal{H}_v^{alg}$ is a positive definite symmetric matrix, check the positive-definiteness of $Q = [Q_{lk}]$ where $Q_{21} = Q_{12}^T$, and positive definiteness of the following matrix (instead of (7.28)):

$$\begin{bmatrix} -Q_{12} + (\mathcal{H}_x^{alg})^T R_v^{-1}\mathcal{H}_v^{alg} & H_x^{alg} \\ H_x^{alg} & H_v^{alg} \end{bmatrix} \succ \mathbf{0} \tag{7.29}$$

in addition to $Q+2[(\mathcal{H}_c^{alg})^T R_v \mathcal{H}_c^{algm}]_{sym} \succ \mathbf{0}$. However, we have found the benefits of using two non-equal non-diagonal $\mathcal{H}_{cx}^{alg}$ and $\mathcal{H}_{cv}^{alg}$ are recoverable in Step 2 of Algorithm 7.2.2 while verifying a set of simpler conditions.

In the next theorem, we prove multiagent systems with nonlinearly coupled agent-layer dynamics (7.14) cooperatively track the reference command if they communicate according to the multi-layer linear cooperative protocol (7.17) over fixed candidate digraphs $\mathcal{G}_{cx}$ and $\mathcal{G}_{cv}$ of Algorithm 7.2.2 with static weights. We further prove that this reference tracking is achieved with an exponential rate, and find an upper-bound on quadratic cost function (7.18). We define $\mathcal{P}_2 = P + \frac{\kappa^2}{2\sigma}\lambda_{max}((\mathcal{H}_c^{alg})^T R_v \mathcal{H}_c^{alg} + (\mathcal{H}_c^{algm})^T R_v \mathcal{H}_c^{algm}) I_{2N}$, and let the exponential tracking behavior $e(t) \leq \kappa exp^{-\sigma t} e(0)$ be specified by two scalars $\kappa = \sqrt{\frac{\lambda_{max}(P)}{\lambda_{min}(P)}}$ and $\sigma = \frac{\lambda_{min}(Q+2[(\mathcal{H}_c^{alg})^T R_v \mathcal{H}_c^{algm}]_{sym})}{2\lambda_{max}(P)}$.

Theorem 7.2.2. *The fixed candidate control-layer communication digraphs $\mathcal{G}_{cx}$ and $\mathcal{G}_{cv}$ in Step 2 of Algorithm 7.2.2 ensure exponential second-order cooperative tracking* (7.15) *by agent-layer dynamics* (7.14) *with a guaranteed upper-bound on quadratic cost function* (7.18) *specified by κ, σ, and $\mathcal{P}_2$.*

Proof. This proof is given at Subsection 7.5.2. □

A discussion similar to Remarks 7.2.3-7.2.4 can be adopted for the result of Theorem 7.2.2, but it is omitted for brevity. In terms of R_{xf} and R_{vf} of Design procedure 7.2.2, we propose the following corollary to establish a bound on the tolerable interconnected time-varying nonlinear uncertainties in agent-layer dynamics by multi-layer linear cooperative tracking protocol (7.17) over the given digraphs $\mathcal{G}_{cx}$ and $\mathcal{G}_{cv}$. For a special scenario, we further discuss guaranteed-cost communication topology design problem based on the given upper-bound matrix $\mathcal{P}_2$ in cost function (7.18).

Corollary 7.2.2. *Let the given fixed communication digraphs $\mathcal{G}_{cx}$ and $\mathcal{G}_{cv}$ be represented by known $\mathcal{H}_{cx}$ and $\mathcal{H}_{cv}$, respectively. The static tracking protocol* (7.17) *can tolerate norm-bounded time-varying nonlinearities g_i in multiagent system* (7.14) *if the reduced-order Laplacian matrices can be decomposed as $\mathcal{H}_{cx} = \mathcal{H}_{cx,s} + \mathcal{H}_{cx,r}$ and $\mathcal{H}_{cv} = \mathcal{H}_{cv,s} + \mathcal{H}_{cv,r}$, and there exists a diagonal input weighting matrix $R_v \in \mathbb{R}^{N\times N} \succ \boldsymbol{0}$ such that the structurally symmetric reduced-order Laplacian matrices $\mathcal{H}_{cx,s}$ and $\mathcal{H}_{cv,s}$, and residual matrices $\mathcal{H}_{cx,r}$ and $\mathcal{H}_{cv,r}$ satisfy the following conditions:*

1. *There exists a symmetric positive definite $Q = [Q_{lk}] \in \mathbb{R}^{2N\times 2N}$ such that $Q + 2[\mathcal{H}_{c,s}^T R_v \mathcal{H}_{c,r}]_{sym} \succ \boldsymbol{0}$ where $\mathcal{H}_{c,s} = [\mathcal{H}_{cx,s}, \mathcal{H}_{cv,s}]$ and $\mathcal{H}_{c,r} = [\mathcal{H}_{cx,r}, \mathcal{H}_{cv,r}]$.*

2. *$R_v\mathcal{H}_{cv,s}$, $2R_v\mathcal{H}_{cx,s}+Q_{22}+R_{vf}$, $\mathcal{H}_{cx,s}^T R_v\mathcal{H}_{cv,s}-Q_{12}$ are symmetric positive definite and:*

$$\begin{bmatrix} \mathcal{H}_{cx,s}^T R_v\mathcal{H}_{cv,s}-Q_{12} & R_v\mathcal{H}_{cx,s} \\ R_v\mathcal{H}_{cx,s} & R_v\mathcal{H}_{cv,s} \end{bmatrix} \succ \boldsymbol{0}$$

3. *$\mathcal{H}_{cx,s}^T R_v\mathcal{H}_{cx,s} \succ R_{xf}$ and $\mathcal{H}_{cv,s}^T R_v\mathcal{H}_{cv,s} \succ 2R_v\mathcal{H}_{cx,s}+R_{vf}$ are satisfied where R_{xf} and R_{vf} are defined in Design procedure 7.2.2,*

For a given upper-bound cost matrix $\mathcal{P}_2$ in (7.18)*, guaranteed-cost communication topologies $\mathcal{G}_{cx}$ and $\mathcal{G}_{cv}$ can be found by searching for diagonal $R_v \succ \boldsymbol{0}$, sign-indefinite $Q_{12} \in \mathbb{R}^{N\times N}$, and decomposition $\mathcal{H}_{cx}=\mathcal{H}_{cx,s}+\mathcal{H}_{cx,r}$ and $\mathcal{H}_{cv}=\mathcal{H}_{cv,s}+\mathcal{H}_{cv,r}$ that satisfy:*

4. $$\begin{bmatrix} \mathcal{H}_{cx,s}^T R_v\mathcal{H}_{cv,s}-Q_{12} & R_v\mathcal{H}_{cx,s} \\ R_v\mathcal{H}_{cx,s} & R_v\mathcal{H}_{cv,s} \end{bmatrix} + \tfrac{\kappa^2}{2\sigma}\lambda_{max}(\mathcal{H}_{c,s}^T R_v\mathcal{H}_{c,s}+\mathcal{H}_{c,r}^T R_v\mathcal{H}_{c,r})I_{2N} \preccurlyeq \mathcal{P}_1$$

with exponential convergence parameters $\kappa,\sigma>0$, and $\mathcal{H}_{c,s}=[\mathcal{H}_{cx,s},\mathcal{H}_{cv,s}]$ and $\mathcal{H}_{c,r}=[\mathcal{H}_{cx,r},\mathcal{H}_{cv,r}]$. □

The proof can be discussed based on the derivations of this subsection, but is omitted for brevity. Both κ and σ can be conservatively estimated using Theorem 7.2.2. Furthermore, the corollary is stated based on three robust cooperative tracking requirements and a robust performance test which should be checked for the given communication topologies $\mathcal{H}_{cx}$ and $\mathcal{H}_{cv}$. However, we can further simplify this corollary assuming $Q_{12}=\mathbf{0}$ for which the condition $\mathcal{H}_{cx,s}^T R_v\mathcal{H}_{cx,s}-Q_{12}$ is always satisfied because $R_v \succ \mathbf{0}$.

7.2.3 Mixed-order cooperative tracking

In the previous two subsections, we designed the single-layer and multi-layer cooperative tracking problems in heterogeneous multiagent systems respectively with first- and second-order agents. Now, we use those fundamental results to handle robust cooperative tracking in mixed-order multiagent systems with physically-coupled agent-layer dynamics. Here, M agents are modeled by second-order dynamics:

$$\begin{aligned} \dot{x}_i(t) = v_i(t), \qquad \dot{v}_i(t) = g_i(y_i(t), t) + u_{vi}(t) \\ y_i(t) = C_{xi} \sum_{j=1}^{N} a_{ij}^{ax}(x_i(t) - x_j(t)) + C_{vi} \sum_{j=1}^{M} a_{ij}^{av}(v_i(t) - v_j(t)) \end{aligned} \tag{7.30}$$

for all $i \in \mathcal{V}_1 = \{1, ..., M\}$ where $1 < M \leq N$, and $N - M$ agents are described by:

$$\dot{x}_i(t) = f_i(z_i(t), t) + u_{xi}(t), \qquad z_i(t) = C_{xi} \sum_{j=1}^{N} a_{ij}^{ax}(x_i(t) - x_j(t)) \tag{7.31}$$

for all $i \in \mathcal{V}_2 = \{M + 1, ..., N\}$. In this multiagent system with unknown agent-layer nonlinearities f_i and g_i, we propose a robust cooperative tracking problem:

$$\lim_{t \to \infty} (x_i(t) - r) = 0 \quad \forall\, i \in \mathcal{V}_1 \cup \mathcal{V}_2 \qquad \textit{and} \qquad \lim_{t \to \infty} v_i(t) = 0 \quad \forall\, i \in \mathcal{V}_1 \tag{7.32}$$

where $r \in \mathbb{R}$ is a constant that can be created using the following reference generator:

$$\dot{x}_0 = 0 \tag{7.33}$$

with a manipulable initial condition $x_0(0) = r$. We are interested in enforcing all agents (7.30)-(7.31) to track this reference r by allowing them to communicate based on the following distributed tracking protocols:

$$u_{vi}(t) = \begin{array}{l} -(\sum_{j=1}^{N} a_{ij}^{cx}(x_i(t) - x_j(t)) + b_i^{cx}(x_i(t) - x_0(t))) \\ -(\sum_{j=1}^{M} a_{ij}^{cv}(v_i(t) - v_j(t)) + b_i^{cv} v_i(t)) \end{array} \quad \forall i \in \mathcal{V}_1 \qquad (7.34)$$

and

$$u_{xi}(t) = -(\sum_{j=1}^{N} a_{ij}^{cx}(x_i(t) - x_j(t)) + b_i^{cx}(x_i(t) - x_0(t))) \qquad \forall i \in \mathcal{V}_2 \qquad (7.35)$$

We introduce a fictitious second state variable $v_0 = 0$ for the virtual command generator (7.33) and define tracking error variables $e_{vi} = v_i - v_0 = v_i$ for second-order agents in $\mathcal{V}_1$. In the presence of unknown time-varying interconnected nonlinearities f_i and g_i, scalars $a_{ij}^{cx}, b_i^{cx}, a_{ij}^{cv}, b_i^{cv} \geq 0$ should be designed to guarantee robust cooperative tracking (7.32) and provide an upper-bound on the following quadratic cost function:

$$\mathcal{J}_3(e(0)) = \int_0^\infty (e^T(t)Qe(t) + u^T(t)Ru(t))dt \leq e^T(0)\mathcal{P}_3 e(0) \qquad (7.36)$$

where $e = col\{e_x, e_v\} \in \mathbb{R}^{N+M}$, $e_x = col\{e_{xi}\} \in \mathbb{R}^N$, $e_{xi} = x_i - x_0$ for $i \in \mathcal{V}_1 \cup \mathcal{V}_2$, $e_v = col\{e_{vi}\} \in \mathbb{R}^M$, $e_{vi} = v_i - v_0 = v_i$ for $i \in \mathcal{V}_1$, $u = col\{u_v, u_x\} \in \mathbb{R}^N$, $u_v = col\{u_{vi}\} \in \mathbb{R}^M$ for $i \in \mathcal{V}_1$, and $u_x = col\{u_{xi}\} \in \mathbb{R}^{N-M}$ for $i \in \mathcal{V}_2$. Furthermore, $Q = Q^T = Q[lk] \in \mathbb{R}^{(N+M)\times(N+M)} \succ \mathbf{0}$ for $l, k \in \{1, 2, 3\}$, $R = R^T = diag\{R_v, R_x\} \in \mathbb{R}^{N\times N} \succ \mathbf{0}$, $R_v \in \mathbb{R}^M \succ \mathbf{0}$, and $R_x \in \mathbb{R}^{N-M} \succ \mathbf{0}$. Also, $\mathcal{P}_3 = \mathcal{P}_3^T \in \mathbb{R}^{(N+M)\times(N+M)} \succ \mathbf{0}$ is either an unknown or a-priori known constant matrix which will be discussed later in this subsection.

Now, we prove the proposed framework for the first- or second-order multiagent systems can be applied to the multi-layer cooperative tracking problem in mixed-order multiagent systems with time-varying nonlinearly interconnected agent-layer

dynamics. We find the aggregated tracking error dynamics for sub-multiagent system of second-order agents:

$$\begin{gathered} \dot{e}_{x\mathcal{V}_1} = e_v \qquad and \qquad \dot{e}_v = u_v + g(y,t), \qquad \forall i \in \mathcal{V}_1 \\ y = y_x + y_v \end{gathered} \tag{7.37}$$

where $e_v = v - \mathbf{1}_M v_0 = v$, $g = col\{g_i\}$, and $e_{x\mathcal{V}_1}, e_v, u_v, y_x, y_v \in \mathbb{R}^M$ for $i \in \mathcal{V}_1$. We also build the aggregated tracking error dynamics for sub-multiagent system of first-order agents:

$$\dot{e}_{x\mathcal{V}_2} = u_x + f(z,t), \qquad \forall i \in \mathcal{V}_2 \tag{7.38}$$

where $e_{x\mathcal{V}_2}, u_x, z$ for $\mathbb{R}^{N-M}$ and $f = col\{f_i\}$ for $i \in \mathcal{V}_2$. We further find:

$$y_v = C_v \mathcal{L}_{av} e_v \qquad and \qquad \begin{bmatrix} y_x \\ z \end{bmatrix} = C_x \mathcal{L}_{ax} e_x$$

where $C_v = diag\{C_{vi}\} \forall i \in \mathcal{V}_1$, and $\mathcal{L}_{av} \in \mathbb{R}^{M \times M}$ is the Laplacian matrix of agent-layer v-variable coupling graph, $e_x = [e_{x\mathcal{V}_1}^T, e_{x\mathcal{V}_2}^T] = col\{e_{xi}\}$, $C_x = diag\{C_{xi}\}$ for $i \in \mathcal{V}_1 \cup \mathcal{V}_2$, and $\mathcal{L}_{ax} \in \mathbb{R}^{N \times N}$ is the Laplacian matrix of agent-layer x-variable coupling graph. With a lumped representation over $\mathcal{G}_{ax}$ and $\mathcal{G}_{av}$, the aggregated multiagent system of mixed-order agents are written as $\dot{e} = Ae + Bu + B\phi(z,y,t)$ where:

$$\begin{bmatrix} \dot{e}_x \\ \dot{e}_v \end{bmatrix} = \begin{bmatrix} A_{11} & A_{12} \\ A_{21} & A_{22} \end{bmatrix} \begin{bmatrix} e_x \\ e_v \end{bmatrix} + \begin{bmatrix} B_1 \\ B_2 \end{bmatrix} \begin{bmatrix} u_v \\ u_x \end{bmatrix} + \begin{bmatrix} B_1 \\ B_2 \end{bmatrix} \begin{bmatrix} g(y,t) \\ f(z,t) \end{bmatrix} \tag{7.39}$$

$$A_{11} = \begin{bmatrix} \mathbf{0}_{M\times M} & \mathbf{0}_{M\times(N-M)} \\ \mathbf{0}_{(N-M)\times M} & \mathbf{0}_{(N-M)\times(N-M)} \end{bmatrix} \quad A_{12} = \begin{bmatrix} I_M \\ \mathbf{0}_{(N-M)\times M} \end{bmatrix}$$
$$A_{21} = \begin{bmatrix} \mathbf{0}_{M\times M} & \mathbf{0}_{M\times(N-M)} \end{bmatrix} \quad A_{22} = \mathbf{0}_{M\times M} \tag{7.40}$$
$$B_1 = \begin{bmatrix} \mathbf{0}_{M\times M} & \mathbf{0}_{M\times(N-M)} \\ \mathbf{0}_{(N-M)\times M} & I_{N-M} \end{bmatrix} \quad B_2 = \begin{bmatrix} I_M & \mathbf{0}_{M\times(N-M)} \end{bmatrix}$$

Also, over $\mathcal{G}_{cx}$ and $\mathcal{G}_{cv}$, the aggregated tracking the aggregated tracking control signal is given bycontrol signal is given by:

$$\begin{bmatrix} u_v \\ u_x \end{bmatrix} = -\mathcal{H}_{cx}e_x - \begin{bmatrix} \mathcal{H}_{cv} \\ \mathbf{0}_{(N-M)\times M} \end{bmatrix} e_v =: -\mathcal{H}_c e \tag{7.41}$$

Let $R_{xf} = r_{xf}I_N$ and $R_{vf} = r_{vf}I_M$ where the two scalars are defined as $r_{xf} = \max_i(\max_i(2\beta_i r_{vi}, \alpha_i r_{xi})\gamma_{cxi}^2)\|\mathcal{L}_{ax}\|^2$ and $r_{vf} = 2\max_i(\beta_i r_{vi}\gamma_{cvi}^2)\|\mathcal{L}_{av}\|^2$ (note that β_i is only defined for $i \in \mathcal{V}_1$ and α_i is only given for $i \in \mathcal{V}_2$). We introduce $Q_m = Q + R_f$ where $Q, R_f \in \mathbb{R}^{(N+M)\times(N+M)}$ are defined as follows:

$$Q = \begin{bmatrix} Q_{11} & \mathbf{0}_{M\times(N-M)} & Q_{13} \\ \mathbf{0}_{(N-M)\times M} & Q_{22} & \mathbf{0}_{(N-M)\times M} \\ Q_{13}^T & \mathbf{0}_{M\times(N-M)} & Q_{33} \end{bmatrix} \quad R_f = \begin{bmatrix} R_{xf} & \mathbf{0}_{N\times M} \\ \mathbf{0}_{M\times N} & R_{vf} \end{bmatrix} \tag{7.42}$$

and propose a control-theoretic design procedure to find two candidate reduced-order Laplacian matrices $\mathcal{H}_{cx} \in \mathbb{R}^{N\times N}$ and $\mathcal{H}_{cv} \in \mathbb{R}^{M\times M}$ corresponding to the required candidate topologies $\mathcal{G}_{cx}$ and $\mathcal{G}_{cv}$, respectively.

Design procedure 7.2.3. *Find* $u = Ke = [K_x, K_v]e$ *that solves modified LQR problem* (7.43)*. Then,* (7.44) *represents the two candidate graph topologies* $\mathcal{G}_{cx}$ *and* $\mathcal{G}_{cv}$ *if condition* (7.45) *is satisfied. Matrix* $P = [P_{lk}] \in \mathbb{R}^{(N+M)\times(N+M)} \succ \boldsymbol{0}$ *is the partitioned solution of ARE* (7.46) *for* $l, k \in \{1, 2, 3\}$ *where* $P_{12} = \boldsymbol{0}$ *and* $P_{23} = \boldsymbol{0}$*.*

$$\begin{aligned} \min_{u \in \mathcal{U}_{3m}} \quad & J_{3m}(e(0)) = \textstyle\int_0^\infty (e^T Q_m e + u^T R u) dt \\ \textit{subject to} \quad & \dot{e} = Ae + Bu \ \ \textit{in (7.39)} \end{aligned} \tag{7.43}$$

$$\left[\begin{array}{c|c} \mathcal{H}_{cx} & \begin{matrix} \mathcal{H}_{cv} \\ \boldsymbol{0} \end{matrix} \end{array}\right] = \left[\begin{array}{cc|c} R_v^{-1} P_{13}^T & \boldsymbol{0} & R_v^{-1} P_{33} \\ \boldsymbol{0} & R_x^{-1} P_{22} & \boldsymbol{0} \end{array}\right] \tag{7.44}$$

$$P_{13}^T \boldsymbol{1}_N \geq \boldsymbol{0}, \qquad P_{22} \boldsymbol{1}_N \geq \boldsymbol{0}, \qquad P_{33} \boldsymbol{1}_N \geq \boldsymbol{0} \tag{7.45}$$

$$\begin{bmatrix} are(1,1) & \boldsymbol{0} & are(1,3) \\ \boldsymbol{0} & are(2,2) & \boldsymbol{0} \\ are(1,3)^T & \boldsymbol{0} & are(3,3) \end{bmatrix} = \boldsymbol{0} \tag{7.46}$$

$$\begin{aligned} are(1,1) &= Q_{11} + R_{xf} - P_{13} R_v^{-1} P_{13}^T \\ are(1,3) &= Q_{13} + P_{11} - P_{13} R_v^{-1} P_{33} \\ are(2,2) &= Q_{22} + R_{xf} - P_{22} R_x^{-1} P_{22} \\ are(3,3) &= Q_{33} + R_{vf} + P_{13} + P_{13}^T - P_{33} R_v^{-1} P_{33} \end{aligned}$$

Note that the existence of a unique stabilizing $P \succ \mathbf{0}$ can be guaranteed based on the controllability and observability of $(Q_m^{1/2}, A, B)$, and we refer to Remark 7.2.2 for a discussion on "modified" LQR problem. A question may arise about the imposed structure on Q in (7.42). In the following remarks, we first

connect this question to the proposed tracking protocol (7.34)-(7.35), and then provide an optimal control-theoretical reason for it.

Remark 7.2.5. *We first mention that assuming a complete matrix* $Q = Q^T = [Q_{lk}] \in \mathbb{R}^{(N+M)\times(N+M)}$ *results in ARE:*

$$\begin{bmatrix} are(1,1) & are(1,2) & are(1,3) \\ are(1,2)^T & are(2,2) & are(2,3) \\ are(1,3)^T & are(2,3)^T & are(3,3) \end{bmatrix} = \boldsymbol{0}$$

$$\begin{aligned} are(1,1) &= Q_{11} + R_{xf} - P_{12}R_x^{-1}P_{12} - P_{13}R_v^{-1}P_{13}^T \\ are(1,2) &= Q_{12} - P_{12}R_x^{-1}P_{22} - P_{13}R_v^{-1}P_{23}^T \\ are(1,3) &= Q_{13} + P_{11} - P_{12}R_x^{-1}P_{23} - P_{13}R_v^{-1}P_{33} \\ are(2,2) &= Q_{22} + R_{xf} - P_{22}R_x^{-1}P_{22} - P_{23}R_v^{-1}P_{23}^T \\ are(2,3) &= Q_{23} + P_{12}^T - P_{22}R_x^{-1}P_{23} - P_{23}R_v^{-1}P_{33} \\ are(3,3) &= Q_{33} + R_{vf} + P_{13} + P_{13}^T - P_{23}^T R_x^{-1}P_{23} - P_{33}R_v^{-1}P_{33} \end{aligned}$$

and the following reduced-order Laplacian matrices:

$$\left[\begin{array}{c|c} \mathcal{H}_{cx} & \mathcal{H}_{cv} \end{array}\right] = \left[\begin{array}{cc|c} R_v^{-1}P_{13}^T & R_v^{-1}P_{23}^T & R_v^{-1}P_{33} \\ R_x^{-1}P_{12}^T & R_x^{-1}P_{22} & R_x^{-1}P_{23} \end{array}\right]$$

which, for $P_{23} \neq \boldsymbol{0}$*, requires using the cooperative algorithm* (7.34) *for all agents in* $\mathcal{V}_1 \cup \mathcal{V}_2$*. We introduced the cooperative algorithm* (7.35) *because we could not see any physical justifications to update* x*-variable of agents in* $\mathcal{V}_2$ *based on the* v*-variable of second-order agents in* $\mathcal{V}_1$*. Thus, we observe that* $P_{23} = \boldsymbol{0}$ *is imposed by cooperative algorithm* (7.35) *for first-order agents in* $\mathcal{V}_2$*. Based on the Design*

procedure 7.2.3, we further mention that the tracking protocol (7.34)-(7.35) *can be rewritten as follows:*

$$u_{vi} = -(\sum_{j=1}^{M} a_{ij}^{cx}(x_i - x_j) + b_i^{cx}(x_i - x_0) + \sum_{j=1}^{M} a_{ij}^{cv}(v_i - v_j) + b_i^{cv} v_i) \quad \forall i \in \mathcal{V}_1$$
$$u_{xi} = -(\sum_{j=M+1}^{N} a_{ij}^{cx}(x_i - x_j) + b_i^{cx}(x_i - x_0)) \quad \forall i \in \mathcal{V}_2$$

which means, if we do not update x-variable of first-order agents in $\mathcal{V}_2$ *based on the v-variable of second-order agents in* $\mathcal{V}_1$*, the optimal topology will necessary be composed by two sets of decoupled communication topologies:* $\mathcal{G}_{cx\mathcal{V}_1}$ *and* $\mathcal{G}_{cv\mathcal{V}_1}$ *for agents in* $\mathcal{V}_1$*, and* $\mathcal{G}_{cx\mathcal{V}_2}$ *for agents in* $\mathcal{V}_2$*.* □

Remark 7.2.6. *We now clarify the reason for proposing a special structure on the state weighting matrix* Q *that, in addition to* $P_{23} = \mathbf{0}$*, results in* $P_{12} = \mathbf{0}$*. We know the solution* P *of this ARE (in Remark 7.2.5) is equal to* $lim_{t\to\infty} P(t)$ *where* $P(t)$ *is the solution of corresponding Riccati equation. In particular, zeros of this* $P(t)$ *(and* P*) can be found using matrix differential equation* (2.29)*. Substituting* (A, B) *from* (7.39) *and a complete matrix* $Q = [Q_{lk}]$ *in the Hamiltonian matrix of* (2.29)*, we find:*

$$\dot{e}_{x\mathcal{V}_1} = e_v, \quad \dot{e}_v = -R_v^{-1} L_{v\mathcal{V}_1}$$
$$\dot{L}_{x\mathcal{V}_1} = -Q_{11} e_{x\mathcal{V}_1} - Q_{12} e_{x\mathcal{V}_2} - Q_{13} e_v$$
$$\dot{L}_{v\mathcal{V}_1} = -Q_{13}^T e_{x\mathcal{V}_1} - Q_{23}^T e_{x\mathcal{V}_2} - Q_{33} e_v - L_{x\mathcal{V}_1}$$

for the second-order agents in $\mathcal{V}_1$ *and*

$$\dot{e}_{x\mathcal{V}_2} = -R_x^{-1} L_{xz\mathcal{V}_2}$$
$$\dot{L}_{x\mathcal{V}_2} = -Q_{12}^T e_{x\mathcal{V}_1} - Q_{22} e_{x\mathcal{V}_2} - Q_{23} e_v$$

for the first-order agents in $\mathcal{V}_2$. Here, based on the notation of (2.29)*, we have used $x \leftarrow [e_{x\mathcal{V}_1}^T, e_{x\mathcal{V}_2}^T, e_v^T]^T$ and $L \leftarrow [L_{x\mathcal{V}_1}^T, L_{x\mathcal{V}_2}^T, L_{v\mathcal{V}_1}^T]^T$. Because $L(t) = P(t)e(t)$, we notice that the proposed structure* (7.42) *(with $Q_{12} = \boldsymbol{0}$ and $Q_{23} = \boldsymbol{0}$) is the only way to ensure $P_{23} = \boldsymbol{0}$. We further observe that it consequently results in $P_{12} = \boldsymbol{0}$. In this situation, the two set of equations for $\mathcal{V}_1$ and $\mathcal{V}_2$ are independent from each other, and we find:*

$$\begin{bmatrix} L_{x\mathcal{V}_1}(t) \\ L_{x\mathcal{V}_2}(t) \\ L_{v\mathcal{V}_1}(t) \end{bmatrix} = \begin{bmatrix} * & \boldsymbol{0} & * \\ \boldsymbol{0} & * & \boldsymbol{0} \\ * & \boldsymbol{0} & * \end{bmatrix} \begin{bmatrix} e_{x\mathcal{V}_1}(t) \\ e_{x\mathcal{V}_2}(t) \\ e_v(t) \end{bmatrix} =: P(t)e(t)$$

where the matrices $\boldsymbol{0}$ indicate those components of $P(t)$ that are always equal to zero (i.e., $P_{12} = \boldsymbol{0}$ and $P_{23} = \boldsymbol{0}$). This finding matches on the structure of (7.44)*. The closed-form solutions for the remaining components of P in ARE* (7.46) *(corresponding to the $*$-components of $P(t)$) will be discussed in the rest of this subsection.* □

The candidate topologies $\mathcal{G}_{cx\mathcal{V}_1}$, $\mathcal{G}_{cx\mathcal{V}_2}$, and $\mathcal{G}_{cv}$ (see end of Remark 7.2.5) can be designed using the existing software packages by solving $(N+M) \times (N+M)$ nonlinear matrix equation (7.46). However, based on $are(1,3)$ and $are(3,1)$ for $Q_{13} = Q_{13}^T$, we know $P_{13}^T = P_{13}$ which results in the following set of matrix equations:

$$\begin{gathered} (Q_{11} + R_{xf}) - P_{13}R_v^{-1}P_{13} = \mathbf{0} \qquad (Q_{22} + R_{xf}) - P_{22}R_x^{-1}P_{22} = \mathbf{0}, \\ (Q_{33} + R_{vf} + 2P_{13}) - P_{33}R_v^{-1}P_{33} = \mathbf{0} \end{gathered} \tag{7.47}$$

These equations can be solved similar to the ARE (7.9) in Design procedure 7.2.1 (we further know $P_{11} = P_{13}R_v^{-1}P_{33} - Q_{13}$ where its positive definiteness is ensured based on a joint observability and stabilizability condition discussed after Design procedure 7.2.3). These explicit solutions are of particular interest for multiagent systems with a high-number of agents, and allow splitting the original $(N+M)\times(N+M)$ ARE (7.46) into three matrix equations with low(er) dimensions $M \times M$, $(N-M)\times(N-M)$, and $M \times M$. We now rely on the discussion after Design procedure 7.2.1 and propose the following closed-form solutions for the candidate communication topologies based on the known design matrices Q, R_x, and R_v:

$$\mathcal{H}_{cx} = \begin{bmatrix} \mathcal{H}_{cx\mathcal{V}_2} & \mathbf{0} \\ \mathbf{0} & \mathcal{H}_{cx\mathcal{V}_1} \end{bmatrix}$$

$$\begin{aligned} \mathcal{H}_{cx\mathcal{V}_2} &= R_v^{-1/2}(R_v^{-1/2}(Q_{11}+R_{xf})R_v^{-1/2})^{1/2}R_v^{1/2} \\ \mathcal{H}_{cx\mathcal{V}_1} &= R_x^{-1/2}(R_x^{-1/2}(Q_{22}+R_{xf})R_x^{-1/2})^{1/2}R_x^{1/2} \\ \mathcal{H}_{cv} &= R_v^{-1/2}[2(R_v^{-1/2}(Q_{11}+R_{xf})R_v^{-1/2})^{1/2} + R_v^{-1/2}(Q_{33}+R_{vf})R_v^{-1/2}]^{1/2}R_v^{1/2} \end{aligned} \tag{7.48}$$

For this coupled cost scenario, various representations can be found following the discussion in Subsection 7.2.1 which is omitted for brevity. We may also consider a decoupled cost function in Design procedure 7.2.3 by introducing $Q = diag\{q_{x\mathcal{V}_1 i}|_{i=1}^{M}, q_{x\mathcal{V}_2 i}|_{i=M+1}^{N}, q_{vi}|_{i=1}^{M}\}$ for $q_{x\mathcal{V}_1 i}, q_{x\mathcal{V}_2 i}, q_{vi} > 0$. This simplification suggests $N+M$ decoupled scalar modified LQR problems, and results in two candidate star topologies:

$$\begin{aligned}\mathcal{H}_{cx} &= diag\{\sqrt{\tfrac{q_x\mathcal{V}_1 i+r_{xf}}{r_{vi}}}|_{i=1}^{M}, \sqrt{\tfrac{q_x\mathcal{V}_2 i+r_{xf}}{r_{xi}}}|_{i=M+1}^{N}\} \\ \mathcal{H}_{cv} &= diag\{\sqrt{2\sqrt{\tfrac{q_x\mathcal{V}_1 i+r_{xf}}{r_{vi}}}+\tfrac{q_{vi}+r_{xf}}{r_{vi}}}|_{i=1}^{M}\}\end{aligned} \tag{7.49}$$

This in fact means, whenever all agents have access to the reference command, no inter-agent communication is necessary to guarantee cooperative tracking in a multiagent system of (7.30)-(7.31). Since v_0 is a fictitious state variable for the virtual reference generator (i.e., $e_v = v_i - v_0 = v_i$), star topology (7.49) requires all agents in $\mathcal{V}_1$ to measure the absolute value of their second state variable. We, however, mention that the coupled cost scenario may result in communication topology (7.48) with only a few absolute velocity measurements.

The following property is satisfied by candidate topologies in both coupled and decoupled cost scenarios.

Property 7.2.3. *The candidate graph topologies $\mathcal{G}_{cx}$ and $\mathcal{G}_{cv}$ in Design procedure 7.2.3 (or $\mathcal{G}_{cx\mathcal{V}_1}$, $\mathcal{G}_{cx\mathcal{V}_2}$, and $\mathcal{G}_{cv}$) satisfy the following equalities:*

$$e^T Q_m e + u^T R u + J_{3m,e}^{\star T}(Ae + Bu) = 0 \qquad\qquad 2u^T R + J_{3m,e}^{\star T} B = \boldsymbol{0}$$

where $J_{3m}^{\star}$ is the optimal cost in (7.43)*, $J_{3m,e}^{\star} = \frac{\partial J_{3m}^{\star}}{\partial e}$, and e, A, and B are defined in* (7.39)*.*

In Remark 7.2.5, we discussed that the proposed cooperative tracking algorithm (7.35) for first-order agents in $\mathcal{V}_2$ has resulted in a block diagonal x-variable reduced-order Laplacian matrix $\mathcal{H}_{cx}$. We also showed the high-order ARE (7.46) could be solved by three low-order AREs (7.47) in which the first and third AREs for $\mathcal{V}_1$ are coupled to each other through P_{13}, and the second ARE corresponds

$\mathcal{V}_2$ is decoupled from the other two AREs. Due to the properties of solutions to ARE (7.46), we further know the resulting communication graphs are necessarily structurally symmetric. In the next algorithm, we propose a systematic approach to find structurally non-symmetric digraphs $\mathcal{G}_{cx}$ and $\mathcal{G}_{cv}$ to be used in multi-layer cooperative tracking protocol (7.34)-(7.35).

Algorithm 7.2.3. *The design problem of $\mathcal{G}_{cx}$ and $\mathcal{G}_{cv}$ (or $\mathcal{G}_{cx\mathcal{V}_1}$, $\mathcal{G}_{cx\mathcal{V}_2}$, and $\mathcal{G}_{cv}$) can be addressed in two independent steps:*

1. *For agents in $\mathcal{V}_2$: Follow the steps of Algorithm 7.2.1 to design structurally non-symmetric communication digraph $\mathcal{G}_{cx\mathcal{V}_2}$ by finding $\mathcal{H}_{cx\mathcal{V}_2}$ that satisfies the following condition for an arbitrarily selected $R_x \in \mathbb{R}^{(N-M)\times(N-M)}$[4],*

$$Q_{22} + 2[(\mathcal{H}_{cx\mathcal{V}_2}^{alg})^T R_x \mathcal{H}_{cx\mathcal{V}_2}^{algm}]_{sym} \succ \boldsymbol{0} \tag{7.50}$$

2. *For agents in $\mathcal{V}_1$: Follow the steps of Algorithm 7.2.2 to design structurally non-symmetric communication digraphs $\mathcal{G}_{cx\mathcal{V}_1}$ and $\mathcal{G}_{cv}$ by finding the two matrices $\mathcal{H}_{cx\mathcal{V}_1}$ and $\mathcal{H}_{cv\mathcal{V}_1}$ that satisfy the following condition for an arbitrarily selected $R_v \in \mathbb{R}^{M\times M}$[5],*

$$\begin{bmatrix} Q_{11} + 2[(\mathcal{H}_{cx\mathcal{V}_1}^{alg})^T R_v \mathcal{H}_{cx\mathcal{V}_1}^{algm}]_{sym} & Q_{13} + 2[(\mathcal{H}_{cx\mathcal{V}_1}^{alg})^T R_v \mathcal{H}_{cv\mathcal{V}_1}^{algm}]_{sym} \\ Q_{13}^T + 2[(\mathcal{H}_{cv\mathcal{V}_1}^{alg})^T R_v \mathcal{H}_{cx\mathcal{V}_1}^{algm}]_{sym} & Q_{33} + 2[(\mathcal{H}_{cv\mathcal{V}_1}^{alg})^T R_v \mathcal{H}_{cv\mathcal{V}_1}^{algm}]_{sym} \end{bmatrix} \succ \boldsymbol{0} \tag{7.51}$$

[4]In Algorithm 7.2.1, replace Q_x by Q_{22} and name the result $\mathcal{H}_{cx\mathcal{V}_2}^{alg}$.

[5]In Algorithm 7.2.2, replace Q_{22} by Q_{33} and name the results $\mathcal{H}_{cx\mathcal{V}_1}^{alg}$ and $\mathcal{H}_{cv\mathcal{V}_1}^{alg}$ for $Q_{13} = \mathbf{0}$.

The outcome of this algorithm is given by

$$\mathcal{H}_c = \left[\begin{array}{cc|c} \mathcal{H}^{alg}_{cx\mathcal{V}_1} & \boldsymbol{0} & \mathcal{H}^{alg}_{cv\mathcal{V}_1} \\ \boldsymbol{0} & \mathcal{H}^{alg}_{cx\mathcal{V}_2} & \boldsymbol{0} \end{array}\right] + \left[\begin{array}{cc|c} \mathcal{H}^{algm}_{cx\mathcal{V}_1} & \boldsymbol{0} & \mathcal{H}^{algm}_{cv\mathcal{V}_1} \\ \boldsymbol{0} & \mathcal{H}^{algm}_{cx\mathcal{V}_2} & \boldsymbol{0} \end{array}\right] =: \mathcal{H}^{alg}_c + \mathcal{H}^{algm}_c$$

where we emphasize that Property 7.2.3 is satisfied only by structurally symmetric components of $\mathcal{G}_{cx}$ and $\mathcal{G}_{cv}$ included in $\mathcal{H}^{alg}_c$. □

We now prove that the multi-layer linear cooperative tracking protocol (7.34)-(7.35) over two candidate communication topologies $\mathcal{G}_{cx}$ and $\mathcal{G}_{cv}$ of Algorithm 7.2.3 ensures robust tracking (7.32) while guaranteeing an upper-bound on cost function (7.36) for a mixed-order multiagent system with unknown interconnected time-varying nonlinear agent-layer dynamics. We define $\kappa = \sqrt{\frac{\lambda_{max}(P)}{\lambda_{min}(P)}}$, $\sigma = \frac{\lambda_{min}(Q+(\mathcal{H}^{alg}_c)^T R\mathcal{H}^{algm}_c)}{2\lambda_{max}(P)}$, and $\mathcal{P}_3 = P + \lambda_{max}((\mathcal{H}^{alg}_c)^T R\mathcal{H}^{alg}_c + (\mathcal{H}^{algm}_c)^T R\mathcal{H}^{algm}_c)$.

Theorem 7.2.3. *The candidate control-layer communication graph topologies $\mathcal{G}_{cx}$ and $\mathcal{G}_{cv}$ characterized by the aggregated reduced-order Laplacian matrix $\mathcal{H}_c$ in Algorithm 7.2.3 ensure exponential distributed cooperative tracking* (7.32) *with a rate specified by $\kappa, \sigma > 0$, and an upper-bound matrix $\mathcal{P}_3$ on quadratic cost function* (7.36)*.*

Proof. The proof is passed to the Subsection 7.5.3. □

For the given communication digraphs $\mathcal{G}_{cx}$ and $\mathcal{G}_{cv}$ that fit on the structure of (7.44), in the next corollary, we unify the findings of this subsection and establish a bound on the tolerable time-varying interconnected nonlinearities f_i and g_i in agent-layer dynamics (7.30)-(7.31) by multi-layer linear cooperative tracking protocol (7.34)-(7.35).

Corollary 7.2.3. *A bound on the maximum tolerable unknown interconnected nonlinearities by distributed cooperative tracking protocol* (7.34)-(7.35) *can be established as the minimum tolerance of the first-order closed-loop multiagent system* $\mathcal{V}_2$ *based on Corollary 7.2.1 and second-order closed-loop multiagent system* $\mathcal{V}_1$ *based on Corollary 7.2.2. For the given upper-cost matrix* $\mathcal{P}_3$*, let* $\mathcal{P}_3' \succcurlyeq \mathcal{P}_3$ *be a matrix with the same pattern as* Q *in* (7.42)*. Then, using* $\mathcal{P}_3'$*, performance-oriented topology design problem is also splittable into two independent parts based on the Corollary 7.2.1 and Corollary 7.2.2.* □

We emphasize that conditions of both Corollaries 7.2.1 and 7.2.2 should be simultaneously satisfied because, e.g., the agent-layer dynamics are physically coupled over the x-variable digraph $\mathcal{G}_{ax}$. However, since the communication topologies can be independently designed, the complexity is not higher than each single Corollary 7.2.1 or 7.2.2.

7.3 Simulation verification

We now verify the feasibility of proposed ideas in Section 7.2 through simulation studies. We provide a comprehensive study on the robust first-order cooperative tracking problem in Subsection 7.3.1. We study the results of second-order cooperative tracking in Subsection 7.3.2. Finally, in Subsection 7.3.3, we discuss a numerical example for the cooperative tracking in a mixed-order multiagent system with unknown agent-layer dynamics.

7.3.1 First-order cooperative tracking

In this subsection, we investigate the results of Subsection 7.2.1 based on a multiagent system with 5 agents and unknown interconnected time-varying nonlinear dynamics $f_1 = \sqrt{0.5}sin(t)tanh(z_1)$, $f_2 = \sqrt{0.4}sin(z_2)$, $f_3 = \sqrt{0.5}z_3$, $f_4 = \sqrt{0.4}z_4$, $f_5 = \sqrt{0.5}cos(t)tanh(z_5)$. We let $z_i = 0.4\sum_{j\in\mathcal{N}_i^{ax}}(x_i - x_j)$ for $i \in \{1, 2, ..., 5\}$ where the physical neighborhoods of agents are shown using an agent-layer coupling graph in the left-side plot of Figure 7.2. This agent-layer dynamics show diverging response to the perturbation in 5^{th} agent's initial condition at time $t_0 = 10s$ (see Figure 7.1).

In the *first numerical study*, we choose a symmetric reduced-order Laplacian matrix Q_x and a diagonal $R_x = diag\{0.5, 1, 0.5, 1, 0.5\}$ in the Design procedure 7.2.1.

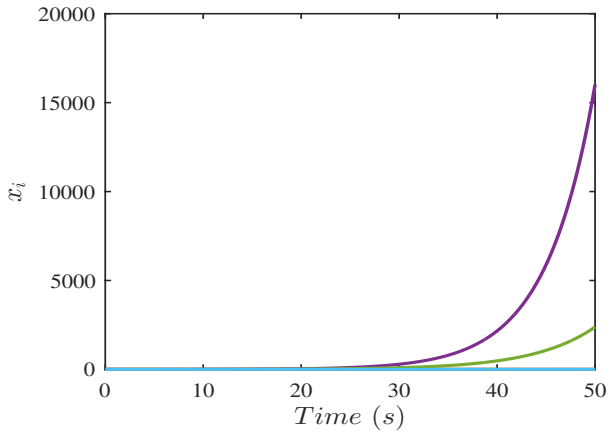

Figure 7.1: A multiagent system with agent-layer dynamics (7.1) and nonlinear functions of Subsection 7.3.1 shows diverging behavior in response to a perturbation in only agent 5's initial condition at time $t_0 = 10s$. As seen, the multiagent system can be sensitive to perturbations in any of its individual components due to the physical couplings.

$$Q_x = \begin{bmatrix} 3.5 & -1.5 & 0 & 0 & -1.5 \\ -1.5 & 2.5 & -1 & 0 & 0 \\ 0 & -1 & 1 & 0 & 0 \\ 0 & 0 & 0 & 1 & -1 \\ -1.5 & 0 & 0 & -1 & 2.5 \end{bmatrix}$$

As discussed before Algorithm 7.2.1, this results in control-layer communication topology $\mathcal{G}_{cx}$ with reduced-order Laplacian matrix $\mathcal{H}_{cx}$:

$$\mathcal{H}_{cx} = \begin{bmatrix} 2.6410 & -0.7522 & -0.0633 & -0.1144 & -0.6315 \\ -0.3761 & 1.5229 & -0.3324 & -0.0354 & -0.0680 \\ -0.0633 & -0.6649 & 1.5625 & -0.0174 & -0.0238 \\ -0.0572 & -0.0354 & -0.0087 & 1.0625 & -0.3136 \\ -0.6315 & -0.1360 & -0.0238 & -0.6272 & 2.2499 \end{bmatrix} \tag{7.52}$$

in which the inter-agent communication topology is complete and, furthermore, all agents should directly receive the reference command. The two-layer closed-loop multiagent system configuration and simulation result are shown in Figure 7.2.

In the *second investigation*, we verify the effectiveness of star topology based on the diagonal weighted communication graph in (7.13). The result is shown in Figure 7.3 where the left-side plot is obtained by taking the diagonal terms of Q_x in all-to-all scenario (7.52) which results in the diagonal reduced-order Laplacian matrix $\mathcal{H}_{cx} = diag\{2.7690, 1.6833, 1.6332, 1.1548, 2.3806\}$, and the right-side plot is achieved by using a four times greater state weighting matrix (compared to the left-side) which ends in $\mathcal{H}_{cx} = diag\{5.3542, 3.2146, 2.9440, 2.0817, 4.5461\}$. This

in fact shows the flexibility of the proposed algorithm to adjust the exponential convergence speed of multiagent systems with unknown time-varying nonlinear dynamics (see Remark 7.2.3 in Subsection 7.2.1). In both cases, R_x is the same as that of all-to-all scenario in Figure 7.2.

In the *third numerical result*, we further investigate the effect of Q_x on the overall topology of $\mathcal{G}_{cx}$. We again choose an incomplete state weighting matrix (compare with the selection in (7.52)); however, the resulting reduced order Laplacian matrix represents an incomplete inter-agent control-layer topology. For the same R_x as the previous two cases, Q_x and $\mathcal{H}_{cx}$ are as follows, and the closed-loop configuration and simulation result are depicted in Figure 7.4.

$$Q_x = \begin{bmatrix} 6.5 & 0 & 0 & 0 & -3 \\ 0 & 5.5 & -2 & 0 & 0 \\ 0 & -2 & 2 & 0 & 0 \\ 0 & 0 & 0 & 2 & -2 \\ -3 & 0 & 0 & -2 & 5 \end{bmatrix}$$

$$\mathcal{H}_{cx} = \begin{bmatrix} 3.5797 & 0 & 0 & -0.1734 & -0.9153 \\ 0 & 2.3278 & -0.4556 & 0 & 0 \\ 0 & -0.9112 & 2.0621 & 0 & 0 \\ -0.0867 & 0 & 0 & 1.3707 & -0.4688 \\ -0.9153 & 0 & 0 & -0.9377 & 3.0643 \end{bmatrix} \tag{7.53}$$

As is seen in Figure 7.4, still all agents must have access to the reference command (based on the discussion before Algorithm 7.2.1, we could expect this requirement because $Q_{xm}\mathbf{1}_5 > \mathbf{0}$). However, we have already shown in Figure 7.3

that the inter-agents communication is unnecessary whenever all agents have access to the reference command. Additionally, these inter-agents communication is still structurally symmetric (bi-direction) due to the symmetry of solution to ARE (7.9). Therefore, *in the fourth simulation*, we verify the feasibility of Algorithm 7.2.1 in finding an incomplete structurally non-symmetric communication topology where only a few agents have access to the reference signal. The closed-loop multiagent system and the corresponding simulation result are shown in Figure 7.5 for $R_x = diag\{0.2, 0.4, 0.2, 0.4, 0.2\}$ and the following set of matrices:

$$\mathcal{H}_x^{alg} = \begin{bmatrix} 1.75 & -0.5 & 0 & 0 & -0.5 \\ -0.5 & 1 & -0.5 & 0 & 0 \\ 0 & -0.5 & 1.25 & 0 & 0 \\ 0 & 0 & 0 & 0.5 & -0.5 \\ -0.5 & 0 & 0 & -0.5 & 1.75 \end{bmatrix}$$

$$\mathcal{H}_{cx}^{alg} = \begin{bmatrix} 8.75 & -2.5 & 0 & 0 & -2.5 \\ -1.25 & 2.5 & -1.25 & 0 & 0 \\ 0 & -2.5 & 6.25 & 0 & 0 \\ 0 & 0 & 0 & 1.25 & -1.25 \\ -2.5 & 0 & 0 & -2.5 & 8.75 \end{bmatrix}$$

$$\mathcal{H}_{cx} = \begin{bmatrix} 7.875 & -2.5 & 0 & 0 & -2.5 \\ -1.875 & 1.875 & 0 & 0 & 0 \\ 0 & -2.5 & 6.25 & 0 & 0 \\ 0 & 0 & 0 & 2.25 & -2.25 \\ -2.5 & 0 & 0 & -2.5 & 7.875 \end{bmatrix}$$

where $\mathcal{H}_x^{alg}$ is a design matrix, $\mathcal{H}_{cx}^{alg}$ is the result of Step 1, and $\mathcal{H}_{cx}$ is a modified result based on the Step 2 of Algorithm 7.2.1. (For such a setup, an alternative incomplete digraph will be discussed in the fifth simulation.)

In the *fifth simulation*, we consider a multi-area large-scale system as depicted in the left-side plot of Figure 7.6 where a cooperative algorithm should be design to ensure reference command tracking in all areas. Here, agents 1 to 5, 6 to 10, and 11 to 15 respectively belong to Area 1, 2, and 3. We assume that the ordered-number agents in each area are described by the same time-varying nonlinearities and inter-area physical couplings as in the first simulation, for example: agents 1, 6, and 10 are modeled by f_1. However, the neighborhoods $\mathcal{N}_i$ in z_i have been modified to further include the intra-area couplings from agent 5 to 8, 10 to 13, and 15 to 3. We require the communication topologies of these areas be independent from each other (e.g., due to the high implementation cost whenever these areas are geographically far from each other). Therefore, we follow the two steps of Algorithm 7.2.1 for $\mathcal{H}_x^{alg} = (I_3 \otimes \mathcal{H}_{xa}^{alg})$ and $R_x = I_3 \otimes R_{x5}$ (R_{x5} is the same weighting matrix as in the fourth simulation scenario), and find $\mathcal{H}_{cx} = (I_3 \otimes \mathcal{H}_{cxa})$:

$$\mathcal{H}_{xa}^{alg} = \begin{bmatrix} 2 & -0.5 & 0 & 0 & -0.5 \\ -0.5 & 1 & -0.5 & 0 & 0 \\ 0 & -0.5 & 1.5 & 0 & 0 \\ 0 & 0 & 0 & 0.5 & -0.5 \\ -0.5 & 0 & 0 & -0.5 & 2 \end{bmatrix} \quad \mathcal{H}_{cxa} = \begin{bmatrix} 4 & -1 & 0 & 0 & -1 \\ -0.5 & 0.5 & 0 & 0 & 0 \\ 0 & -2 & 3.6 & 0 & 0 \\ 0 & 0 & 0 & 1 & -1 \\ -1 & 0 & 0 & 0 & 3 \end{bmatrix}$$

The simulation result for this multi-area multiagent system is shown in the right-plot of Figure 7.6. Note that we have considered the same inter-area communications for brevity in the presentation, and Algorithm 7.2.1 is in fact valid for three different communication structures: $\mathcal{H}_{cx} = diag\{\mathcal{H}_{cxk}\}$ for $k \in \{1, 2, 3\}$.

The result of Corollary 7.2.1 can be verified by reverse engineering based on the provided information for Figure 7.2 to Figure 7.6, and we do not present any new results for brevity. We just mention that, for example, a 10-minute simulation using incomplete structure of Figure 7.5 results in the cost 3.66 (left-hand side of inequality (7.5)) and the analytical worst-case calculation provides guaranteed bound 80.675 for approximated $\kappa = 1$ and $\sigma = 0.4$ to be used in that corollary (right-hand side of inequality (7.5)).

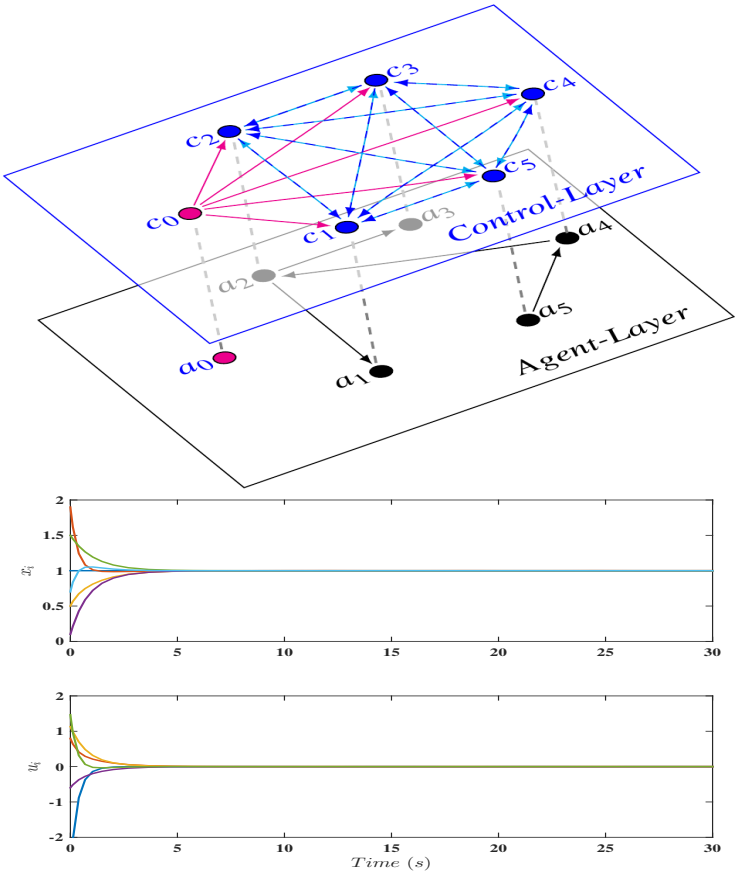

Figure 7.2: An incomplete state weighting matrix Q_x in Design procedure 7.2.1 will not necessarily result in an incomplete communication topology $\mathcal{G}_{cx}$ (see the discussion before Algorithm 7.2.1). *Top)* The two-layer closed-loop multiagent system configuration using the all-to-all communication graph $\mathcal{G}_{cx}$ of (7.52). *Black* items build the physically coupled multiagent system, and *blue* items create the control-layer communication topology. The control-layer graph is structurally symmetric with bi-directed communication links which have been shown in two colors *blue* and *cyan*. Also, *Magenta* items correspond to the (virtual) command generator which is physically decoupled from other agents (to be interpreted as the main control room in large-scale systems). *Bottom)* Distributed first-order cooperative tracking in a multiagent system of (7.1) modeled by nonlinear functions of Subsection 7.3.1.

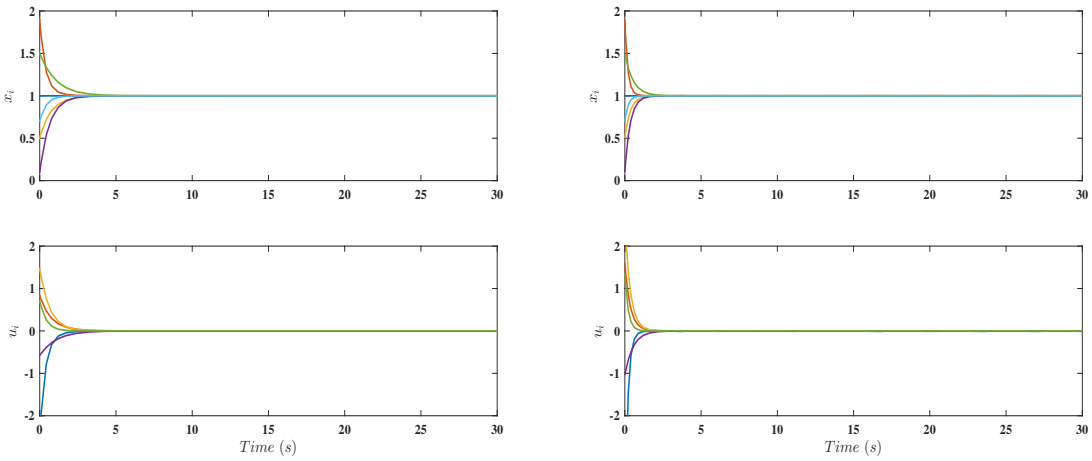

Figure 7.3: First-order cooperative tracking using star topology $\mathcal{G}_{cx}$ where all agents receive the reference command over five directed edges (consider only *magenta* arrows in the left-side plot of Figure 7.2). The norm of state weighting matrix Q_x in the right-plot is four times greater than that of the left-plot which, as expected from LQR optimal control theory, has resulted in a faster convergence compared to the left-side plot with more aggressive control actions.

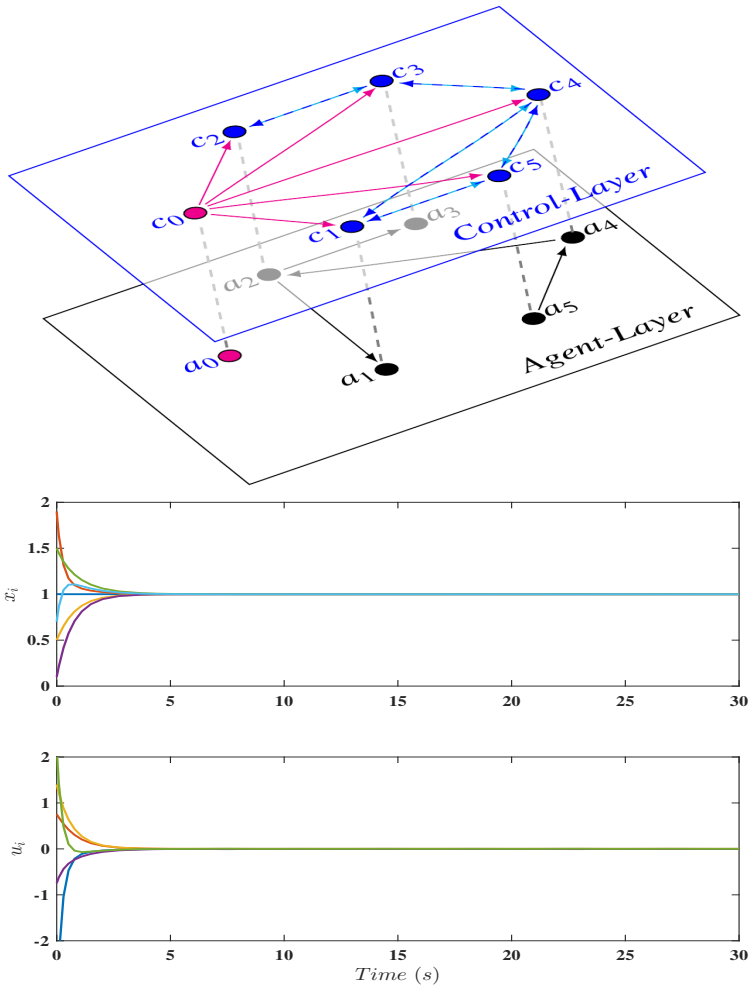

Figure 7.4: The (incomplete) structure of control-layer communication topology highly depends on the selection of state weighting matrix Q_x in Design procedure 7.2.1: *Top)* Closed-loop multiagent system configuration using $\mathcal{H}_{cx}$ in (7.53). *Bottom)* Numerical simulation results.

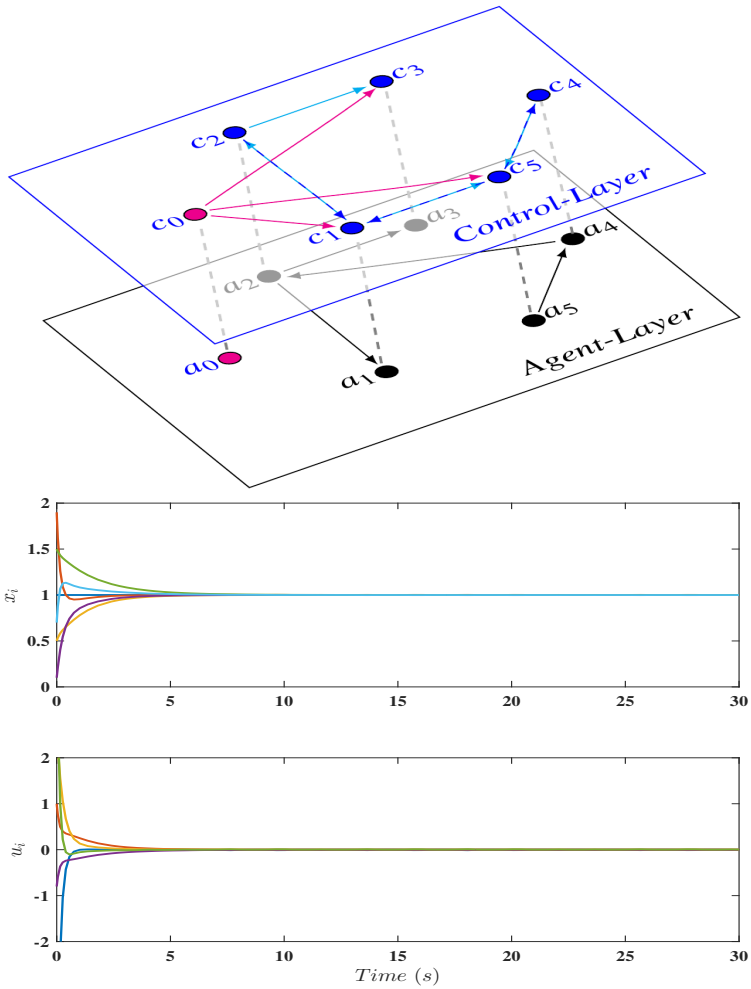

Figure 7.5: *Top)* Closed-loop interconnected multiagent system configuration with a structurally non-symmetric control-layer that is designed based on Algorithm 7.2.1. *Bottom)* First-order cooperative tracking behavior using linear distributed protocol with communication topology $\mathcal{G}_{cx}$ of the fourth simulation.

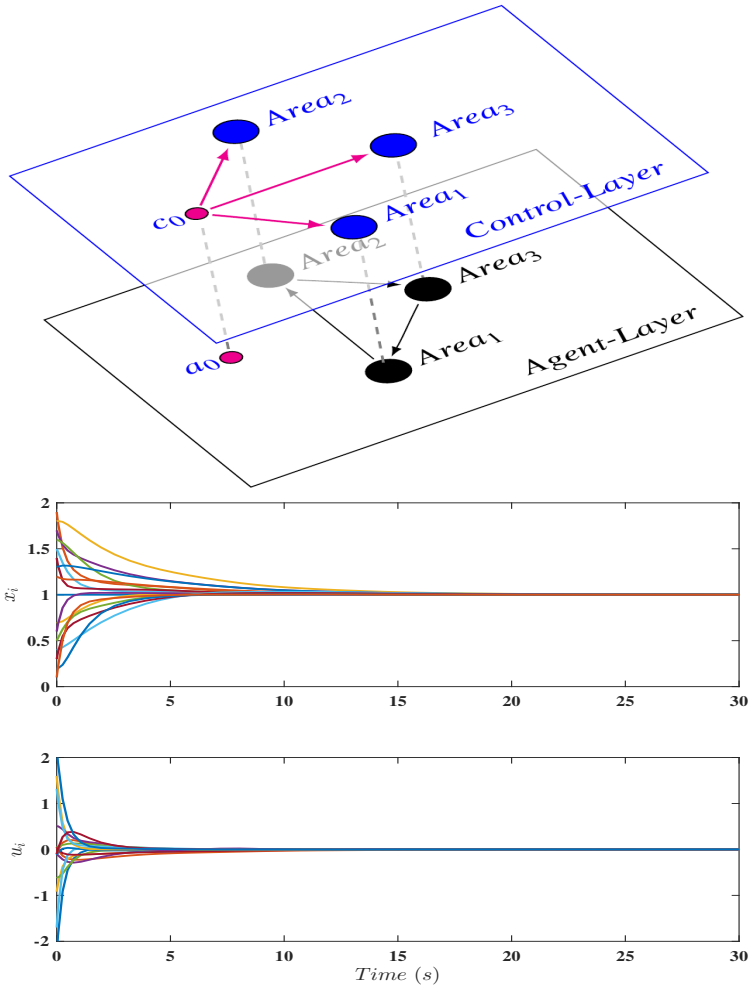

Figure 7.6: *Top)* In a high-dimension physically coupled multiagent system of fifteen agents, we can use Algorithm 7.2.1 and divide the cooperative protocol design problem into three subproblems where, in each area, the five agents exchange information over a communication graph similar to that of Figure 7.5-Top with a set of new edge-weights and no information exchange from agent 4 to 5. *Bottom)* First-order cooperative tracking in multi-area multiagent system subject to unknown inter- and intra-area time-varying nonlinear physical couplings.

7.3.2 Second-order cooperative tracking

We now verify the results of Subsection 7.2.2 using a multiagent system of second-order coupled agents where the time-varying nonlinearities are assumed to be the same as in the first-order tracking scenario in Subsection 7.3.1 replacing f_i by g_i, α_i by β_i, and z_i by $y_i = 0.4\sum_{j\in\mathcal{N}_i^{ax}}(x_i - x_j) + 0.4\sum_{j\in\mathcal{N}_i^{av}}(v_i - v_j)$ in which the physical coupling neighborhoods $\mathcal{N}_i^{ax}$ and $\mathcal{N}_i^{av}$ are shown as agent-layer graphs in Figure 7.7. This configuration models a multiagent system with diverging trajectories which is not shown for brevity. In the rest of this subsection, we discuss two design scenarios based on the Algorithm 7.2.2. A comprehensive study can be made following the discussion in Subsection 7.3.1.

In the *first simulation*, we choose $R_v = diag\{0.5, 1, 0.5, 1, 0.5\}$, $\mathcal{H}_x^{alg} = 2R_v$, and $\mathcal{H}_v^{alg}$; and find $\mathcal{H}_{cx}$ and $\mathcal{H}_{cv}$ given by the aggregated matrix $\mathcal{H}_c$:

$$\mathcal{H}_v^{alg} = \begin{bmatrix} 9 & -2 & 0 & 0 & -2 \\ -2 & 6 & -4 & 0 & 0 \\ 0 & -4 & 9 & 0 & 0 \\ 0 & 0 & 0 & 4 & -4 \\ -2 & 0 & 0 & -4 & 11 \end{bmatrix}$$

$$\mathcal{H}_c = \left[\begin{array}{c|c} \mathcal{H}_{cx} & \mathcal{H}_{cv} \end{array}\right] = \left[\begin{array}{ccccc|ccccc} 2 & 0 & 0 & 0 & 0 & 18 & -4 & 0 & 0 & -4 \\ 0 & 2 & 0 & 0 & 0 & -2 & 6 & -4 & 0 & 0 \\ 0 & 0 & 2 & 0 & 0 & 0 & 0 & 18 & 0 & 0 \\ 0 & 0 & 0 & 2 & 0 & 0 & 0 & 0 & 4 & -4 \\ 0 & 0 & 0 & 0 & 2 & -4 & 0 & 0 & -8 & 22 \end{array}\right] \tag{7.54}$$

where the left-side partition represents a star communication graph $\mathcal{G}_{cx}$ and the right-side partition models a structurally non-symmetric communication topology $\mathcal{G}_{cv}$ to be used in cooperative tracking protocol (7.17). The closed-loop multiagent system and simulation result are shown in Figure 7.7.

In the *second simulation*, we choose the aforementioned R_v and $\mathcal{H}_v^{alg}$, and set $\mathcal{H}_x^{alg} := \mathcal{H}_v^{alg}$. Based on the first step of Algorithm 7.2.2, we find two reduced-order Laplacian matrices $\mathcal{H}_{cx}^{alg}$ and $\mathcal{H}_{cv}^{alg}$ and, based on the second step, we end in $\mathcal{H}_c = [\mathcal{H}_x^{alg}|\mathcal{H}_v^{alg}]$:

$$\mathcal{H}_{cx}^{alg} = \mathcal{H}_{cv}^{alg} = \begin{bmatrix} 22 & -6 & 0 & 0 & -6 \\ -3 & 9 & -6 & 0 & 0 \\ 0 & -12 & 22 & 0 & 0 \\ 0 & 0 & 0 & 6 & -6 \\ -6 & 0 & 0 & -12 & 28 \end{bmatrix}$$

$$\mathcal{H}_c = \left[\begin{array}{ccccc|ccccc} 16 & -6 & 0 & 0 & 0 & 22 & -6 & 0 & 0 & -6 \\ -3 & 9 & -6 & 0 & 0 & -3 & 9 & -6 & 0 & 0 \\ 0 & -12 & 22 & 0 & 0 & 0 & 0 & 22 & 0 & 0 \\ 0 & 0 & 0 & 6 & -6 & 0 & 0 & 0 & 6 & -6 \\ 0 & 0 & 0 & -12 & 25 & -6 & 0 & 0 & -12 & 28 \end{array}\right] \tag{7.55}$$

where the left- and right-side partitions of $\mathcal{H}_c$ correspond to $\mathcal{G}_{cx}$ and $\mathcal{G}_{cv}$, respectively. The multi-layer closed-loop multiagent system and simulation result are given by Figure 7.8 in which the initial state values of the (virtual) reference generator have been manipulated to create the desired command.

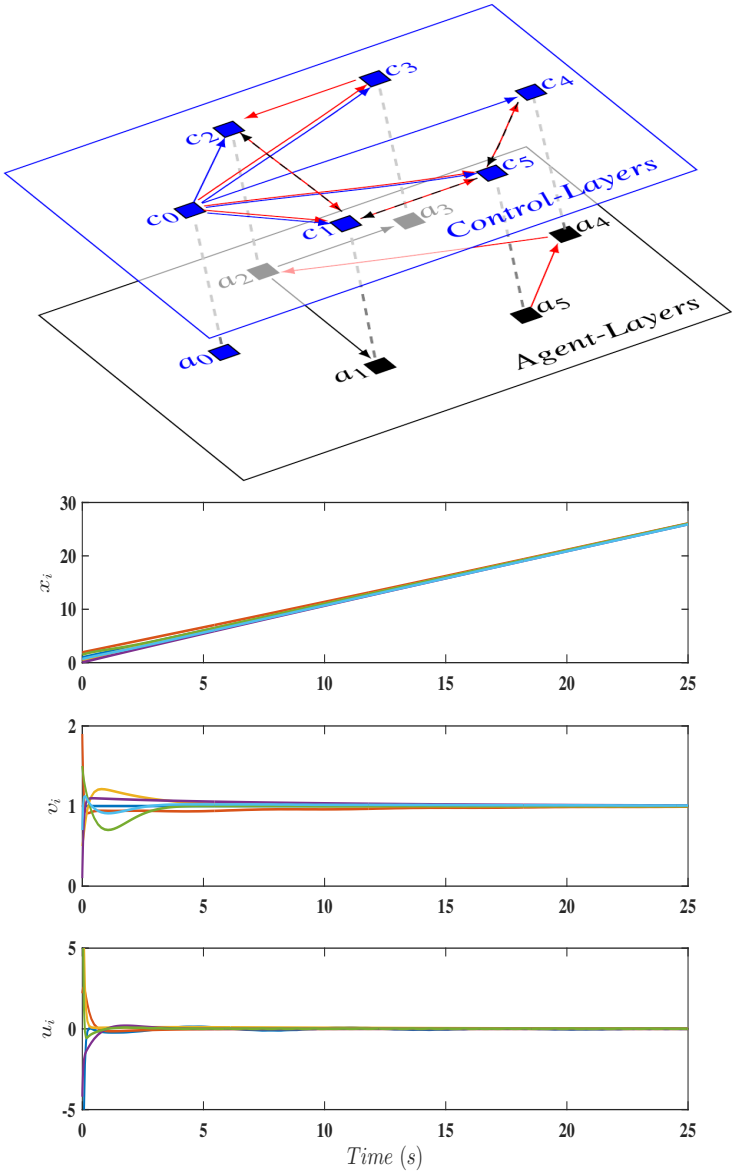

Figure 7.7: Multi-layer second-order cooperative tracking: *Top)* Closed-loop configuration using communication topologies represented by $\mathcal{H}_c$ in (7.54). Over the agent-layers, *black* arrows represent x-variable physical couplings and *red* arrows indicates v-variable interconnections. Over the control-layers, *blue* arrows denotes x-variable communication topology and *red/black* arrows stand for v-variable information exchange graph. *Bottom)* The corresponding numerical simulation result to the left-side configuration.

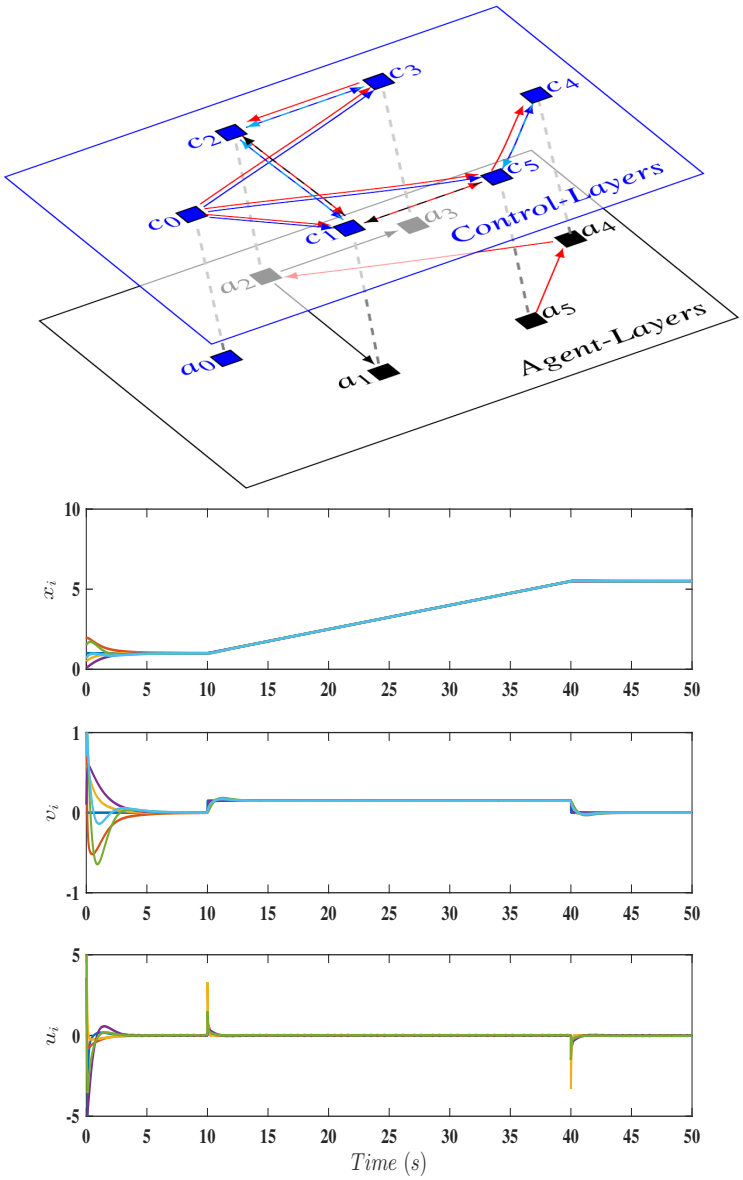

Figure 7.8: Multi-layer second-order cooperative tracking: *Top)* Closed-loop configuration using communication topologies represented by $\mathcal{H}_c$ in (7.55). Symbols and colors are defined similar to Figure 7.7. *Bottom)* The simulation result corresponding to the left-side multi-layer structure.

7.3.3 Mixed-order cooperative tracking

In this subsection, we consider the mixed-order multiagent system of Subsection 7.2.3 with $M = 2$ second order agents (7.30) and $N - M = 3$ first-order agents (7.31). The nonlinearities of second-order agents are the same as the first two agents in Subsection 7.3.2 (i.e., $i \in \mathcal{V}_1 = \{1, 2\}$), and those of first-order agents are the same as the last three agents in Subsection 7.3.1 (i.e., $i \in \{3, 4, 5\}$). The physical couplings have been shown as agent-layer graphs in the left-side plot of Figure 7.9.This physically coupled multiagent system shows unstable behavior which is not shown in this chapter due to the space consideration. In the Algorithm 7.2.3, we choose $R_v = diag\{0.2, 0.4\}$, $R_x = diag\{0.2, 0.4, 0.2\}$, the following $\mathcal{H}^{alg}_{x\mathcal{V}_1}$, $\mathcal{H}^{alg}_{v\mathcal{V}_1}$, and $\mathcal{H}^{alg}_{x\mathcal{V}_2}$, and find structurally symmetric communication topologies $\mathcal{G}_{cx\mathcal{V}_1}$, $\mathcal{G}_{cx\mathcal{V}_2}$, and $\mathcal{G}_{cv\mathcal{V}_1}$ represented by $\mathcal{H}^{alg}_c$:

$$\mathcal{H}^{alg}_{x\mathcal{V}_1} = \mathcal{H}^{alg}_{v\mathcal{V}_1} = \begin{bmatrix} 1.5 & -1.5 \\ -1.5 & 3.5 \end{bmatrix} \qquad \mathcal{H}^{alg}_{x\mathcal{V}_2} = \begin{bmatrix} 1.7 & -0.7 & 0 \\ -0.7 & 0.7 & 0 \\ 0 & 0 & 1 \end{bmatrix}$$

$$\mathcal{H}^{alg}_c = \left[\begin{array}{ccccc|cc} 7.5 & -7.5 & 0 & 0 & 0 & 7.5 & -7.5 \\ -3.75 & 8.75 & 0 & 0 & 0 & -3.75 & 8.75 \\ 0 & 0 & 8.5 & -3.5 & 0 & 0 & 0 \\ 0 & 0 & -1.75 & 1.75 & 0 & 0 & 0 \\ 0 & 0 & 0 & 0 & 5 & 0 & 0 \end{array}\right]$$

in which $\mathcal{H}_c^{alg}$ is partitioned according to (7.44). We further continue Algorithm 7.2.3 and find three structurally non-symmetric communication topologies:

$$\mathcal{H}_c = \left[\begin{array}{ccccc|cc} 6.75 & -6.75 & 0 & 0 & 0 & 5.55 & -5.55 \\ 0 & 5 & 0 & 0 & 0 & 0 & 4.5625 \\ 0 & 0 & 4.575 & -3.5 & 0 & 0 & 0 \\ 0 & 0 & -1.75 & 3.25 & -1.5 & 0 & 0 \\ 0 & 0 & 0 & 0 & 4.75 & 0 & 0 \end{array}\right] \tag{7.56}$$

to be used in mixed-order cooperative tracking protocol (7.34)-(7.35) as depicted in the left-side plot of Figure 7.9 and result in cooperative reference tracking response shown by the right-side plot of this figure.

7.4 Summary and bibliography

We consider cooperative reference tracking problems for three classes of heterogeneous multiagent systems with interconnected nonlinear first-, second, and mixed-order agent-layer dynamics. We introduce a multi-layer framework and propose linear distributed cooperative protocols in which, by treating each communication link as a proportional gain (controller), we appropriately design the control-layer communication topologies to ensure robust tracking and performance in the closed-loop interconnected multiagent system.

We develop optimal control-theoretic formulation to design these control layers, incorporate matrix-algebraic tools to solve the resulting nonlinear matrix equations, and propose analytical solutions to the control-layers design problems

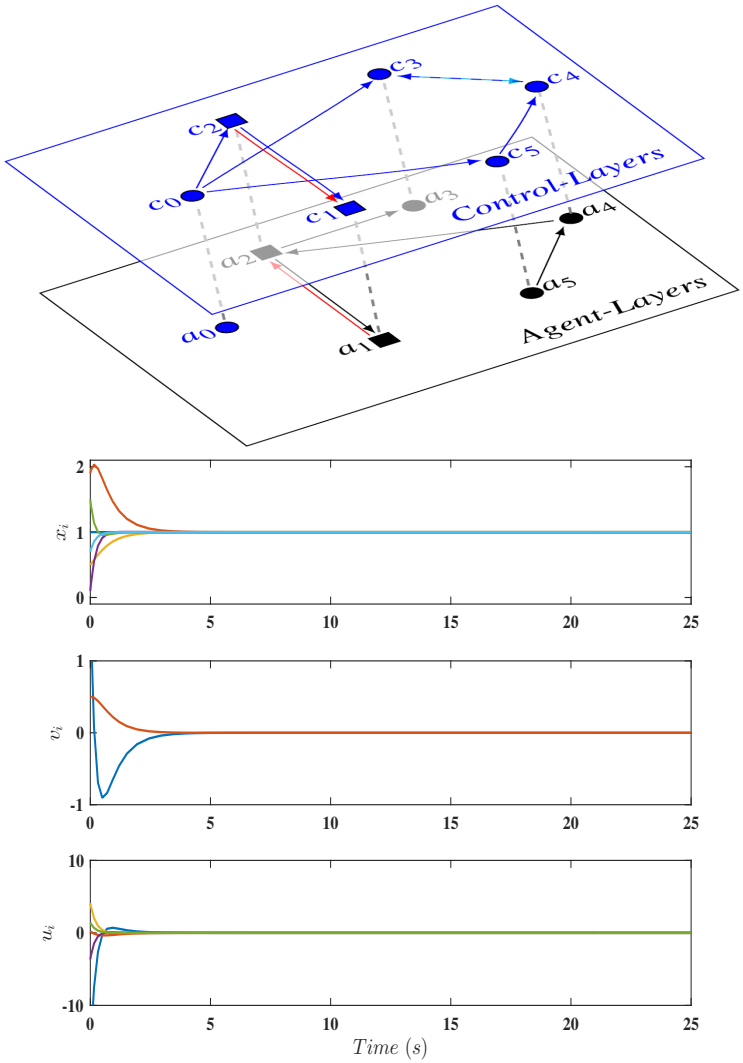

Figure 7.9: Multi-layer cooperative tracking in mixed-order multiagent systems of Subsection 7.3.3: *Top)* Closed-loop configuration where *squares* and *circles* denote second-order and first-order agents, respectively. The *colors* have been explained in Figure 7.7. *Bottom)* Numerical simulation result for the proposed configuration in the left-side plot.

which relate the communication topologies to the multiagent system-level design matrices and our partial knowledge about agent-layer interconnected dynamics. We also develop several algorithms to systematically design structurally symmetric

and non-symmetric control-layers which ensure robust tracking and guaranteed-performance in the presence of partially-known agent-layer dynamics.

These algorithms, in particular, can be used to incorporate a-priori knowledge about the required control-layer structures and find appropriate communication strengths (e.g., due to the implementation cost of communication links whenever agents are geographically far from each other). In each case, for the given control-layer communication topologies, we further establish a bound on the uncertainties in agent-layer dynamics that can be tolerated by this chapter's linear distributed protocol. Noticing the fact that nonlinear matrix equations in second- and mixed-order tracking problems are decomposed into reduced-dimension equations with the same structure as in the first-order tracking problem, the proposed ideas can be used to address (mixed) high-order tracking problems based on the low-dimension matrix equations corresponding to a multiagent system of single integrators.

The problems of this chapter are inspired by the reference tracking challenge in large-scale systems (versus stability issues in Chapters 5 and 6) from a cyber-physical viewpoint in which we assume the unknown agent-layer dynamics are time-varying and interconnected. This viewpoint is inspired by [157], in part. From a multi-agent systems' viewpoint, compared to [73] and [158]-[159], we consider an unknown communication topology and treat it as a design degree of freedom, and each agent's modeling uncertainty dependents on its own as well as its neighbors' internal variables.

Also, note that we consider the global performance of multiagent systems that guarantee convergence rate maximization and quadratic cost function minimization in the presence of modeling uncertainties in the agent-layer dynamics.

References [153]-[154] discussed numerical optimization approaches to find communication graphs with maximum convergence rate as the performance metric. Nevertheless, these references did not provide any closed-form solutions to represent their optimal communication topologies. Under various assumptions on the number of nodes and edges in undirected graphs, [155] proposed several analytical solutions as the graphs with maximum consensus convergence rate. However, similar to [153]-[154], the result was limited to undirected graphs. Based on globally coupled linear-quadratic cost function, [84] proposed an inverse-optimal control technique to achieve cooperative tracking in multiagent systems. But the result was limited to a-priori known "detailed balanced digraphs" and needed local controller implementations. Reference [86] used a linear-quadratic regulatory (LQR) formulation and proved the minimum of global cost could be achieved by inter-agent communication over bi-directed complete digraphs. Additionally, for a decoupled cost function (i.e., sum of agent-level local cost functions), [88]-[89] derived star graph as the optimal communication topology assuming all followers' access to the leader's information. Nevertheless, all of these designs were limited to linear multiagent systems, without any sort of physical interconnections in the open-loop (control communication-free) multiagent systems, and without any modeling uncertainties. Furthermore, these results covered only undirected and some special classes of digraphs to be used as communication topologies.

Nonlinearities in multiagent systems have also been investigated in the literature of distributed control. References [160]- [161] designed nonlinear protocols to ensure consensus in linear multiagent systems. Reference[66] proposed a feedback linearizion-based approach in order to synchronize multiagent systems of

nonlinear agents (see [73], [159], and [162] too). Although the result of applying nonlinear control is theoretically strong, these techniques are still unpopular in industries due to the extra complexity and unclarity compared to linear control methods [163]. In the previous chapters, using linear techniques, we proposed distributed controllers for multiagent systems with Lur'e-type nonlinear agents. In Section 5.3, we considered a special class of multiagent systems with unknown nonlinear physical couplings in the distributed decoupling problem where the result was limited to completely known physical coupling topologies among agents and communication graph was the same as the coupling topology. We addressed these issues in Section 6.1; however, there was no discussion on the closed-loop multiagent system's global performance and the method was still limited to a-priori known undirected communication topology. Similar to the completely linear scenarios in [77]-[78], the designer required local agent-level control manipulations for the implementation purpose. Additionally, there are some applications that do not fit the proposed physical coupling structure of these references.

Although we do not cover any particular applications in this chapter, we mention that the proposed approaches can be used for the coordination control purpose in wind farms (see [144]) under the time-varying nonlinear effects of wake which couple the down-stream turbines to the up-stream ones [164]. The large-scale power system with inter-area couplings can be viewed as another application for the proposed ideas of this chapter [165]. The proposed methods can be applied to the cooperative tracking problem in multi-robot systems in the absence of physical interconnections. In this case the nonlinearities are due to the inaccurate transformation that converts robot's nonlinear dynamics to integrator (see [44]). Without

any physical interconnections and nonlinearities, the results of this chapter can be used to design optimal structurally non-symmetric directed communication topologies which ensure consensus in linear multiagent systems with a guaranteed convergence rate and linear quadratic cost (see [19] and [166] for the application of consensus algorithms).

We acknowledge that the results of this chapter are based on the matrix-algebraic definitions and findings in [99] and [167]. In particular, a comprehensive discussions on M-matrices and functions of matrices are provided in [167].

7.5 Appendix: proofs

Proofs of all theorems are gathered in this section.

7.5.1 Proof of Theorem 7.2.1 (page 264)

We prove this theorem in two steps by showing $u_x = -\mathcal{H}_{cx}e$ of Step 2 in Algorithm 7.2.1 ensures *1)* robust exponential first-order cooperative tracking (7.2) for multiagent systems of agents (7.1) with unknown physically-coupled time-varying nonlinearities f_i, and *2)* robust performance by guaranteeing an upper-bound $\mathcal{P}_1$ on the quadratic cost function (7.5) subject to unknown trajectories of (7.1).

Step 1) We write the first part of this proof by letting the input of multiagent system (7.6) be written as $u_x = \tau_x + \tau_{xm}$ where $\tau_x = -\mathcal{H}_{cx}^{alg}e_x$, $\tau_{xm} = -\mathcal{H}_{cx}^{algm}e_x$, and $\mathcal{H}_{cx}^{alg}$ and $\mathcal{H}_{cx}^{algm}$ are defined in Step 2 of Algorithm 7.2.1. We propose a candidate Lyapunov function $V(e_x) = e_x^T P e_x \succ \mathbf{0}$ where $P \succ \mathbf{0}$ is the solution of ARE (7.9). We first note that $J_{1m}^{\star} = e_x^T(0)Pe_x(0)$ is the optimal cost in Design procedure 7.2.1. Thus, the pair (e_x, τ_x) with $\tau_x = -\mathcal{H}_{cx}^{alg}e_x = -R_x^{-1}Pe_x$ satisfies

Property 7.2.1 if we replace $J_{1m}^{\star}$ by V, and u_x by τ_x. Now, along the uncertain trajectories of (7.6), we find:

$$\begin{aligned}\dot{V}(e_x) &= V_{e_x}^T(f+\tau_x+\tau_{xm}) = -e_x^T Q_{xm} e_x - \tau_x^T R_x \tau_x - 2\tau_x^T R_x (f+\tau_{xm}) \\ &\leq -e_x^T (Q_x + 2[(\mathcal{H}_{cx}^{alg})^T R_x \mathcal{H}_{cx}^{algm}]_{sym}) e_x \prec 0\end{aligned}$$

where the inequality is obtained based on the condition in Step 2 of Algorithm 7.2.1 and the fact that $f^T R_x f \leq e_x^T R_{xf} e_x$. Using Rayleigh-Ritz inequality, we further find $\lambda_{min}(P)\|e_x\|^2 \leq V(e_x) \leq \lambda_{max}(P)\|e_x\|^2$ and $\dot{V}(e_x) \leq -\lambda_{min}(Q)\|e_x\|^2$. Now, global exponential stability of the origin in error dynamics (7.6) is proved in the presence of unknown time-varying interconnected nonlinearities f. This further indicates that the first-order distributed cooperative tracking problem (7.2) is achieved by agents (7.1) with an exponential rate specified by positive scalars κ and σ (defined before the main statement of this theorem).

Step 2) Based on the results in Step 1, we know $V_{e_x}^T(f+u_x) \leq -e_x^T(Q_x + 2(\mathcal{H}_{cx}^{alg})^T R_x \mathcal{H}_{cx}^{algm}) e_x$. Substituting $V_{e_x}^T = 2e_x^T P$ and adding $u_x^T R_x u_x$ to both sides of this inequality, we find $e_x^T Q_x e_x + u_x^T R_x u_x \leq -\frac{d}{dt}(e_x^T P e_x) + u_x^T R_x u_x - 2e_x^T (\mathcal{H}_{cx}^{alg})^T R_x \mathcal{H}_{cx}^{algm} e_x$. Now, we integrate both sides over $[0,\infty)$ and find:

$$\begin{aligned}\mathcal{J}_1(e_x(0)) \leq\ & e_x^T(0) P_1 e_x(0) + \textstyle\int_0^\infty (u_x^T R_x u_x - 2e_x^T (\mathcal{H}_{cx}^{alg})^T R_x \mathcal{H}_{cx}^{algm} e_x) dt \\ \leq\ & e_x^T(0) P_1 e_x(0) \\ & + \tfrac{\kappa^2}{2\sigma} (\lambda_{max}[(\mathcal{H}_{cx}^{alg})^T R_x \mathcal{H}_{cx}^{alg} + (\mathcal{H}_{cx}^{algm})^T R_x \mathcal{H}_{cx}^{algm}]) e_x^T(0) e_x(0) \\ & = e_x^T(0) \mathcal{P}_1 e_x(0)\end{aligned}$$

where we use $\lim_{t\to\infty} e_x(t) = \mathbf{0}$, $u_x = -\mathcal{H}_{cx}e_x$, $\|e_x(t)\| \leq \kappa\ exp^{-\sigma t}\|e_x(0)\|$, and the fact that:

$$e_x^T\mathcal{H}_{cx}^T R_x \mathcal{H}_{cx} e_x = e_x^T((\mathcal{H}_{cx}^{alg})^T R_x \mathcal{H}_{cx}^{alg} + (\mathcal{H}_{cx}^{algm})^T R_x \mathcal{H}_{cx}^{algm} + 2(\mathcal{H}_{cx}^{alg})^T R_x \mathcal{H}_{cx}^{algm})e_x$$

7.5.2 Proof of Theorem 7.2.2 (page 275)

The detail of this proof is similar to that of Theorem 7.2.1. We briefly discuss a two-step proof to show exponential reference tracking using the weighted information exchange digraphs $\mathcal{G}_{cx}$ and $\mathcal{G}_{cv}$, and establish an upper-bound bound on quadratic cost function (7.5).

Step 1) To prove exponentially cooperative second-order tracking, we introduce $V(e) = e^T P e \succ \mathbf{0}$ as the candidate Lyapunov function where $P \succ \mathbf{0}$ is the solution of ARE (7.23). We let $u_v = \tau_v + \tau_{vm}$ where $\tau_v = -\mathcal{H}_c^{alg} e$ and $\tau_{vm} = -\mathcal{H}_c^{algm} e$, and $\mathcal{H}_c^{alg}$ and $\mathcal{H}_c^{algm}$ are defined in Algorithm 7.2.2. We know any pairs (τ_v, e) satisfy Property 7.2.2 replacing u_v by τ_v and $J_{2m}^\star$ by V (since the ARE of Design procedure 7.2.2 is satisfied). Now, along the uncertain trajectories of (7.19) with unknown interconnected nonlinearities $g(y,t)$, we find:

$$\begin{aligned}
\dot{V}(e) = \ & -e^T Q e - (\tau_v^T R_v \tau_v + 2\tau_v^T R_v g + g^T R_v g) - (e^T R_f e - g^T R_v g) \\
& -2e^T(\mathcal{H}_c^{alg})^T R_v \mathcal{H}_c^{algm} e \\
& \leq -e^T(Q + 2[(\mathcal{H}_c^{alg})^T R_v \mathcal{H}_c^{algm}]_{sym})e \prec 0
\end{aligned}$$

We know $\lambda_{min}(P)e^Te \leq V(e) \leq \lambda_{max}(P)e^Te$ and the following inequality can be established using Rayleigh-Ritz inequality:

$$\dot{V}(e) \leq -\lambda_{min}(Q + 2[(\mathcal{H}_c^{alg})^T R_v \mathcal{H}_c^{algm}]_{sym})e^Te$$

This ensures global exponential stability of the origin in error dynamics (7.19) with predefined converging behavior specified by $e(t) \leq \kappa exp^{-\sigma t}e(0)$, κ and σ.

Step 2) Based on the result of Step 1, we know:

$$V_e^T(\begin{bmatrix} \mathbf{0} \\ I_N \end{bmatrix} g + \begin{bmatrix} e_v \\ u_v \end{bmatrix}) \leq -e^T(Q + 2(\mathcal{H}_c^{alg})^T R_v \mathcal{H}_c^{algm})e$$

We further use the fact $V_e^T = 2e^TP$ in order to find $\frac{d}{dt}(e^TPe) \leq -e^T(Q + 2[(\mathcal{H}_c^{alg})^T R_v \mathcal{H}_c^{algm}]_{sym})e$ and, by integrating over $[0, \infty)$, we know $\int_0^\infty (e^TQe + u_v^T R_v u_v)dt \leq e^T(0)Pe(0) + \int_0^\infty (u_v^T R_v u_v - 2(\mathcal{H}_c^{alg})^T R_v \mathcal{H}_c^{algm})dt$ because of the limit behavior $lim_{t\to\infty}e(t) = \mathbf{0}$. With some manipulation, we find $\mathcal{J}_2(e(0)) \leq e^T(0)\mathcal{P}_2e(0)$ where $\mathcal{P}_2$ is defined before the main statement of this Theorem.

7.5.3 Proof of Theorem 7.2.3 (page 289)

This proof follows that of Theorem 7.2.2. In the *first step*, we propose a candidate Lyapunov function $V(e) = e^TPe \succ \mathbf{0}$, decompose $u = \tau + \tau_m$ where $u = [u_v^T, u_x^T]^T = \mathcal{H}_c e$, $\tau = [\tau_v^T, \tau_x^T]^T = \mathcal{H}_c^{algm}e$, and $\tau_m = [\tau_{vm}^T, \tau_{xm}^T]^T = \mathcal{H}_c^{algm}e$ are defined based on Algorithm 7.2.3. Along the unknown trajectories of the coupled error dynamics (7.39), we find:

$$\begin{aligned}\dot{V}(e) = & \; -e^T Q e - (u^T R u + 2u^T R\phi + \phi^T R\phi) - (e^T R_f e - \phi^T R\phi) - 2\tau^T R\tau_m \\ \leq & \; -e^T (Q + 2[(\mathcal{H}_c^{alg})^T R \mathcal{H}_c^{algm}]_{sym}) e \prec 0\end{aligned}$$

and conclude exponential stationary tracking behavior in the closed-loop multiagent system of mixed-order agents (7.30)-(7.31). Note that:

$$(\mathcal{H}_c^{alg})^T R \mathcal{H}_c^{algm} = \begin{bmatrix} (\mathcal{H}_{cx\mathcal{V}_1}^{alg})^T R_v \mathcal{H}_{cx\mathcal{V}_1}^{algm} & \mathbf{0} & (\mathcal{H}_{cx\mathcal{V}_1}^{alg})^T R_v \mathcal{H}_{cv\mathcal{V}_1}^{algm} \\ \mathbf{0} & (\mathcal{H}_{cx\mathcal{V}_2}^{alg})^T R_x \mathcal{H}_{cx\mathcal{V}_2}^{algm} & \mathbf{0} \\ (\mathcal{H}_{cv\mathcal{V}_1}^{alg})^T R_v \mathcal{H}_{cx\mathcal{V}_1}^{algm} & \mathbf{0} & (\mathcal{H}_{cv\mathcal{V}_1}^{alg})^T R_v \mathcal{H}_{cv\mathcal{V}_1}^{algm} \end{bmatrix}$$

Thus, using the transformation $e_{\mathcal{T}} = \mathcal{T}^T e$ for a row permutation matrix $\mathcal{T} \in \mathbb{R}^{(N+M)\times(N+M)}$, this condition can be rearranged as $\dot{V} \leq -e_{\mathcal{T}}^T \Delta e_{\mathcal{T}} \prec \mathbf{0}$ in which $\Delta = diag\{(7.50),\ (7.51)\}$. Therefore, the positive definiteness of matrix $Q + 2[(\mathcal{H}_c^{alg})^T R \mathcal{H}_c^{alg}]_{sym}$ can be verified by two independent lower-order tests (7.50) and (7.51) in Algorithm 7.2.3. In the *second step*, we find:

$$\begin{aligned}\mathcal{J}_3(e(0)) = & \; \int_0^\infty (e^T Q e + u^T R u) dt \leq e^T(0) P e(0) \\ & + \int_0^\infty (u^T R u - 2e^T ((\mathcal{H}_c^{alg})^T R \mathcal{H}_c^{algm}) e) dt\end{aligned}$$

which, substituting $u = \tau + \tau_m$ as defined in the first step, can be rewritten as $\mathcal{J}_3(e(0)) \leq e^T(0) \mathcal{P}_3 e(0)$ with the given $\mathcal{P}_3$ in this theorem.

Chapter 8

Overview and Future Work

"Do not be satisfied with the stories that come before you. Unfold your own myth."

Mawlana — Poet (1207-1273)

A comprehensive summary of results is included at the end of each chapter. Now, at first, we provide a brief chapter-by-chapter overview of this dissertation and, later, propose some theoretical and practical future work ideas.

In Chapter 3, we propose four distributed algorithms and study the challenges of graph-theoretic consensus in physically decoupled multiagent systems. In that chapter, the presence of modeling uncertainties increases the challenges compared to the major part of the literature. We show the agreement is on an unknown value that depends on the initial conditions of agents. After ensuring agreement among agents of a multiagent system, we also prove that an agreement on zero can be guaranteed by imposing some further requirements on the closed-loop multiagent system.

In Chapter 4, motivated by the results of Section 3.1 for multi-vehicle systems, we propose a leaderless stationary consensus protocol which ensures all vehicles agree on a position and come to stop in the presence of unknown persistent disturbances with a few absolute measurements. We further develop a leader-follower stationary protocol which can be applied to the multi-vehicle and multi-robot systems with second-order dynamics.

In Chapter 5, based on the results of Section 3.2, we interpret the agreement on zero as the stabilization of a large-scale system around the origin. Particularly, we discuss some benefits of using distributed algorithms to stabilize large-scale systems. We introduce the notion of physically coupled (interconnected) multiagent systems, and propose two problems based on the structure of available information about the multiagent system: distributed decoupling control and stabilization. In that chapter, we only address the distributed decoupling problem and, moreover, assume the physical coupling topology is completely known (although its effect appears through some unknown linear or nonlinear functions).

In Chapter 6, we assume the physical coupling topology is unknown and propose multi-layer distributed control configurations for both decoupling and stabilization problems in physically interconnected multiagent systems. In this formulation, agents interact over the agent-layer physical coupling topology and controllers exchange information over the control-layer communication topology.

In the distributed decoupling, we have access to all absolute measurements of agents and implement the decoupling algorithm in a hierarchical manner. We stabilize some residual dynamics using lower-level local controllers, and use relative measurements in order to design a higher-level distributed protocol to mitigate

the adverse effects of physical couplings and stabilize the entire interconnected multiagent system (see Sections 5.2, 5.3, and 6.1). In the distributed stabilization, we assume only a few agents provide their absolute measurements. Thus, the stabilization is guaranteed with less measurements compared to the distributed control problem (see Section 6.2).

Although heterogeneous, in Chapters 5 and 6, all agents are modeled by dynamical systems with the same order and the results were limited to the decoupling and stability issues. In all cases, the control-layer communication graph is structurally symmetric and we are able to manipulate the agent-layer dynamics by implementing local controllers. In Chapter 7, we address these challenges by considering the entire control-layer as a manipulable control variable to be designed based on the unknown agent-layer's time-varying nonlinearly interconnected dynamics. By treating each inter-agent communication link as a proportional gain, we use modified LQR formulation and find closed-form solutions for the control-layer purely based on the design matrices and our partial information about the agent-layer dynamics. We show the proposed approach can be used for the performance-oriented design of multi-layer cooperative tracking protocols in mixed-order multiagent systems and, further, establish bounds on the maximum agent-layer modeling uncertainties that can be tolerated by the given communication topologies.

We can further think about the results of Chapters 5 to 7 based on the model of multiagent systems and distributed control protocol. Regarding the modeling, we consider heterogeneous multiagent systems in Chapters 5 to 7. In Section 5.2, we use relative-output measurements, and design an observer-based distributed

decoupling system for a parameter-dependent multiagent system where agents could operate at different operating points. Another result is about the static relative-state feedback approach. In Section 5.3, we consider time-invariant Lur'e nonlinear multiagent systems with matched or unmatched state-coupled nonlinearities, and in Section 6.1, we generalize the model to another Lur'e multiagent system with mixed matched and unmatched time-varying nonlinear modeling uncertainties. In Section 6.2, we introduce a class of linear time-invariant multiagent systems with both state- and input-coupled modeling uncertainties. In Section 7.2, we consider three classes of multiagent systems with unknown interconnected nonlinear modeling uncertainties in their state-space realization.

Regarding the distributed formulation, we address the decoupling and stabilization problems using leaderless consensus protocols (see Section 5.2), and leader-follower consensus strategies (see Section 5.3, and Chapters 5-7). Regarding the developments in Chapter 5, although they appear through some unknown functions and result in modeling uncertainties, we completely know the physical coupling topology. Hence, we use the same topology to design distributed decoupling system. In Chapter 6, we relax this assumption by proposing a multilayer distributed control framework. We further propose some fixed-gain fully distributed algorithms that can be designed without any global knowledge about the coupling and communication graph topologists. In Chapter 7, we propose a set of linear cooperative tracking protocols to ensure robust exponential stability and performance in interconnected multiagent systems. In this formulation, unlike Chapters 5 and 6, the entire control-layer has been teated as the manipulable variable for the control design purpose.

An itemized summary of this Dissertation is given in Table 8.1. Note that, in Section 5.1, we connect the literature of multiagent systems to that of large-scale systems by proposing distributed decoupling and stabilization problems for interconnected multiagent systems. Also, in Section 5.4, we discuss the proposed distributed decoupling problem includes many of the existing distributed consensus problems as special cases. We have considered modeling uncertainties in all designs which can be interesting from practical viewpoints. Thus, we may imagine many future work ideas that cover all theoretical and practical aspects of both multiagent and large-scale systems along with the proposed synergistic foundation in Figure 1.1, page 26. In the rest of this chapter, we discuss the future work ideas under both theoretical and practical categories.

8.1 Theoretical aspect

There are many potential theoretical extensions to this dissertation. As a few immediate ideas, we mention *communication delay* and *quantization*[1]. Additionally, the distributed algorithm may receive imperfect *noisy measurements*. In this case, we can propose *stochastic models* of interconnected multiagent systems and (potentially) prove the same results "on average" (for a zero-mean noise). Moreover, based on the fully distributed developments in Chapter 5, we know that our

[1] A special quantization on a lumped relative-measurement has been discussed in [168]. Based on that, we propose a logarithmic quantizer for a multiagent system of integrators, we write it as $\dot{x}_i = u_i'$ where $u_i' = g_q(\sum_{j\in\mathcal{N}_i}(x_i - x_j))$, $g_q(u_i)$ denotes the quantization function which satisfies $|g_q(u_i) - u_i| \leq \gamma_q |u_i|$ with a constant γ_q. We rewrite it as $\dot{x}_i = u_i + f_q(u_i)$ where $f_q(u_i) = g_q(u_i) - u_i$. Letting $f_q(u_i)$ be a modeling uncertainty, the proposed approaches of this dissertation can be used to handle the quantization problem. However, the general quantization problem will remain as a future work idea.

Table 8.1: Itemized overview of this dissertation.

Chapter/Section	**Model**	**Source of modeling uncertainty**	**Distributed control objective**	**Design level**
3.1	Linear	Disturbances	Leaderless & Leader-Follower Consensus	Local (agent-level)
3.2	Linear	Varying operating point	Leaderless Consensus	Local
4	Linear	Disturbances	Leaderless & Leader-follower Stationary Consensus	Local
5.2	Linear	Varying operating points & Interconnection	Decoupling & Performance	Local
5.3	Nonlinear	Nonlinear interconnection	Decoupling	Local
6.1	Nonlinear	Nonlinearity & Interconnection	Decoupling	Local
6.2	Linear	Interconnection	Stabilization	Local
7	Nonlinear	Nonlinearity & Interconnection	Tracking & Performance & Graph design	Global (multiagent system-level)

ideas have the following features: *1)* The control gains are found independent of graph topologies. Therefore, the design is robust with respect to both coupling and communication topologies "as long as they are fixed and time-invariant in each run," and *2)* They allow a post-design of the communication graph topology. In fact, the initial communication network can be arbitrarily chosen to meet some specific properties (e.g., at least it needs to be a connected graph). However, depending on the optimality requirements, we may re-design and upgrade the communication network to optimize it with respect to some new criteria without being worried about its effects on the decoupling control gains.

In this sense, the proposed fully distributed ideas recover the interconnected multiagent system after any failures in coupling and communication topologies which cause (temporary) shut-downs. However, we emphasize this is different from the switching-based scenarios that may happen in multiagent or large-scale systems. To be clear, while the proposed approached may work under switching scenarios, the proofs do not provide any theoretical guarantees for the stability in any switching interconnected multiagent systems. Thus, *switching control* of *switched systems* can be another future work direction (see [169]). Although we have already found "closed-form" solution for a special class with quadratic cost functions, we consider *communication topology optimization* problem with *non-quadratic cost functions* as another future work idea. The coupling and communication *faults* can be discussed in a similar manner proposing a weighted graph Laplacian (see Remark 2.2.1); however, *resilient control* of interconnected multiagent systems is left as a future challenge. Proposing a multi-layer LQR-based formulation for the distributed consensus (or decoupling) of "uncertain" multi-

agent systems over *signed graphs* where the adjacency matrix has both positive and negative weights is another future work idea. In this case, the multiagent system has antagonistic communication which results in a collaborative-competitive condition [105]. Designing a multi-layer LQR-based formulation in the *discrete-time domain* may open a new window to use the existing results and address the aforementioned quantization, delay, switching, hybrid, and sampled-data control problems. Also, developing a modification of the proposed ideas to handle completely nonlinear interconnected multiagent systems will definitely widen the application of proposed ideas in this research work.

8.2 Practical aspect

In addition to the discussion in previous section, we note that *1)* we have added different sources of modeling uncertainties to each model of multiagent system (unavoidable in real world applications), and *2)* we have addressed our control problems using the well-known LQR approach. The proofs might be less obvious, or possibly complicated; however, the statements of final results are purely based on the modified LQR formulations which should be understandable to a wide range of control theoreticians and practitioners. Although we need some modifications to systematically handle the presence of unknown interconnections in distributed stabilization and decoupling problems, we still provide the conventional degrees of freedom in tuning the system and control input matrices based on the well-known existing rule-of-thumbs (e.g., see [110]). Therefore, we believe the ideas should be sufficiently interesting for people with practical interests (see [163]).

Note that the result of Chapter 3 is already developed with an application viewpoint. However, we further mention that our distributed decoupling and stabilization ideas are applicable to both multi-machine power systems and smart grids. Thinking about the old-style multi-machine power systems, the proposed approaches can be used instead of the existing decentralized techniques (e.g., compared to [15], the proposed LQR formulations in this dissertation need some less-restrictive structural assumptions on the distributed generators' state space models). On the other hand, dealing with a (tomorrow's) smart grid, we notice two main points: *1)* the presence of communication between smart grid's building blocks (e.g., microgrids) fits the multi-layer viewpoint of this research, and *2)* each microgrid's capability to operate in either islanded or grid-connected mode shows the need for a hierarchical framework in the fully distributed decoupling algorithms where agents can be locally stabilized using their absolute measurements. Moreover, we may consider the distributed coordination of wind turbines in the wind farm as another direct application of our ideas.

References

[1] Bennett S., "A Brief History of Automatic Control," *IEEE Control Systems*, Vol. 16, No. 3, pp. 17-25, 1996.

[2] Siljak D., *Large-Scale Dynamic Systems,* North-Holland, 1978.

[3] Lunze J., *Feedback Control of Large-Scale Systems,* Prentice Hall, 1992.

[4] Couzin I., Krause J., Franks N., Levin S., "Effective Leadership and Decision Making in Animal Groups on the Move," *Nature*, Vol. 433, No. 3, pp. 513-516, 2005.

[5] Vicsek T., Czirok A., Ben-Jacob E., Cohen I., Shochet O., "Novel type of phase transition in a system of self-driven particles," *Physical Review Letters,* Vol. 75, No. 6, pp. 1226-1229, 1995.

[6] Seiler P., Pant A., Hedrick J., "A Systems Interpretation for Observations of Bird V-Formations," *Journal of Theoretical Biology*, Vol. 221, No. 2, pp. 279-287, 2003.

[7] Seiler P., *Coordinated Control of Unmanned Aerial Vehicles,* Ph.D. dissertation, University of California, Berkeley, USA, 2001.

[8] Pant A. Seiler P., Koo T. Hedrick K., "Mesh Stability of Unmanned Aerial Vehicle Clusters," *IEEE Transactions on Automatic Control*, Vol. 1, pp. 62-68, 2002.

[9] Fax R., Murray R., "Graph Laplacian and Stabilization of Vehicle Formations," *IFAC World Congress*, Spain, 2002.

[10] Olfati-Saber R., Murray R., "Distributed Structural Stabilization and Tracking for Formations of Dynamic Multi-Agents," *IEEE Conference on Decision and Control*, USA, 2002.

[11] Jadbabaie A., Lin J., Morse S., "Coordination of Groups of Mobile Autonomous Agents Using Nearest Neighbor Rules," *IEEE Transactions on Automatic Control,* Vol. 48, No. 6, pp. , 988-1001, 2003.

[12] Zhao Y., Minero P., Gupta V., "On Disturbance Propagation in Leader-Follower Systems with Limited Leader Information," *Automatica*, Vol. 50, No. 2, pp. 591-598, 2014.

[13] Schoenwald D., "AUVs: In Space, Air, Water, and on the Ground," *IEEE Control Systems Magazine*, Vol. 20, No. 6, pp. 15-18, 2000.

[14] Cruz D., McClintock J., Perteet B., Orqueda O., Cao Y., Fierro R., "Decentralized Cooperative Control: A Multivehicle Platform for Research in Networked Embedded Systems," *IEEE Control Systems Magazine*, 2007.

[15] Wang Y., Hill D., Guo G., "Robust Decentralized Control for Multimachine Power Systems," *IEEE Trans. on Circuits and Systems - I: Fundamental Theory and Applications*, Vol. 44, No. 3, pp. 271-279, 1998.

[16] Murray R., "Recent Research in Cooperative Control of Multivehicle Systems," *Journal of Dynamic Systems, Measurement, and Control*, Vol. 129, No. 5, pp. 571-583, 2007.

[17] DeGroot M., "Reaching a Consensus," *Journal of the American Statistical Association*, Vol. 69, No. 345, pp. 118-121, 1974.

[18] Tsitsiklis J., Bertsekas D., Athans M., "Distributed Asynchronous Deterministic and Stochastic Gradient Optimization Algorithms," *IEEE Transactions on Automatic Control*, Vol. 31, No. 9, pp. 803-812, 1986.

[19] Olfati-Saber R., Fax A, Murray R., "Consensus and Cooperation in Networked Multiagent Systems," *Proceedings of the IEEE*, Vol. 95, No. 1, pp. 215-233, 2007.

[20] Cao Y., Yu W., Ren W., Chen G., "An Overview of Recent Progress in the Study of Distributed Multi-agent Coordination," *IEEE Transactions on Industrial Informatics*, Vol. 9, No. 1, pp. 427-438, 2013.

[21] Lin J., Morse A., Anderson B., "The Multi-agent Rendezvous Problem," *IEEE Conference on Decision and Control*, USA, 2003.

[22] Cortes J., Martinez S., Bullo F., "Robust Rendezvous for Mobile Autonomous Agents via Proximity Graphs in Arbitrary Dimensions," *IEEE Transactions on Automatic Control*, Vol. 51, No. 8, pp. 1289-1298, 2006.

[23] Tanner H., Jadbabaie A., Pappas G., "Stable Flocking of Mobile Agents, Part I: Fixed Topology," *IEEE Conference on Decision and Control*, USA, 2003.

[24] Tanner H., Jadbabaie A., Pappas G., "Stable Flocking of Mobile Agents, Part II: Dynamic Topology," *IEEE Conference on Decision and Control*, USA, 2003.

[25] Olfati-Saber R., "Flocking for Multiagent Dynamic Systems: Algorithms and Theory," *IEEE Transactions on Automatic Control*, Vol. 51, No. 3, pp. 401-420, 2006.

[26] Barca J., Y.A. Sekercioglus Y., "Swarm Robotics Reviewed," *Robotica*, Vol. 31, No. 3, pp. 349-359, 2013.

[27] Ren W., "Formation Keeping and Attitude Alignment for Multiple Spacecraft Through Local Interactions," *Journal of Guidance, Control, and Dynamics*, Vol. 30, No. 2, pp. 633-638, 2007.

[28] Cortes J., "Global and Robust Formation-Shape Stabilization of Relative Sensing Networks," *Automatica*, Vol. 45, No. 12, pp. 2754-2762, 2009.

[29] Olfati-Saber R., "Distributed Kalman Filtering for Sensor Networks," *IEEE Conference on Decision and Control*, USA, 2007.

[30] Ren W., Beard R., Atkins E., "A Survey of Consensus Problems in Multi-agent Coordination," *American Control Conference*, USA, 2005.

[31] Ren W., Beard R., Atkins E., "Information Consensus in Multivehicle Cooperative Control," *IEEE Control Systems Magazine*, Vol. 27, No. 2, pp. 71-82, 2007.

[32] Oh K-K., Park M-C., Ahn H-S., "A Survey of Multi-Agent Formation Control," *Automatica*, Vol. 53, pp. 424-440, 2015.

[33] Wang X., Zeng Z., Cong Y., "Multi-agent Distributed Coordination Control: Developments and Directions via Graph Viewpoint," *Neurocomputing*, Vol. 199, pp. 204-218, 2016.

[34] Wang Q., Gao H., Alsaadi F., Hayat T., "An Overview of Consensus Problems in Constrained Muli-Agent Coordination" *Systems Science and Control Engineering*, Vol. 2, pp. 275-284, 2014.

[35] Olfati-Saber R., Murray R., "Consensus Problems in Networks of Agents with Switching Topologies and Time Delays," *IEEE Transactions on Automatic Control*, Vol. 49, No. 9, pp. 1520-1233, 2004.

[36] Moreau L., "Stability of Continuous-Time Distributed Consensus Algorithms," *IEEE Conference on Decision and Control*, USA, 2004. Full version available at arXiv:math/0409010.

[37] Tanner H., "On the Controllability of Nearest Neighbor Interconnections," *IEEE Conference on Decision and Control*, USA, 2004.

[38] Lu J., Chen G., "A Time-Varying Complex Dynamical Network Model and Its Controlled Synchronization Criteria," *IEEE Transactions on Automatic Control*, Vol. 50, No. 6, pp. 841-846, 2005.

[39] Jiang H., Zhang L., Yu J., Zhou C., "Consensus of Multi-Agent Systems with Dead-Zone Nonlinearity," *International Journal of Control, Automation, and Systems*, Vol. 10, No. 4, pp. 824-829, 2012.

[40] Ren W., Atkins E., "Distributed Multi-Vehicle Coordinated Control via Local Information Exchange," *International Journal of Robust and Nonlinear Control*, Vol. 17, No. 10, pp. 1002-1033, 2007.

[41] Ren W., "On Consensus Algorithms for Double-Integrator Dynamics," *IEEE Transactions on Automatic Control*, Vol. 53, No. 6, pp. 1503-1509, 2008.

[42] Yu W., Chen G., Cao M., "Some Necessary and Sufficient Conditions for Second-Order Consensus in Multi-Agent Dynamical Systems," *Automatica*, Vol. 46, No. 6, pp. 1089-1095, 2010.

[43] Xie G., Wang L., "Consensus Control for a Class of Networks of Dynamic Agents," *International Journal of Robust and Nonlinear Control*, Vol. 17, pp. 941-959, 2007.

[44] Lawton J., Beard R., Young B., "A Decentralized Approach to Formation Maneuvers," *IEEE Transactions on Robotics and Automation*, Vol. 19, No. 6, 2003.

[45] Yu W., Chen G., Cao M., Kurths J., "Second-Order Consensus for Multiagent Systems with Directed Topologies and Nonlinear Dynamics," *IEEE Transactions on Systems, Man, and Cybernetics - Part B: Cybernetics*, Vol. 40, No. 3, pp. 881-891, 2010.

[46] Wang P., Jia Y., "Robust H_∞ Containment Control for Second-Order Multi-agent Systems with Nonlinear Dynamics in Directed Networks," *Neurocomputing*, Vol. 153, pp. 235-241, 2015.

[47] Song Q., Cao J., Yo W., "Second-Order Leader-Following Consensus of Nonlinear Multi-agent Systems via Pinning Control," *Systems and Control Letters*, Vol. 59, No. 9, pp. 553-562, 2010.

[48] Fan M-C., Chen Z., Zhang H-T., "Semi-Global Consensus of Nonlinear Second-Order Multi-Agent Systems With Measurement Output Feedback," *IEEE Transactions on Automatic Control*, Vol. 59, No. 8, pp. 2222-2227, 2014.

[49] Meng Z., Lin Z., Ren W., "Robust Cooperative Tracking for Multiple Non-Identical Second-Order Nonlinear Systems," *Automatica*, Vol. 49, No. 8, pp. 2363-2372, 2013.

[50] Das A., Lewis F., "Cooperative Adaptive Control for Synchronization of Second-Order Systems with Unknown Nonlinearities," *International Journal of Robust and Nonlinear Control*, Vol. 21, No 13, pp. 15091524, 2011.

[51] Zheng Y., Zhu Y., Wang L., "Consensus of Heterogeneous Multi-agent Systems," *IET Control Theory and Applications*, Vol. 5, No. 16, pp. 1881-1888, 2011.

[52] Ren W., Moore K., Chen Y., "High-Order and Model Reference Consensus Algorithms in Cooperative Control of Multi-Vehicle Systems," *Journal of Dynamic Systems, Measurement, and Control*, Vol. 129, No. 5, pp. 678-688, 2006.

[53] Liu Y., Jia Y., "Consensus problem of high-order multi-agent systems with external disturbances: An H analysis approach," *International Journal of Robust and Nonlinear Control*, Vol. 20, No. 14, pp. 1579-1593, 2010.

[54] Liu T., Jiang Z., "Distributed Output-Feedback Control of Nonlinear Multi-Agent Systems," *IEEE Transactions on Automatic Control*, Vol. 58, No. 11, 2013.

[55] Wang X., Ji H., "Leader-Follower Consensus for a Class of Nonlinear Multi-Agent Systems," *International Journal of Control, Automation, and Systems*, Vol. 10, No. 1, pp. 27-35, 2012.

[56] Zhang X., Liu L., Feng G., "Leader-Follower Consensus of Time-Varying Nonlinear Multi-Agent Systems," *Automatica*, Vol. 52, pp. 8-14, 2015.

[57] Cheng L., Wang Y., Ren W., Hou Z-G., Tan M., "On Convergence Rate of Leader-Following Consensus of Linear Multiagent Systems with Communication Noise," *IEEE Transactions on Automatic Control*, Vol. 61, No. 11, pp. 3586-3592, 2016.

[58] Fax A., Murray R., "Information Flow and Cooperative Control of Vehicle Formations," *IEEE Transactions on Automatic Control*, Vol. 49, pp. 1465-1476, 2004.

[59] Scardovi L., Sepulchre R., "Synchronization in Networks of Identical Linear Systems," *Automatica*, Vol. 45, No. 11, pp. 2557-2562, 2009.

[60] Ma C-Q., Zhang J-F., "Necessary and Sufficient Conditions for Consensusability of Linear Multiagent Systems," *IEEE Transactions on Automatic Control*, Vol. 55, No. 5, pp. 1263-1268, 2010.

[61] Li Z., Liu X., Lin P., Ren W., "Consensus of Linear Multi-Agent Systems with Reduced-Order Observer-Based Protocols," *Systems and Control Letters,* Vol. 60, pp. 510-516, 2011.

[62] Li Z., Liu X., Fu M., "Global Consensus Control of Lipschitz Nonlinear Multi-Agent Systems," *IFAC World Congress*, Italy, 2011.

[63] Li Z., Ren W., Liu X., Fu M., "Consensus of Multi-Agent Systems With General Linear and Lipschitz Nonlinear Dynamics Using Distributed Adaptive Protocols," *IEEE Transactions on Automatic Control*, Vol. 58, No. 7, pp. 1786-1791, 2013.

[64] Peng Z., Wang D., Zhang H., Lin Y., "Cooperative output feedback adaptive control of uncertain nonlinear multi-agent systems with a dynamic leader," *Neurocomputing*, Vol. 149, pp. 132141, 2015.

[65] Hu J., Cao J., Yu J., Hayat T., "Consensus of Nonlinear Multiagent Systems with Observer-Based Protocols," *Systems and Control Letter*, Vol. 72, pp. 71-79, 2014.

[66] Bidram A., Lewis F., Davoudi A., "Synchronization of Nonlinear Heterogeneous Cooperative Systems using Input-Output Feedback Linearization," *Automatica*, Vol. 50, pp. 2578-2585, 2014.

[67] Chopra N., Spong M., "On Exponential Synchronization of Kuramoto Oscillators," *IEEE Transactions on Automatic Control,* Vol. 54, No. 2, pp. 353-357, 2009.

[68] Li Z., Duan Z., Xie L., and Liu X., "Distributed Robust Control of Linear Multi-agent Systems with Parameter Uncertainties," *International Journal of Control*, Vol. 85, No. 8, pp. 1039-1050, 2012.

[69] Wang J., Duan Z., Wen G., Chen G., "Distributed Robust Control of Uncertain Linear Multi-Agent Systems," *International Journal of Robust and Nonlinear Control*, Vol. 25, No. 13, pp. 2162-2179, 2015.

[70] Zhao Y., Duan Z., Wen G., Li Z., Chen G., "Fully Distributed Tracking Control for Non-Identical Multi-agent Systems with Matching Uncertainty," *International Journal of Adaptive Control and Signal Processing*, Vol. 29, No. 8, pp. 1024-1037, 2015.

[71] Cheng F., Yu W., Wan Y., and Cao J., "Distributed Robust Control for Linear Multi-Agent Systems with Intermittent Communications and Parameter Uncertainties," *IEEE Transactions on Circuits and Systems II: Express Briefs*, Vo. 63, No. 9, pp. 838-842, 2016.

[72] Zhang H. Lewis F., "Adaptive Cooperative Tracking Control of Higher-Order Nonlinear Systems with Unknown Dynamics," *Automatica*, Vo. 48, No. 7, pp. 1432-1439, 2012.

[73] Li Z., Duan Z., Lewis F., "Distributed Robust Consensus Control of Multiagent Systems with Heterogeneous Matching Uncertainties," *Automatica*, Vol. 50, No. 3, pp. 883-889, 2014.

[74] Mesbahi M., "On State-Dependent Dynamic Graphs and Their Controllability Properties," *IEEE Transactions on Automatic Control*, Vol. 50, No. 3, pp. 387-392, 2005.

[75] Carmela M., Jadbabaie A., "Decentralized Control of Connectivity for Multi-Agent Systems," *IEEE Conference on Decision and Control*, USA, 2006.

[76] Zelazo D., *Graph-theoretic Methods for the Analysis and Synthesis of Networked Dynamic Systems,* Ph.D. Dissertation, University of Washington, 2009.

[77] Oh K-K., Moore K., Ahn H-S., "Disturbance Attenuation in a Consensus Network of Identical Linear Systems: An H_∞ Approach," *IEEE Transactions on Automatic Control*, Vol. 59, No. 8, pp. 2164-2169, 2014.

[78] Cheng Y., Ugrinovskii V., "Gain-Scheduled Leader-Follower Tracking Control for Interconnected Parameter Varying Systems," *International Journal of Robust and Nonlinear Control*, 26:461-488, 2016.

[79] Borrelli F., Keviczky T., "Distributed LQR Design for Identical Dynamically Decoupled Systems," *IEEE Transactions on Automatic Control*, Vol. 53, No. 8, pp. 1901-1912, 2008.

[80] Langbort C., Delvenne J-C., "Distributed Desing Methods for Linear Quadratic Control and Their Limitation," *IEEE Transactions on Automatic Control*, Vol. 55, No. 9, pp. 2085-2093, 2010.

[81] Dong W., "Distributed optimal control of multiple systems," *International Journal of Control*, Vol. 83, No. 10, pp. 2067-2079, 2010.

[82] Tuna. S-E., "LQR-Based Coupling Gain for Synchronization of Linear Systems," *Arxiv*, 2008.

[83] Zhang H., Lewis F., Das A., "Optimal Design for Synchronization of Cooperative Systems: State Feedback, Observer and Output Feedback," *IEEE Transactions on Automatic Control*, Vol. 56, No. 8, pp. 1948-1952, 2011.

[84] Movric K., Lewis F., "Cooperative Optimal Control for Multi-Agent Systems on Directed Graph Topologies," *IEEE Transactions on Automatic Control*, Vol. 59, No. 3, pp. 769-774, 2014.

[85] Zhang H., Feng T., Yang GH, Liang H., "Distributed Cooperative Optimal Control for Multiagent Systems on Directed Graphs: An Inverse Optimal Approach," *IEEE Transactions on Cybernetics*, Vol. 45, No. 7, pp. 1315-1326, 2015.

[86] Cao Y., Ren W., "Optimal Linear Consensus Algorithms: An LQR Perspective," *IEEE Transactions on Systems, Man, and Cybernetics - Part B: Cybernetics*, Vol. 40, No. 3, pp. 819-830, 2010.

[87] Deshpande P., Menon P., Edwards C., Postlethwaite I., "A Distributed Control Law with Guaranteed LQR Cost for Identical Dynamically Coupled Linear Systems," *American Control Conference*, USA, 2011.

[88] Ma J., Zheng Y., Wang L., "LQR-based Optimal Topology of Leader-Following Consensus," *International Journal of Robust and Nonlinear Control*, Vol. 25, No. 17, pp. 3404-3421, 2015.

[89] Wang H., Ma J., "Optimal Topology for Consensus of Heterogeneous Multi-Agent Systems," *Neurocomputing*, Vol. 177, pp. 594-599, 2016.

[90] Nguyen D-H., "A sub-Optimal Consensus Design for Multi-Agent Systems based on Hierarchical LQR," *Automatica*, Vol. 55, pp. 88-94, 2015.

[91] Kim Y., Mesbahi M., "On Maximizing the Second Smallest Eigenvalue of a State-Dependent Graph Laplacian," *IEEE Transactions on Automatic Control*, Vol. 51, No. 1, pp. 116-120, 2006.

[92] Xiao L., Boyd S., "Fast Linear Iterations for Distributed Averaging," *Systems and Control Letters*, Vol. 52, pp. 65-78, 2004.

[93] Li Z., Duan Z., Chen G., Huang L., "Consensus of Multiagent Systems and Synchronization of Complex Networks: A Unified Viewpoint," *IEEE Transactions on Circuits and Systems I: Regular Papers*, Vol. 57, No. 1, pp. 213-224, 2010.

[94] Li Z., Liu X., Ren W., Xie L., "Distributed Tracking Control for Linear Multiagent Systems with a Leader of Bounded Unknown Input," *IEEE Transactions on Automatic Control*, Vol. 58, No. 2, pp. 518-523, 2013.

[95] Li Z., Wen G., Duan Z., Ren W., "Consensus of Linear Multi-Agent Systems with Fully Distributed Control Gains under a General Directed Graph," *IEEE Transactions on Automatic Control*, Vol. 60, No. 4, pp. 1152-1157, 2015.

[96] Ferrari-Trecate G., Galbusera L., Marciandi M., Scattolini R., "Model Predictive Control Schemes for Consensus in Multi-Agent Systems with Single- and Double-Integrator Dynamics," *IEEE Transactions on Automatic Control*, Vol. 54, No. 11, pp. 2560-2572, 2009.

[97] Wang W., Huang J., Wen C., Fan H., "Distributed Adaptive Control for Consensus Tracking with Application to Formation Control of Nonholomonic Mobile Robots," *Automatica*, Vol. 50, No. 4, pp. 1254-1263, 2014.

[98] Chen F., Ren W., Lan W., Chen G.,"Distributed Average Tracking for Reference Signals With Bounded Accelerations," *IEEE Transactions on Automatic Control*, Vol. 60, No. 3, pp.863-869, 2015.

[99] Horn R., Johnson C., *Matrix Analysis*, Cambridge University Press, 2013.

[100] Langville A., Stewart W., "The Kronecker Product and Stochastic Automata Networks," *Journal of Computational and Applied Mathematics*, Vol. 167, No. 2, pp. 429-447, 2004.

[101] Doyle J., Francis B., Tannenbaum A., *Feedback Control Theory*, Macmillan Publishing Co., 1990.

[102] Schizas C., Evans F., "A Graph Theoretic Approach to Multiavriable Control System Design," *Automatica*, Vol. 17, No. 2, pp. 371-377, 1981.

[103] Wang F., Cameron I., "Graph Theoretical Methods in Control Systems Analysis," *Chemical Engineering Science*, Vol. 48, No. 22, pp. 3777-3782, 1993.

[104] Mesbahi M., Egerstedt M., *Graph Theoretic Methods in Multiagent Networks*, Princeton, 2010.

[105] Altafini C., "Consensus problems on networks with antagonistic interactions," *IEEE Transactions Automatic Control*, Vol. 58, No. 4, pp. 935-946, 2013.

[106] Khalil H., *Nonlinear Control*, Prentice Hall, 2014.

[107] Chen C-T., *Linear System: Theory and Design,* 3rd Ed., Oxford University Press, 1999.

[108] Ioannou P., Sun J., *Robust Adaptive Control,* Dover Publication, 2012.

[109] Kirk D., *Optimal Control Theory: An Introduction*, Prentice Hall, 1970.

[110] Dorato P., Abdallah C., Cerone V., *Linear Quadratic Control: An Introduction*, Krieger, 2000.

[111] Rezaei V., Stefanovic M., "Distributed Leaderless and Leader-Follower Consensus of Linear Multiagent Systems under Persistent Disturbances," *Mediterranean Conference on Control and Automation*, Greece, 2016.

[112] Rezaei V., Stefanovic M., "Distributed Optimal Leaderless Consensus of Linear Multiagent Systems with Polynomial State Space Models," *IEEE Multi-Conference on Systems and Control*, Argentina, 2016.

[113] Rezaei V., Stefanovic M., "Distributed Output Feedback Stationary Consensus of Multi-Vehicle Systems in Unknown Environments," *Control Theory and Technology,* Vol. 16, No. 2, pp. 93-109, 2018.

[114] Ni W., Cheng D., "Leader-Following Consensus of Multi-agent Systems under Fixed and Switching Topologies," *Systems and Control Letters*, Vol. 59, No. 3-4, pp. 209-217, 2010.

[115] Johnson C., "Disturbance Accommodating Control: An Overview," *American Control Conference*, USA, 1986.

[116] Yucelen T., Egerstedt M., "Control of Multiagent Systems under Persistent Disturbance," *American Control Conference*, Canada, 2012.

[117] Anderson M., Dimarogonas D., Sandberg H., Johansson K., "Distributed Control of Networked Dynamical Systems: Static Feedback, Integral Action and Consensus," *IEEE Transactions on Automatic Control*, Vol. 59, No. 7, pp. 1750-1764, 2014.

[118] Cao W., Zhang J., Ren W., "Leader-Follower Consensus of Linear Multi-agent Systems with Unknown External Disturbances," *Systems and Control Letters*, Vol. 82, pp. 64-70, 2015.

[119] Ajorlou A., Asadi M., Aghdam A., Blouin S., "Distributed Consensus Control of Unicycle Agents in the Presence of External Disturbances," *Systems and Control Letters,* Vol. 82, pp. 86-90, 2015.

[120] Rezaei V., "Advanced Control of Wind Turbines: Briesf Survey, Categorization, and Challenges," *American Control Conference*, USA, 2015.

[121] Marcos A., Balas G., "Development of Linear Parameter Varying Models for Aircraft," *Journal of Guidance, Control, and Dynamics*, Vol. 27, No. 2, pp. 218-228, 2004.

[122] Lin F., *Robust Control Design: An Optimal Control Approach*, Wiley, 2007.

[123] Douglas J., Athans M., "Robust Linear Quadratic Designs with Real Parameter Uncertainty," *IEEE Transactions on Automatic Control*, Vol. 39, No. 1, pp. 107-111, 1994.

[124] Petersen I., McFarlane D., "Optimal Guaranteed Cost Control and Filtering for Uncertain Linear System," *IEEE Transactions on Automatic Control*, Vol. 39, No. 9, pp. 1971-1977, 1994.

[125] Bento L., Parafita R., Nunes U., "Inter-Vehicle Sensor Fusion for Accurate Vehicle Localization supported by V2V and V2I Communications," *International Conference on Intelligent Transportation Systems,* 2012.

[126] Langari R., "Autonomous Vehicles: A Tutorial on Research and Development Issues," *American Control Conference,* USA, 2017.

[127] Ren W., Atkins E., "Distributed MultiVehicle Coordinated Control via Local Information Exchange," *International Journal of Robust and Nonlinear Control*, Vol. 17, No. 10-11, pp. 1002-1033, 2007.

[128] Xue R., Cai G., "Formation Flight Control of Multi-UAV System with Communication Constraints," *Journal of Aerospace Technology Management,* Vol. 8, No. 2, pp. 203-210, 2016.

[129] Yucelen T., Johnson E., "Control of Multi-Vehicle Systems in the presence of Uncertain Dynamics," *International Journal of Control,* Vol. 86, No. 9, pp. 1540-1553, 2013.

[130] Huang N., Duan Z., Chen G., "Some Necessary and sufficient Conditions for Consensus of Second-Order Multi-Agent Systems with Sampled Position Data," *Automatica,* Vol 63, pp. 148-155, 2016

[131] Liu C-L., Liu F., "Stationary Consensus of Heterogeneous Multi-Agent Systems with Bounded Communication Delays," *Automatica*, Vol. 47, pp. 2130-2133, 2011.

[132] Qin J., Yu C., Hirche S., "Stationary Consensus of Asynchronous Discrete-Time Second-Order Multi-Agent Systems under Switching Topology," *IEEE Transactions on Industrial Informatics,* Vol. 8, No. 4, pp. 986-994, 2012.

[133] Feng Y., Xu S., Lewis F., Zhang B., "Consensus of Heterogeneous First- and Second-Order Multi-Agent Systems with Directed Communication Topologies," *International Journal of Robust and Nonlinear Control,* Vol. 25, pp. 362-375, 2015.

[134] Pei Y., Sun J., "Necessary and Sufficient Conditions of Stationary Average Consensus for Second-Order Multi-Agent Systems," *International Journal of Systems Science,* Vol. 47, No. 15, pp. 3631-3636, 2016.

[135] Gohrle C., Schindler A., Wagner A., Sawodny O., "Road Profile Estimation and Preview Control for Low-Bandwidth Active Suspension Systems," *IEEE/ASME Transactions on Mechatronics,* Vol. 20, No. 5, pp. 2299-2310, 2015.

[136] Youn I., Khan M., Uddin N., Tomizuka M., "Road Disturbance Estimmation for the Optimal Preview Control of an Active Suspension System Based on Tracked Vehicle Model," *International Journal of Automotive Technology,* Vol. 18, No. 2, pp. 307-316, 2017.

[137] Cho A., Kim S., Kee C., "Wind Estimation and Airspeed Calibration using a UAV with a Single-Antenna GPS Receiver and Pitot Tube," *IEEE Transactions on Aerospace and Electronic Systems,* Vol. 47, No. 1, pp. 109-117, 2011.

[138] Arain B., Kendoul F., "Real-Time Wind Speed Estimation and Compensation for Improved Flight," *IEEE Transactions on Aerospace and Electronic Systems,* Vol. 50, No. 2, pp. 1599-1606, 2014.

[139] Shen H., Li N., Griffiths H., Rojas S., "Tracking Control of a Small Unmanned Air Vehicle with Airflow Awareness," *American Control Conference,* USA, 2017.

[140] Rezaei V., Stefanovic M., "Distributed Stabilization of Linear Multiagent Systems with Coupled State and Input Uncertainties," *IEEE Conference on Control Technology and Applications*, USA, 2017.

[141] Rezaei V., Stefanovic M., "Distributed Decoupling of Partially-Unknown Interconnected Linear Multiagent Systems: State and Output Feedback Approaches," *IFAC World Congress*, France, 2017.

[142] Rezaei V., Stefanovic M., "Distributed Decoupling of Linear Multiagent Systems with Interconnected Nonlinear Uncertainties," *IEEE Conference on Decision and Control*, USA, 2016.

[143] Lam J., Yang G-H., "Balanced Model Reduction of Symmetric Composite Systems," *Internation Journal of Control*, Vol. 65, No. 6, pp. 1031-1043, 1996.

[144] Madjidian M., Mirkin L., "Distributed Control with Low-Rank Coordination," *IEEE Transactions on Control of Network Systems*, Vol. 1, No. 1, pp. 53-63, 2014.

[145] Wang S., Davison E., "On the Stabilization of Decentralized Control Systems," *IEEE Transactions on Automatic Control,* Vol. 18, No. 5, pp. 473-478, 1973.

[146] Sojoudi S. Lavaei J., Aghdam A., *Structurally Constrained Controllers: Analysis and Synthesis*, Springer, 2011.

[147] Zhang X., Lin Y., "Nonlinear Decentralized Control of Large-Scale Systems with Strong Interconnections," *Automatica*, Vol. 50, pp. 2419-2423, 2014.

[148] Skogestad S. and Postlethwaite I., *Multivariable Feedback Control: Analysis and Design*, Wiley, 2005.

[149] Ouyang H., Petersen I., Ugrinovskii V., "Lagrange Stabilization of Pendulum-Like Systems: A Pseudo H_∞ Control Approach," *IEEE Transactions on Automatic Control*, Vol. 57, No. 3, pp. 649-662, 2012.

[150] Rezaei V., Stefanovic M., "Distributed Decoupling of Linear Multiagent Systems with Mixed Matched and Unmatched State-Coupled Nonlinear Uncertainties," *American Control Conference*, USA, 2017.

[151] Jiang F., Wang L., "Consensus Seeking of High-Order Dynamic Multi-Agent Systems with Fixed and Switching Topologies," *International Journal of Control*, Vol. 82, No. 2, pp. 404-420, 2010.

[152] Su H., Wang X., Lin Z., "Flocking of Multi-Agents with a Virtual Leader," *IEEE Transactions on Automatic Control*, Vol. 45, No. 2, pp. 293-307, 2009.

[153] Rafiee M., Bayen A., "Optimal Network Topology Design in Multi-Agent Systems for Efficient Average Consensus," *IEEE Conference on Decision and Control,* USA, 2010.

[154] Dai R., Mesbahi M., "Optimal Topology Design for Dynamic Networks," *IEEE Conference on Decision and Control,* USA, 2011.

[155] Ogiwara K., Fukami T., Takahashi N., "Maximizing Algebraic Connectivity in the Space of Graphs with a Fixed Number of Vertices and Edges," *IEEE Transactions on Control of Network Systems,* Vol. 4, No. 2, pp. 359-368, 2017.

[156] Chowdhury D., Khalil H., "Fast Consensus in Multi-Agent Systems With Star Topology Using High Gain Observers," *IEEE Control Systems Letters*, Vol. 1, No. 1, pp. 188-193, 2017.

[157] Antsaklis P. "Goals and Challenges in Cyber-Physical Systems Research: Editorial of the Editor in Chief," *IEEE Transactions on Automatic Control*, Vol. 59, No. 12, pp. 3117-3119, 2014.

[158] Wang J., Duan Z., Wen G., Chen, G., "Distributed Robust Control of Uncertain Linear Multi-Agent Systems," *International Journal of Robust and Nonlinear Control,* Vol. 25, No. 13, pp. 2162-2179, 2015.

[159] Ai X., Yu J., Jia Z., Shen Y., Ma P., Yang D. "Adaptive Robust Consensus Tracking for Nonlinear Second-Order Multi-Agent Systems with Heterogeneous Uncertainties," *International Journal of Robust and Nonlinear Control,* Vol. 27, pp. 5082-5096, 2017.

[160] Olfati-Saber R., Murray R., "Consensus protocols for networks of Dynamic Agents," *American Control Conference*, USA, 2003.

[161] Liu X., Chen T., Lu W., "Consensus Problem in Directed Networks of Multi-Agents via Nonlinear Protocols," *Physics Letters A,* Vol. 373, No. 35, pp. 3122-3127, 2009.

[162] Zhang H., Lewis F., "Adaptive Cooperative Tracking Control of Higher-Order Nonlinear Systems with Unknown Dynamics," *Automatica*, Vol. 48, No. 7, pp. 1432-1439, 2012.

[163] Samad T., "A Survey on Industry Impact and Challenges Thereof," *IEEE Control Systems Magazine,* Vol. 37, No. 1, pp. 17-18, 2017.

[164] Gonzalez J., Payan M., Santos J., Rodriguez A., "Maximizing the Overall Production of Wind Farms by Setting the Individual Operating Point of Wind Turbines," *Renewable Energy,* Vol. 80, pp. 219-229, 2015.

[165] Nabavi S-B., Chakrabortty A., "Topology Identification for Dynamic Equivalent Models of Large Power System Networks, *American Control Conference*, USA, 2013.

[166] Ren W., Beard R., Atkins E., "A Survey of Consensus Problems in Multi-agent Coordination," *American Control Conference,* USA, 2005.

[167] Higham N., *Functions of Matrices: Theory and Computation,* SIAM, 2008.

[168] Nedic A., Olshevsky A., Ozdaglar A., Tsitsiklis J., "On Distributed Averaging Algorithms and Quantization Effects," *IEEE Transactions on Automatic Control*, Vol. 54, No. 11, pp. 2506-2517, 2009.

[169] Liberzon D., *Switching in Systems and Control*, Birkhauser, 2003.